ISTANBUL UNIVERSITY PRESS

Indexed in Web of Science

İstanbul Journal of Pharmacy

VOLUME 54 • ISSUE 2 • AUGUST 2024

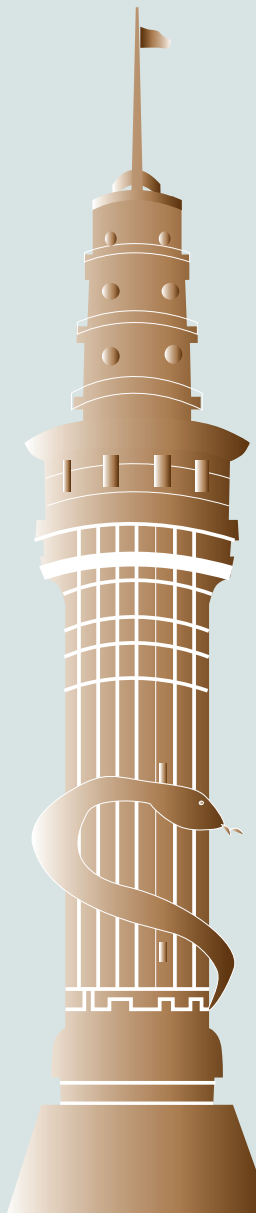

ijp.istanbul.edu.tr

EISSN 2587-2087

İstanbul Journal of Pharmacy
AUGUST 2024,
VOLUME 54, ISSUE 2

INDEXING AND ABSTRACTING

Web of Science - Emerging Sources Citation Index (ESCI)
TÜBİTAK-ULAKBİM TR Dizin
CAS Source Index
SOBİAD
EBSCO Central & Eastern European Academic Source
EBSCO Academic Search Ultimate
Cabells Journalytics
Gale Cengage

OWNER
Prof. Dr. Sevda SÜZGEÇ SELÇUK
İstanbul University, Faculty of Pharmacy, Department of Pharmacognosy, İstanbul, Türkiye

RESPONSIBLE MANAGER
Assoc. Prof. Dr. Bahar GÜRDAL ABAMOR
İstanbul University, Faculty of Pharmacy, Department of Pharmaceutical Botany, İstanbul, Türkiye

CORRESPONDENCE ADDRESS
İstanbul University, Faculty of Pharmacy,
Department of Pharmaceutical Botany,
Beyazıt, 34116, Fatih / İstanbul, Türkiye
Phone: +90 212 440 02 75
Fax: +90 212 440 02 52
E-mail: akaline@istanbul.edu.tr
https://dergipark.org.tr/tr/pub/iujp
https://iupress.istanbul.edu.tr/tr/journal/ijp/home

PUBLISHER
İstanbul University Press
İstanbul University Central Campus,
34452 Beyazit, Fatih, İstanbul, Türkiye
Phone: +90 212 440 00 00

The publication languages of the journal is English.

This is a scholarly, international, peer-reviewed and open-access journal published triannually in April, August and December.

Publication Type: Periodical

İstanbul Journal of Pharmacy
AUGUST 2024,
VOLUME 54, ISSUE 2

EDITORIAL MANAGEMENT BOARD

İSTANBUL UNIVERSITY PRESS

EDITORIAL MANAGEMENT BOARD

İstanbul Journal of Pharmacy
AUGUST 2024,
VOLUME 54, ISSUE 2

EDITORIAL BOARD

İSTANBUL UNIVERSITY PRESS

EDITORIAL BOARD

AIMS AND SCOPE

İstanbul Journal of Pharmacy (Istanbul J Pharm) is an international, scientific, open access periodical published in accordance with independent, unbiased, and double-blinded peer-review principles. The journal is the official publication of İstanbul University Faculty of Pharmacy and it is published triannually on April, August, and December. The publication language of the journal is English.

İstanbul Journal of Pharmacy (Istanbul J Pharm) is an international, scientific, open access periodical published in accordance with independent, unbiased, and double-blinded peer-review principles. The journal is the official publication of İstanbul University Faculty of Pharmacy and it is published triannually on April, August, and December. The publication language of the journal is English.

The target audience of the journal includes specialists and professionals working and interested in all disciplines of pharmaceutical, also medicinal, biological and chemical sciences.

The editorial and publication processes of the journal are shaped in accordance with the guidelines of the International Committee of Medical Journal Editors (ICMJE), World Association of Medical Editors (WAME), Council of Science Editors (CSE), Committee on Publi- cation Ethics (COPE), European Association of Science Editors (EASE), and National Information Standards Organization (NISO). The journal is in conformity with the Principles of Transparency and Best Practice in Scholarly Publishing (https://publicationethics.org/resources/guidelines-new/principles-transparency-and-best-practice-scholarly-publishing).

İstanbul Journal of Pharmacy is currently indexed in Web of Science-Emerging Sources Citation Index, TUBITAK ULAKBIM TR Index and CAS database.

Processing and publication are free of charge with the journal. No fees are requested from the authors at any point throughout the evaluation and publication process. All manuscripts must be submitted via the online submission system, which is available at http://dergipark.gov.tr/iujp. The journal guidelines, technical information, and the required forms are available on the journal's web page.

All expenses of the journal are covered by the İstanbul University.

Statements or opinions expressed in the manuscripts published in the journal reflect the views of the author(s) and not the opinions of the İstanbul University Faculty of Pharmacy, editors, editorial board, and/or publisher; the editors, editorial board, and publisher disclaim any responsibility or liability for such materials.

PUBLICATION POLICIES

The journal is committed to upholding the highest stan- dards of publication ethics and pays regard to Principles of Transparency and Best Practice in Scholarly Publishing published by the Committee on Publication Ethics (COPE), the Directory of Open Access Journals (DOAJ), the Open Access Scholarly Publishers Association (OASPA), and the World Association of Medical Editors (WAME) on https:/ / publicationethics.org/resources/guidelines-new/principles-transparency-and-best-practice-scholarly-publishing

The subjects covered in the manuscripts submitted to the Journal for publication must be in accordance with the aim and scope of the Journal.

Changing the name of an author (omission, addition or order) in papers submitted to the Journal requires written permission of all declared authors.

Plagiarism, duplication, fraud authorship/denied authorship, research/data fabrication, salami slicing/salami publication, breaching of copyrights, prevailing conflict of interest are unethical behaviors. All manuscripts not in accordance with the accepted ethical standards will be removed from the publication. This also contains any possible malpractice discovered after the publication.

Plagiarism

Submitted manuscripts that pass preliminary control are scanned for plagiarism using iThenticate software. If plagi-arism/self-plagiarism will be found authors will be informed. Editors may resubmit manuscript for similarity check at any peer-review or production stage if required. High similarity scores may lead to rejection of a manuscript before and even after acceptance. Depending on the type of article and the percentage of similarity

score taken from each article, the overall similarity score is generally expected to be less than 15 or 20%.

Double Blind Peer-Review

After plagiarism check, the eligible ones are evaluated by the editors-in-chief for their originality, methodology, the importance of the subject covered and compliance with the journal scope. The editor provides a fair double-blind peer review of the submitted articles and hands over the papers matching the formal rules to at least two national/international referees for evaluation and gives green light for publication upon modification by the authors in accordance with the referees' claims.

Editorial Policy

The editorial and publication processes of the journal are shaped in accordance with the guidelines of the International Council of Medical Journal Editors (ICMJE), the World Association of Medical Editors (WAME), the Council of Science Editors (CSE), the Committee on Publication Ethics (COPE), the European Association of Science Editors (EASE), and National Information Standards Organization (NISO). The journal conforms to the Principles of Transparency and Best Practice in Scholarly Publishing (doaj.org/bestpractice). Originality, high scientific quality, and citation potential are the most important criteria for a manuscript to be accepted for publication. Manuscripts submitted for evaluation should not have been previously presented or already published in an electronic or printed medium. The journal should be informed of manuscripts that have been submitted to another journal for evaluation and rejected for publication. The submission of previous reviewer reports will expedite the evaluation process. Manuscripts that have been presented in a meeting should be submitted with detailed information on the organization, including the name, date, and location of the organization.

Open Access Statement

The journal is an open access journal and all content is freely available without charge to the user or his/her institution. Except for commercial purposes, users are allowed to read, download, copy, print, search, or link to the full texts of the articles in this journal without asking prior permission from the publisher or the author. This is in ac- cordance with the BOAI definition of open access.

The open access articles in the journal are licensed under the terms of the Creative Commons Attribution-NonCommercial 4.0 International (CC BY-NC 4.0) license.

Article Processing Charge

All expenses of the journal are covered by the İstanbul University. Processing and publication are free of charge with the journal. There is no article processing charges or submission fees for any submitted or accepted articles.

Copyright Notice

Authors publishing with the journal retain the copyright to their work licensed under the Creative Commons Attribution-NonCommercial 4.0 International license (CC BY-NC 4.0) (https://creativecommons.org/licenses/by-nc/4.0/) and grant the Publisher non-exclusive commercial right to publish the work. CC BY-NC 4.0 license permits unrestricted, non-commercial use, distribution, and reproduction in any medium, provided the original work is properly cited.

PEER REVIEW POLICIES

Only those manuscripts approved by its every individual author and that were not published before in or sent to another journal, are accepted for evaluation.

Submitted manuscripts that pass preliminary control are scanned for plagiarism using iThenticate software. After plagiarism check, the eligible ones are evaluated by editor-in-chief for their originality, methodology, the importance of the subject covered and compliance with the journal scope.

The selected manuscripts are sent to at least two national/international external referees for evaluation and publica- tion decision is given by editor-in-chief upon modification by the authors in accordance with the referees' claims.

Editor-in-Chief evaluates manuscripts for their scientific content without regard to ethnic origin, gender, sexual orientation, citizenship, religious belief or political philosophy of the authors. He/She provides a fair double-blind peer review of the submitted articles for publication and ensures that all the information related to submitted manuscripts is kept as confidential before publishing.

Editor-in-Chief is responsible for the contents and overall quality of the publication. He/She must publish errata pages or make corrections when needed.

Editor-in-Chief does not allow any conflicts of interest between the authors, editors and reviewers. Only he has the full authority to assign a reviewer and is responsible

for final decision for publication of the manuscripts in the Journal.

Reviewers must have no conflict of interest with respect to the research, the authors and/or the research funders. Their judgments must be objective.

Reviewers must ensure that all the information related to submitted manuscripts is kept as confidential and must report to the editor if they are aware of copyright infringement and plagiarism on the author's side.

A reviewer who feels unqualified to review the topic of a manuscript or knows that its prompt review will be impossible should notify the editor and excuse himself from the review process.

The editor informs the reviewers that the manuscripts are confidential information and that this is a privileged interaction. The reviewers and editorial board cannot discuss the manuscripts with other persons. The anonymity of the referees must be ensured. In particular situations, the editor may share the review of one reviewer with other reviewers to clarify a particular point.

PEER REVIEW PROCESS

Only those manuscripts approved by its every individual author and that were not published before in or sent to another journal, are accepted for evaluation.

Submitted manuscripts that pass preliminary control are scanned for plagiarism using iThenticate software. After plagiarism check, the eligible ones are evaluated by Editor-in-Chief for their originality, methodology, the importance of the subject covered and compliance with the journal scope. Editor-in-Chief evaluates manuscripts for their scientific content without regard to ethnic origin, gender, sexual orientation, citizenship, religious belief or political philosophy of the authors and ensures a fair double-blind peer review of the selected manuscripts.

The selected manuscripts are sent to at least two nation- al/international external referees for evaluation and publication decision is given by Editor-in-Chief upon modification by the authors in accordance with the referees' claims.

Editor-in-Chief does not allow any conflicts of interest between the authors, editors and reviewers and is responsible for final decision for publication of the manuscripts in the Journal.

Reviewers' judgments must be objective. Reviewers' comments on the following aspects are expected while conducting the review.

- Does the manuscript contain new and significant information?
- Does the abstract clearly and accurately describe the content of the manuscript?
- Is the problem significant and concisely stated?
- Are the methods described comprehensively?
- Are the interpretations and consclusions justified by the results?
- Is adequate references made to other Works in the field?
- Is the language acceptable?

Reviewers must ensure that all the information related to submitted manuscripts is kept as confidential and must report to the editor if they are aware of copyright infringement and plagiarism on the author's side.

A reviewer who feels unqualified to review the topic of a manuscript or knows that its prompt review will be impossible should notify the editor and excuse himself from the review process.

The editor informs the reviewers that the manuscripts are confidential information and that this is a privileged interaction. The reviewers and editorial board cannot discuss the manuscripts with other persons. The anonymity of the referees is important.

PUBLICATION ETHICS AND MALPRACTICE STATEMENT

An approval of research protocols by the Ethics Committee in accordance with international agreements (World Medical Association Declaration of Helsinki "Ethical Principles for Medical Research Involving Human Subjects," amended in October 2013, www.wma.net) is required for experimental, clinical, and drug studies. If required, ethics committee reports or an equivalent official document will be requested from the authors. For manuscripts concerning experimen- tal research on humans, a statement should be included that shows that written informed consent of patients and volunteers was obtained following a detailed explanation of the procedures that they may undergo. For studies carried out on animals, the measures taken to prevent pain and suffering of the animals should be stated clearly. Information on patient consent, the name of the ethics committee, and the ethics committee approval number should also be stated in the Materials and Methods section of the manu script. It is the authors' responsibility to carefully protect the patients' anonymity. For photographs

that may reveal the identity of the patients, signed releases of the patient or of their legal representative should be enclosed.

All submissions are screened by a similarity detection soft- ware (iThenticate by CrossCheck) at any point during the peer-review or production process. Even if you are the au- thor of the phrases or sentences, the text should not have unacceptable similarity with the previously published data.

When you are discussing others' (or your own) previous work, please make sure that you cite the material correctly in every instance.

In the event of alleged or suspected research misconduct, e.g., plagiarism, citation manipulation, and data falsification/fabrication, the Editorial Board will follow and act in accordance with COPE guidelines.

Research Ethics

İstanbul Journal of Pharmacy adheres to the highest standards in research ethics and follows the principles of international research ethics as defined below. The authors are responsible for the compliance of the manuscripts with the ethical rules.

- Principles of integrity, quality and ransparency should be sustained in designing the research, reviewing the design and conducting the research.
- The research team and participants should be fully informed about the aim, methods, possible uses and requirements of the research and risks of participation in research.
- The confidentiality of the information provided by the research participants and the confidentiality of the respondents should be ensured. The research should be designed to protect the autonomy and dignity of the participants.
- Research participants should participate in the research voluntarily, not under any coercion.
- Any possible harm to participants must be avoided. The research should be planned in such a way that the participants are not at risk.
- The independence of research must be clear; and any conflict of interest or must be disclosed.
- In experimental studies with human subjects, written informed consent of the participants who decide to participate in the research must be obtained. In the case of children and those under wardship or with confirmed insanity, legal custodian's assent must be obtained.
- If the study is to be carried out in any institution or organization, approval must be obtained from this institution or organization.
- In studies with human subject, it must be noted in the method's section of the manuscript that the informed consent of the participants and ethics committee approval from the institution where the study has been conducted have been obtained.

Author's Responsibilities

It is authors' responsibility to ensure that the article is in accordance with scientific and ethical standards and rules. And authors must ensure that submitted work is original. They must certify that the manuscript has not previously been published elsewhere or is not currently being considered for publication elsewhere, in any language. Applicable copyright laws and conventions must be followed. Copyright material (e.g. tables, figures or extensive quotations) must be reproduced only with appropriate permission and acknowledgement. Any work or words of other authors, contributors, or sources must be appropriately credited and referenced.

All the authors of a submitted manuscript must have di- rect scientific and academic contribution to the manuscript. The author(s) of the original research articles is defined as a person who is significantly involved in "conceptualization and design of the study", "collecting the data", "analyzing the data", "writing the manuscript", "reviewing the manuscript with a critical perspective" and "planning/conducting the study of the manuscript and/or revising it". Fund raising, data collection or supervision of the research group are not sufficient roles to be accepted as an author. The author(s) must meet all these criteria described above. The order of names in the author list of an article must be a codecision and it must be indicated in the **Copyright Agreement Form**. The individuals who do not meet the authorship criteria but contributed to the study must take place in the acknowledgement section. Individuals providing technical support, assisting writing, providing a general support, providing material or financial support are examples to be indicated in acknowledgement section.

All authors must disclose all issues concerning financial relationship, conflict of interest, and competing interest that may potentially influence the results of the research or scientific judgment. When an author discovers a significant error or inaccuracy in his/her own published paper, it is the author's obligation to promptly cooperate

with the Editor to provide retractions or corrections of mistakes.

Human Subjects and Animal Use in Research, Ethics Committee Approval and Informed Consent

The Journal takes as principle to comply with the ethical standards of World Medical Association (WMA) Declaration of Helsinki – Ethical Principles for Medical Research Involving Human Subjects and WMA Statement on Animal Use in Biomedical Research.

An approval of research protocols by the Ethics Committee in accordance with international standards mentioned above is required for experimental, clinical, and drug studies and for some case reports. If required, ethics committee reports or an equivalent official document will be requested from the authors. For manuscripts concerning experimental research on humans, a statement should be included that shows that written informed consent of patients and volunteers was obtained following a detailed explanation of the procedures that they may undergo. For studies carried out on animals, the measures taken to prevent pain and suffering of the animals should be stated clearly. Information on patient consent, the name of the ethics committee, and the ethics committee approval number should also be stated in the Materials and Methods section of the manuscript. It is the authors' responsibility to carefully protect the patients' anonymity. For photographs that may reveal the identity of the patients, signed releases of the patient or of their legal representative should be enclosed.

Conflict of Interest

İstanbul Journal of Pharmacy requires and encourages the authors and the individuals involved in the evaluation process of submitted manuscripts to disclose any existing or potential conflicts of interests, including financial, consultant, and institutional, that might lead to potential bias or a conflict of interest. Any financial grants or other support received for a submitted study from individuals or institutions should be disclosed to the Editorial Board. To disclose a potential conflict of interest, the ICMJE Potential Conflict of Interest Disclosure Form should be filled in and submitted by all contributing authors. Cases of a potential conflict of interest of the editors, authors, or reviewers are resolved by the journal's Editorial Board within the scope of COPE and ICMJE guidelines. The Editorial Board of the journal handles all appeal and complaint cases within the scope of COPE guidelines. In such cases, authors should get in direct contact with the editorial office regarding their appeals and complaints. When needed, an ombudsperson may be assigned to resolve cases that cannot be resolved internally. The Editor in Chief is the final authority in the decision-making process for all appeals and complaints.

Responsibility for the Editor and Reviewers

Editor-in-Chief evaluates manuscripts for their scientific content without regard to ethnic origin, gender, sexual orientation, citizenship, religious belief or political philosophy of the authors. He/She provides a fair double-blind peer review of the submitted articles for publication and ensures that all the information related to submitted manuscripts is kept as confidential before publishing.

Editor-in-Chief evaluates manuscripts for their scientific content without regard to ethnic origin, gender, sexual orientation, citizenship, religious belief or political philosophy of the authors. He/She provides a fair double-blind peer review of the submitted articles for publication and ensures that all the information related to submitted manuscripts is kept as confidential before publishing.

Editor-in-Chief does not allow any conflicts of interest between the authors, editors and reviewers. Only he has the full authority to assign a reviewer and is responsible for final decision for publication of the manuscripts in the Journal.

Reviewers must have no conflict of interest with respect to the research, the authors and/or the research funders. Their judgments must be objective.

Reviewers must ensure that all the information related to submitted manuscripts is kept as confidential and must report to the editor if they are aware of copyright infringement and plagiarism on the author's side.

A reviewer who feels unqualified to review the topic of a manuscript or knows that its prompt review will be impossible should notify the editor and excuse himself from the review process.

The editor informs the reviewers that the manuscripts are confidential information and that this is a privileged interaction. The reviewers and editorial board cannot discuss the manuscripts with other persons. The anonymity of the referees must be ensured. In particular situations, the editor may share the review of one reviewer with other reviewers to clarify a particular point.

MANUSCRIPT PREPARATION

The manuscripts should be prepared in accordance with ICMJE-Recommendations for the Conduct, Reporting, Ed- iting, and Publication of Scholarly Work in Medical Journals (updated in December 2015 - http://www.icmje.org/icmje-recommendations.pdf). Authors are required to prepare manuscripts in accordance with the CONSORT guidelines for randomized research studies, STROBE guidelines for observational original research studies, STARD guidelines for studies on diagnostic accuracy, PRISMA guidelines for systematic reviews and meta-analysis, ARRIVE guidelines for experimental animal studies, and TREND guidelines for non-randomized public behavior.

Manuscripts can only be submitted through the journal's online manuscript submission and evaluation system, available at http://ijp.istanbul.edu.tr/en/_. Manuscripts submitted via any other medium will not be evaluated.

Manuscripts submitted to the journal will first go through a technical evaluation process where the editorial office staff will ensure that the manuscript has been prepared and submitted in accordance with the journal's guidelines. Submissions that do not conform to the journal's guidelines will be returned to the submitting author with technical correction requests.

Authors are required to submit the following:

- Copyright Agreement Form
- Author Form
- Title Page

during the initial submission.

The manuscript should be prepared in MS Word format by using Times New Roman font (12 pt) and double-spaced on one side of the paper with adequate margins (2.5 cm).

Preparation of the Manuscript

Title page: A separate title page should be submitted with all submissions and this page should include:

- The full title of the manuscript as well as a short title (running head) of no more than 50 characters,
- Name(s), affiliations, and highest academic degree(s) and ORCID ID(s) of the author(s),
- Grant information and detailed information on the other sources of support,
- Name, address, telephone (including the mobile phone number) and fax numbers, and email address of the corresponding author,
- Acknowledgment of the individuals who contributed to the preparation of the manuscript but who do not fulfill the authorship criteria.

Abstract: An structured abstract should be submitted with Original Articles (Background and Aims, Methods, Results, Conclusion). Please check Table 1 below for word count specifications.

Keywords: Each submission must be accompanied by a minimum of three to a maximum of six keywords for subject indexing at the end of the abstract. The keywords should be listed in full without abbreviations. The keywords should be selected from the National Library of Medicine, Medical Subject Headings database (https://www.nlm.nih.gov/mesh/MBrowser.html).

Manuscript Types

Original Articles: This is the most important type of article since it provides new information based on original research. The main text of original articles should be structured with Introduction, Materials and Methods, Results, Discussion, and Conclusion subheadings. Results and Discussion sections can be combined under "Result and Discussion" heading. Please check Table 1 for the limitations for Original Articles.

Statistical analysis to support conclusions is usually necessary. Statistical analyses must be conducted in accordance with international statistical reporting standards (Altman DG, Gore SM, Gardner MJ, Pocock SJ. Statistical guidelines for contributors to medical journals. Br Med J 1983: 7; 1489-93). Information on statistical analyses with specified statistical software and descriptive details of the chemical used should be provided with a separate subheading under the Materials and Methods section.

Units should be prepared in accordance with the International System of Units (SI).

Editorial Comments: Editorial comments aim to provide a brief critical commentary by reviewers with expertise or with high reputation in the topic of the research article published in the journal. Authors are selected and invited by the journal to provide such comments. Abstract, Keywords, and Tables, Figures, Images, and other media are not included.

Review Articles: Reviews prepared by authors who have extensive knowledge on a particular field and whose scientific background has been translated into a high

Table 1. Limitations for each manuscript type

Type of manuscript	Word limit	Abstract word limit	Table limit	Figure limit
Original Article	3500	250 (Structured)	6	7 or total of 15 images
Review Article	5000	250 (Unstructured)	6	10 or total of 20 images
Short Paper	1000	200	No tables	10 or total of 20 images
Letter to the Editor	500	No abstract	No tables	No media

volume of publications with a high citation potential are welcomed. These authors may even be invited by the journal. Reviews should describe, discuss, and evaluate the current level of knowledge of a topic in clinical practice and should guide future studies. Please check Table 1 for the limitations for Review Articles.

Short Papers: Please check Table 1 for the limitations for Short Papers.

Letters to the Editor: This type of manuscript discusses important parts, overlooked aspects, or lacking parts of a previously published article. Articles on subjects within the scope of the journal that might attract the readers' attention, particularly educative cases, may also be submitted in the form of a "Letter to the Editor." Readers can also present their comments on the published manuscripts in the form of a "Letter to the Editor." Abstract, Keywords, and Tables, Figures, Images, and other media should not be included. The text should be unstructured. The manuscript that is being commented on must be properly cited within this manuscript.

Tables

Tables should be included in the main document, presented after the reference list, and they should be numbered consecutively in the order they are referred to within the main text. A descriptive title must be placed above the tables. Abbreviations used in the tables should be defined below the tables by footnotes (even if they are defined within the main text). Tables should be created using the "insert table" command of the word processing software and they should be arranged clearly to pro- vide easy reading. Data presented in the tables should not be a repetition of the data presented within the main text but should be supporting the main text.

Figures and Figure Legends

Figures, graphics, and photographs should be submitted as separate files (in TIFF or JPEG format) through the submission system. The files should not be embedded in a Word document or the main document. When there are figure subunits, the subunits should not be merged to form a single image. Each subunit should be submitted separately through the submission system. Images should not be labeled (a, b, c, etc.) to indicate figure sub- units. Thick and thin arrows, arrowheads, stars, asterisks, and similar marks can be used on the images to support figure legends. Like the rest of the submission, the figures too should be blind. Any information within the images that may indicate an individual or institution should be blinded. The minimum resolution of each submitted figure should be 300 DPI. To prevent delays in the evaluation process, all submitted figures should be clear in resolution and large in size (minimum dimensions: 100 x 100 mm). Figure legends should be listed at the end of the main document.

All acronyms, abbreviations, and symbols used in the manuscript must follow international rules and should be defined at first use, both in the abstract and in the main text. The abbreviation should be provided in parentheses following the definition.

For plant materials, herbarium name (or acronym), number, name and surname of the person who identified the plant materials should be indicated in the Materials and Methods section of the manuscript.

When a drug, product, hardware, or software program is mentioned within the main text, product information, including the name of the product, the producer of the product, and city and the country of the company (including the state if in USA), should be provided in parentheses in the following format: "Discovery St PET/CT scanner (General Electric, Milwaukee, WI, USA)"

All references, tables, and figures should be referred to within the main text, and they should be numbered consecutively in the order they are referred to within the main text. Limitations, drawbacks, and the shortcomings of original articles should be mentioned in the Discussion section before the conclusion paragraph.

REFERENCES

Reference Style and Format

İstanbul Journal of Pharmacy complies with APA (American Psychological Association) style 6th Edition for referencing and quoting. For more information:

- American Psychological Association. (2010). Publication manual of the American Psychological Association (6^{th} ed.). Washington, DC: APA.
- http://www.apastyle.org

Accuracy of citation is the author's responsibility. All references should be cited in text. Reference list must be in alphabetical order. Type references in the style shown below

Citations in the Text

Citations must be indicated with the author surname and publication year within the parenthesis.

If more than one citation is made within the same paranthesis, separate them with (;).

Samples:
More than one citation;
(Esin et al., 2002; Karasar, 1995)
Citation with one author;
(Akyolcu, 2007)
Citation with two authors;
(Sayıner & Demirci, 2007)
Citation with three, four, five authors;
First citation in the text: (Ailen, Ciambrune, & Welch, 2000) Subsequent citations in the text: (Ailen et al., 2000)
Citations with more than six authors;
(Çavdar et al., 2003)

Citations in the Reference

All the citations done in the text should be listed in the References section in alphabetical order of author surname without numbering. Below given examples should be considered in citing the references.

Basic Reference Types

Book

a) Turkish Book
Karasar, N. (1995). *Araştırmalarda rapor hazırlama* (8^{th} ed.) [Preparing research reports]. Ankara, Turkey: 3A Eğitim Danışmanlık Ltd.
b) Book Translated into Turkish
Mucchielli, A. (1991). *Zihniyetler* [Mindsets] (A. Kotil, Trans.). İstanbul, Turkey: İletişim Yayınları.
c) Edited Book
Ören, T., Üney, T., & Çölkesen, R. (Eds.). (2006). *Türkiye bilişim ansiklopedisi* [Turkish Encyclopedia of Informatics]. İstanbul, Turkey: Papatya Yayıncılık.
d) Turkish Book with Multiple Authors
Tonta, Y., Bitirim, Y., & Sever, H. (2002). *Türkçe arama motorlarında performans değerlendirme* [Performance evaluation in Turkish search engines]. Ankara, Turkey: Total Bilişim.
e) Book in English
Kamien R., & Kamien A. (2014). *Music: An appreciation*. New York, NY: McGraw-Hill Education.
f) Chapter in an Edited Book
Bassett, C. (2006). Cultural studies and new media. In G. Hall & C. Birchall (Eds.), *New cultural studies: Adventures in theory* (pp. 220–237). Edinburgh, UK: Edinburgh University Press.
g) Chapter in an Edited Book in Turkish
Erkmen, T. (2012). Örgüt kültürü: Fonksiyonları, öğeleri, işletme yönetimi ve liderlikteki önemi [Organization culture: Its functions, elements and importance in leadership and business management]. In M. Zencirkıran (Ed.), *Örgüt sosyolojisi* [Organization sociology] (pp. 233–263). Bursa, Turkey: Dora Basım Yayın.
h) Book with the same organization as author and publisher
American Psychological Association. (2009). *Publication manual of the American psychological association* (6^{th} ed.). Washington, DC: Author.

Article

a) Turkish Article
Mutlu, B., & Savaşer, S. (2007). Çocuğu ameliyat sonrası yoğun bakımda olan ebeveynlerde stres nedenleri ve azaltma girişimleri [Source and intervention reduction of stress for parents whose children are in intensive care unit after surgery]. *İstanbul University Florence Nightingale Journal of Nursing, 15*(60), 179–182.
b) English Article
de Cillia, R., Reisigl, M., & Wodak, R. (1999). The discursive construction of national identity. *Discourse and Society, 10*(2), 149–173. http://dx.doi.org/10.1177/0957926599010002002
c) Journal Article with DOI and More Than Seven Authors
Lal, H., Cunningham, A. L., Godeaux, O., Chlibek, R., Diez-Domingo, J., Hwang, S.-J. ... Heineman, T. C. (2015). Efficacy of an adjuvanted herpes zoster subunit

vaccine in older adults. *New England Journal of Medicine, 372*, 2087–2096. http://dx.doi.org/10.1056/NEJMoa1501184

d) Journal Article from Web, without DOI

Sidani, S. (2003). Enhancing the evaluation of nursing care effectiveness. *Canadian Journal of Nursing Research, 35*(3), 26-38. Retrieved from http:/ / cjnr.mcgill.ca

e) Journal Article wih DOI

Turner, S. J. (2010). Website statistics 2.0: Using Google Analytics to measure library website effectiveness. *Technical Services Quarterly, 27*, 261–278. http:/ / dx.doi.org/10.1080/07317131003765910

f) Advance Online Publication

Smith, J. A. (2010). Citing advance online publication: A review. *Journal of Psychology*. Advance online publication. http://dx.doi.org/10.1037/a45d7867

g) Article in a Magazine

Henry, W. A., III. (1990, April 9). Making the grade in today's schools. *Time, 135*, 28–31.

Doctoral Dissertation, Master's Thesis, Presentation, Proceeding

a) Dissertation/Thesis from a Commercial Database

Van Brunt, D. (1997). *Networked consumer health information systems* (Doctoral dissertation). Available from ProQuest Dissertations and Theses database. (UMI No. 9943436)

b) Dissertation/Thesis from an Institutional Database

Yaylalı-Yıldız, B. (2014). *University campuses as places of potential publicness: Exploring the politicals, social and cultural practices in Ege University* (Doctoral dissertation). Retrieved from Retrieved from: http://library.iyte.edu.tr/tr/hizli-erisim/iyte-tez-portali

c) Dissertation/Thesis from Web

Tonta, Y. A. (1992). *An analysis of search failures in online library catalogs* (Doctoral dissertation, University of California, Berkeley). Retrieved from http://yunus.hacettepe.edu.tr/~tonta/yayinlar/phd/ickapak.html

d) Dissertation/Thesis abstracted in Dissertations Abstracts International

Appelbaum, L. G. (2005). Three studies of human information processing: Texture amplification, motion representation, and figure-ground segregation. *Dissertation Abstracts International: Section B. Sciences and Engineering, 65*(10), 5428.

e) Symposium Contribution

Krinsky-McHale, S. J., Zigman, W. B., & Silverman, W. (2012, August). Are neuropsychiatric symptoms markers of prodromal Alzheimer's disease in adults with Down syndrome? In W. B. Zigman (Chair), *Predictors of mild cognitive impairment, dementia, and mortality in adults with Down syndrome*. Symposium conducted at the meeting of the American Psychological Association, Orlando, FL.

f) Conference Paper Abstract Retrieved Online

Liu, S. (2005, May). *Defending against business crises with the help of intelligent agent based early warning solutions*. Paper presented at the Seventh International Conference on Enterprise Information Systems, Miami, FL. Abstract retrieved from http://www.iceis.org/iceis2005/abstracts_2005.htm

g) Conference Paper - In Regularly Published Proceedings and Retrieved Online

Herculano-Houzel, S., Collins, C. E., Wong, P., Kaas, J. H., & Lent, R. (2008). The basic nonuniformity of the cerebral cortex. *Proceedings of the National Academy of Sciences, 105*, 12593–12598. http://dx.doi.org/10.1073/pnas.0805417105

h) Proceeding in Book Form

Parsons, O. A., Pryzwansky, W. B., Weinstein, D. J., & Wiens, A. N. (1995). Taxonomy for psychology. In J. N. Reich, H. Sands, & A. N. Wiens (Eds.), *Education and training beyond the doctoral degree: Proceedings of the American Psychological Association National Conference on Postdoctoral Education and Training in Psychology* (pp. 45–50). Washington, DC: American Psychological Association.

i) Paper Presentation

Nguyen, C. A. (2012, August). *Humor and deception in advertising: When laughter may not be the best medicine*. Paper presented at the meeting of the American Psychological Association, Orlando, FL.

Other Sources

a) Newspaper Article

Browne, R. (2010, March 21). This brainless patient is no dummy. *Sydney Morning Herald, 45*.

b) Newspaper Article with no Author

New drug appears to sharply cut risk of death from heart failure.(1993, July 15). *The Washington Post*, p. A12.

c) Web Page/Blog Post

Bordwell, D. (2013, June 18). David Koepp: Making the world movie-sized [Web log post]. Retrieved from http://www.davidbordwell.net/blog/page/27/

d) Online Encyclopedia/Dictionary

Ignition. (1989). (2^{nd} ed.). Retrieved from http://dictionary.oed.com

Marcoux, A. (2008). Business ethics. In E. N. Zalta (Ed.). *The Stanford encyclopedia of philosophy*. Retrieved from

http://plato.stanford.edu/entries/ethics-business/

e) Podcast

Dunning, B. (Producer). (2011, January 12). *inFact: Conspiracy theories* [Video podcast]. Retrieved from http://itunes.apple.com/

f) Single Episode in a Television Series

Egan, D. (Writer), & Alexander, J. (Director). (2005). Failure to communicate. [Television series episode]. In D. Shore (Executive producer), *House*; New York, NY: Fox Broadcasting.

g) Music

Fuchs, G. (2004). Light the menorah. On *Eight nights of Hanukkah* [CD]. Brick, NJ: Kid Kosher..

REVISIONS

When submitting a revised version of a paper, the author must submit a detailed "Response to the reviewers" that states point by point how each issue raised by the reviewers has been covered and where it can be found (each reviewer's comment, followed by the author's reply and line numbers where the changes have been made) as well as an annotated copy of the main document. Revised manuscripts must be submitted within 30 days from the date of the decision letter. If the revised version of the manuscript is not submitted within the allocated time, the revision option may be cancelled. If the sub- mitting author(s) believe that additional time is required, they should request this extension before the initial 30- day period is over.

Accepted manuscripts are copy-edited for grammar, punctuation, and format. Once the publication process of a manuscript is completed, it is published online on the journal's webpage as an ahead-of-print publication before it is included in its scheduled issue. A PDF proof of the accepted manuscript is sent to the corresponding author and their publication approval is requested within 2 days of their receipt of the proof.

Editor in Chief: Emine AKALIN
Address: İstanbul University Faculty of Pharmacy, İstanbul, Turkiye
Phone: +90 212 440 02 75
Fax: +90 212 440 02 52
E-mail: jfacpharm@istanbul.edu.tr
Publisher: İstanbul University Press
Address: İstanbul University Central Campus, 34452 Beyazit, Fatih / İstanbul, Turkiye
Phone: +90 212 440 00 00

İstanbul Journal of Pharmacy
AUGUST 2024,
VOLUME 54, ISSUE 2

İSTANBUL UNIVERSITY PRESS

CONTENTS

ORIGINAL ARTICLES

İstanbul Journal of Pharmacy
AUGUST 2024,
VOLUME 54, ISSUE 2

İSTANBUL UNIVERSITY PRESS

CONTENTS

İstanbul Journal of Pharmacy
Istanbul J Pharm2024, 54 (2): 108–121
DOI: 10.26650/IstanbulJPharm.2024.1269717

Original Article

Flurbiprofen-encapsulated microsphere laden into heat-triggered *situ* gel for ocular delivery

Heybet Kerem Polat[1], Sedat Ünal[2]

[1]Republic of Turkey Ministry of Health, Turkish Medicines and Medical Devices Agency, Ankara, Türkiye
[2]Erciyes University, Faculty of Pharmacy, Department of Pharmaceutical Technology, Kayseri, Türkiye

ABSTRACT

Background and Aims: This investigation aimed to enhance flurbiprofen's (FB) pre-corneal residence period and ocular availability in the postoperative management of ocular inflammation.

Methods: The microsphere (MS) material was poly (lactic-co-glycolic acid) PLGA, and FB-laden microspheres were prepared using a single emulsification/solvent evaporation process, loaded onto thermosensitive in situ gels, and then characterised.

Results: The size of the microparticles was measured as 19.3±2.1 µm. Entrapment efficiency, zeta potential, and *in vitro* release; it was observed that the microspheres were released for six days. The optimum gelling capacity was obtained using 15% Poloxamer 407, 8% Poloxamer 188, and 1% HEC (viscosity 80-125 cp). Poloxamer 407 concentration was reduced, resulting in increased gelation temperature and duration. It was determined that the gelling temperature of the selected formulation was 35±0.1 °C, the pH was 6.9±0.02, and the viscosity at the gelling temperature was 11042±247 cP. The addition of hydroxyethyl cellulose increased the mucoadhesive strength. - in vitro release of FB from FB-PLGA MS followed the Korsmeyer-Peppas model , –, and the in situ gel preparation was found to be compatible with the Peppas-Sahlin model. In addition, MTT analysis of the ARPE-19 cell line revealed that the in situ gel formulation was biocompatible.

Conclusion: Flurbiprofen release was sustained, ocular availability was improved, and residence time was increased when flurbiprofen-loaded microspheres were incorporated into in situ gel bases.

Keywords: Flurbiprofen, Poloxamer Gel, Ocular Gel, PLGA Microsphere, Release Kinetics

INTRODUCTION

Flurbiprofen (FB) has recently been used to reduce pain and inflammation during ocular surgery; eye drops are the most common type of market FB preparations for ocular administration. However, ocular drops have several drawbacks, such as rapid tear turnover. Numerous experiments have been conducted to enhance the ocular bioavailability of FB (Anderson & Shive, 1997).

A technique used to increase the bioavailability of hydrophobic medicines is the development of PLGA microspheres. To prevent the drug from being metabolised by enzymatic processes in the tear film and to provide consistent and extended drug release, the medication is completely integrated into the polymer matrix (Samatı, Yüksel, & Tarımcı, 2006).

The development of in-situ gel when in contact with the ocular surface as a result of the action of pH, salts, or temperature is the subject of the most current study to address the problem may address the drawbacks of commercial eye drops (Khan, Warade, & Singhavi, 2018).

An optimised formulation was developed using poloxamer 188 (P188) and poloxamer 407 (P407) with FB-loaded PLGA MSs, which forms gelat the corneal temperature, to enhance its bioavailability in ocular tissues. In this study, FB-loaded MC was produced, and the zeta potential, polydispersity index, and particle size were used to describe MSs. UV spectrophotometry was used to determine the effectiveness of FB encapsulation (Samatı et al., 2006). Later, FB-loaded microspheres were included into an optimised in situ gel formulations, which were created to extend the residence period of the microspheres on the ocular surface. The addition of HEC to poloxamer at various concentrations improved bioadhesion properties of the gel the . Then, the optimum formulation was selected, release research was conducted using this formulation, and *in vitro* characterisation experiments of the produced in situ gels were performed.

Corresponding Author: Heybet Kerem Polat **E-mail:** kerem_hybt@hotmail.com
Submitted: 23.03.2023 • **Revision Requested:** 25.10.2023 • **Last Revision Received:** 06.11.2023 • **Accepted:** 27.07.2024

Release and kinetic studies were performed to evaluate the selected optimum gel formulation.

MATERIALS AND METHODS

Materials

From Sigma-Aldrich (St. Louis, MO, USA), we obtained flurbiprofen, PLGA, poloxamer 407, poloxamer 188, hydroxyethyl cellulose (HEC) (125 cp), Benzalkonium chloride (BAC), NaCl, dichloromethane, PVA, and phosphate buffered saline (PBS) tablets.

Production of Flurbiprofen-loaded PLGA microspheres

FB-loaded PLGA MCs were produced using a slightly modified single emulsification/solvent evaporation technique (O/W) (Momoh, Adedokun, Lawal, & Ubochi, 2014). Briefly, 400 mg of PLGA and 200 mg of FB were dissolved in 5 mL of dichloromethane (DCM) to create the organic phase. The O/W emulsion was created by emulsifying the organic phase into an aqueous phase (30 mL) prepared with PVA as a dispersion agent in water (3% w/v) and homogenised (9000 rpm for 4 min) with Ultra-Turrax (IKA, Germany). Following the homogenisation step that created the emulsion, 20 ml of distilled water was added, and mixing was carried out at the same speed for the next minute. The immature microspheres were agitated for 5 h at 500 rpm while suspended in 100 mL of distilled water to produce a completely O/W emulsion. The organic solvent removed throughout the night by stirring. (RCT Simple-Ika). The microspheres separated with centrifugation at 5000 rpm for 10 min in a Thermo ScientificTM SL 16R. They were dried overnight at room temperature following three washings with deionised water. The dried microspheres were stored in a desiccator for further examination. The same method was applied to create PLGA microspheres that were blank and did not contain FB. Figure 1 shows a schematic of microsphere production.

Spectrophotometric Analysis of Flurbiprofen

Using a Shimadzu UV-1800 Spectrophotometer (Japan), the amount of FB in vitro was measured spectrophotometrically at 246 nm, as previously described (Akyüz, Duman, & Murat, 2017).

In vitro characterisation of Flurbiprofen-loaded PLGA Microspheres

Particle size and zeta potential: The distributions of particle size, mean zeta potential, and particle size of the produced microspheres were calculated using Mastersizer 2000 and the light scattering principle (Malvern corporation, UK). Each measurement was performed three times.

Surface morphology of FB-loaded PLGA MSs: The morphological properties and surface traits of PLGA MSs were observed by scanning electron microscopy (SEM) (Zeiss Evo LS-10, Germany).

Determination of drug loading capacity: To determine how well the microspheres were entrapped, perfectly measured (20 mg) FB-loaded PLGA microspheres were dissolved in 1 mL of DCM and then transferred to 9 mL of methanol. The suspension was centrifuged, and the supernatant was then filtered through a 0.45-m membrane. The supernatant was examined using a UV/visible spectrophotometer set at 246 nm. A calibration curve was created using previously known standard solutions of FB in DCM/methanol mixtures (1:9). For each batch, measurements were performed in triplicate. The spectrophotometric method was validated following the recommendations of the ICH. Within the scope of the validation of the spectrophotometric method used for FB quantification, linearity, accuracy, precision, repeatability, limit of detection (LOD), and limit of quantification (LOQ) were determined. The regression coefficient (r^2), which expresses linearity, was determined for FB as $r^2 = 0.9898$. The LOD and LOQ, which express the sensitivity of the method, were determined as 0.0217 µg/mL and 0.0719 µg/mL, respectively. The following equation is used to compute the encapsulation efficiency:

$$EE\ \% = (actual\ drug\ content / theoretical\ drug\ content) \times 100 \quad (1)$$

In Vitro release of FB from FB Loaded PLGA MCs. The collection and separation approach, which is often employed for polymeric microparticles, was used to conduct in vitro release tests. Evaluation of FB release from PLGA MCs was carried out under sink conditions based on FB solubility (5 g/mL) (D'Souza & DeLuca, 2006). Briefly, 40 mL of PBS (pH 7.4) containing 10 mg of microspheres was agitated horizontally at 30 rpm for six days at 37 ºC. The samples taken at certain time intervals were analysed spectrophotometrically (0, 1, 2, 4, 8, 12, 24, 36, 48, 72, 96, 120, and 144 hours). Sample replacement was performed using the same amount of new-release medium (Samdancioglu, Calış, Sumnu, & Atilla Hincal, 2006). It was feasible to determine the cumulative proportion of total FB emitted at each time point using the previously disclosed confirmed spectrophotometric approach.

Release kinetics

DDSolver, a programme developed to speed up calculations and avoid computational mistakes, was used to investigate the release profiles of microspheres and microspheres embedded in in situ gel formulations. Data were computed using the DDSolver programme after acquiring the *in vitro* release profiles of microspheres to identify the most vital and significant four criteria; coefficient of determination (R2), adjusted coefficient of determination (R2adjusted), Akaike Information Criterion (AIC), and model selection criteria (MSC). The resulting data were fitted to multiple kinetic models (Zero order, First order, Hixson-

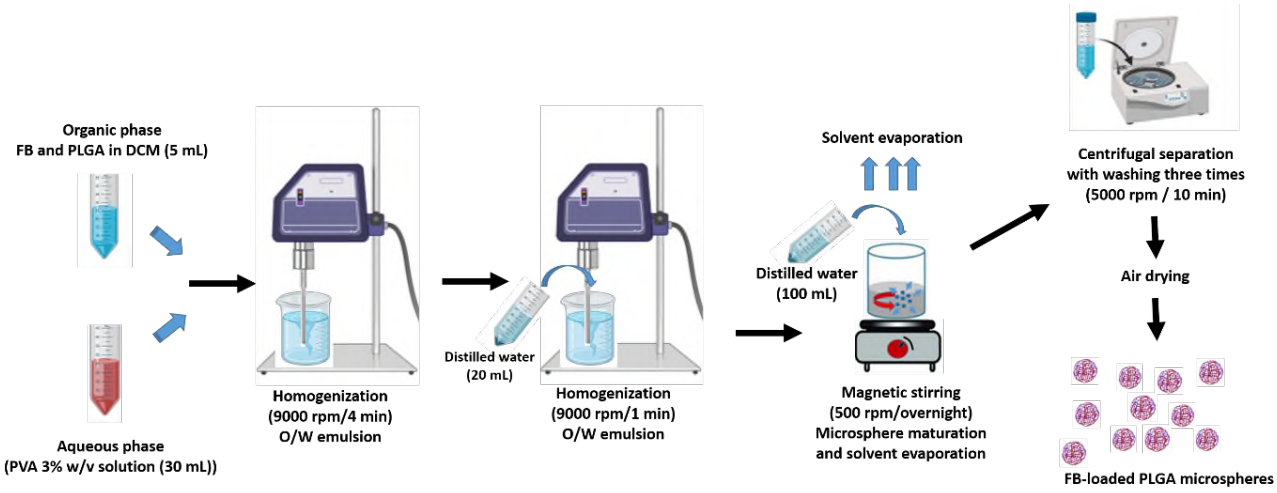

Figure 1. The method for producing FB-loaded PLGA MC.

Crowell, Higuchi, Weibull, Korsmeyer-Peppas, Peppas-Sahlin, and Hopfenberg model) (Zhang et al., 2010). The highest R^2, $R^2_{adjusted}$, MSC, and AIC values were used to evaluate the different kinetic models. Additionally, DDSolver was used to calculate the release differences between AS-free and FB-loaded PLGA MSs using the "difference (f1)" and "similarity (f2)" factors (Puthli & Vavia, 2009).

In situ gel preparation

Using the cold technique, in situ gels were prepared (H Kerem POLAT, 2022). Other PX 407 and PX 188 concentrations with mucoadhesive HECs were used to produce FB-loaded MS-in situ-forming gels. The components of the ready formulations are listed in Table 1. For the formulations, the projected amount of cold water in a vial with a magnetic bar was gradually increased for PX 407 and PX 188. The mixture was continually stirred with a magnetic stirrer (Thermomac-TM19). The Pluronic solutions were partially dissolved and occasionally blended to create clear homogeneous solutions. Additional amounts of the mucoadhesive HEC polymers (0, 0.5, and 1%) (wt/wt) were added to the total poloxamer content during preparation (Table 1). Each sample was stored at 4°C before use. In all formulations, Benzalkonium chloride (BAC), NaCl, and FB-loaded MC (%0.03) were added.

In vitro characterisation of *in situ* gels

pH: The pH was determined using a pH metre (Fungilab viscometer (USA). Three measurements were taken (n=3). For ocular formulations, isotonicity is a crucial factor to consider preventing ocular irritation and tissue damage. The test was conducted using the hemolytic technique (H Kerem POLAT, 2022)

Clarity: Following gelation, the in situ gel formulation's clarity was assessed by holding it up to bright light while contrasting it with a dark background (Polat, 2022).

Gelation Temperature: Each polymer solution (10 ml) was stirred with a magnetic stirrer in a water bath. The heated polymer solutions were swirled at 100 rpm and 1 °C/min (Thermomac-TM19). The temperature at which the magnetic bar stopped moving was recorded as the gelling temperature. Each sample was subjected to three measurements. (Polat, 2022).

Determination of gelation time: A test tube containing 2 ml of sample kept at 4 °C was placed in a water bath heated to the gelation temperature (35 °C). By frequently turning the test tube upside down, the in situ gel was checked for gelation. In cases in which the test tube did not flow when turned upside down, the gelation time was recorded (Asasutjarit, Thanasanchokpibull, Fuongfuchat, & Veeranondha, 2011).

Table 1. Compositions of *in situ* gelling formulations

Code	Formulation's ingredients (%, w/w)						
	FB-loaded MCs	PX 407	PX 188	HEC (80-125 cP)	Benzalkonium chloride (BAC)	NaCl	Water
A1	0.03	12	8	0	0.001	0.2	100
A2	0.03	12	8	1	0.001	0.2	100
A3	0.03	12	8	1.5	0.001	0.2	100
A4	0.03	15	8	0	0.001	0.2	100
A5	0.03	15	8	1	0.001	0.2	100
A6	0.03	15	8	1.5	0.001	0.2	100
A7	0.03	18	8	0	0.001	0.2	100
A8	0.03	18	8	1	0.001	0.2	100
A9	0.03	18	8	1.5	0.001	0.2	100

*Excipient ratios were kept constant throughout the study.

Viscosity: The viscosities of the samples were evaluated using a Fungilab rotating viscometer (USA) with an R5 spindle at 10 rpm. At 25 and 35 °C, the viscosity values of all MS-loaded in situ gels were measured (Table 2) (Polat, 2022).

Rheological behavious: The rheological behaviours of the samples were measured using a Fungilab rotating viscometer (USA) with an R5 spindle at different (1, 2.5, 5, 10, 20, and 50) rpm. Viscosities were evaluated at various angular velocities, and flow curves were computed.

Determination of the Mucoadhesive Force

The *in vitro* bioadhesive force on sheep cornea tissue obtained locally from butchers was measured using a piece of equipment known as a texture analyser (TA.XT Plus, StableMicro Systems, UK). Bioadhesion studies were conducted on all formulations. The in situ gel was applied to one of the texture analyser's arms, and the eye was placed on the others. The probe used to apply the membrane to the basis decreased at a force of 0.2 N and a speed of 0.1 mm/s during the 60-s contact period. The effectiveness of the in situ gel bioadhesive was evaluated by testing resistance to probe removal (Polat et al., 2023). At 35 °C, triplicate measurements of each bioadhesion were performed.

***In vitro* Release of FB from FB-MC–loaded in situ gels**

The in vitro release study was conducted using the dialysis bag method (Polat et al., 2022). The dialysis membrane (Sigma, D9277) was then sealed, 100 µL of MHM was added, and 10 mL of an isotonic phosphate buffer (pH 7.4) was placed at 35 °C. This describes the sink condition is provided. All media were removed at different time points, and 10 mL of the new buffer media was introduced (0, 1, 2, 4, 8, 12, 24, 36, 48, 72, 96, 120, and 144 hours). The amount of FB was measured using a UV-Vis spectrophotometer.

Biocompatibility studies (MTT assay)

A 37°C humidified 5% CO2 incubator was used to culture ARPE-19 cells in DMEM/F-12 medium containing 10% foetal bovine serum, 50 unit/mL penicillin, and 50 mg/mL streptomycin. The MTT assay was used to assess how the inserted formulations affected the viability of ARPE-19 cells. After counting the cells using the Thoma slide counting chamber, a 96-well plate was seeded with 5000 cells per well at a density of 50000 cells/ml. The contents of the wells were removed overnight. FB-loaded mc-containing in situ gels were used to treat cells at dosages of 5, 10, 15, 20, and 25 µg/ml. (Aksungur et al., 2011; -Polat et al. (2023). DMEM was used to manufacture blank in situ gel stock solutions, and complete medium was used to make dilutions. After injecting the medication and in situ gel, the cells were cultured for 2 h. Then, 25 µl of MTT solution (5 mg/ml) was added to each well, and the cells were incubated for 24 h. Following the addition of 200 µl of DMSO to each well, absorbance was measured using an Elisa Plate Reader.

***Ex vivo* Corneal Transport Studies**

Ex vivo corneal transport investigations were performed using locally obtained sheep corneal tissue from butchers. For evaluating the passage and participation of FBs through ocular tissues, the formulations were compared with commercial preparations. Transport studies were conducted with n = 3. Two distinct formulations were examined, one of which could be purchased (Flubord®). The "vertical diffusion Franz cells" -system was used in transport studies.

The donor side of the tissue transport cells was towards the surface of the outer cornea, and its contact area was 0.785 cm^2. The donor side received 2 mL of the in situ gel formulation and commercial product, whereas the acceptor side received 4 mL of PBS (pH 7.4) as the buffer. Without the use of a stirring element, the system was maintained at 34°C in a light-proof container. After 2 h, samples were collected from the recipient cell into vials, and a UV-vis spectrophotometer was used to measure the FB drug loading capacity.

Statistical analysis

Using unpaired one-way ANOVA and Tukey's multiple comparisons test, statistical significance was determined. (labelled as * = P < 0.05, ** = P < 0.01, *** = P < 0.001, **** = P < 0.0001 and ns = not significant.

RESULTS

In vitro characterisation of FB-loaded PLGA MCs

Table 2 shows the average zeta potentials, encapsulation efficiencies, particle sizes, and distributions of FB-loaded and blank PLGA MCs. The average particle size of FB-loaded microspheres was 19.3 µm. The average particle size of blank microspheres was discovered to be 24.1 µm.

Figure 2 shows a SEM image of the shapes of FB-loaded and -unloaded PLGA microspheres. The microspheres were mostly spherical in shape and had tiny sporadic pits all over their surfaces. Surface holes were more noticeable in microspheres loaded with FB. Moreover, greater magnifications allowed for a more detailed observation of the microsphere surfaces, and the particle size distribution in the photographs matched the results of the mastersinger device (Figure 3).

The in vitro release of FB from PLGA MCs was continued over a period of six days in accordance with the extended-release goal of the study, as illustrated in Figure 4. According to previous studies, two- or three-phase release profiles can be observed when drugs are released from biodegradable polymers through both diffusion and erosion of the polymeric matrix. The initial and immediate release of the burst effect continued for eight hours. After 72 hours, a second rapid release phase appeared. Subsequently, a continuous release profile was observed through day 6 of the experiment.

In vitro Gel Characterisation

To find the best compositions for use as in situ gels, systems with various concentrations of PX188 and PX407 and different concentrations of HEC were created and examined for gelling capacity. Table 3 presents the gelling properties of the formulations.

The lowest polymer-containing samples, A1, A2, and A3 (13% PX407, 8% PX188), demonstrated a sol (liquid) state under non-physiological (4°C) and physiological (35°C) conditions with no gelation, indicating that they could not gel.

The pH of the FB-loaded MS-loaded in situ gel compositions was measured using a pH meter that had already been calibrated. The pH of the in situ gel compositions was found to range between 6.78±0.04 and 7.02 ± 0.01 (Table 3).

Rheology and viscosity

Figure 5 shows the viscosity measurements of FB-loaded MSs in situ gelling systems at different shear rates. At the moment of gelation, all the produced formulations exhibited shear-thinning flow characteristics.

This study investigated the changes in viscosity with increasing temperature (Figure 6).

Determination of the Mucoadhesive Force

The mucoadhesive force, which extends the formulation's precorneal residence time by preventing quick drainage, is a crucial physicochemical characteristic for the in situ production of ophthalmic gels. Figure 7 presents the analysis of the mucoadhesive forces of all the created in situ gels.

In Vitro Release of FB from FB-MC-loaded In Situ Gels

Experiments on the in vitro release of medication were performed using in situ gels at 35 °C in an isotonic phosphate buffer (pH 7.4) and MHM (0.03%). The in situ gels loaded with MHM (0.03%) and the MSs loaded with FB underwent 144 h of *in vitro* release profile analysis (Fig 4).

Biocompatibility studies (MTT assay)

Drug delivery vehicles should be biocompatible as novel ocular drug delivery systems. Figure 8 shows the biocompatibility of the in situ gel.

Ex vivo Transport Studies

The *ex vivo* transport study results (Fig. 9) showed that MHM provided an enhanced drug concentration compared with the marketed product, Flubord (P < 0.01).

Table 2. Results of FB-loaded and blank PLGA MCs' *in vitro* characterisation (n=3)

Blank PLGA MCs					**FB-loaded PLGA MCs**					
Particle size (µm)			**Zeta Potential (mV)**	**Polydispersity Index (PDI)**	**Particle size (µm)**			**Zeta Potential (mV)**	**Polydispersity Index (PDI)**	**Entrapment Efficiency (%)**
$D_{10\%}$	*Mean Particle Size* $D_{50\%}$	$D_{90\%}$			$D_{10\%}$	*Mean Particle Size* $D_{50\%}$	$D_{90\%}$			
2.2± 0.4	**19.3 ± 2.1**	37.4 ± 2.7	-33.6± 2.1	0.316 ± 0.011	3.8 ± 1.3	**24.1± 4.6**	42.7 ± 3.9	-42.6 ± 1.9	0.388 ± 0.024	67.4 ± 2.3

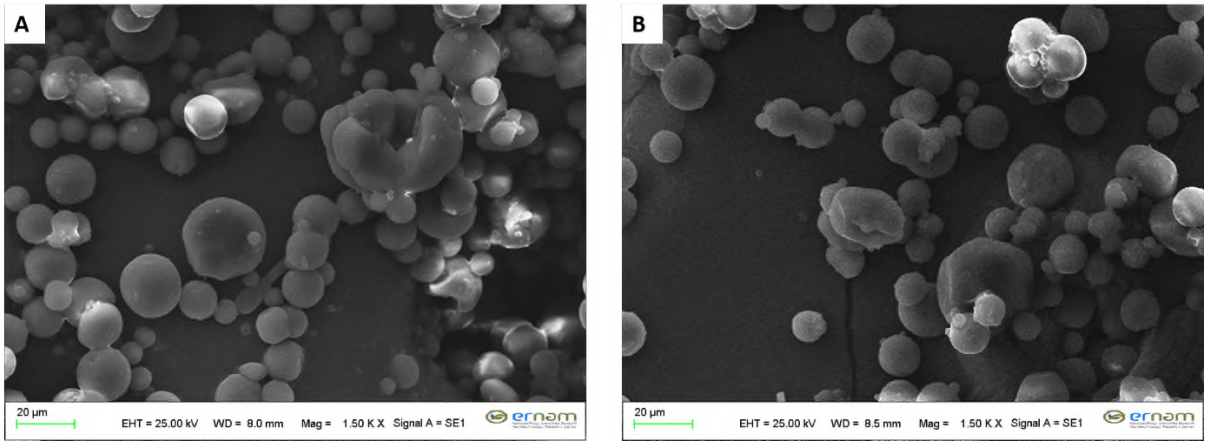

Figure 2. SEM photo of blank PLGA MCs (A) and (B) FB-loaded PLGA MCs.

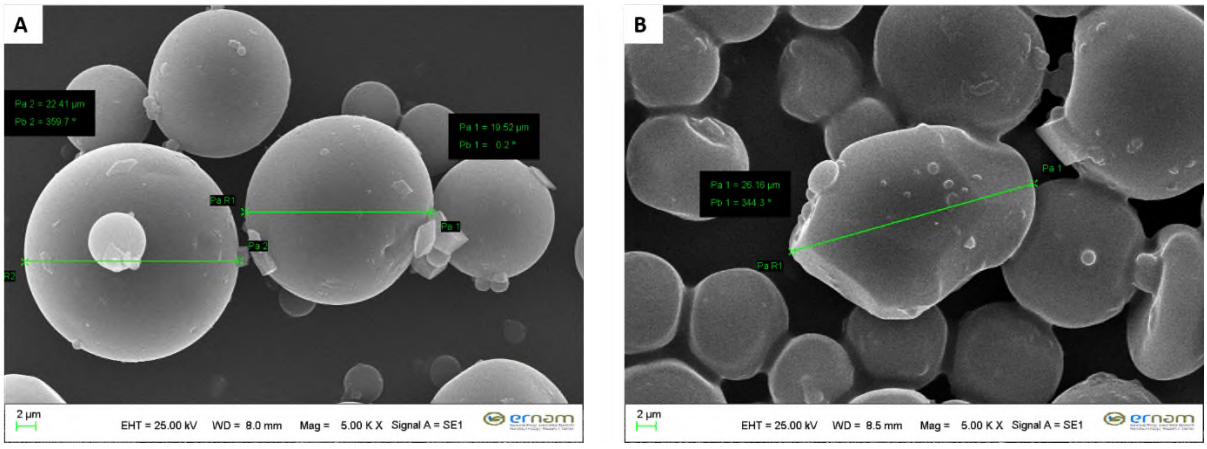

Figure 3. SEM image that was magnified considerably to allow for a closer look at the microsphere surface. Blank PLGA MCs(A) and (B) FB-loaded PLGA MCs

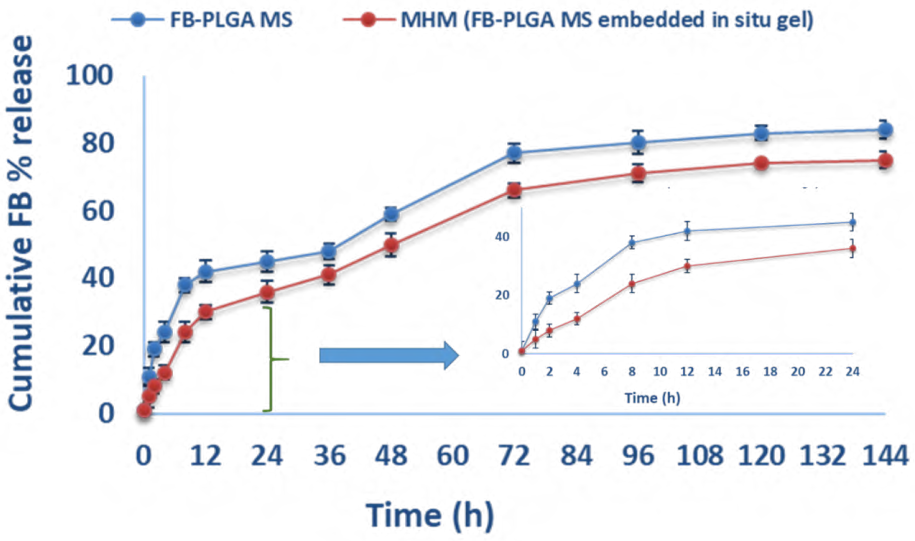

Figure 4. Cumulative FB release from microspheres and in situ gel formulation with FB-loaded microspheres (n=3)

Table 3. Results of *in vitro* characterisation of *in situ* gels.

Formulation	pH (±SD)	Gelation temperature (°C±SD)	Gelation time (s)	Viscosity (cP) = 25 °C	Viscosity (cP) = 35 °C	Clarity
A1	7.02±0.01	41±0.5	51±0.5	272±25	842±98	+
A2	7.00±0.02	40±0.3	44±0.9	333±44	978±123	+
A3	6.97±0.03	39±0.4	38±0.3	359±41	1045±152	+
A4	6.96±0.02	38±0.6	43±0.5	352±39	7872±141	+
A5	6.93±0.01	36±0.7	38±0.7	384±56	10088±212	+
A6	6.9±0.02	35±0.1	33±0.2	422±38	11042±247	+
A7	6.89±0.06	30±0.4	35±0.1	425±55	16642±432	+
A8	6.82±0.03	29±0.4	32±0.3	497±68	19482±479	+
A9	6.78±0.04	26±0.2	27±0.2	944±87	22813±574	+

DISCUSSION

In vitro characterisation of FB-loaded PLGA MCs

The encapsulation of FB in microspheres may cause an increase in particle sizes of the drug-containing microspheres. There are trials employing microspheres made for treating eye infections ranging in size from 8.5 µm to 25 µm. (Ding et al., 2018). Hence, the particle size of the obtained FB-loaded PLGA microspheres was suitable for an ocular controlled release system.

The drug release from the created microspheres experienced a burst impact, as observed by approximately 40% release at the conclusion of the eighth hour. From the eighth to the third hour of this time, a slower release was noticed, which was attributed to ongoing diffusion-based release from the polymeric microspheres. A second rapid release profile with a 36-to 72-hour duration was found. This was understood to mean that the accelerated breakdown of the polymeric matrix boosted drug release. The expansion of microsphere pores and activation of new diffusion routes are also relevant in this context (Siep-

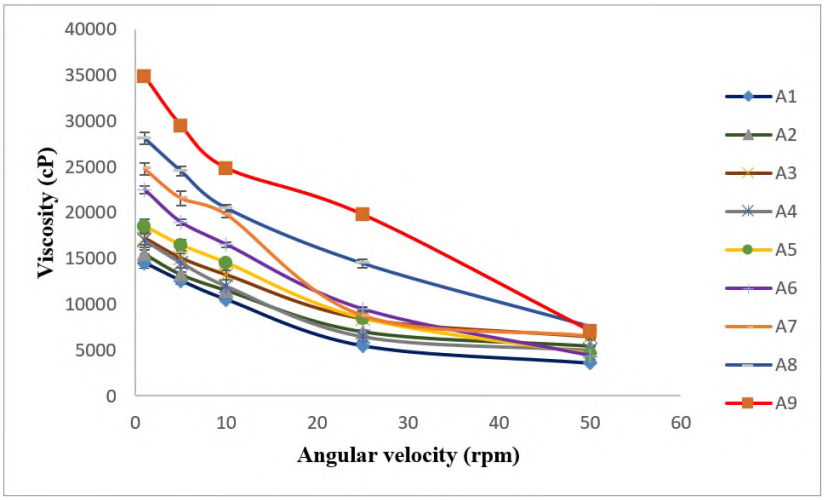

Figure 5. Rheological characteristics of in situ gelling systems' - (n=3)

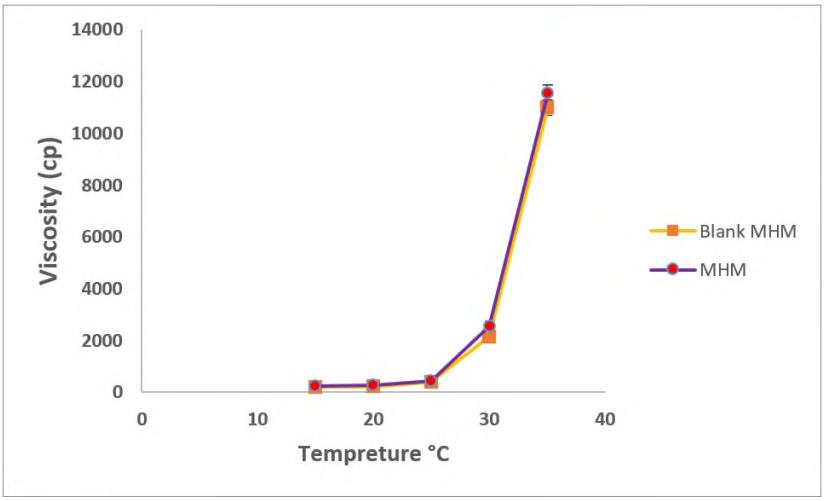

Figure 6. Viscosity profiles of MHM (n=3) at different temperatures (n=3).

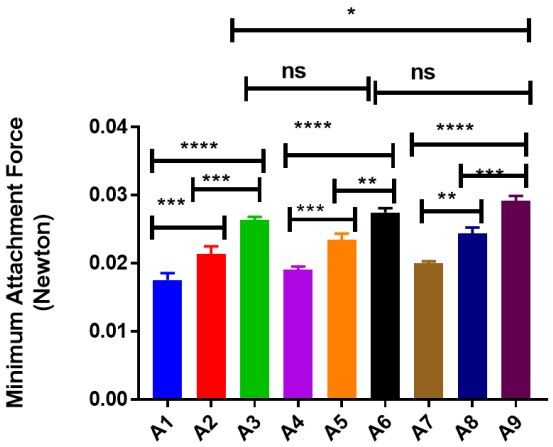

Figure 7. Mucoadhesion study results for ın situ gels (n=3).

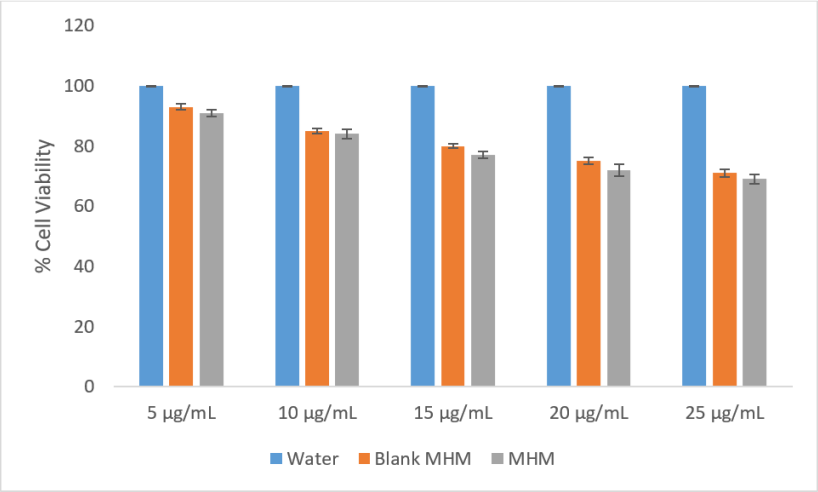

Figure 8. The biocompatibility of water, blank MHM, and MHM was investigated using an MTT assay with ARPE-19 cells (n=3)

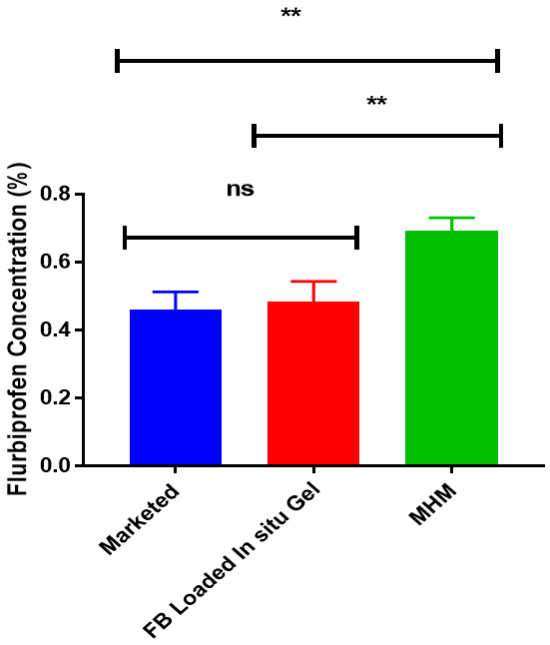

Figure 9. Cumulative corneal transport of commercially available product and formulations prepared in this study (n=3).

mann, Faisant, & Benoit, 2002). From the 72nd to the 144th hour, a more regulated release profile was observed as the drug concentration in the microspheres decreased with time, and the bursting effect of the degradation process subsided. The profile began to plateau at the 96th hour. After examining the release profile, it was discovered that at the end of the fifth day, approximately 80% of the encapsulated drug had been released from the polymeric matrix. A regulated release was observed because of the drug's diffusion, breakdown, and polymer degradation over the course of six days (Yasukawa, Kimura, Tabata, & Ogura, 2001).

In vitro Gel Characterisation

These findings show poloxamer gel's thermosensitivity is strongly influenced by the concentration; a higher PX 407 concentration accelerated gelation at a lower gelation temperature. To decrease the polymer concentration of the in situ gel while enhancing the gelling properties and rheological behaviour, the interaction of in situ gelling polymers with HEC as a viscosity-modifying agent was explored. A9 (PX 407 and HEC) exhibited optimal gelation at concentrations of 17% and 1.5%, respectively. It is hypothesised that HEC molecule entanglement and

substantial hydrogen bonding result in firmly aligned gel formations within Pluronic micelle routes.

Precise formulations must be used for ocular applications. Despite the efficacy of drug delivery methods, such as ointments, patient compliance is low because they cause blurred vision. Regardless of the effectiveness of the medication, outcomes cannot be reached if the patient does not follow instructions. For this reason, the compositions intended for ocular use must be transparent (Patel, Cholkar, Agrahari, & Mitra, 2013).

According to a literature review, a pH range of 4–8 is appropriate for eyes (Patel et al., 2013). Ophthalmic thermo reversible gels' sol-gel transition temperatures of ophthalmic thermo-reversible gels are between 25 and 34°C, making them appropriate for ocular delivery. When t thermosensitive formulation's gelation temperature is less than 25°C, a gel may form at room temperature. When > 34°C, a liquid dosage form persists at the ocular surface temperature, causing the formulation to drain from the eyes. When the two poloxamer grades are combined, it is possible to control the gelation temperature to remain within the permissible range (25-34°C) (Abd Elhady, Mortada 6Awad, & Zaki,- 2003).

Two polymer grades were researched and employed to form in situ forming gels to select formulations with an adequate sol-gel transition temperature and the lowest total poloxamer concentration. The formulations of P407/P188 (15/8 %, wt/wt) for the in situ-forming gel of FB-loaded MSs produced satisfactory results. The in situ gel formation temperatures for all FB-loaded MS formulations were between 26°C and 41°C, particularly for A5 and A6, which are suitable for ocular administration. The data in Table 3 show this.

To generate poloxamer, an amphiphilic synthetic copolymer, two hydrophilic blocks of polyethylene oxide (PEO) are sandwiched between two hydrophobic blocks of polypropylene oxide (PPO). Amphiphilic block copolymer molecules form small micellar subunits when mixed together in aqueous liquids. Polymer molecules join to form a vast micellar cross-linked network when concentrations above a particular level, known as the critical micelle concentration, are reached (Heybet Kerem Polat et al., 2023). The temperature also significantly affects micelle formation. The PEO and PPO blocks are hydrated when the temperature falls below the critical micelle temperature. In aqueous solutions, PPO is also largely soluble. The PPO chains interact hydrophobically as the temperature rises, becoming dehydrated and less soluble than the PEO chains. It is difficult for these micelles to disperse in the solution independently, so they interact and tangle with other micelles. Because of this entanglement, a three-dimensional network structure was created (Wanka, Hoffmann, & Ulbricht, 1994), and elation required higher temperature at lower P-407-127 concentrations.

The gelation temperature of the in situ-forming gels was lowered by adding mucoadhesive polymers like HEC, as shown in Table 3. The transition temperature gradually decreased when the polymer concentration was increased from 0 to 1 and 1.5%. Such mucoadhesive polymers' ability to bind to polyoxyethylene chains found in poloxamer molecules may explain their ability to reduce gelation temperatures. Including mucoadhesive polymers, which allow attachment of the formulations to the corneal mucin, would significantly minimise the drainage of ophthalmic formulations from the pre-corneal surface. As a result, dehydration is encouraged, enhancing intermolecular hydrogen bonding and the entanglement of nearby molecules, resulting in gelation at lower temperatures (Gilbert, Richardson, Davies, & Hadgraft, 1987).

The system is expected to gel instantly or quickly upon exposure to its gelation temperature, preventing rapid evacuation by tear fluid (Venkatesh, Kamlesh, & Kumar, 2013). The gelation times of A1 and A9 were approximately 51 and 27 s, respectively (Table 3). Additionally, A9, which exhibited higher concentrations of PX 407 and HEC, required less gelation time. This finding shows that shorter gelation times are associated with reduced effective sol-gel transition temperatures caused by increased pluronic and HEC concentrations (Ricci, Lunardi, Nanclares, & Marchetti, 2005).

Determination of the Mucoadhesive Force

The formulations comprising mucoadhesive polymers, such as HEC, considerably improved the mucoadhesive force of the ciprofloxacin HCl in situ-producing gels. The mucoadhesive force dramatically increased with increasing polymer concentrations ($p < 0.0001$).

Mansour et al. (Mansour, Mansour, Mortada, & Abd ElHady, 2008) developed ciprofloxacin-loaded poloxamer in situ gels. Different concentrations of HPMC and HEC were used to increase the in situ mucoadhesion of the gels. Because of their mucoadhesion study, they determined that the use of increasing concentrations of HPMC and HEC significantly increased mucoadhesion. In another study, fluconazole-loaded in situ gels were prepared and HEC was used to increase the viscosity of the gels. In a mucoadhesion study, it was determined that the mucoadhesive properties of HEC increased with increasing doses (Gonjari et al., 2009).

Rheology and viscosity

According to a literature review, the recommended viscosity for effective ocular delivery is 50–50,000 cp. As the formulation spends more time in the dead end region of the eye, its bioavailability will increase in proportion to the increase in viscosity. To determine the viscosity values of all formulations, 10 rpm measurements at 25°C and 35°C. The data analysis showed that the viscosity changed depending on the polymer content (Table 3). The significance of the effect of polymer concentration on viscosity is illustrated by the above example. The above example shows the significance of the effect of polymer

concentration viscosity. The results were consistent, according to a literature review (Fathalla et al., 2017).

When using excessively viscous in situ gels, several problems could arise; however, when using in situ gels that are low in viscosity, tears can be cleared from the surface of the eye quickly. High-viscosity ocular formulations should be avoided because they frequently leave a noticeable residue on the side of the eyelid where they are administered. Adopting in situ gel formulations with pseudo-plastic behaviour makes it feasible to decrease the adverse effects of ocular reflexes, such as blinking, in the formulation. The pseudo-plastic flow of the formulation allows for a more pleasant application and longer corneal contact time. The viscosity increased as the PX 407 content increased from 12% to 18% (wt/wt). This may be explained by the fact that the poloxamer is a nonionic triblock copolymer composed of polyoxyethylene, polyoxypropylene, and polyoxyethylene that aggregates into micelles at 34°C because of the dehydration of the polymer blocks with temperature. Micellar packing and enlargement lead to gel development, and the gel becomes more twisted at greater poloxamer concentrations. These micelle entanglements prevent the micelles from simply separating from one another, which explains the hard and viscous gel with high poloxamer concentrations is hard and viscous (Cabana, Aıt-Kadi, & Juhász, 1997). We can infer that higher concentrations of the mucoadhesive improve the viscosity of the formulations by examining the impact of various mucoadhesive concentrations, such as HEC, on the viscosity of the poloxamer in situ-forming gels. The theory that block copolymer PX407 thermosensitive gels are produced via hydrogen bonding in aqueous systems, which is brought about by the attraction between the oxygen atom of the poloxamer aether and the protons of water, may explain this. The addition of substances containing hydroxyl groups, such as the studied cellulose derivatives, is anticipated to increase the number of hydrogen bonds, thereby increasing the measured viscosity of the resulting formulations.

When the in vitro characterisation results were examined, it was decided that the A6 formulation could be applied ocularly due to its gelling temperature, viscosity, and mucoadhesive properties. After this stage, the A6 formulation code was changed to MHM, and the study continued with this formulation.

Rheological experiments were conducted at various temperatures to determine the thermoreversible characteristics of the formulations under accelerated thermal fluctuations. The formulations were subjected to a heat cycle between 10°C and 40°C before rheological testing. The results showed that rising temperature caused the formulation viscosity to increase. At 25°C, the viscosity of MHM was found to be 436±35 cP, whereas it increased to 11542±321 cP at 35°C.

In vitro Release

The overall release percentage of FB-loaded MSs was 74 ±0.8%. Fig. 8 indicates that from 0 h to 8 h, the cumulative release percentage of FB-loaded MSs was 39±0.74%, whereas that of MS-loaded in situ gel was 23± 0.48. It can be seen that there is a difference in burst effect between in situ gels and microspheres. Compared with MHM, FB-loaded MSs had a significantly higher burst release percentage.

It is thought that this difference in the burst effect is caused by the in situ gel. The following two actions may have been included in the in situ gel release profiles: First, the nanoparticles were simultaneously freed from the skeletal carrier as the in situ gel slowly decomposed. The second stage was the gradual release of the medication from the PLGA nanoparticles. It was now clear why there were differences between the release characteristics of the two formulations. The gel initially prevented MSs loaded with FB from contacting the release medium. An increase in the number of microparticles discharged as the gel gradually degraded. All nanoparticles were released at a rate comparable to that of FB-loaded MSs 24 h after the gel had dissolved, indicating their release behaviour was dependent on a diffusion process. After examining the literature, it is possible to show that the results are consistent (Morsi, Ghorab, Refai, & Teba, 2016).

Hu et al. determined that when they developed a rifampicin-loaded PLGA microsphere and loaded it onto an in situ gel containing sodium alginate, the burst effects were lower due to the dual structure of the in situ gels (Hu, Feng, & Zhu, 2012). Beg et al. loaded moxifloxacin-loaded nanoparticles, which they produced in another study, onto in situ poloxamer gels. Because of the release study, we determined that the burst effect of nanoparticle-loaded in situ gels was lower than that of drug-loaded nanoparticles. In another study, PLGA nanoparticles loaded with fluorometholone were prepared for use in ocular inflammation and loaded in situ gels. The release study determined that the burst release of in situ gels was significantly lower than that of nanoparticles (Gonzalez-Pizarro et al., 2019).

Release kinetics

The results obtained from *in vitro* release studies were fitted into various mathematical models, including first-order and zero-order Higuchi, Korsmeyer, Hollenberg, Baker-Lonsdale, Peppas-Sahlin, and Weibull models, to investigate the FB release kinetics. DDSolver software was used for the best-fitted mathematical model with the highest R^2, $R^2_{adjusted}$, MSC, and AIC values. The release kinetic parameters are listed in Table 4.

Table 4. Release kinetic modelling and results of FB-loaded PLGA- and FB-loaded in situ gels

Model and equation / Formulation		Evaluation criteria						
		Parameter		R^2	$R^2_{adjusted}$	AIC	MSC	n/m*
Zero-order	FB-PLGA MS	k0	0.776	0.3932	0.3932	114.7558	0.3457	-
F=k0*t	MHM in situ gel	k0	0.679	0.6842	0.6842	105.3656	0.9987	-
First-order	FB-PLGA MS	k1	0.022	0.8160	0.8160	99.2406	1.5392	-
F=100*[1-Exp(-k1*t)]	MHM in situ gel	k1	0.014	0.9179	0.9179	87.8525	2.3459	-
Higuchi	FB-PLGA MS	kH	8.131	0.9106	0.9106	89.8625	2.2606	-
F=kH*t^0.5	MHM in situ gel	kH	6.962	0.9771	0.9771	71.2804	3.6206	-
Korsmeyer-Peppas	FB-PLGA MS	kKP	15.742	0.9774	0.9753	73.9900	3.4815	0.347
F=kKP*t^n	MHM in situ gel	kKP	8.650	0.9820	0.9803	70.1525	3.7074	0.450
Hopfenberg	FB-PLGA MS	kHB	0.000	0.8160	0.7993	101.2424	1.3852	-
F=100*[1-(1-kHB*t)^n]	MHM in situ gel	kHB	0.000	0.9178	0.9104	89.8605	2.1914	-
Baker-Lonsdale	FB-PLGA MS	kBL	0.002	0.9674	0.9674	76.7531	3.2690	-
3/2*[1-(1-F/100)^(2/3)]-F/100=kBL*t	MHM in situ gel	kBL	0.001	0.9857	0.9857	65.1459	4.0925	-
Peppas-Sahlin	FB-PLGA MS	k1	14.752	0.9787	0.9744	75.2343	3.3858	0.413
F=k1*t^m+k2*t^(2*m)	MHM in situ gel	k1	6.036	0.9901	0.9882	64.3082	4.1570	0.621
Weibull	FB-PLGA MS	β	0.530	0.9744	0.9693	77.5887	3.2047	-
F=100*{1-Exp[-((t-Ti)^β)/α]}	MHM in situ gel	β	0.631	0.9895	0.9874	65.1102	4.0953	-

The data obtained from *the in vitro* drug release of FB-PLGA were fitted to the Korsmeyer model with the highest R2, R2adjusted, MSC, and AIC values. Korsmeyer-Peppas model, also known as "Power low," portrays the release mechanisms, including the diffusion of water into the matrix and swelling or dissolution of the matrix, using the "n" value in the Korsmeyer-Peppas. The "release exponent n" value elucidates the drug-release mechanism. If the "n" value is less than 0.45, drug release corresponds to Fickian diffusion. When these data were examined using the Korsmeyer-Peppas model, FB release from PLGA NPs was compatible with Fickian diffusion. On the other hand, the Peppas-Sahlin model exhibited superior describing the release mechanisms of FB from MHM in situ gels. "m" diffusional exponent is equal to the "n" value in the Korsmeyer model. If "m" is less than 0.45, then Fickian diffusion. If "m" is between 0.45 and 0.85, drug release depends on non-Fickian diffusion. If m = 0.85, drug release occurs through case II transport (Supramaniam, Adnan, Mohd Kaus, & Bushra, 2018). The "m" value was examined; it was 0.621 for the MHM-in situ gel. It was observed that there was non-Fickian diffusion considering the diffusional exponent parameter of the Peppas-Sahlin model.

Biocompatibility studies (MTT assay)

The cytotoxicity of ARPE-19 cells, as measured using in situ gel microscopy, was found to be acceptable. Consequently, the created in situ gel system is biocompatible. Applications were made to the in situ gel cell line at different concentrations. It was determined that cell viability decreases with increasing concentrations. Although there was no significant change in the positive control group at the lowest dose, a statistically significant change was observed at the highest dose ($P < 0.01$). Another eye study demonstrated that the cytotoxicity of flurbiprofen changed in a dose-dependent manner (Vasconcelos et al., 2015).

One of the numerous polymeric drug delivery vehicles is PLGA, which is crucial in applications that integrate targeting, imaging, diagnostics, and therapy. Furthermore, this polymer readily hydrolyses to monomers like lactic acid or glycolic acid, which are then excreted from the body via normal metabolic pathways. There was no discernible difference between the formulations of the blank in situ gel (loaded just with PLGA microspheres) and FB microsphere-filled in situ gel after evaluation. When the literature is examined, it is seen that there are similar results (Öztürk, Yenilmez, Şenel, Kıyan, & Güven, 2020).

Ex vivo Transport Studies

In situ gel formulations were used in transport investigations of sheep corneal tissue for a 2-hour period together with a commercially available medication (suspension), and the tissue was not harmed (Aytekin et al., 2020). Similar findings were often reported in the literature review. Veiga et al. In a study they conducted, they produced Nepafenac-loaded microparticles. In their ex vivo study, they determined that the microparticles loaded with Nepafenac passed more than the market preparation (Lorenzo-Veiga, Diaz-Rodriguez, Alvarez-Lorenzo, Loftsson, & Sigurdsson, 2020).

CONCLUSION

In this study, flurbiprofen-loaded PLGA microspheres were formed and evaluated. Additionally, the study investigated adding microspheres into a thermosensitive in situ gel preparation for ophthalmic delivery. A significantly modified single-emulsification/solvent evaporation process (O/W), proper particle size, zeta potential, and sustained release were used to prepare FB-loaded PLGA microspheres. The elucidation of the in vitro release kinetics of FB-PLGA MSs as mathematical modelling has also been demonstrated by our study. Our study has also demonstrated the elucidation of the *in vitro* release kinetics of FB-PLGA MSs as mathematical modelling. Furthermore, a release kinetic analysis was performed for the gel system containing MS. After the comprehensive characterisation study, we determined that FB-PLGA MS and gel systems fit different mathematical models. A6 (MHM) was therefore selected to be incorporated into a thermosensitive in situ gel prepared with 15% PX-407 + 8% PX-407 + 1.5% HEC, which displayed the optimum gelling capacity, a mucoadhesive structure, and sustained release and good rheological behaviour. - MTT analysis of the ARPE-19 cell line showed that the in situ gel formulation was biocompatible. In addition, the ex vivo corneal transition study showed that MHM had higher corneal penetration than that of the marketed product. The optimized his formulation could be considered a viable ocular drug delivery method for treating postoperative inflammation due to its decreased administration interval.

Peer-review: Externally peer-reviewed.

Author Contributions: Conception/Design of Study- H.K.P., S.Ü.; Data Acquisition- H.K.P., S.Ü.; Data Analysis/Interpretation- H.K.P., S.Ü.; Drafting Manuscript- H.K.P., S.Ü.; Critical Revision of Manuscript- H.K.P., S.Ü.; Final Approval and Accountability- H.K.P., S.Ü.

Conflict of Interest: The authors have no conflict of interest to declare.

Financial Disclosure: The authors declared no financial support.

ORCID IDs of the authors

Heybet Kerem Polat 0000-0001-5006-3091
Sedat Ünal 0000-0002-1518-010X

REFERENCES

Abd Elhady, S. S., Mortada, N. D., Awad, G. A., and Zaki, N. M. (2003). Development of an in situ gelling and much adhesive mebeverine hydrochloride solution for rectal administration. *Saudi Pharmaceutical Journal, 11*.

Aksungur, P., Demirbilek, M., Denkbaş, E. B., Vandervoort, J., Ludwig, A., Ünlü, N. (2011). Development and characterisation of Cyclosporine A loaded nanoparticles for ocular drug delivery: Cellular toxicity, uptake, and kinetic studies. *Journal of controlled release, 151*(3), 286-294.

Akyüz, L., Duman, F. and Murat, K. (2017). Encapsulation of flurbiprofen by chitosan using a spray drying method with in vitro drug release and molecular docking. *Turkish Journal of Pharmaceutical Sciences, 14*(1), 34.

nderson, J. M., & Shive, M. S. (1997). Biodegradation and biocompatibility of PLA and PLGA microspheres. *Advanced drug delivery reviews, 28*(1), 5-24.

Asasutjarit, R., Thanasanchokpibull, S., Fuongfuchat, A., and Veeranondha, S. (2011). Optimisation and evaluation of thermoresponsive diclofenac sodium ophthalmic in situ gels. *International Journal of Pharmaceutics, 411*(1-2), 128-135.

Aytekin, E., Öztürk, N., Vural, İ., Polat, H. K., Çakmak, H. B., Çalış, S., and Pehlivan, S. B. (2020). Design of ocular drug delivery platforms and in vitro-in vivo evaluation of riboflavin in the cornea using a non-interventional (epi-on) technique for keratoconus treatment. *J Control Release, 324*, 238-249. doi:10.1016/j.jconrel.2020.05.017

Cabana, A., Aıt-Kadi, A., & Juhász, J. (1997). Study of the gelation process of polyethylene oxidea–polypropylene oxideb–polyethylene oxideacopolymer (poloxamer 407) aqueous solutions. *Journal of colloid and interface science, 190*(2), 307-312.

D'Souza, S. S., and DeLuca, P. P. (2006). Methods to assess in vitro drug release from injectable polymeric particulate systems. *Pharmaceutical Research, 23*, 460-474.

Ding, D., Kundukad, B., Somasundar, A., Vijayan, S., Khan, S. A., & Doyle, P. S. (2018). Design of mucoadhesive PLGA microparticles for ocular drug delivery. *ACS Appl Biomater, 1*(3), 561-571.

Dumortier, G., Grossiord, J. L., Agnely, F., & Chaumeil, J. C. (2006). A review of poloxamer 407 pharmaceutical and pharmacological characteristics. *Pharmaceutical Research, 23*, 2709-2728.

Fathallae, Z. M., Mangala, A., Longan, M., Khaled, K. A., Hussein, A. K., El-Garhy, O. H., & Alan, R. G. (2017). Poloxamer-based thermoresponsive ketorolac tromethamine in situ gel preparations: Design, characterisation, toxicity and transcorneal permeation studies. *European Journal of Pharmaceutics and Biopharmaceutics, 114*, 119-134.

Gilbert, J. C., J. L. Richardson, M. C. Davies, K. J., & Hadgraft, J. (1987). Effects of solutes and polymers on the gelation properties of pluronic F-127 solutions for controlled drug delivery. *Journal of controlled release, 5*(2), 113-118.

Gonjari, I. D., A. H. Hosmani, A. B. Karmarkar, A. S. Godage, S. B. Kadam, and P. N. (2009). Formulation and evaluation of an in situ thermoreversible mucoadhesive gel of fluconazole. *Drug*

Discovery and Therapeutics, 3(1).

Gonzalez-Pizarro, R., Carvajal-Vidal, P., Halbault Bellows, L., alpena, A. C., spina, M., & García, M. L. (2019). In-situ forming gels containing fluorometholone-loaded polymeric nanoparticles for ocular inflammatory conditions. *Colloids Surf B Biointerfaces, 175*, 365-374. doi:10.1016/j.colsurfb.2018.11.065

Hu, C., Feng, H., & Zhu, C. (2012). Preparation and characterisation of rifampicin-PLGA microspheres/sodium alginate in situ gel combination delivery system. *Colloids Surf B Biointerfaces, 95*, 162-169. doi:10.1016/j.colsurfb.2012.02.030

Ishibashi, T., Yokoi, N., Bron, A. J., Tiffany, J. M., Komuro, A., and Kinoshita, S. (2003). Reversible retention of thermo-gelling timolol on the human ocular surface studied by video meniscometry. *Current eye research, 27*(2), 117-122.

Khan, S., Parade, S., & Qinghai, D. J. (2018). Improvement in ocular bioavailability and prolonged delivery of tobramycin sulphate following topical ophthalmic administration of drug-loaded mucoadhesive microparticles incorporated in a thermosensitive in situ gel. *Journal of ocular pharmacology and therapeutics, 34*(3), 287-297.

Lorenzo-Veiga, B., Diaz-Rodriguez, P., Alvarez-Lorenzo, C., Loftsson, T., and Sigurdsson, H. H. (2020). In Vitro and Ex Vivo Evaluation of Nepafenac-Based Cyclodextrin Microparticles for Treatment of Eye Inflammation. *Nanomaterials (Basel), 10*(4). doi:10.3390/nano10040709

Mansour, M., Mansour, S., Mortada, N. D., & Abd ElHady, S. S. (2008). Ocular poloxamer-based ciprofloxacin hydrochloride in situ forming gels. *Drug development and industrial pharmacy, 34*(7), 744-752.

Momoh, M., Adedokun, M., Lawal S, Ubochi G. (2014). Formulation and in vitro evaluation of ibuprofen-loaded poly (D, L-lactide-co-glycolide) microparticles. *Tropical Journal of Pharmaceutical Research, 13*(10), 1571-1576.

Morsi, N., Ghorab, D., Refai H, Teba H. (2016). Ketoroloactromethamine-loaded nanodispersion incorporated into thermosensitive in situ gel for prolonged ocular delivery. *International Journal of Pharmaceutics, 506*(1-2), 57-67.

Öztürk, A. A., Yenilmez, E., Şenel, B., Kıyan, H. T., and Güven, U. M. (2020). Effect of different molecular weight PLGA on flurbiprofen nanoparticles: formulation, characterisation, cytotoxicity, and in vivo anti-inflammatory effects using the HET-CAM assay. *Drug Dev Ind Pharm, 46*(4), 682-695. doi:10.1080/03639045.2020.1755304

Patel, A., Cholkar, K., Agrahari, V. and Mitra, A. K. (2013). Ocular drug delivery systems: An overview. *World journal of pharmacology, 2*(2), 47–49, 2018.

Polat, H. K., (2022). Design of a Metformin–HCl and Moxifloxacin–HCl-loaded Thermosensitive In Situ Gel. *Journal of Research in Pharmacy, 26*(5).

Polat, H. K., Arslan, A., Ünal, S., Haydar, M. K., Aytekin, E., Gözcü S., Mokhtare, B. (2023). Development of a Dual Drug-Loaded Thermosensitive Ocular In Situ Gel Using Factorial Design. *Journal of Pharmaceutical Innovation*, 1-21.

Polat, H. K., Kurt, N., Aytekin, E., Akdağ Çaylı, Y., Bozdağ Pehlivan, S., & Çalış, S. (2022). Design of Besifloxacin HCl-loaded nanostructured lipid carriers: in vitro and ex vivo evaluation. *Journal of ocular pharmacology and therapeutics, 38*(6), 412-423.

Polat, H. K., Ünal, S., Aytekin, E., Karakuyu, N. F., Pezik, E., Haydar, M. K., Mokhtare, B. (2023). Development of a Lornoxicam-loaded heat-triggered ocular in situ gel using factorial design. *Drug Dev Ind Pharm*, 1-15. doi:10.1080/03639045.2023.2264932

Puthli, S., and Vavia, P. R. (2009). Stability studies of a microparticulate system using piroxicam as model drug. *Aaps Pharmscitech, 10*, 872-880.

Ricci, E., Lunardi, L. O., Nanclares, D., and Marchetti, J. M. (2005). Sustained release of lidocaine from Poloxamer 407 gels. *International journal of pharmaceutics, 288*(2), 235-244.

Samatı, Y., Yüksel, N., & Tarimcı, N. (2006). Preparation and characterisation of poly (D, L-lactic-co-glycolic acid) microspheres containing flurbiprofen sodium. *Drug Delivery, 13*(2), 105-111.

Samdancioglu, S., Calis, S., Sumnu, M. and Atilla Hincal, A. (2006). Formulation and in vitro evaluation of bisphosphonate-loaded microspheres for implantation in osteolysis. *Drug development and industrial pharmacy, 32*(4), 473-481.

Siepmann, J., Faisant, N., & Benoit, J.-P. (2002). A new mathematical model for quantifying drug release from bioerodible microparticles using Monte Carlo simulations. *Pharmaceutical Research, 19*, 1885-1893.

Signatella, R., Bulolo, C., pedaliers, G., Maltese, A., & Puglisi, G. (2002). Flurbiprofen-loaded acrylate polymer nanosuspensions for ophthalmic application. *Biomaterials, 23*(15), 3247-3255.

Supramaniam, J., Adnan, R., Mohd Kaus, N. H., & Bushra, R. (2018). Magnetic nanocellulose alginate hydrogel beads as a potential drug delivery system. *Int J Biol Macromol, 118*(Pt A), 640-648. doi:10.1016/j.ijbiomac.2018.06.043

Vasconcelos, A., Vega, E., Pérez, Y., Gómara, M. J., García, M. L., & Haro, I. (2015). Conjugation of cell-penetrating peptides with poly(lactic-co-glycolic acid)-polyethylene glycol nanoparticles improves ocular drug delivery. *Int J Nanomedicine, 10*, 609-631. doi:10.2147/ijn. S71198

Venkatesh, D., Kamlesh, L. and Kumar, P. (2013). Development and evaluation of chitosan-based thermosensitive in situ gels of pilocarpine. *Int J Pharm Pharmaceut Sci, 5*, 164-169.

Wanka, G., Hoffmann, H. and Ulbricht, W. (1994). Phase diagrams and aggregation behaviours of poly (oxyethylene)-poly (oxypropylene)-poly (oxyethylene) triblock copolymers in aqueous solutions. *Macromolecules, 27*(15), 4145-4159.

Yasukawa, T., Kimura, H., Tabata, Y., & Ogura, Y. (2001). Biodegradable scleral plugs for vitreoretinal drug delivery. *Advanced drug delivery reviews, 52*(1), 25-36.

How cite this article

Polat, H.K., & Ünal, S (2024). Flurbiprofen-encapsulated microsphere laden into heat-triggered situ gel for ocular delivery. *İstanbul Journal of Pharmacy, 54*(2), 108–121. DOI: 10.26650/IstanbulJPharm.2024.1269717

İstanbul Journal of Pharmacy
Istanbul J Pharm2024, 54 (2): 122–127
DOI: 10.26650/IstanbulJPharm.2024.1444072

Original Article

Synthesis and evaluation of the antibacterial and antifungal activity of new ibuprofen hydrazone derivatives

Çağla Begüm Apaydın[1], Emel Mataracı Kara[2]

[1]İstanbul University, Faculty of Pharmacy, Department of Pharmaceutical Chemistry, İstanbul, Türkiye
[2]İstanbul University, Faculty of Pharmacy, Department of Pharmaceutical Microbiology, İstanbul, Türkiye

ABSTRACT

Background and Aims: The pursuit of new antimicrobial agents to address antimicrobial resistance remains a fundamental effort in supporting sustainable global health endeavours. Hydrazone compounds possess numerous advantages as biologically active agents because of their diverse properties. In our work, a series of hydrazone derivatives (**4a-f**) containing the ibuprofen moiety were synthesised and evaluated as antibacterial and antifungal agents.

Methods: Novel hydrazone derivatives were synthesised through the condensation of 2-[4-(2-methylpropyl)phenyl]propanehydrazide with suitable cyclohexanone derivatives. The structure of the new compounds was confirmed using spectral methods such as IR, ^{1}H-NMR, ^{13}C-NMR (APT) and electrospray ionisation mass spectrometry (ESI-MS). Testing involved six compounds and their standards against a range of bacterial and fungal strains, including Gram-positive and Gram-negative bacteria, as well as *Candida* spp. MIC values were determined using the microbroth dilution method.

Results: Each of the tested molecules exhibited varying inhibitory effects across six distinct targets, resulting in different MIC values. Compounds **4a, 4e,** and **4f** showed moderate antimicrobial activity compared with the standards.

Conclusion: Among the tested compounds, compound **4a** demonstrated the most potent antimicrobial activity against the *P. mirabilis* strain, with an MIC value of 312.5 µg/mL. Further modification and development of ibuprofen-hydrazone derivatives against targets may result in new antimicrobial drug candidates in the near future.

Keywords: Hydrazone; ibuprofen; antibacterial activity; antifungal activity; gram-positive bacteria; gram-negative bacteria.

INTRODUCTION

Antimicrobial resistance (AMR) is a critical health problem and development threat to the entire world. AMR occurs as a result of bacteria, fungi, viruses, and parasites changing over time and not responding to drugs; this makes infections more difficult to treat and increases the risk of disease spread, morbidity, and mortality (WHO 2023). The increase in high resistance rates observed after antibiotic treatment causes prolonged hospitalisations, treatment failures, and seriously high costs (Dadgostar, 2019). New antibiotics that are effective against resistant microorganisms are urgently needed.

Hydrazide-hydrazones have demonstrated a wide range of pharmacological activities, including anticancer, antimicrobial, antidiabetic, anticonvulsant, antitumor, anti-tuberculosis, antidepressant, antiinflammatory, and antiviral activities (Angelova, Karabeliov, Andreeva-Gateva, & Tchekalarova, 2016; Koçyiğit-Kaymakçıoğlu et al., 2006; Nasr, Bondock, & Youns, 2014; Paprocka et al., 2018; Salgin-Goksen et al., 2021; Taha et al., 2017; Tian et al., 2009). Among the biological activity profiles of hydrazide-hydrazones, antimicrobial properties are the most prevalent in the scientific literature. Several hydrazone have been reported to possess wide spectra of activity against both Gram-(+) and Gram-(-) bacteria as antibacterial agents (Masunari & Tavares, 2007), and some of them have also been reported to have an inhibitory effect on fungi (Evranos, Gürpinar, & Eryilmaz, 2020; Tatar et al., 2016; Vicini, Zani, Cozzini, & Doytchinova, 2002).

In this paper, we report the synthesis of novel hydrazone obtained from the condensation of 2-[4-(2-methylpropyl)phenyl]propanehydrazide and appropriate cyclohexanone derivatives. All the synthesised compounds were also screened for their in vitro antibacterial and antifungal activities.

Corresponding Author: Çağla Begüm Apaydın **E-mail:** cagla.apaydin@istanbul.edu.tr
Submitted: 27.02.2024 • **Revision Requested:** 20.05.2024 • **Last Revision Received:** 22.05.2024 • **Accepted:** 23.05.2024

MATERIALS AND METHODS

Chemistry

Commercially available chemicals were purchased from Sigma-Aldrich or Merck. Melting points were determined in open capillary tubes using a Buchi B-540 melting point apparatus and are uncorrected. ^{1}H-NMR and ^{13}C-NMR spectra were run on Bruker 500 MHz and Bruker 600 MHz spectrophotometers. Microanalyses were performed using a Thermo Finnigan Flash EA 1112 elemental analyser. An AgilentAgilent 1260 Infinity II ESI/MS mass spectrometer was used to record the mass spectra with electrospray ionisation (IR: Infrared radiation, ^{1}H-NMR: Proton nuclear magnetic resonance, ^{13}C-NMR: Carbon-13 nuclear magnetic resonance, APT: Attached proton test).

Methyl 2-[4-(2-methylpropyl)phenyl]propanoate (2)

Racemic acid (**1**) (0.1 mol) and a few drops of sulphuric acid (%98) in methanol (0.5 mol) were heated under reflux for 24 h. Saturated sodium bicarbonate was added, and the solvent was evaporated under vacuum. The solution was extracted with chloroform and dried over sodium sulphate. The yellowish oily residue was used without further purification (Allegretti et al., 2005) (CAS number: 61566-34-5).

2-[4-(2-Methylpropyl)phenyl]propanehydrazide (3)

A mixture of **2** (0.01 mol), ethanol (20 ml), and hydrazine hydrate was heated under reflux for 6 h. The resulting white powders were filtered off and recrystallised from C_2H_5OH (Bülbül et al., 2023) (CAS number: 127222-69-9).

General procedure for the synthesis of 2-[4-(2-methylpro pyl) phenyl]-N'-[4-(non)-substitutedcyclohexylidene] propanehydrazide (4a-f)

A solution of **3** (0.005 mol) in ethanol (25 ml) and an appropriate cyclohexanone (0.006 mol) was refluxed for 4-6 h. The resulting white solid was filtered off and recrystallised from C_2H_5OH-H_2O mixture.

N-(4-methylcyclohexylidene)-2-[4-(2-methylpropyl)phenyl] propanehydrazide (4b)

White crystals (84%); m.p. 122-124°C; IR(KBr): ν_{max} 3213, 3169 (N-H), 1656 (C=O), 1539, 1496, 1456 (C=N, C=C); ^{1}H-NMR ($CDCl_3$/600MHz): 8.49, 8.03 (1H, 2s, NH), 7.31-7.27, 7.26-7.21, 7.16-7.12, 7.08-7.03 (4H, 4m, Ar-H), 4.69-4.60, 3.69-3.60 (1H, 2m, -CH-CH_3), 2.63-2.38, 2.23-2.04, 1.92-1.43, 1.26-0.90 (18H, 4m, cyc-H, $(CH_3)_2$C**H**-, -CH-CH_2- and -CH-C**H**$_3$), 0.89 (6H, d, *J*= 6.6 Hz, CH_3); ^{13}C-NMR ($CDCl_3$/150MHz): 176.4, 170.2 (C=O), 161.2, 161.1, 154.8, 154.3 (C=N), 141.1, 139.8, 138.9, 138.8, 137.7 (C1, C4), 129.8, 129.0, 127.7, 127.5 (C2, C3, C5, C6), 45.9, 40.7, 40.5 (-CH-CH_3), 45.1, 44.9 (-CH-CH_2-), 35.0, 34.9, 34.8, 34.7, 34.6, 33.7, 33.5, 25.4, 25.0 (cyc-CH_2), 31.8, 31.6 (cyc-CH), 30.1 ($(CH_3)_2$CH), 22.4, 22.2 ($(CH_3)_2$CH-), 21.3, 21.2 (CH_3), 18.2, 18.1 (-CH-CH_3). LC-MS (ESI (+)) $C_{20}H_{30}N_2O$ $[M+H]^+$: 315.24309; Found: 315.2 (100, $[M+H]^+$), 316.2 (20, $[M+2H]^+$), 337.2 (95, $[M+Na]^+$), 338.2 (20, $[M+H+Na]^+$). Anal. calcd. for $C_{20}H_{30}N_2O$ (314.46) C: 76.39, H: 9.62, N: 8.91. Found C: 76.77, H: 9.13, N: 8.98.

N-(4-ethylcyclohexylidene)-2-[4-(2-methylpropyl)phenyl] propanehydrazide (4c)

White powders (88%); m.p. 112-114°C; IR(KBr): ν_{max} 3223, 3176 (N-H), 1660 (C=O), 1541, 1512, 1463 (C=N, C=C); ^{1}H-NMR ($CDCl_3$/500MHz): 8.52, 8.17 (1H, 2s, NH), 7.31, 7.25, 7.15, 7.07 (4H, 4d, *J*=7.8 Hz, Ar-H), 4.70-4.64, 3.71-3.62 (1H, 2m, -CH-CH_3), 2.68-0.80 (20H, m, cyc-H, $(CH_3)_2$C**H**-, -C**H**-CH_2- and -CH-C**H**$_3$),0.91 (6H, d, *J*= 6.6 Hz, CH_3); ^{13}C-NMR ($CDCl_3$/125MHz): 176.4 (C=O), 155.3, 154.8 (C=N), 141.0, 139.9, 138.8, 137.6 (C1, C4), 129.7, 129.0, 127.7, 127.5 (C2, C3, C5, C6), 45.8, 40.7, 40.5 (-**C**H-CH_3), 45.0, 44.9 (-CH-**C**H_2-), 38.5, 38.4 (cyc-CH), 34.7, 34.4, 32.6, 32.4, 31.4,25.6, 25.0 (cyc-CH_2), 28.7, 28.5, 28.2 (CH_2), 30.1 ($(CH_3)_2$**C**H-), 22.4, 22.2 ($(CH_3)_2$CH-), 18.2, 18.1 (-CH-**C**H_3), 11.5 (CH_3). LC-MS (ESI (+)) $C_{21}H_{32}N_2O$ $[M+H]^+$: 329.25874; Found: 329.2 (100, $[M+H]^+$), 351.2 (90, $[M+Na]^+$), 352.3 (25, $[M+H+Na]^+$). Anal. calcd. for $C_{21}H_{32}N_2O$ (328.49) C: 76.78, H: 9.82, N: 8.53, Found C: 76.99, H: 9.46, N: 8.59.

N-(4-propylcyclohexylidene)-2-[4-(2-methylpropyl)phenyl] propanehydrazide (4d)

White crystals (80%); m.p. 122-124°C; IR(KBr): ν_{max} 3224, 3174 (N-H), 1660 (C=O), 1541, 1512, 1456 (C=N, C=C); ^{1}H-NMR ($CDCl_3$/600MHz): 8.46, 8.02 (1H, 2s, NH), 7.29, 7.24 (2H, 2d, *J*= 7.8 Hz, Ar-H), 7.16-7.12, 7.08-7.03 (2H, 2m, Ar-H), 4.68-4.61, 3.68-3.62 (1H, 2m, -C**H**-CH_3), 2.62-2.39, 2.22-2.05, 1.95-0.85 (22H, 3m, cyc-H, $(CH_3)_2$C**H**-, -CH-C**H**$_2$- and -CH-C**H**$_3$), 0.89 (6H, d, *J*= 6.6 Hz, CH_3); ^{13}C-NMR ($CDCl_3$/150MHz): 176.4, 170.2 (C=O), 161.6, 161.5, 155.1, 154.7 (C=N), 141.1, 139.9, 139.8, 138.9, 137.7 (C1, C4), 129.8, 129.0, 127.7, 127.5 (C2, C3, C5, C6), 45.9, 40.7, 40.5 (-**C**H-CH**3**), 45.1, 44.9 (-**C**H-CH_2-), 38.2, 38.1 (CH_2), 36.5, 36.3, 36.2 (cyc-CH), 34.7, 34.5, 33.0, 32.8, 32.5, 25.4, 25.0 (cyc-CH_2), 31.7, 31,6, 31.5 ($(CH_3)_2$**C**H-), 22.4, 22.2 ($(CH_3)_2$CH-), 20.1(CH2), 18.3, 18.2, 18.1 (-CH-CH_3), 14.2 (CH_3). LC-MS (ESI (+)) $C_{22}H_{34}N_2O$ $[M+H]^+$: 343.27439; Found: 343.2 (10, $[M+H]^+$). Anal. calcd. for $C_{22}H_{34}N_2O$ (342.51): C: 77.14, H: 10.01, N: 8.18. Found C: 77.50, H: 10.20, N: 8.27.

***N*-(4-*tert*-butylcyclohexylidene)-2-[4-(2-methylpropyl) phenyl]propanehydrazide (4e)**

White crystals (81%); m.p. 113-125°C; IR(KBr): ν_{max} 3219, 3169 (N-H), 1662 (C=O), 1543, 1512, 1450 (C=N, C=C); ^{1}H-NMR ($CDCl_3$/600MHz): 8.43, 8.01 (1H, 2s, NH), 7.29, 7.24 (2H, 2d, *J*= 7.8 Hz, Ar-H), 7.17-7.12, 7.08-7.03 (1H, 2m, -C**H**-CH_3), 4.68-4.61, 3.68-3.62 (1H, 2m, -C**H**-CH_3), 2.63-2.40, 2.22-2.06, 1.97-0.85 (24H, 3m, cyc-H, $(CH_3)_2$C**H**-, -C(C**H**$_3)_3$ and -CH-CH_3**)**, 0.89 (6H, d, *J*= 6.6 Hz, CH_3); ^{13}C-NMR ($CDCl_3$/150MHz): 176.3, 170.2 (C=O), 161.6, 161.5, 155.1, 154.6 (C=N), 141.1, 139.9, 139.8, 138.9, 137.6 (C1, C4), 129.8, 129.0, 128.9, 127.7, 127.5, 127.3 (C2, C3, C5, C6), 45.9, 40.7, 40.6 (-**C**H-CH_3), 45.1, 44.9 (-CH-CH_2-), 38.5, 38.4, 38.3, 38.2 (cyc-CH), 34.7, 34.6, 34.5, 32.6, 32.4, 32.1, 31.4, 31.2, 25.4, 25.0 (cyc-CH_2), 30.1 (($CH_3)_2$CH-), 28.7, 28.5 (-C$(CH_3)_3$), 22.4, 22.2 (($\mathbf{C}H_3)_2$CH-), 18.3, 18.2, 18.1 (-CH-**C**H_3), 11.5 (CH_3). LC-MS (ESI (+)) $C_{23}H_{36}N_2O$; $[M+H]^+$: 357.29004; Found: 357.3 (10, $[M+H]^+$). Anal. calcd. for $C_{23}H_{36}N_2O$ (356.54) C: 77.48, H: 10.18, N: 7.86, Found C: 77.08, H: 10.22, N: 7.88.

Determination of Minimum Inhibitory Concentrations (MICs)

The ibuprofen hydrazone analogues in vitro antibacterial properties were determined through the application of the Clinical and Laboratory Standards Institute's microbroth dilution procedure (CLSI, 2008; CLSI, 2020).

The compounds were tested for their minimum inhibitory concentrations (MICs) against the following bacteria: *Escherichia coli* ATCC 25922, *Proteus mirabilis* ATCC 14153, *Staphylococcus aureus* ATCC 29213, *Staphylococcus epidermidis* ATCC 12228, *Klebsiella pneumoniae* ATCC 4103, and three yeasts: *Candida albicans* ATCC 10231, *Candida parapsilosis* ATCC 22019, and *Candida tropicalis* ATCC 750. As test media, Mueller-Hinton broth (MHB) (Difco, Detroit, MI, USA) was created for the bacteria through serial 2-fold dilutions ranging from 1250 to 0.6 µg/mL, while RPMI-1640 medium (Sigma, St. Louis, MO, USA) was prepared for the yeasts and buffered to pH 7.0 using MOPS. For the molecules, dimethyl sulfoxide (DMSO) was used as a solvent. To achieve a final concentration of 5 x10^5 CFU/mL for the bacteria and 0.5 x10^3 to 2.5 x10^3 CFU/mL for the yeasts in the test trays, respectively, 50 µl of a 4–6 h broth culture was added to each well. To prevent the trays from evaporating, they were covered and sealed in plastic bags. Trays containing MHB were incubated for 24 h at 37 °C, whereas trays containing RPMI-1640 media were incubated for 48 h at 30 °C. The minimum inhibitory concentration (MIC) is the lowest concentration of a chemical that completely inhibits observable development. The antibacterial properties of DMSO were examined using test microorganisms as a control. The values of the controls were used to evaluate the outcomes.

RESULTS AND DISCUSSION

Chemistry

The synthetic pathways for the preparation of the target products are illustrated in Figure 1. The reaction of 2-[4-(2-methylpropyl)phenyl]propanehydrazide and appropriate cyclohexanones in ethanol gives the corresponding hydrazone/hydrazide compounds in good to excellent yields. The molecular structure of the synthesized compounds was confirmed by spectroscopic methods including ^{1}H NMR, ^{13}C NMR, and mass spectrometry. In addition, compounds **4a** and **4f**, previously described by Halim et al. in the literature (Apaydın, Hasbal Çelikok, Yılmaz Özden, & Cihan Üstündağ, 2022), were synthesized and confirmed by spectral and analytical data (experimental information for these molecules was given in the Supplementary Material).

In the IR spectra, some significant stretching bands due to N–H, C=O, C=N, and C=C were at 3226-3169 cm^{-1}, 1662-1656 cm^{-1} and 1543-1448 cm^{-1} respectively.

The ^{1}H NMR spectra of **4a-f** displayed two sets of signals for most of the protons. NH protons were observed as two separate singlets at about δ 8.69-8.01 ppm. In the ^{1}H NMR spectra of **4a-f**, protons were observed at δ 2.84-0.85 ppm due to the existence of aliphatic protons in the cyclohexylidene residue.

Carbon resonances were assigned using the APT experiments. Observation of C=N (δ 161.6-153.2 ppm) resonances in the ^{13}C NMR spectra of **4a-f** verified the presence of hydrazone compounds. The ^{13}C NMR spectra of compound **4a-f** showed the characteristic amide C = O carbon at δ 176.5-170.2 ppm as two signal sets, except for **4c**. N-acylhydrazone can exist in four possible forms, as geometric isomers (E/Z) regarding the C=N double bonds and as rotamers (cis/trans) regarding the amide N-C(O) (Apaydın, Hasbal Çelikok, Yılmaz Özden, & Cihan Üstündağ, 2022; Cihan Üstündağ, Mataracı Kara, & Çapan, 2019). All compounds were found to exist as racemic mixtures of two isomers, as indicated by ^{1}H-NMR and ^{13}C-NMR spectra.

Protonated $[M+H]^+$ molecular ions observed in ESI-MS confirmed the molecular weights of the compounds.

In vitro Antibacterial and Antifungal Activity

Ibuprofen is approved for over-the-counter (OTC) usage at a dosage of 200 mg per single dose, with a maximum daily limit of 1200 mg (Moore, 2007). Antimicrobial properties are usually discovered later and considered as side effects in non-antibiotic drugs (Obad J, Suskovic J, & Kos, 2015). Similarly, the antimicrobial capabilities of ibuprofen are viewed solely as a side effect and are not addressed in the patient information leaflets accompanying ibuprofen drugs. In the disc diffusion test conducted to investigate the antimicrobial properties of ibuprofen, inhibition zones were obtained with concentrations greater than

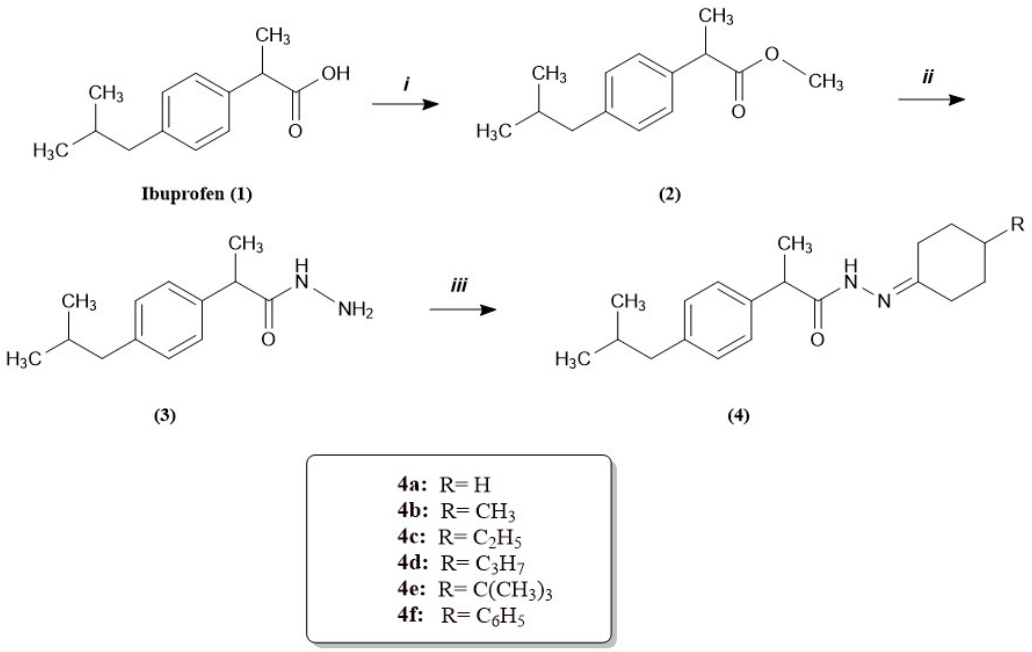

Figure 1. Synthesis route of hydrazide-hydrazone derivatives (**4a-f**) (i): CH_3OH, conc. H_2SO_4, reflux, 24 h; (ii): $NH_2NH_2.H_2O/C_2H_5OH$, reflux, 6 h (iii): C_2H_5OH/cyclic ketones, 4-6 h.

Table 1. Antimicrobial properties of compounds 4a-f against selected bacteria and fungi

	MIC (µg/mL)						
Microorganism	**4a**	**4b**	**4c**	**4d**	**4e**	**4f**	**Reference antimicrobials**
***S. aureus* ATCC 29213**	-[a]	-	-	-	-	-	**1.2 (Cefuroxime-Na)**
***P. mirabilis* ATCC 14153**	**312.5**	-	-	-	**625**	**625**	**2.4 (Cefuroxime-Na)**
***S. epidermidis* ATCC 1228**	**625**	-	-	-	**625**	**625**	**9.8 (Cefuroxime)**
***E. coli* ATCC 25922**	**625**	-	-	-	-	**625**	**4.9 (Cefuroxime-Na)**
***E. fecalis* ATCC 29212**	**625**	-	-	-	**625**	**625**	**128 (Amikacin)**
***K. pneumoniae* ATCC 4352**	**625**	-	-	-	-	-	**4.9 (Cefuroxime-Na)**
***P. aeruginosa* ATCC 27853**	-	-	-	-	-	-	**2.4 (Ceftazidime)**
***C. albicans* ATCC 10231**	-	-	-	-	-	**625**	**4.9 (Clotrimazole)**
***C. tropicalis* ATCC 750**	-	-	-	-	-	-	**1 (Amphotericin B)**
***C. parapsilosis* ATCC 22019**	-	-	-	-	-	-	**0.5 (Amphotericin B)**

[a] No activity at the highest concentration tested.

62.5 µg and 250 µg for *Staphylococcus aureus*, 125 µg and 250 µg for *Bacillus subtilis*, 31.3 µg and 125 µg for *Candida albicans*, 31.3 µg and 62.5 µg for *Aspergillus brasiliensis* using ibuprofen/disc and ibuprofen lysine/disc, respectively. However, inhibition zones were not obtained for *Escherichia coli, Pseudomonas aeruginosa*, and *Salmonella typhimurium* (Obad J, Suskovic J, & Kos, 2015).

The antibacterial and antifungal activities of the new hydrazone derivatives (**4a-f**) were evaluated *in vitro* against the following strains: four Gram-negative bacteria [*Pseudomonas*

aeruginosa (ATCC 27853), *Escherichia coli* (ATCC 25922), *Klebsiella pneumoniae* (ATCC 4352), and *Proteus mirabilis* (ATCC 14153), three Gram-positive bacteria [*Staphylococcus aureus* (ATCC 29213), *Staphylococcus epidermidis* (ATCC 12228), and Enterococcus faecalis (ATCC 29212); and three yeasts [*Candida albicans* (ATCC 10231), *Candida parapsilosis* (ATCC 22019), and *Candida tropicalis* (ATCC 750). The structures of the new hydrazone derivatives used in this work and their MICs compared with standard agents are shown in **Table 1.** With regard to the antibacterial activity, **4b, 4c**, and **4d** exhibited no activity against any of the tested reference strains. Surprisingly, **4a, 4e**, and **4f** showed weak activity against some Gram-positive and Gram-negative *strains*, with an MIC value at 625 g/mL. The best antimicrobial activity result from our study was obtained from **4a** when tested against the P. mirabilis strain with a MIC value at 312.5 g/mL. Additionally, antifungal activity was observed against *C. albicans* with **4f**.

CONCLUSION

In this study, we evaluated the ibuprofen hydrazone derivatives in terms of antibacterial and antifungal efficacy. The structures of newly hydrazone products were verified by ^{1}H-NMR, ^{13}C-NMR, MS, and elemental analysis. The compounds **4a, 4e** and **4f** showed moderate antibacterial activity. The data obtained from the antimicrobial activity studies showed that some ibuprofen hydrazone analogs have a potential for the further studies.

Peer-review: Externally peer-reviewed.

Author Contributions: Conception/Design of Study- C.B.A., E.M.K.; Data Acquisition- C.B.A., E.M.K.; Data Analysis/Interpretation- C.B.A., E.M.K.; Drafting Manuscript- C.B.A.; Critical Revision of Manuscript- C.B.A., E.M.K.; Final Approval and Accountability- C.B.A., E.M.K.

Conflict of Interest: The authors have no conflict of interest to declare.

Financial Disclosure: The authors declared no financial support.

ORCID IDs of the authors

Çağla Begüm Apaydın 0000-0001-6703-9389
Emel Mataracı Kara 0000-0002-4428-5066

REFERENCES

Allegretti, M., Bertini, R., Candida, M.C., Bizzarri, C., Di Bitondo, R., Di Cioccio, ... Colotta, F. (2005). 2-Arylpropionic CXC Chemokine Receptor 1 (CXCR1) Ligands as Novel Noncompetitive CXCL8 Inhibitors, *Journal of Medicinal Chemistry, 48*, 4312-https://doi.org/4331. 10.1021/jm049082i.

Angelova, V., Karabeliov, V., Andreeva-Gateva, P.A., Tchekalarova, J. (2016). Recent Developments of Hydrazide/Hydrazone Derivatives and Their Analogs as Anticonvulsant Agents in Animal Models. *Drug Development Research, 77*(7), 379–392. https://doi.org/10.1002/ddr.21329.

Antimicrobial resistance 2023. https://www.who.int/news-room/fact-sheets/detail/antimicrobial-resistance (accessed Jan 27, 2023).

Apaydın, Ç.B., Hasbal Çelikok, G., Yılmaz Özden, T., Cihan Üstündağ, G. (2022). Design, synthesis and biological evaluation of novel sulfonamide hydrazones as α-glucosidase and α-amylase inhibitors. *İstanbul Journal of Pharmacy, 52*(2), 108-113. https://doi.org/10.26650/IstanbulJPharm.2022.1018698.

Bülbül, B., Ding, K., Zhan, C., Çiftçi, G., Yelekçi, K., Gürboğa, M., ... Küçükgüzel, İ. (2023). Novel 1,2,4-triazoles derived from Ibuprofen: synthesis and in vitro evaluation of their mPGES-1 inhibitory and antiproliferative activity, *Molecular Diversity, 27*, 2185–2215. https://doi.org/10.1007/s11030-022-10551-0.

Cihan Üstündağ, G., Mataracı Kara, E., Çapan G. (2019). Synthesis, characterization, antibacterial and antifungal evaluation of novel cyclohexanone benzoylhydrazones. *İstanbul Journal of Pharmacy, 49*(3): 142-147. https://doi.org/10.26650/istanbuljpharm.2019.19022.

CLSI, Clinical and Laboratory Standards Institute Performance Standards for Antimicrobial Susceptibility Testing, Clinical and Laboratory Standards Institute. 950 West Valley Road, Suite 2500, Wayne, Pennsylvania 19087, USA, 2020.

CLSI, Clinical and Laboratory Standards Institute Reference Method for Broth Dilution Antifungal Susceptibility Testing of Yeasts; Approved Standard M27-A3.2008, Wayne, 2008.

Dadgostar, P. (2019). Antimicrobial Resistance: Implications and Costs. *Infection and Drug Resistance, 12*, 3903–3910. https://doi.org/10.2147/IDR.S234610.

Evranos-Aksöz, B., Gürpinar, S.S., Eryilmaz, M. (2020). Antimicrobial activities of some pyrazoline and hydrazone derivatives. *Turkish Journal Of Pharmaceutical Sciences, 17*(5), 500–505. https://doi.org/10.4274/tjps.galenos.2019.42650.

Koçyiğit-Kaymakçıoğlu, B., Elçin, O., Seda, U., Fatma, K., Nathaly, S., Sevim, R., Dimoglo, A. (2006). Synthesis and characterization of novel hydrazide-hydrazones and the study of their structure-antituberculosis activity. *European Journal of Medicinal Chemistry, 41*(11), 1253–1261. https://doi.org/10.1016/j.ejmech.2006.06.009.

Masunari, A., Tavares, L.C. (2007). A new class of nifuroxazide analogues: Synthesis of 5-nitrothiophene derivatives with antimicrobial activity against multidrug-resistant Staphylococcus aureus. *Bioorganic Medicinal Chemistry, 15*(12): 4229–4236. https://doi.org/10.1016/j.bmc.2007.03.068.

Moore, N. (2007). Ibuprofen: A Journey from Prescription to Over-the-Counter Use. *Journal of the Royal Society of Medicine*, 100, 2-6. https://doi.org/10.1177/014107680710004801s01.

Nasr, T., Bondock, S., Youns, M. (2014). Anticancer activity of new coumarin substituted hydrazide-hydrazone derivatives. *European Journal of Medicinal Chemistry, 76*(9), 539–548. https://doi.org/10.1016/j.ejmech.2014.02.026.

Obad, J., Šuškovic, J., Kos, B. (2015). Antimicrobial activity of ibuprofen: New perspectives on an "Old" non-antibiotic drug. *European Journal of Pharmaceutical Sciences*, 71, 93-98. http://dx.doi.org/10.1016/j.ejps.2015.02.011.

Paprocka, R., Wiese-Szadkowska, M., Helmin-Basa, A., Mazur, L., Kutkowska, J., Michałkiewicz, J., ... Pazderski, L. (2018). Synthesis and evaluation of new amidrazone-derived hydrazides as a potential anti-inflammatory agents. *Monatshefte für Chemie*, 149,

1493–1500. https://doi.org/10.1007/s00706-018-2197-8.

Salgin-Goksen, U., Telli, G., Erikci, A., Dedecengiz, E., Tel, B.C., Kaynak, F.B., ... Gokhan-Kelekci, N. (2021). New 2-Pyrazoline and Hydrazone Derivatives as Potent and Selective Monoamine Oxidase A Inhibitors. *Journal of Medicinal Chemistry, 64*(4): 1989–2009. https://doi.org/10.1021/acs.jmedchem.0c01504.

Taha, M., Shah, S.A.A., Imran, S., Afifi, M., Chigurupati, S., Selvaraj, M., ... Vijayabalan, S. (2017). Synthesis and in vitro study of benzofuran hydrazone derivatives as novel alpha-amylase inhibitor. *Bioorganic Chemistry, 75*, 78–85. https://doi.org/10.1016/j.bioorg.2017.09.002.

Tatar, E., Şenkardeş, S., Sellitepe, H.E., Küçükgüzel, Ş.G., Karaoğlu, Ş.A., Bozdeveci, A., De Clercq, E., Pannecouque, C., Ben Hadda, T., Küçükgüzel, I. (2016). Synthesis, and prediction of molecular properties and antimicrobial activity of some acylhydrazones derived from N-(arylsulfonyl)methionine. *Turkish Journal of Chemistry, 40*(3), 510–534. https://doi.org/10.3906/kim-1509-21.

Tian, B., He, M., Tang, S., Hewlett, I., Tan, Z., Li, J., ... Yang, M. (2009). Synthesis and antiviral activities of novel acylhydrazone derivatives targeting HIV-1 capsid protein. *Bioorganic & Medicinal Chemistry Letters, 19*(8): 2162–2167. https://doi.org/10.1016/j.bmcl.2009.02.116.

Vicini, P., Zani, F., Cozzini, P., Doytchinova, I. (2002). Hydrazones of 1,2-benzisothiazole hydrazides: Synthesis, antimicrobial activity and QSAR investigations. *European Journal of Medicinal Chemistry, 37*(7), 553–564. https://doi.org/10.1016/S0223-5234(02)01378-8.

How cite this article

Apaydın, Ç.B., & Mataracı Kara, E. (2024). Synthesis and evaluation of the antibacterial and antifungal activity of new ibuprofen hydrazone derivatives. *İstanbul Journal of Pharmacy, 54*(2), 122–127. DOI:10.26650/IstanbulJPharm.2024.1444072

İstanbul Journal of Pharmacy
Istanbul J Pharm2024, 54 (2): 128–132
DOI: 10.26650/IstanbulJPharm.2024.1462752

Original Article

Spectrophotometric determination of ichthammol in topical formulations

Gamze Ergin Kızılçay[1]

[1]İstanbul University, Faculty of Pharmacy, Department of Analytical Chemistry, İstanbul, Türkiye

ABSTRACT

Background and Aims: This study developed a new, simple, and rapid spectrophotometric method for determining ichthammol as a local antiseptic in topical formulations. The developed spectrophotometric method for determining ichthammol was applied to topical formulations.

Methods: The linearity range of the ichthammol was 5.0-50.0 µg/mL at a wavelength of 235 nm. Ethanol:water (50:50; v/v) was used as the solvent. The method was validated using the limit of quantification, limit of detection, linearity, selectivity, robustness, recovery, precision, stability, and accuracy of the method using the International Conference on Harmonisation guidelines for validation of analytical procedures: text and methodology Q2 (R1).

Results: The limits of detection and quantification were calculated to be 0.044 µg/mL and 0.148 µg/mL, respectively. Intra-day and inter-day relative standard deviation values were calculated to be less than 1.024 %. The assay recovery and precision of ichthammol from topical formulations at 5.0, 20.0, and 50.0 µg/mL were evaluated. The mean recoveries for ichthammol in the topical formulation were calculated at 97.944-99.860%. It was determined that the ichthammol sample solution was stable for 24 h at 4.0°C. The validated method was applied to the cream formulation, and the amount of ichthammol in the cream was determined to be 97.442%.

Conclusion: The validated method was successfully applied to determine ichthammol in topical formulations. The proposed method is reproducible and reliable and can be safely used for routine analysis.

Keywords: Ichthammol, spectrophotometric method, topical formulation, validation

INTRODUCTION

Ichthammol, also known as dark sulphonated shale oil, is a black, oily compound with a characteristic odour. From elemental analysis, the composition of ichthammol was calculated to be $C_{28}H_{36}S_5O_6(NH_4)_2$ (Baumann & Schotten, 1883). It is an ammonium salt of dark sulphonated shale oil (bituminous schists) produced via distillation, followed by sulfonation and neutralisation (Österreichischen Ichthyol Gesellschaft, 1884). An active substance belonging to the class of antiseptics and disinfectants, it is used topically (Boyd, 2010). Ichthammol can be used as a local antiseptic or in the treatment of inflammatory diseases of the skin (such as eczema, abscess, and boil) due to its irritant properties and as an aid in the treatment of chronic skin diseases together with other antiseptics (Shi, Hsiao, Lowes, & Hamzavi, 2021).

Although the first use of ichthammol for treating dermatological diseases was reported by Paul Unna in 1882 (Unna, 1882), scientific data regarding its effectiveness for treating dermatological diseases are quite limited. The majority of research on the topic is from Europe (Boyd, 2010). Currently, products containing ichthammol are used as a local antiseptic for eczema, furunculosis, psoriasis, and acne. Due to its irritating effect on the skin, it is used together with other antiseptics to treat boil-like inflammations and skin diseases such as erysipelas (snapworm) and lupus erythematosus (erythematous skin tuberculosis). It is also popularly advocated for use as a "drawing ointment" for use in relieving glass or wood splinters, spider bites, arthropod attacks, and abscesses (Boyd, 2010).

Ichthammol is available over-the-counter in many forms but is most commonly included in pharmaceutical formulations along with zinc, paraffin, and beeswax, usually in concentrations of 5-20%. In the case of boils, topical application is thought to accelerate their “marking” by more easily expelling their contents (i.e., “drawing”). There are no absolute contraindications to the use of ichthammol, but because it is believed to have anti-inflammatory, antibacterial, and antimycotic qualities, it is accessible as an active ingredient in over-the-

Corresponding Author: Gamze Ergin Kızılçay **E-mail:** gamze.erginkizilcay@istanbul.edu.tr
Submitted: 01.04.2024 • **Revision Requested:** 12.06.2024 • **Last Revision Received:** 25.06.2024 • **Accepted:** 27.06.2024

counter treatments for the treatment of conditions like offensive odour and skin irritation. (DrugBank, 2006).

Since topical ointments are non-prescription and have been used by the public since antiquity, there is no reliable method to measure the amount of ichthammol present in them. Despite this, topical ointments are frequently used in dermatology. Existing methods in pharmacopoeias (USP Pharmacopoeia, 2012) and the literature (Perevozchikova & Savelyeva, 1981; Kalde Ya, 1976; Saveleva & Kudymov, 1963; Suprun, 1961) are indirect methods based on the determination of molecules such as iodine, sulphur, and ammonia.

In this study, we aimed to develop a fast, easy, and inexpensive spectrophotometric method for the analysis of this compound from pharmaceutical preparations in ointment formulations. The developed method was validated according to the International Conference on Harmonisation (ICH) Harmonised Tripartite Guideline Validation of analytical procedures: text and methodology Q2 (R1) (ICH Q2 (R1), 2005) rules and was applied to analyse topical pharmaceutical preparations containing commercial ingredients on the market.

MATERIAL AND METHODS

Chemicals

Ichthammol was purchased from Österreichischen Ichthyol Gesellschaft m.b. H. & Co. KG. Ultrapure water from an Elga-branded water system was used in the research laboratory. ACS-grade ethanol was obtained from Merck (Germany). A pharmaceutical topical formulation was purchased fom a pharmacy in Turkey.

Solutions

The stock solution of ichthammol (1.0 mg/mL) was prepared in ethanol-water (50:50, v/v), and it was diluted using ethanol-water (50:50, v/v) to obtain a second stock solution of 100.0 µg/mL. Volumes of 0.5 mL were taken from the second stock solution, and 0.1-0.5 mL were taken from the stock solution diluted to 10.0 mL using the ethanol-water to prepare six practical ichthammol solutions at different concentrations (5-50 µg/mL). The linearity range of ichthammol was 5.0, 10.0, 20.0, 30.0, 40.0, and 50.0 µg/mL.

Instrumentation

A UV-160 A spectrophotometer of the Shimadzu brand (Kyoto, Japan) was used in this study. Measurements were carried out at a wavelength of 235 nm using 1-cm quartz cells.

Preparation of the sample and placebo solutions

The sample and placebo solutions were prepared in ethanol:water (50:50, v/v). The topical formulation and placebo were weighed at 50.0 mg into a 250.0 mL volumetric flask and dissolved in ethanol-water (50:50, v/v). The sample solution was stirred in a vortex mixer for 2.0 min and then placed in an ultrasonic bath at 40.0 °C for 30.0 min. It was completed to its volume with ethanol-water. The solution was brought to room temperature by keeping it under tap for 2.0 min and completed to its volume with ethanol-water (50:50; v/v) solution. Vortexing was performed for 2.0 min. The absorbance of the sample was measured at 235 nm against a blank (ethanol:water (50:50; v/v), which was selected as the maximum wavelength. The amount of substance in the topical formulation was calculated by substituting the resulting absorbance into the calibration equation.

Method development and validation

During method development, the measurement wavelength was first determined. Then, measurements were taken at different solvent ratios, and the best solvent ratio was determined. For sample preparation conditions, the ultrasonic bath holding time and temperature were tested. The developed method was validated using the ICH Guidelines Q2 (R1) as a reference (ICH Q2 (R1), 2005).

Taking into consideration the concentration of ichthammol present in the preparation containing solution, the linearity of ichthammol was investigated in the range of 5.0-50.0 µg/mL (n=3). The limits of detection (LOD) and limits of quantitation (LOQ) were calculated using the formula LOD or LOQ = κSDa/b, where the value of K is 3 and 10 for LOD and LOQ, respectively.

By selecting the three calibration curve concentrations, absolute recoveries were evaluated by adding placebo to concentrations in three selected calibration curves. A placebo solution was prepared in a similar manner to the sample solution. Three different concentrations of standard ichthammol solutions (5.0, 20.0, and 50.0 µg/mL (n=3), were filled to their volume with the placebo solution, and these mixtures were analysed using the proposed method.

Precision studies on the method were examined for inter-day and intra-day precision. Therefore, separate standard solutions were prepared at concentrations of 5.0, 20.0, and 50.0 µg/mL (n=3). The standards from the same day and different days were analysed and assessed by calculating the relative standard deviation (RSD) percentages of the field values.

The stability of ichthammol in the topical formulation solution was studied at the end of the 12th and 24th hours while the samples were kept under 4.0°C conditions. Stability was assessed by comparing the initial results with the results obtained at the conclusion of the analyses at the end of the 12th and 24th hours. The robustness parameter was evaluated by varying the wavelength and solvent ratio. Three replicates were determined using a standard solution for each robustness parameter. The standard solution was initially prepared in ethanol:water

(50:50, v/v). Subsequently, measurements were conducted after preparing the standard solutions using solvent ratios of 48:52, v/v ethanol to 52:48, v/v water. A similar approach was adopted for wavelength, with initial measurements made at the method-specified wavelength of 235 nm. The standard solution was measured by adjusting the wavelength from 233 to 237 nm. The measured values obtained were analysed for the RSD value, which was selected as the system suitability parameter.

RESULTS AND DISCUSSION

During the method development studies, the best spectrophotometric measurement results were obtained using the solution ratio of ethanol-water (50:50, v/v) (Figure 1). The highest absorbance values were obtained at 40.0 °C (Figure 2) and 30.0 min (Figure 3) in the ultrasonic bath for sample preparation. The measurement wavelength was 235 nm. Validation studies under these conditions were conducted as follows.

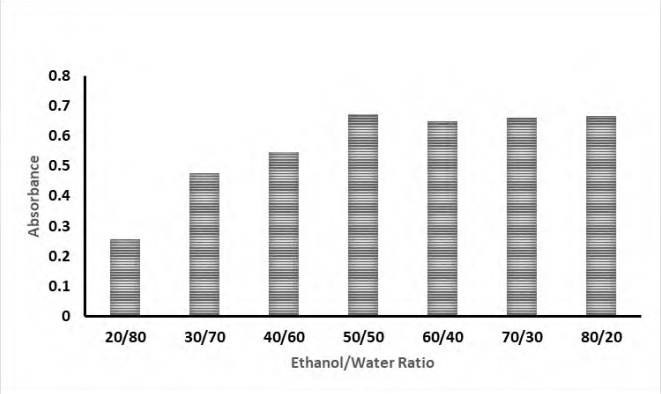

Figure 1. Effect of solvent ratio on the absorbance of the ichthammol solubility

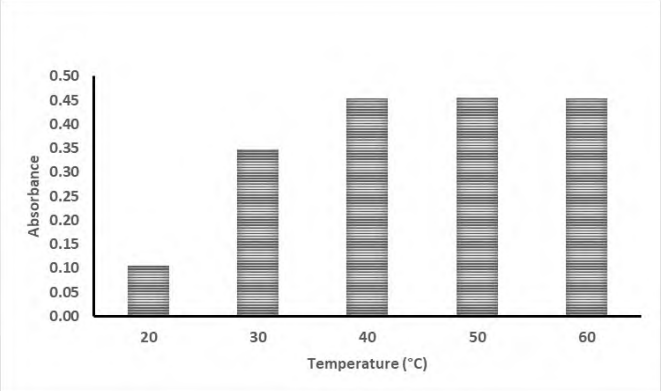

Figure 2. Effect of temperature on absorbance in sample preparation

Selectivity

To assess method selectivity, absorbance was measured in the solvent, ichthammol standard solution, topical formulation, and placebo solutions. During the ichthammol spectrum, no absorbance was observed due to the solvent or placebo, as depicted in Figure 4.

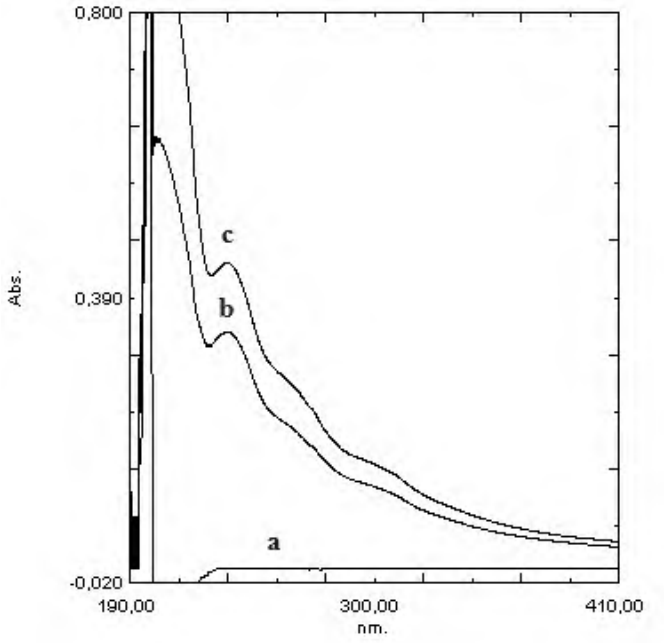

Figure 4. The absorption spectrum of a) the placebo solution, b) the standard ichthammol solution (20.0 µg/mL), c) the cream formulation (10%)

Linearity and sensitivity

Considering the analysed ichthammol formulation, the linearity of the proposed method was studied in the concentration range of 5.0-50.0 µg/mL. The average regression formula can be expressed as A = 0.0191 C + 0.0633 (R^2=0.9992) with C representing the concentration of ichthammol (µg/mL) and A represents the absorbance. The linearity results obtained by the proposed method are displayed in Table 1. In accordance with

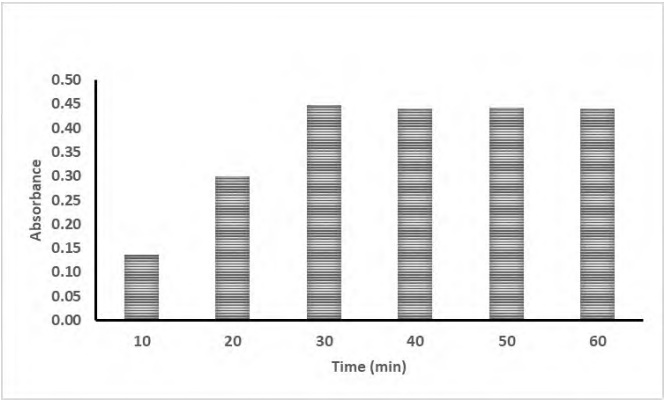

Figure 3. Effect of time on absorbance in sample preparation

the study parameters, LOD and LOQ were calculated at 0.044 µg/mL and 0.148 µg/mL, respectively.

Table 1. Linearity results obtained by the developed method

Parameter	Ichthammol
Linearity range (µg/mL)	5.0-50.0
Regression equation	A = 0.0191 C + 0.0633
Slope ± SD	0.0191± 4.71x 10^{-5}
Intercept ± SD	0.0633± 2.83 x10^{-4}
Mean correlation coefficient, R^2	0.9992
LOD[a] (µg/mL)	0.044
LOQ[b] (µg/mL)	0.148

[a] Limit of Detection; [b] Limit of Quantitation

Recovery

As shown in Table 2, the absolute recovery values of ichthammol in the topical formulations were between 97.944 and 99.860%. The average ichthammol recovery was 98.806%.

Table 2. Recovery results for the assay of ichthammol (n=3)

Concentration (µg/mL)		Recovery (%)	RSD[b] (%)
Added	**Found (mean ± SD[a])**		
5.0	4.993±0.030	99.860	0.605
20.0	19.723±0.091	98.613	0.460
50.0	48.972±0.132	97.944	0.269

[a] Standard deviation; [b] Relative standard deviation

Precision

Precision assessments were performed for both intra-day and inter-day repeatability, as previously described. The RSD% for intra-day repeatability ranged from 0.394% to 1.024%, and for inter-day repeatability, it ranged from 0.280% to 0.593%. Table 3 lists the precision values of the method. These results are in accordance with the statement that the RSD% should be less than 2.0%.

Stability

By comparing the preliminary findings with those obtained at the end of the studies after 12 and 24 h, the developed method

Table 3. Intra-day & inter-day precision and accuracy of ichthammol (n=3)

Concentration (µg/mL)			
Added	**Found (mean ± SD[a])**	**RSD[b] (%)**	**RME[c] (%)**
Intra-day			
5.0	5.115 ± 0.052	1.024	2.304
20.0	20.316 ± 0.080	0.394	1.579
50.0	49.827 ± 0.262	0.525	-0.346
Inter-day			
5.0	5.098 ± 0.030	0.593	1.955
20.0	20.211 ± 0.080	0.396	1.056
50.0	49.513 ± 0.138	0.280	-0.974

[a] Standard deviation; [b] Relative standard deviation; [c] Relative mean error

stability under specified conditions for the ichthammol solution was evaluated. Upon analysing the obtained values, it was evident that the variations ranged from 100.59% to 101.04% (Table 4). These results show that there was no noticeable change in the absorbance.

Table 4. Stability results of ichthammol obtained by the proposed method (n=3)

Time (hour)	Concentration (µg/mL) (mean±SD)	RSD (%)	Variation (%)
0	20.281±0.030	0.149	100.00
12	20.525±0.030	0.147	101.04
24	20.421±0.030	0.148	100.59

Robustness

To evaluate the robustness of the method, the results obtained by changing the solvent ratio and wavelength were evaluated. The RSD% value determined using the proposed method was 0.128 at a solvent ratio of 50:50, v/v, and wavelength of 235 nm. During the robustness assessment of the proposed method, adjustments were made to the solvent ratio and wavelength as previously outlined. The resulting RSD% values were within the range of 0.126-0.129 and 0.129-0.131, respectively. Additionally, the variation% was 99.630-101.554 for solvent ratio and 98.881-99.030 for wavelength changes. It was determined that the proposed method was not affected by minor changes.

The developed and validated spectrophotometric method is

simple to prepare, selective, reproducible, rapid, and reliable, enabling the analysis of ichthammol from topical formulations.

Determination of Ichthammol in Topical Formulation

The percentage of ichthammol in the cream formulation, as determined using the proposed method, was calculated to range from 9.536% to 9.924% (Table 5). This result proves the successful application of the method in analysing ichthammol within the cream preparation.

Table 5. Determination of ichthammol in topical formulation (n=6)

n	g / 20 g	%
1	1.962	9.812
2	1.985	9.924
3	1.952	9.758
4	1.931	9.655
5	1.907	9.536
6	1.956	9.780
Mean	1.949	
SD[a]	0.027	
RSD[b]	1.373	

[a] Standard deviation; [b] Relative standard deviation

CONCLUSION

In this study, a fast, easy, and inexpensive spectrophotometric method was developed for the analysis of ichthammol, which is widely used among the public for pharmaceutical preparations in ointment form. The developed method was validated according to the ICH guidelines and applied to the analysis of topical pharmaceutical preparations commercially available on the market.

The developed method was carried out directly via spectrophotometric measurement for the analysis of ichthyol and is the first direct method ever published. In contrast, previously published methods were based on the indirect analysis of substances such as sulphur and ammonia in the content of ichthammol (Perevozchikova & Savelyeva, 1981; Kalde Ya, 1976; Saveleva & Kudymov, 1963; Suprun, 1961). Additionally, the method's sample preparation step is straightforward for topical formulations because it only requires 30.0 min of ultrasonic bath heating at 40.0°C. Method validation studies have demonstrated that this approach is appropriate for highly accurate, precise, and robust quantification of drugs from topical formulations.

As a result, the proposed method allows the analysis of ichthammol in topical pharmaceutical preparations to be performed directly, simply, and quickly, with high accuracy, precision, and robustness, and the method can be easily applied to routine analyses.

Peer-review: Externally peer-reviewed.

Conflict of Interest: The author has no conflict of interest to declare.

Financial Disclosure: The author declared no financial support.

ORCID IDs of the authors

Gamze Ergin Kızılçay 0000-0002-1089-7195

REFERENCES

Baumann, E., & Schotten, C. (1883). Über das "Ichthyol"". *Monatshefte für praktische Dermatologie*, 2, 257.

Boyd, A.S. (2010). Ichthammol revisited. *International Journal of Dermatology*, 49(7), 757– 760. https://doi.org/10.1111/j.1365-4632.2010.04551.x

DrugBank Online (2006). Retrieved from https://go.drugbank.com/drugs/DB11341 (Updated at September 28, 2021).

ICH Q2 (R1). (2005). Validation of Analytical Procedures: Text and Methodology, https://database.ich.org/sites/default/files/Q2%28R1%29%20Guideline.pdf. (Accessed October 8, 2023).

Kalde Ya., L. (1976). Determination of sulphate sulfur in ichthyol by the titrimetric method (Russian). *Farmatsiya*, 25(2), 69-71.

Österreichischen Ichthyol Gesellschaft m.b.H. & Co. KG (1884). Retrieved from https://www.ichthyol.de/en/raw-materials-for-corporate-customers/ ichthammol/

Perevozchikova, G.G., & Savelyeva, G.I. (1981). Quantitative determination of potassium iodide in suppositoria with ichthyol. *Farmatsiya*, 30(2), 62-63.

Saveleva, G.I., & Kudymov, G.I. (1963). Qualitative Determination of Thiophene Sodium in Ichthyol. | Kolıchestvennoe Opredelenıe Tıofenovo I Sery V Ikhtıole. *Aptechnoe delo*, 12, 62-65.

Shi, V.Y., Hsiao, J.L., Lowes, M.A., & Hamzavi, I.H. (2021). A Comprehensive Guide to Hidradenitis Suppurativa. Elsevier. https://doi.org/10.1016/C2019-0-04427-5.

Suprun, P.P. (1961). Iodo-chlorometric method for quantitative determination of ichthyol in. *Aptechnoe delo*, 10, 38-42.

The United States Pharmacopeia (USP) 35 (2012). Ichthammol, 3474-3475.

Unna, P.G. (1882). Aphorismen über Schwefeltherapie und Schwefelpräparate. IV. Ichthyol. *Monatsheft Praktische Dermatologie*, 1, 328-333.

How cite this article

Ergin Kızılçay, G. (2024). Spectrophotometric determination of ichthammol in topical formulations. *İstanbul Journal of Pharmacy, 54*(2), 128–132. DOI: 10.26650/IstanbulJPharm.2024.1462752

İstanbul Journal of Pharmacy
Istanbul J Pharm2024, 54 (2): 133–143
DOI: 10.26650/IstanbulJPharm.2024.1225463

Original Article

Effects of chromatographic conditions on retention behaviour of different psychoactive agents in high-performance liquid chromatography: A machine-learning-based approach

Abdullahi Garba Usman[1], Emine Erdağ[2], Selin Işık[1]

[1]Near East University, Faculty of Pharmacy, Department of Analytical Chemistry, Nicosia, Cyprus
[2]Near East University, Faculty of Pharmacy, Department of Pharmaceutical Chemistry, Nicosia, Cyprus

ABSTRACT

Background and Aims: High-pressure liquid chromatography (HPLC) data on the effects of various chromatographic conditions on the retention behaviour of three different psychotropic drugs; clonazepam, diazepam, and oxazepam) were considered for simulation using a machine learning approach.

Methods: For the simulation of selected psychoactive compounds using HPLC, different machine learning techniques were used in this study: adaptive neuro-fuzzy inference system, multilayer perceptron, Hammerstein-Weiner model, and a traditional linear model in the form of stepwise linear regression. Four evaluation criteria were used to assess the effectiveness of the models: coefficient of determination, root mean squared error, mean squared error, and correlation coefficient.

Results: The results show that machine learning approaches, especially multilayer perceptions, are more reliable than classical linear models with an average coefficient of determination value of 0.98 in both calibration and validation phases.

Conclusion: The performance results also demonstrate that these models can be improved using additional approaches, such as hybrid models, ensemble machine learning, evolving algorithms, and optimisation techniques.

Keywords: Machine learning, clonazepam, diazepam, oxazepam, validation, evaluation metrics

INTRODUCTION

Psychiatrists and general practitioners typically prescribe psychoactive medications. These medications are categorised into several classes, including antipsychotics, mood stabilisers, anticonvulsants (also known as anti-epileptics), and antidepressants (Jouyban et al., 2009). They are also substances that can depress brain activity, such as alcohol, benzodiazepines (e.g., Alprazolam, Diazepam), and barbiturates. These drugs may promote relaxation, sedation, and euphoria. However, they can also cause side effects like impaired coordination, slurred speech, and respiratory depression, when taken at high doses (Jouyban et al., 2009). Previously, antidepressants were only used to treat depression, anti-epileptic drugs were only used to treat epilepsy, antipsychotic drugs were only used to treat acute mania and schizophrenia, and mood stabilisers were only used to treat bipolar disorders. The analytical techniques employed in the clarification and identification of various psychoactive substances, particularly benzodiazepines like clonazepam (CLO), diazepam (DIA), and oxazepam (OXA), have been covered in previous research (Cunha, Mendes, & Marques, 2019). It is crucial to develop a practical analytical method that can be used to identify these compounds due to problems like adulteration, fraud, and abuse of pharmaceutical medications. Technical research articles have therefore used a variety of approaches to determine the qualitative and quantitative features of these psychoactive compounds, including spectroscopy, chromatography, and chemometrics. It is necessary to optimise the chromatographic conditions to achieve the global optimum conditions that can be used in either qualitative determination, quantitative determination, or hybrid determination of the analyte of interest to develop protocols for determining any analyte using chromatographic methods like HPLC (Usman, Isik, & Abba, 2020). Since HPLC is one of the most frequently used analytical methods for pharmaceutical, food, and chemical analysis, simulation of the retention behaviour is one of the crucial topics in the chemometrics approach. Analytes are typically resolved using HPLC based on their distribution between mobile and stationary phases, which is presented in the form of retention time (tR) or occasionally informed of retention factor (k), especially if the retention of the mobile phase, known as the dead

Corresponding Author: Emine Erdağ **E-mail:** emine.erdag@neu.edu.tr
Submitted: 29.12.2022 • **Revision Requested:** 11.04.2024 • **Last Revision Received:** 18.04.2024 • **Accepted:** 27.06.2024

time, is taken into consideration (Usman, Isik, & Abba, 2020). In HPLC, tR is an important parameter for both qualitative and quantitative analysis. The values of tR increased when the analyte interacted strongly with the stationary phase and decreased when the analyte interacted strongly with the mobile phase. As a result, tR is linked to three different parameters. These parameters can be summarised as the structure of the stationary phase, the chemical properties of the analyte, and the physicochemical behaviour of the mobile phase (Usman, Isik, & Abba, 2021). One commonly used technique to enhance the performance of HPLC systems involves increasing solvent strength by adding an organic modifier to the aqueous medium. This increases the resolution of two or more subsequent peaks. Another parameter that influences tR is also taken into account, and that is the column temperature. Traditionally, an expensive and time-consuming trial-and-error method is used to adjust the mobile phase composition, column temperature, and other chromatographic parameters (Ghali et al., 2020). Chemometric techniques can be used to predict chromatographic variables under ideal conditions, such as tR and resolution (Silva et al., 2020).

Currently, several chemical and pharmaceutical branches use chemometrics-based methodologies that were established through regression analysis, classification analysis, and molecular structure descriptors (Erdag, Haskologlu, Mercan, Abacioglu, & Sehirli, 2023; Sultanoglu, Erdag, & Ozverel, 2023; Tomić et al., 2020). However, as these approaches typically use linear regression techniques, such as stepwise linear regression (SWLR), single linear regression (SLR), and multilinear regression (MLR), it is often difficult to make physical sense of these models (D'Archivio, 2019). These descriptors are often multidimensionally complex; thus, non-linear approaches such as artificial intelligence (AI) technologies are the only way to address them (Rodríguez-Díaz & Sánchez-León, 2019). Conventional linear, static analysis, and other statistical techniques are generally used in tR prediction. Statistical/chemometric and experimental design methodologies should be combined to evaluate the properties of various analytes and improve their physical behaviours (Tayyebi, Hajjar, & Soltanali, 2019). Regression analysis seems straightforward and uncomplicated; however, it has some disadvantages when dealing with several independent variables and reduces accuracy. The accuracy of predicted parameters can be improved using multiple regression analysis when creating a model (Abba et al., 2020). Recent technical research has used artificial intelligence and optimisation techniques to address complicated issues in chromatography and other instrumental methods of investigation. For instance, previous studies have described the use of machine learning to predict the retention characteristics of distinct small compounds under various HPLC settings (Osipenko et al., 2020). With an average absolute error of 46 s, the proposed strategy outperformed previously used learning algorithms. A recent study reported the use of artificial intelligence and ensemble machine learning to predict the presence of methyclothiazide and amiloride drugs using the HPLC technique (Usman, Isik, & Abba, 2020). The proposed strategy for estimating the k-values of agents demonstrated robust performance. Furthermore, the use of hybrid models to predict the retention behaviour of thymoquinone using HPLC has been recently demonstrated (Usman, Isik, & Abba, 2020). The method exhibits the hybrid technique's capacity to more effectively simulate both the linear and nonlinear characteristics of the data.

In addition, a method for selecting an appropriate solvent gradient for separating preparative peptides using machine learning was developed (Samuelsson, Eiriksson, Åsberg, Thorsteinsdóttir, & Fornstedt, 2019). The procedure demonstrated that the machine learning approach was effective in showing how chromatographic settings affect retention behaviour. Artificial neural networks (ANN) were used in a previous study to clarify different types of amino acids using the HPLC technique (D'Archivio, 2019). In this study, multilayer perceptions (MLP), adaptive neuro-fuzzy inference systems (NF), Hammerstein-Weiner (HW), and SWLR were used to simulate the effects of selected psychoactive agents using HPLC for the first time. The main goal of this study was to use various machine learning approaches to investigate the physicochemical effects of two chromatographic conditions; column temperature and mobile phase, on the retention behaviour of three psychotropic substances.

MATERIALS AND METHODS

Machine learning techniques

Any data-driven technique must consider scientific principles and data knowledge (Elkiran, Nourani & Abba, 2019). Temperature and mobile phase were used as independent variables to model the tR of three psychoactive substances (CLO, DIA, and OXA). This research used machine learning approaches, such as MLP, NF, HW, and SWLR models. MATLAB 9.3 was used to perform the simulation. Then, the data were divided into 60% calibration and 40% verification. The best way to obtain unbiased estimates of model performance for a small dataset is to use the k-fold cross-validation technique, which is used to test the performance of models for validation purposes. A flowchart of the model process is shown in Figure 1.

The dataset was standardised to range from zero to one (standard scale) to increase the data integrity and reduce redundancy using Equation (**1**).

$$X_i = \frac{x_u - x_{min}}{x_{max} - x_{min}} \quad (1)$$

"X_i" served as a normalised quantity, "x_u" served as an unnormalised quantity, "x_{min}" served as the minimum, and "x_{max}" served as the maximum quantity of the dataset.

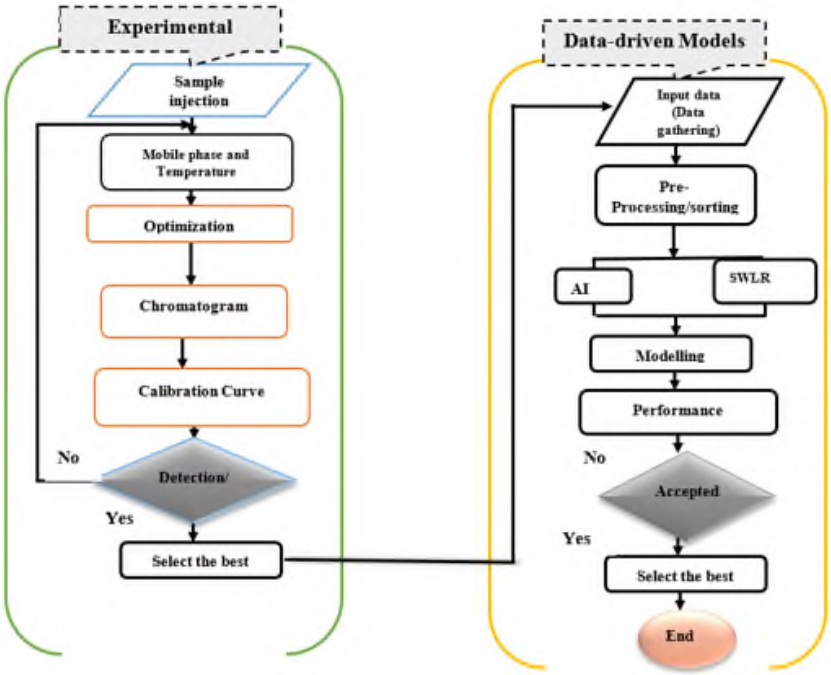

Figure 1. The flow chart of the proposed methodology.

Neuro-fuzzy algorithm

Neuro-fuzzy, a data-intelligence algorithm, mixes fuzzy logic (FL) and neural network learning to handle ambiguous phenomena in collaborative operations. NF is employed as an assessment tool in the field because of its capacity to resemble real functions. On the other hand, the surgeon approach has wider application areas (Choubin, Khalighi-Sigaroodi, Malekian & Kişi, 2016). The defuzzifier and defuzzifier are the basic building blocks of a fuzzy database system. Fuzzy logic involves the use of membership functions to transform input data into fuzzy values ranging from 0 to 1. Nodes that serve as membership functions (MFs) make the input-output relationship modelling possible. Numerous shapes and sizes of the main functions exist, including triangular, sigmoid, gaussian, and trapezoidal (Shojaeimehr & Rahimpour, 2018).

Considering that a first-order Sugeno fuzzy has two inputs (x_1 and x_2) and one output (f), the following principles apply, as shown in Equations (**2**) and Equation (**3**).

$$\text{Law 1 : If } \mu(x_1) is\ A_1\ and\ \mu(x_2) is\ B_1\ then\ f_1 = p_1x_1 + q_1x_2 \quad (2)$$

$$\text{Law 2 : If } \mu(x_1) is\ A_2\ and\ \mu(x_2) is\ B_2\ then\ f_2 = p_2x_2 + q_2x_2 \quad (3)$$

Parameters A_1, B_1, A_2, and B_2 are the main functions for the x_1 and x_2 inputs. The parameters of the outlet function were p_1, q_1, r_1, and p_2, q_2, r_2. The NF structure and formulation were based on a five-layer neural network architecture. Extensive studies have been conducted on the NF model in the literature (Karimi, Kisi, Shiri & Makarynskyy, 2013; Abba, Hadi & Abdullahi, 2017).

Hammerstein-Weiner model

A nonlinear block precedes or opposes a linear dynamic structure in the Hammerstein-Wiener model. The HW was created as a black-box model to identify nonlinear systems. The HW structure is composed of parallel and series-connected nonlinear dynamic and static blocks. Unlike other typical ANNs, the HW model block has been identified as an excellent example that is directly related to linear and nonlinear systems (Abba et al., 2020). The HW model also includes a simple and flexible approach to selecting parametric values for nonlinear models, effectively capturing the physical details of the system properties (Pham et al., 2019).

Multilayer perceptron neural network

A multilayer perception neural network is one of the most prevalent types of ANNs that can handle a nonlinear environment. Compared with other classes of ANNs, researchers consider

this universal approximator (Ghorbani, Deo, Yaseen, Kashani & M0hammadi, 2017). The structure of the MLP consists of an input layer, a hidden layer, and an output layer, as in other well-known ANNs (Kim & Singh, 2014). The signal is translated and sent using weights and biases from the input layer to the output layer through a series of mathematical processes. The Levenberg-Marquardt algorithm was employed as the learning algorithm to reduce the error between the observed and predicted values. The set training procedures were repeated until the intended results were obtained. MLP has an input, one or more hidden layers, and output layers in a structure similar to an ANN.

$$y_i = \sum_{j=1}^{N} w_{ji} x_j + w_{i0} \tag{4}$$

In Equation (**4**), the total number of nodes within the top layer of a node is denoted by N. w_{ji} was the weight between nodes *i* and *j* in the upper layer; x_j was the output derived from node *j*; w_{i0} was the bias in the node *i* and y_i was the input signal of node *i* that crosses through the transfer function.

Evaluation metrics and machine learning methods

In general, linear regression (LR) is one of the most commonly used computational techniques for modelling various input and output variables is linear regression (LR). When choosing the optimal set of parameters for the best prediction accuracy of the output variable, it is important to keep in mind that there is a link between single and multiple variables. According to several modellers, systematic regression is an advancement in selection that makes use of the optimal input dataset by removing or including variables while considering the residual sum of the squares into account (Abba et al., 2020). The SWLR model adheres to the variables' systematic shifts by assessing their effects. To reduce the impact of any variable, each variable that does not support and fulfil the mechanism of the model is eliminated one by one. MLR can be used to explain the concept of the SWLR model (Lee, Han, Lee, & Yoon, 2017).

Any data-driven approach's output accuracy is often evaluated using a variety of metrics based on a comparison of calculated and anticipated values (Usman, Isik, Abba & Meriçli, 2021). To determine the determination coefficient (DC) (Equation (**5**)), correlation coefficient (CC) (Equation (**6**)), and evaluation of the two models (Chandwani, Vyas, Agrawal, & Sharma, 2015), we used two statistical errors, namely root-mean-squared error (RMSE) and mean-squared error (MSE), as shown in Equations (**7**) and (**8**).

$$DC = 1 - \frac{\Sigma_{j=1}^{N}[(Y)_{obs,j} - (Y)_{com,j}]^2}{\Sigma_{j=1}^{N}[(Y)_{obs,j} - \overline{(Y)}_{obs,j}]^2} \tag{5}$$

$$CC = \frac{\Sigma_{i=1}^{N}(Y_{obs} - \overline{Y}_{obs})(Y_{com} - \overline{Y}_{com})}{\sqrt{\Sigma_{i=1}^{N}(Y_{obs} - \overline{Y}_{obs})^2}\Sigma_{i=1}^{N}(Y_{com} - \overline{Y}_{com})^2} \tag{6}$$

$$MSE = \sqrt{\frac{\Sigma_{i=1}^{N}(Y_{obsi} - Y_{comi})^2}{N}} \tag{7}$$

$$MSE = \frac{1}{N}\Sigma_{i=1}^{N}(Y_{obsi} - Y_{comi})^2 \tag{8}$$

Here, N, Y_{obsi}, $\overline{Y}$ *and* Y_{comi} were data number, data observed, average value of the data observed, and computed values, respectively.

Data set and model validation

The data used in the present study were collected from a previous experimental study (Jouyban et al., 2009). The main objective of successful data-driven techniques is to ensure that the model provides a set of data from indicators that can be used as a basis for reliably predicting unknown variables. Considering restrictions like overfitting, the satisfactory training performance may not always match the testing performance. The most important advantage of the k-fold cross-validation procedure is that the validation set and training sets are independent in each round (Samuelsson et al., 2019). Therefore, taking into account k-fold cross-validation, we divided the data in this study into 60% for the calibration (training) phase and 40% for validation. Thus, we have demonstrated the importance of validating the dataset using additional techniques, as reported in a similar study (Abba, Usman, & Isik, 2020).

RESULTS AND DISCUSSION

Retention time is critically important for detecting fraud and misuse in complex matrix media such as food, drinks, drugs, and environmental samples. First, when substances are analysed using chromatographic techniques like HPLC, the retention time serves as a unique fingerprint for the compounds. Deviations from the expected retention times may indicate fraud, such as the addition of foreign chemicals as adulterants or illegal drugs. Analysts can detect potential fraud or adulteration by comparing the retention times of suspicious samples with those of genuine reference standards (Zhang et al., 2024).

Second, in the pharmaceutical industry, retention time is essential for verifying the authenticity of medication compositions. Genuine pharmaceuticals may exhibit different retention properties compared to counterfeit drugs due to the use of substandard or inactive ingredients. Analysts can identify discrepancies that may counterfeit medications by examining the

retention times of excipients and active pharmaceutical ingredients (APIs) (Fine, Mann, & Aggarwal, 2024).

Third, retention time is utilised in forensic toxicology and drug testing to detect and quantify drugs of abuse in biological samples, such as blood, urine, and hair. Variations in the retention time may indicate adulterants or illicit drug analogues, which are substances used to mask drugs in standard screening procedures. Forensic laboratories can enhance the detection of new chemicals or adulterants in biological specimens by developing retention time libraries for well-known drugs and their metabolites (Zhang et al., 2024).

The way machine learning works is based on learning interactions and identifying complex nonlinear patterns in empirical data. These techniques are also effective in the absence of predetermined regression equations with deliberate choices. A regression problem with temperature and mobile phase as independent variables was used to predict and simulate the retention characteristics of psychotropic substances. In this study, the experimental data from previous analyses were applied under various chromatographic conditions. Before modelling, the data were preprocessed with data normalisation and partitioning.

Although HPLC is a well-established technique for determining retention times, it can be time-consuming and resource-intensive. Machine learning models built on existing HPLC data can potentially predict benzodiazepine retention times more quickly and efficiently. This approach might be particularly useful in scenarios requiring rapid analysis or high-throughput screening (Osipenko et al., 2020). However, conducting HPLC experiments, especially with numerous samples or compounds, can be expensive due to the need for specialised equipment, reagents, and skilled personnel. Predictive models can help reduce these costs by minimising the number of samples required for experimental analysis, allowing researchers to focus on the most promising candidates (Sahu et al., 2018).

Furthermore, machine learning models can reveal complex relationships between molecular structures and retention behaviours that are not evident through traditional analytical methods. By analysing a large dataset of benzodiazepines with known retention times, these models can identify structural features or descriptors that significantly influence retention behaviour, offering insights into the molecular mechanisms involved (Usman, Isik, & Abba, 2022).

In analytical laboratories, predictive models can also serve as valuable tools for quality assurance and control. Researchers can quickly identify potential deviations or anomalies by comparing predicted retention times with experimental data, ensuring the accuracy and reliability of analytical results (Isik, Usman, & Abba, 2023). Additionally, machine learning models based on retention time data can be integrated into virtual screening pipelines to prioritise drugs for further experimental validation. By predicting retention times for large libraries of virtual compounds, researchers can accelerate the drug development process by prioritising candidates with suitable retention properties for synthesis or biological testing.

Moreover, while retention time data are crucial for qualitative analysis, particularly in chromatographic separations, analysts must consider the potential impact of matrix effects on retention time predictions. They should take steps to mitigate these effects through method optimisation, sample preparation, and the use of complementary analytical techniques, such as mass spectrometry (MS), to confirm compound identity based on molecular weight, fragmentation patterns, and other structural information. Additionally, calibration curves or standard addition methods can help address matrix effects by accounting for variations in sample composition, ensuring accurate compound identification in complex samples (Gibbs, 2014).

Equation (**1**) was used to standardise the input and target data prior to using the machine learning techniques. The purpose of the normalisation process is to eliminate redundant information and create a uniform scale for the data. The data integrity was improved using the traditional normalisation procedure. The descriptive data and basi details were reported in a previous study (Hadi et al., 2019). The dependent variables CLO, DIA, and OXA have mean and mean values of 3.45%, 4.96%, and 3.75%, respectively. According to the low skewness values, the experimental data were considered reliable for analysis.

The correlation matrix of past experimental data is linearly presented in Figure 2 to highlight the key input variables. Furthermore, the matrix exhibited a weak inverse relationship with temperature and a strong inverse relationship between the mobile phase and the tR of CLO, DIA, and OXA, respectively. The application of traditional modelling techniques to such complex interactions is trivial, as evidenced by the weakness of correlation values; thus, it is imperative to develop more robust and flexible tools.

The optimal architectures for the MLP, HW, SWLR, and NF models was optimised and selected using trial and error. RMSE and MSE were used to describe the error depicted by the models in both the calibration and validation phases, while DC and CC were used to evaluate the simulation results in terms of agreement between the experimental and predicted values. NF and MLP showed a strong agreement between the simulated and experimental tR values. With DC values of 0.9999 and 0.9999 in the calibration and validation phases, respectively, NF exhibited higher performance capabilities than the other three approaches according to a close comparative examination of Table 1.

The ability of these models to handle highly chaotic and complex nonlinear data is demonstrated by the better goodness-of-fit information for DC and CC and the lower RMSE and MSE performance error information for NF and MLP. Performance error of models reporting MSE. A further comparison of performance capabilities revealed that NF improved the prediction

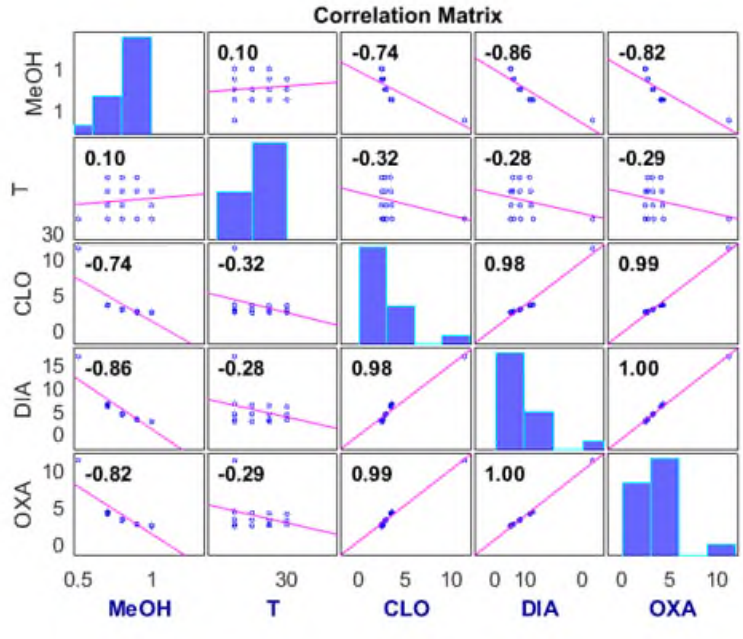

Figure 2. Correlation matrix of the variables.

Table 1. Performance of four different techniques in modelling Clonazepam.

	Calibration				Verification			
	DC	**CC**	**MSE**	**RMSE**	**DC**	**CC**	**MSE**	**RMSE**
NF	0.9999	0.9999	7.60559E-10	2.76E-05	0.9999	0.9999	7.81E-10	2.79E-05
HW	0.647846	0.804889	0.031259399	0.176803	0.6387	0.799187	0.043567	0.208727
MLP	0.999939	0.99997	5.39E-06	0.002321	0.824609	0.90808	9.01E-06	0.003002
SWLR	0.637429	0.798391	0.032184117	0.179399	0.734241	0.856879	1.37E-05	0.003696

accuracy of HW, MLP, and SWLR by 36.03%, 17.53%, and 26.57%, respectively, in the validation phase.

The statistical indices (R2, CC, MSE, and RMSE) used to evaluate the performance prediction of the proposed study were sufficient to assess the effectiveness of the model, taking into account both errors and goodness-of-fit standards. As shown in Table 2, it was possible to observe how well each model performed in terms of the statistical criteria. With an average performance efficiency of 98% compared to 47% for the linear model, the performance results demonstrate the reliability of the non-linear models NF, HW, and MLconcerning SWLR.

To compare the performance results obtained in the current study with those reported in recent literature, Pasin et al. utilised an MLP model to predict the retention time of various new psychoactive substances (NPS), achieving DC values of 0.942. In contrast, the results from our current work using MLP and NF models surpassed those reported by Pasin et al., as indicated by higher DC values (Pasin, Mollerup, Rasmussen, Linnet, & Dalsgaard, 2021). Additionally, previous research implemented a genetic algorithm (GA), multiple linear regression (MLR), and partial least squares (PLS), as well as nonlinear regression techniques, such as kernel PLS (KPLS) and the Levenberg–Marquardt artificial neural network (L–M ANN), to model the retention times of different sedative agents. The correlation coefficients (CC) of the GA-KPLS and L–M ANN models for the training and test sets were 0.921, 0.960, 0.892, and 0.925, respectively. In comparison, the best-performing model in our study, namely NF, demonstrated an exceptional average CC value of 0.9999 in both the training and testing sets for the three psychoactive agents (Noorizadeh, & Noorizadeh, 2012).

Furthermore, Lee et al. applied three models—ANN, support vector machine (SVM), and k-nearest neighbour (k-NN)—to predict the retention times of unknown controlled substances and new psychoactive substances. Using 193 LC–MS-MS barcode spectra as an external test set, the accuracy of the ANN,

Table 2. Performance of four different data-driven technique in modelling Diazepam.

	Calibration				Verification			
	DC	**CC**	**MSE**	**RMSE**	**DC**	**CC**	**MSE**	**RMSE**
NF	0.9998	0.9999	7.968E-10	2.82E-05	0.999997	0.999999	5.41E-10	2.33E-05
HW	0.99911	0.999555	8.47124E-05	0.009204	0.477211	0.690805	0.000108	0.01039
MLP	0.985413	0.99268	0.001389049	0.03727	0.964295	0.981985	7.37E-06	0.002715
SWLR	0.47615	0.690036	0.049883222	0.223346	0.216053	0.464815	0.000162	0.012724

SVM, and k-NN models was 72.5%, 90.0%, and 94.3%, respectively. However, these figures are comparatively lower than those obtained in our current study, particularly for our best-performing models, namely, the NF and MLP (Lee et al., 2022). Hence, based on the literature review, it is evident that the NF and MLP models are robust and serve as effective tools for predicting retention times.

The performance of the models was illustrated using a scatter plot to show the performance errors according to the goodness of fit and the corresponding RMSE values (Figure 3).

The results demonstrate that the three machine learning-based models outperform the traditional SWLR in predicting the tR of the DIA in terms of both goodness of fit and performance error. In addition, the Taylor diagram provides a useful visual tool for comparing the performance of the models (Figure 4). Several statistical measures are described in the Taylor diagram, including standard deviation, CC, DC, and RMSE. Due to its wide range of applications, the Taylor diagram has been used in numerous disciplines, including hydrological modelling, wastewater management, and water engineering. As shown in Figure 4, all machine learning techniques (NF, MLP, and HW) demonstrated greater fitness throughout both the calibration and verification phases. The graph generally indicates that all models demonstrated higher performance and can be used to model the DIA.

Table 3 presents a comparison of four different data-driven methods (MLP, NF, HW, and SWLR models) for OXA simulation in the development of HPLC methods. The results indicate that the MLP model has the most robust predictive capability, marginally surpassing the NF model based on the evaluation parameters employed in this study. The hierarchical order MLP>ANFIS>SWLR>HW can be used to demonstrate the performance effectiveness of the models. In this study, the performance of the models was examined using the CC evaluation metric in both the calibration and validation phases.

Consequently, the principal limitations of the current study include the limited training data and the complexity of retention behaviour. The retention behaviour of psychoactive agents in HPLC is influenced by multiple factors, such as compound structure, polarity, ionisation state, and interactions with the stationary and mobile phases. Accurately capturing the full complexity of retention behaviour in a machine learning model requires advanced feature engineering and sophisticated algorithmic approaches.

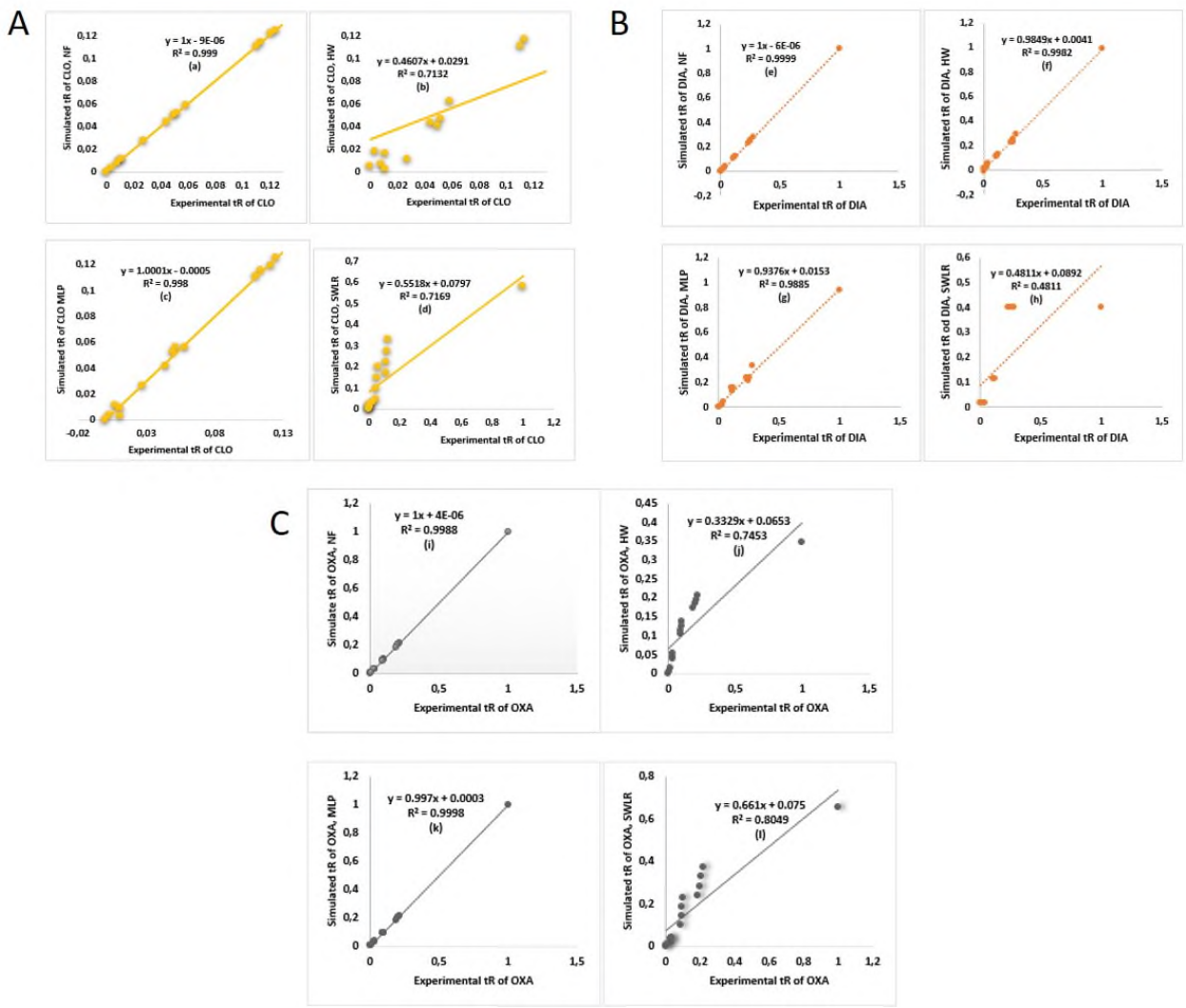

Figure 3. Scatter plots of NF, HW, MLP, and SWLR modelling for tR of CLO (A), DIA (B), and OXA (C), respectively.

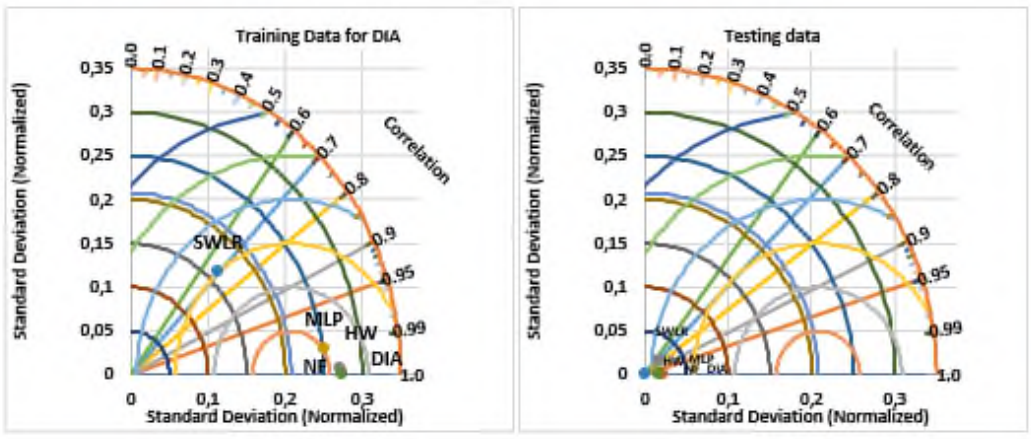

Figure 4. Taylor plot modelling for DIA.

Table 3. Performance of four different data-driven techniques in modelling Oxazepam.

	Calibration				Verification			
	DC	**CC**	**MSE**	**RMSE**	**DC**	**CC**	**MSE**	**RMSE**
NF	0.9988	0.9998	1.84858E-09	4.3E-05	0.999999	0.999999	1.68E-10	1.3E-05
HW	0.470921	0.686237	0.04790947	0.218882	0.221635	0.470781	9.78E-05	0.009891
MLP	0.999881	0.999941	1.07481E-05	0.0032	0.923293	0.960882	9.64E-06	0.003105
SWLR	0.759768	0.871647	0.021753598	0.147491	0.764478	0.874345	2.96E-05	0.005441

CONCLUSION

The effects of different chromatographic settings often influence the estimation of different analytes. In this study, the retention characteristics of three different psychoactive drugs (CLO, DIA, and OXA were modelled under two different mobile phase and column temperature . The performances obtained by the agents demonstrate the accuracy of the machine learning techniques, in particular NF and MLP, which predicted all three drugs with superior performance in both training and testing phases using four different evaluation criteria. The correlation matrix revealed a significant inverse relationship between the dependent variable tR and the mobile phase, leading to the mobile phase as the dominant parameter of column temperature.

In conclusion, the models proposed by MLP and NF can simulate the retention behaviour of each of the three agents. Furthermore, it is recommended to use additional models and optimisation techniques such as support vector machine (SVM), extreme learning machine (ELM), Harris Hawks optimisation (HHO) technique, genetic algorithms (GA), and particle swarm optimisation (PSO), to improve tR in psychoactive drug prediction.

Acknowledgments: The authors appreciate the work by Jouyban et al. (2009) and acknowledge their permission to use the curated data from their study (https://doi.org/10.1002/jssc.200900389) in our current research.

Peer-review: Externally peer-reviewed.

Author Contributions: Conception/Design of Study- A.G.U., E.E., S.I.; Data Acquisition- A.G.U., E.E., S.I.; Data Analysis/Interpretation- A.G.U., E.E., S.I.; Drafting Manuscript- A.G.U., E.E., S.I.; Critical Revision of Manuscript- A.G.U., E.E., S.I.; Final Approval and Accountability- A.G.U., E.E., S.I.

Conflict of Interest: The authors have no conflict of interest to declare.

Financial Disclosure: The authors declared no financial support.

ORCID IDs of the authors

Abdullahi Garba Usman 0000-0001-5660-4581
Emine Erdağ 0000-0002-1431-935X
Selin Işık 0000-0001-7601-3746

REFERENCES

Abba, S.I., Hadi, S.J., & Abdullahi, J. (2017). River water modelling prediction using multi-linear regression, artificial neural network, and adaptive neuro-fuzzy inference system techniques. *Procedia Computer Science, 120*, 75-82. https://doi.org/10.1016/j.procs.2017.11.212

Abba, S. I., Hadi, S. J., Sammen, S. S., Salih, S. Q., Abdulkadir, R. A., Pham, Q. B., Yaseen, Z. M. (2020). Evolutionary computational intelligence algorithm coupled with a self-tuning predictive model for water quality index determination. *Journal of Hydrology, 587*, 124974. https://doi.org/10.1016/j.jhydrol.2020.124974

Abba, S., Usman, A., & I, S. (2020). Simulation for response surface in the HPLC optimization method development using artificial intelligence models: A data-driven approach. *Chemometrics and Intelligent Laboratory Systems, 201*, 104007. https://doi.org/10.1016/j.chemolab.2020.104007

Abba, S. I., Linh, N. T. T., Abdullahi, J., Ali, S. I. A., Pham, Q. B., Abdulkadir, R. A., ... & Anh, D. T. (2020). Hybrid machine learning ensemble techniques for modeling dissolved oxygen concentration. *IEEE Access, 8*, 157218-157237. https://doi.org/10.1109/ACCESS.2020.3017743

Chandwani, V., Vyas, S. K., Agrawal, V., & Sharma, G. (2015). Soft computing approach for rainfall-runoff modelling: a review. *Aquatic Procedia, 4*, 1054-1061. https://doi.org/10.1016/j.aqpro.2015.02.133

Choubin, B., Khalighi-Sigaroodi, S., Malekian, A., & Kişi, Ö. (2016). Multiple linear regression, multi-layer perceptron network and adaptive neuro-fuzzy inference system for forecasting precipitation based on large-scale climate signals. *Hydrological Sciences Journal, 61*(6), 1001-1009. https://doi.org/10.1080/02626667.2014.966721

Cunha, D. L., Mendes, M. P., & Marques, M. (2019). Environmental risk assessment of psychoactive drugs in the aquatic environment. *Environmental Science and Pollution Research, 26*(1), 78-90. https://doi.org/10.1007/s11356-018-3556-z

D'Archivio, A. A. (2019). Artificial neural network prediction of retention of amino acids in reversed-phase HPLC under application of linear organic modifier gradients and/or pH gradients. *Molecules, 24(3)*, 632. https://doi.org/10.3390/molecules24030632

Elkiran, G., Nourani, V., & Abba, S. I. (2019). Multi-step ahead modelling of river water quality parameters using ensemble artificial intelligence-based approach. *Journal of Hydrology, 577*, 123962. https://doi.org/10.1016/j.jhydrol.2019.123962

Erdag, E., Haskologlu, I. C., Mercan, M., Abacioglu, N., & Sehirli, A. O. (2023). An in silico investigation: Can melatonin serve as an adjuvant in NR1D1-linked chronotherapy for amyotrophic lateral sclerosis?. *Chronobiology International, 40*(10), 1395–1403. https://doi.org/10.1080/07420528.2023.2265476

Fine, J., Mann, A. K. P., & Aggarwal, P. (2024). Structure Based Machine Learning Prediction of Retention Times for LC Method Development of Pharmaceuticals. *Pharmaceutical Research, 41*(2), 365–374. https://doi.org/10.1007/s11095-023-03646-2

Ghali, U. M., Usman, A. G., Chellube, Z. M., Degm, M. A. A., Hoti, K., Umar, H., & Abba, S. I. (2020). Advanced chromatographic technique for performance simulation of anti-Alzheimer agent: an ensemble machine learning approach. *SN Applied Sciences, 2*(11), 1-12. https://doi.org/10.1007/s42452-020-03690-2

Ghorbani, M.A., Deo, R.C., Yaseen, Z.M., H. Kashani, M., Mohammadi, B. (2017). Pan evaporation prediction using a hybrid multilayer perceptron-firefly algorithm (MLP-FFA) model: case study in North Iran.*Theoretical and Applied Climatology, 133* , 1119–1131. https://doi.org/10.1007/s00704-017-2244-0

Hadi, S. J., Abba, S. I., Sammen, S. S., Salih, S. Q., Al-Ansari, N., & Yaseen, Z. M. (2019). Non-linear input variable selection approach integrated with non-tuned data intelligence model for streamflow pattern simulation. *IEEE Access, 7*, 141533-141548. https://doi.org/10.1109/ACCESS.2019.2943515

Işık, S., Usman, A., & Abba, S. I. (2023). A chemometrics-based approach for the determination of thymoquinone from Nigella sativa L. (Black Cumin) seeds of different geographical regions using the HPLC technique. İstanbul *Journal of Pharmacy, 53*(3), 320-328. https://doi.org/10.26650/IstanbulJPharm.2023.1181298

Jouyban, A., Soltanpour, S., Acree Jr, W. E., Thomas, D., Agrafiotou, P., & Pappa-Louisi, A. (2009). Modeling the effects of different mobile phase compositions and temperatures on the retention of various analytes in HPLC. *Journal of Separation Science, 32*(22), 3898-3905. https://doi.org/10.1002/jssc.200900389

Karimi, S., Kisi, O., Shiri, J., & Makarynskyy, O. (2013). Neuro-fuzzy and neural network techniques for forecasting sea level in Darwin Harbor, Australia. *Computers & Geosciences, 52*, 50-59. https://doi.org/10.1016/j.cageo.2012.09.015

Kim, S., & Singh, V. P. (2014). Modeling daily soil temperature using data-driven models and spatial distribution. *Theoretical and Applied Climatology, 118*(3), 465-479. https://doi.org/10.1007/s00704-013-1065-z

Lee, J. K., Han, W. S., Lee, J. S., & Yoon, C. N. (2017). A Novel Computational Method for Biomedical Binary Data Analysis: Development of a Thyroid Disease Index Using a Brute-Force Search with MLR Analysis. *Bulletin of the Korean Chemical Society, 38*(12), 1392-1397. https://doi.org/10.1002/bkcs.11308

Lee, S. Y., Lee, S. T., Suh, S., Ko, B. J., & Oh, H. B. (2022). Revealing unknown controlled substances and new psychoactive substances using high-resolution LC–MS-MS machine learning models and the hybrid similarity search algorithm. *Journal of Analytical Toxicology, 46*(7), 732-742. https://doi.org/10.1093/jat/bkab098

Noorizadeh, H., & Noorizadeh, M. (2012). QSRR-based estimation of the retention time of opiate and sedative drugs by comprehensive two-dimensional gas chromatography. *Medicinal Chemistry Research, 21*, 1997-2005. https://doi.org/10.1007/s00044-011-9727-9

Osipenko, S., Bashkirova, I., Sosnin, S., Kovaleva, O., Fedorov, M., Nikolaev, E., & Kostyukevich, Y. (2020). Machine learning to predict retention time of small molecules in nano-HPLC. *Analytical and Bioanalytical Chemistry, 412*(28), 7767-7776. https://doi.org/10.1007/s00216-020-02905-0

Pasin, D., Mollerup, C. B., Rasmussen, B. S., Linnet, K., & Dalsgaard, P. W. (2021). Development of a single retention time prediction model integrating multiple liquid chromatography systems: application to new psychoactive substances. *Analytica Chimica Acta, 1184*, 339035. https://doi.org/10.1016/j.aca.2021.339035

Pham, Q. B., Abba, S. I., Usman, A. G., Linh, N. T. T., Gupta, V., Malik, A., ... & Tri, D. Q. (2019). Potential of hybrid data-intelligence algorithms for multi-station modelling of rainfall. *Water Resources Management, 33*(15), 5067-5087. https://doi.org/10.1007/s11269-019-02408-3

Rodríguez-Díaz, J. M., & Sánchez-León, G. (2019). Optimal designs for multiresponse models with double covariance structure. *Chemometrics and Intelligent Laboratory Systems, 189*, 1-7. https://doi.org/10.1016/j.chemolab.2019.03.009

Sahu, P. K., Ramisetti, N. R., Cecchi, T., Swain, S., Patro, C. S., & Panda, J. (2018). An overview of experimental designs in HPLC method development and validation. *Journal of Pharmaceutical and Biomedical Analysis, 147*, 590-611. https://doi.org/10.1016/j.jpba.2017.05.006

Samuelsson, J., Eiriksson, F. F., Åsberg, D., Thorsteinsdóttir, M., & Fornstedt, T. (2019). Determining gradient conditions for peptide purification in RPLC with machine-learning-based retention time predictions. *Journal of Chromatography A, 1598*, 92-100. https://doi.org/10.1016/j.chroma.2019.03.043

Shojaeimehr, T., & Rahimpour, F. (2018). Retention time modeling of short-chain aliphatic acids in aqueous ion-exclusion chromatography systems under several conditions using computational intelligence methods (artificial neural network and adaptive neuro-fuzzy inference system). *Journal of Liquid Chromatography & Related Technologies, 41*(12), 810-817. https://doi.org/10.1080/10826076.2018.1518846

Silva, J. M., Azcárate, F. J., Knobel, G., Sosa, J. S., Carrizo, D. B., & Boschetti, C. E. (2020). Multiple response optimization of a QuEChERS extraction and HPLC analysis of diclazuril, nicarbazin and lasalocid in chicken liver. *Food Chemistry, 311*, 126014. https://doi.org/10.1016/j.foodchem.2019.126014

Sultanoglu, N., Erdag, E., & Ozverel, C. S. (2023). A single antiviral for a triple epidemic: is it possible?. *Future Virology, 18*(10), 633-642. https://doi.org/10.2217/fvl-2023-0048

Tayyebi, S., Hajjar, Z., & Soltanali, S. (2019). A novel modified training of radial basis network: Prediction of conversion and selectivity in 1-hexene dimerization process. *Chemometrics and Intelligent Laboratory Systems, 190*, 1-9. https://doi.org/10.1016/j.chemolab.2019.05.005

Tomić, J., Ivković, B., Oljačić, S., Nikolić, K., Maljurić, N., Protić, A., & Agbaba, D. (2020). Chemometrically assisted RP-HPLC method development for efficient separation of ivabradine and its eleven impurities. *Acta Chromatographica, 32*(1), 53-63. https://doi.org/10.1556/1326.2019.00659

Usman, A. G., Işik, S., & Abba, S. I. (2020). A novel multi-model data-driven ensemble technique for the prediction of retention factor in HPLC method development. *Chromatographia, 83*(8), 933-945. https://doi.org/10.1007/s10337-020-03912-0

Usman, A. G., Işik, S., & Abba, S. I. (2021). Hybrid data-intelligence algorithms for the simulation of thymoquinone in HPLC method development. *(7)*Journal of the Iranian Chemical Society, 18, 1537-1549. https://doi.org/10.1007/s13738-020-02124-5

Usman, A. G., Işik, S., & Abba, S. I. (2022). Qualitative prediction of Thymoquinone in the high-performance liquid chromatography optimization method development using artificial intelligence models coupled with ensemble machine learning. *Separation Science Plus, 5*(10), 579-587. https://doi.org/10.1002/sscp.202200071

Usman, A. G., Işik, S., Abba, S. I., & Meriçli, F. (2021). Chemometrics-based models hyphenated with ensemble machine learning for retention time simulation of isoquercitrin in Coriander sativum L. using high-performance liquid chromatography. *Journal of Separation Science, 44*(4), 843-849. https://doi.org/10.1002/jssc.202000890

Zhang, Y., Liu, F., Li, X. Q., Gao, Y., Li, K. C., & Zhang, Q. H. (2024). Generic and accurate prediction of retention times in liquid chromatography by post–projection calibration. *Communications Chemistry, 7*(1), 54. https://doi.org/10.1038/s42004-024-01135-0

How cite this article

Usman, A.G., & Erdağ, E., & Işık, S. (2024). Effects of chromatographic conditions on retention behaviour of different psychoactive agents in high-performance liquid chromatography: A machine-learning-based approach. *İstanbul Journal of Pharmacy, 54*(2), 133–143. DOI: 10.26650/IstanbulJPharm.2024.1225463

İstanbul Journal of Pharmacy
Istanbul J Pharm2024, 54 (2): 144–153
DOI: 10.26650/IstanbulJPharm.2024.1362394

Original Article

Detection of antibiotic resistance genes in bacterial isolates from most touched surfaces of public transports in Sagamu, Ogun state, Nigeria

Oluwatoyin B. Famojuro[1], Tayo I. Famojuro[2], Monioluwa E. Mayungbe[3], Oluremi B. Oluwatobi[4]

[1]Olabisi Onabanjo University, Department of Pharmaceutical Microbiology, Ogun State, Nigeria
[2]Bingham University, Department of Pharmacognosy, Karu, Nasarawa State, Nigeria
[3]Olabisi Onabanjo University, Department of Pharmaceutical Microbiology, Ogun State, Nigeria
[4]University of Ibadan, Department of Pharmaceutical Microbiology, Ibadan, Nigeria

ABSTRACT

Background and Aims: The role of fomites in the transmission of infectious diseases is becoming more important because of the possibility that contaminated surfaces act as reservoirs of diseases. The aim of this study was to ascertain the level of bacterial contamination and the prevalence of antibiotic-resistant genes on the most touched surfaces on public transport.

Methods: One hundred samples were collected from door handles and armrests of buses and tricycles, respectively at Isale-Oko motor garage, Sagamu. Bacteria were isolated from the samples and identified following standard microbiological techniques. Antibiotic susceptibility testing was done with the Kirby-Bauer disc diffusion method. The presence of antibiotic-resistant genes-*vanA, drfA, dfrG* genes, and extended-spectrum betta-lactamase (ESBL) genes in Gram-negatives were screened by polymerase chain reaction (PCR) method.

Results: Out of the samples tested, 91% were positive for bacterial contamination. Among the 91 positive samples, 126 bacteria were identified, comprising 98 Gram-positive and 28 Gram-negative bacterial isolates. *Staphylococcus aureus* had the highest overall frequency of occurrence with 62 (49.2%) isolates. Among the Gram-positives, azithromycin resistance was present in 35(56.5%) *S. aureus* and 19(52.8%) *Staphylococcus epidermidis. Salmonella* species was the most resistant to ciprofloxacin (100%). *dfrG* was the most detected among trimethoprim-resistant genes occurring in 11(55%) of multidrug-resistant *S. aureus* and 6(54.6%) of *S. epidermidis*. *vanA* gene was present in *S. aureus* (20%). *dfrA* was present in only *Klebsiella pneumoniae* and *Esherichia coli. E. coli* and *Shigella* species carried bla_{TEM} while bla_{SHV} was found in *Pseudomonas aeruginosa*.

Conclusion: The most-touched surfaces of public transportation can serve as a substantial source of spread for potentially harmful bacteria.

Keywords: Antibiotic resistance, Extended-spectrum beta-lactamase, Bacterial isolates, Public transportation

INTRODUCTION

Any environment including soil, air, water, food, and other organisms, as well as environmental surfaces or items, might include pathogenic organisms (Nwankwo, Okey-kalu, & Eze, 2023). The transportation networking system is constantly increasing to fulfill the demand of carrying heavy loads of products and the movement of people from one location to another. There have been countless reports of how the development and extension of global transportation networks have promoted widespread outbreaks of communicable illnesses (Guimera, Mossa, Turtschi, & Amara, 2005; Tatem, Rogers, & Hay, 2006; Rodrigue, 2020). The effectiveness and accessibility of contemporary transportation networks put people in danger of novel strains of pathogenic microbes (Tatem *et al*., 2006). The World Health Organization has issued a warning about the pandemic status of several diseases resulting from the global dissemination of pathogenic microbes (WHO, 2020).

Handles, chairs, anchors, floors, and windows of public buses are all potential breeding grounds for infectious germs (Rusin, Maxwell, & Gerba, 2002; Chowdhury *et al*., 2016). Buses in use are hardly ever cleaned, and when they are, the technique is limited to the removal of visible dirt or stains (Yeh, Simon, Millar, Alexander, & Franklin, 2011). The unsanitary and humid conditions of buses contribute to the accumulation of microbes on contact surfaces and human contact with microbes from these reservoirs can cause mild to serious infection that can be harmful to humans (Rusin *et al*., 2002; Chowdhury *et al*., 2016). Passengers who do not cover their mouths when

Corresponding Author: Oluwatoyin B. Famojuro **E-mail:** olaniran.oluwatoyin@oouagoiwoye.edu.ng
Submitted: 20.09.2023 • **Revision Requested:** 03.12.2023 • **Last Revision Received:** 04.01.2024 • **Accepted:** 08.02.2024

coughing or sneezing can significantly increase the number of microorganisms in the air (Birteksöz Tan, & Erdoğdu, 2017). People sitting closely together in a confined setting and breathing the same air pose the greatest risk for respiratory-related infectious diseases in these vehicles (Furuya, 2007). A serious worry is the spread of infectious diseases by contact with hands. Hand washing, which is widely recognized as the first step in stopping the transmission of infections, has been neglected and must be strongly promoted by individuals, families, schools, and medical practitioners (Nwankwo *et al*., 2023).

Much research had been done on microbial contamination on public hand-touched surfaces such as those on buses, trains, cellphones, hand knobs, ATMs, hospitals, shopping carts, and other surfaces (Choudhary *et al*., 2016; Bhatta *et al*., 2018; Kahsay, Asgedom, & Weldetinsaa, 2019). *Escherichia coli*, multidrug-resistant *Staphylococcus aureus*, coagulase-negative staphylococci, and *Enterococcus* species are among the commonly reported pathogens that have been isolated from hand-touch surfaces (Ashgar and El-Said, 2012; Chowdhury *et al*., 2016; Birteksöz Tan, and Erdoğdu, 2017; Kahsay *et al*., 2019). Antimicrobial resistance (AMR) has become a public health problem (Allcock *et al*., 2017). The dangers presented by AMR to people's health are especially worrying in developing countries due to limited access to healthcare services, high prevalence of transmissible diseases in the general population, and increased risk of community-acquired resistant infections resulting in greater mortality, extended hospital stays, and more expensive healthcare (WHO, 2021). Although several studies have reported the presence of pathogenic bacteria in public transport, information on antibiotic susceptibility patterns and genes associated with antibiotic resistance is scanty.

It has been established that resistant bacteria can spread to people in a variety of environments, most especially, crowded locations in densely populated urban areas such as public transportation, sporting venues, and schools (Cave, Cole, & Mkrtchyan, 2021). Bacteria from the hospital can also be spread to the community through the public transport system. The Isale-Oko motor garage was chosen as our sample location due to its proximity to the second gate of Olabisi Onabanjo University Teaching Hospital, where most patients and their guests normally board. This study investigated the bacterial burden of buses and tricycles in the Isale-Oko motor garage to determine the role of commuter transport in the transmission of bacteria that could cause serious infections in people and to detect antibiotic resistance genes in bacterial isolates from public transports.

MATERIALS AND METHODS

Sampling site

Samples were collected from randomly selected inter-state public buses and armrests of tricycles in Isale-Oko Motor Garage, Sagamu. Isale-Oko Car Park in Sagamu is one of the motor garages in Sagamu for intra- and inter-state transportation, and it is quite close to the second gate of Olabisi Onabanjo University Teaching Hospital, Sagamu, Ogun state, Nigeria.

Collection of samples

One hundred (100) samples were taken from door handles of public buses and armrests of tricycles. Samples were taken from each area by swabbing a 4 cm^2 section with a sterile cotton swab stick that had been dipped in sterile normal saline and transported to Pharmaceutical Microbiology Laboratory, Faculty of Pharmacy, Olabisi Onabanjo University, Sagamu, Ogun State within 15 minutes of collection for culturing.

Isolation and identification of bacterial isolates

The swab was inoculated into nutrient broth and incubated at 37°C for 24 hours. A loopful from a 24-hour-old culture was used to inoculate the surface of Mannitol salt agar, MacConkey agar, cetrimide agar, and Salmonella-Shigella agar. The culture plates were incubated at 37°C for 24 hours and observed for growth and colony appearance. Lactose-fermenters were streaked on the surface of Eosin methylene blue agar. Biochemical characteristics of the isolates were determined according to standard protocol (Cheesbrough, 2006).

Antibiotic susceptibility testing

Antibiotic susceptibility tests for selected isolates were performed according to the method of Bauer, Kirby, Sherris, & Turck, (1966). The antibiotic sensitivity of enteric bacterial isolates was evaluated using commonly available standard antibiotic discs of imipenem (10 µg), cefotaxime (30 µg), ciprofloxacin (5 µg), cefepime (30 µg), cephalexin (30 µg), azithromycin (15 µg), meropenem (10 µg), Trimethoprim (5 µg), cefoxitin (30 µg), amoxicillin-clavulanic acid (20/10 µg), amikacin (30 µg), ceftazidime (30 µg) and aztreonam (30 µg) [Mast Group, United Kingdom]. The required bacterial suspension was made in nutrient broth by inoculating 5 ml sterile nutrient broth with 3-4 colonies from 18 hours old culture of the isolate and the turbidity of the culture was adjusted to 0.5 McFarland standard. A cotton swab was dipped in the culture suspension and streaked over the solidified Mueller-Hinton agar medium's surface to create a homogenous inocula. Using a sterile pair of forceps, the antibiotic discs were then arranged appropriately on the surface of the seeded plates and left on the bench at 25°C for 30 minutes to diffuse the antibiotic in the media. Following a 24-hour incubation period at 37°C, the diameter of the clear zone growth of inhibition was measured and interpreted in accordance with the standard provided by the Clinical and Laboratory Standards Institute (CLSI, 2022).

Amplification of antibiotic resistance genes in Gram-positive isolates

DNA was extracted using the previously known quick alkaline lysis procedure (Dutka-Malen, Evers, & Courvalin, 1990). PCR was performed on a DNA thermal cycler (Applied Biosystem, USA) in a final volume of 25 µL containing 1 µL of DNA template; 1 µL each of forward and reverse primer (0.2 pmol/µL), 12.5 µL of master mix (Wizbiosolutions, South Korea) and 9.5 µL of sterile filtered water. The primer sequence used in this study is presented in Table 1.

The PCR condition comprised initial denaturation at 95°C for 10 minutes, followed by 30 cycles of 45 seconds at 94°C, 45 seconds at 54°C (*vanA*), 55oC (*dfrA* and *dfrG*), and 1 minute at 72oC, with a final extension for 8 minutes at 72oC.

The PCR condition for ESBL genes involves initial denaturation at 94°C for 10 minutes and 30 cycles of denaturation at 94°C for 40 seconds, annealing at 50°C (bla_{TEM} and bla_{SHV}), 56°C (bla_{CTX-M}) for 40 seconds and elongation 72°C for 1 minute with a final elongation step at 72°C for 7 minutes.

Electrophoresis of PCR products was performed on a 1.5% agarose gel containing 0.5 mg/ml of ethidium bromide at 100 volts for 1 hour using a 100 bp marker as standard. The varied bands were seen after migration while illuminated by UV light.

Statistical analysis

The descriptive data were presented in terms of relative frequency.

RESULTS

Collection and culturing of samples and identification of bacterial isolates from public transport door handles

Out of the 100 public transport door handles swabbed, 91 samples were positive for bacterial growth. Table 1 shows the number of isolates and the types of bacterial species found on the door handles of the vehicles swabbed. One hundred and twenty-six (126) bacterial isolates were cultured from the 91 positive samples, including 98 Gram-positive- and 28 Gram-negative bacterial isolates. The bacteria species found were *S. aureus, S. epidermidis, P. aeruginosa, E. coli, K. pneumoniae, K. oxytoca, Shigella* species, and *Salmonella* species. *S. aureus* had the highest overall frequency of occurrence with a total of 62 (49.2%) isolates followed by *S. epidermidis* with 36 (28.6%) isolates out of the total 126 bacterial isolates while *K. oxytoca* and *Salmonella species* were the least having the same frequency of 1 (0.8%) isolate.

Antibiotic resistance patterns of bacteria isolated from the door handle

The susceptibility patterns of the bacterial isolates to antibiotics are presented in Table 2. Resistance to cefoxitin was found in 35 (56.5%) of *S. aureus* and 15 (44.4%) of *S. epidermidis*. Also, 21 (58.3%) and 43 (69.4) of *S. epidermidis* and *S. aureus*, respectively were resistant to trimethoprim. Only *S. aureus* and *E. coli* were resistant to imipenem with *E. coli* being the most resistant isolate (14.3%). The highest resistance to cefotaxime (55.6%) was observed in *S. epidermidis* while *K. oxytoca* and *Salmonella* species were totally sensitive to cefotaxime. *Salmonella* species was the most resistant to ciprofloxacin (100%) while only *S. aureus* was resistant to meropenem (1.6%). *Salmonella* species was totally resistant to ciprofloxacin, cefepime, and aztreonam (100%). Table 3 shows the antibiotic resistance profile of multidrug-resistant isolates. Among the Gram-positive isolates, 31(31.6%) out of 98 isolates were resistant to three or more classes of antibiotics, 20(64.5%) of which were *S. aureus* isolates the remaining 11 (35.5%) were *S. epidermidis*. Only 4(14.3%) out of 28 Gram-negative bacterial isolates were multidrug resistant.

Detection of antibiotic resistance genes in MDR Gram-positive and Gram-negative isolates from public transport

Twenty multidrug-resistant *S. aureus* and 11 multidrug-resistant *S. epidermidis* were screened for the occurrence of trimethoprim resistance genes (*dfrA, dfrD*, and *dfrG*) and vancomycin resistance gene *vanA*, out of which 3 (15%) and 11 (55%) of the multidrug-resistant *S. aureus* carried *dfrA* and *dfrG*, respectively. The *dfrA* and *dfrG* genes were found in 1 (9.1%) and 6 (54.6%) *S. epidermidis*, respectively (Table 4). *vanA* gene was present in 4 (20%) of *S. aureus* but not found in *S. epidermidis* (Figure 1). The coexistence of *dfrA* and *dfrG* was discovered in one *S. aureus*. Among the Gram-negative bacteria, *dfrA* was present in only *K. pneumoniae* and *E. coli* (Figures 2-3)

Three (75.0%) of multidrug resistant Gram-negative isolates (*E. coli, P. aeruginosa* and *Shigella* species) had ESBL genes. *E. coli* and *Shigella* species carried bla_{TEM} while bla_{SHV} was found in only *P. aeruginosa*. None of the four MDR isolates had bla_{CTX-M} (Figure 4).

Table 1. Primer sequences of antibiotic resistance genes

Genes	Primer sequence	Amplicon sizes (bp)	Reference
dfrA	F: 5´-AGCTACTCTTTAAAGCCTTGACGTA-3´	341	Grape *et al.* (2007)
	R: 5´-GTGTTGCTCAAAAACAACTTCG-3´		
dfrG	F: 5´-TGCTGCGATAAGAA-3´	405	Argudin *et.al.* (2011)
	R: 5´-TGGGCAAATACCTCATTCC-3´		
vanA	F-5'GGGAAAACGACAATTGC-3'	732	Dutka-Maleen *et.al.* (1995)
	R-5'GTACAATGCGGCCGTTA-3'		
bla_{SHV}	F-5'TCGCCTGTGTATTATCTCCC-3'	768	Maynard *et al.* (2003)
	R-5' CGCAGATAAATCACCACAATG-3'		
bla_{TEM}	F-5'GAGTATTCAACATTTTCGT-3'	857	Maynard *et al.* (2003)
	R-5' ACCAATGCTTAATCAGTGA-3'		
bla_{CTX-M}	F-5'TTTGCGATGTGCAGTACCAGTAA-3'	544	Edelstein *et al.* (2003)
	R-5'CGATACGTTGGTGGTGCCATA-3'		

Table 2. Frequency of isolated bacterial species

Isolated bacterial species	No of isolated bacteria	Isolated bacteria (%)
S. aureus	62	49.2
S. epidermidis	36	28.6
P. aeruginosa	11	8.7
E. coli	7	5.6
K. pneumoniae	4	3.2
K. oxytoca	1	0.8
Shigella species	4	3.2
Salmonella species	1	0.8
Total	**126**	**100**

Table 3. Antibiotic resistance profile of bacterial isolates

Isolate (Number)	Number of bacterial isolates (%)												
	IMI	CTX	CIP	CFP	CLX	AZM	TM	MEM	FOX	AUG	AK	CAZ	ATM
S. aureus (62)	2(3.2)	31(50)	11(17.7)	19(30.6)	10(16.1)	35(56.5)	43(69.4)	1(1.6)	35(56.5)	5(8.1)	4(6.5)	52(83.9)	-
CoNS (36)	0(0.0)	20(55.6)	7(19.4)	10(27.8)	3(8.3)	19(52.8)	21(58.3)	0(0.0)	15(44.4)	0(0.0)	1(2.8)	31(86.1)	-
P. aeruginosa (11)	0(0.0)	2(18.2)	1(9.1)	1(9.1)	9(81.8)	-	-	0(0.0)	3(27.3)	1(9.1)	0(0.0)	1(9.1)	2(18.2)
E. coli (7)	1(14.3)	1(14.3)	2(28.6)	2(28.6)	5(71.4)	-	-	0(0.0)	3(42.9)	1(14.3)	0(0.0)	1(14.3)	1(14.3)
K. pneumoniae (4)	0(0.0)	1(25)	0(0.0)	0(0.0)	2(50.0)	-	-	0(0.0)	1(25)	0(0.0)	0(0.0)	1(25)	1(25)
K. oxytoca (1)	0(0.0)	0(0.0)	0(0.0)	0(0.0)	0(0.0)	-	-	0(0.0)	1(100)	0(0.0)	0(0.0)	0(0.0)	0(0.0)
Shigella species (4)	0(0.0)	1(25)	0(0.0)	0(0.0)	1(25.0)	-	-	0(0.0)	2(50)	1(25)	0(0.0)	1(25.0)	1(25)
Salmonella species (1)	0(0.0)	0(0.0)	1(100)	1(100)	1(25.0)	-	-	0(0.0)	0(0.0)	0(0.0)	0(0.0)	0(0.0)	1(100)

Note: IMI = imipenem; CTX = cefotaxime; CIP = ciprofloxacin; CFP = cefepime; CLX = cephalexin; AZM = azithromycin; TM = trimethoprim; MEM = meropenem; FOX = cefoxitin; AUG = amoxicillin clavulanic acid; AK = amikacin; CAZ = ceftazidime; ATM = aztreonam

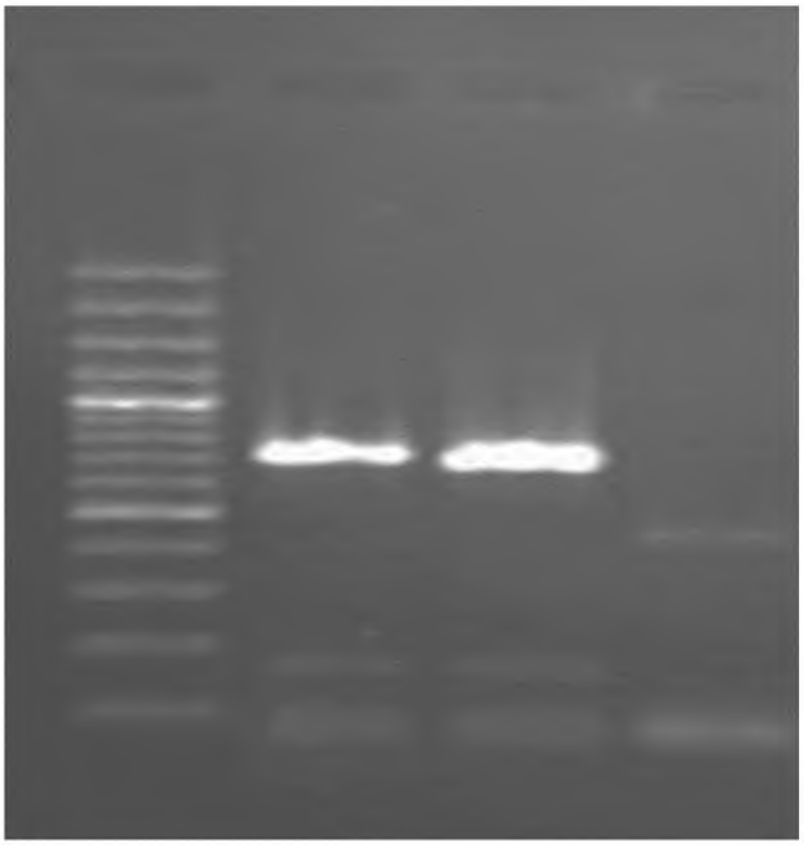

Figure 1. Gel representation of amplified *vanA* (732 bp). *(L = 100bp ladder; lanes 2-4 = S. aureus)*

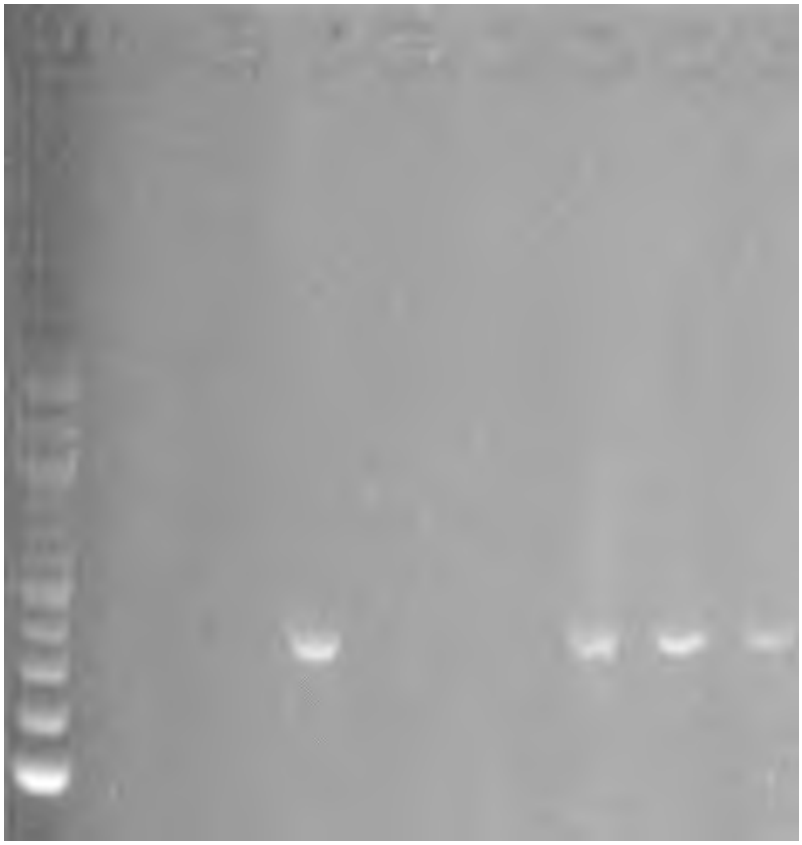

Figure 2. Gel representation of amplified dfrA5 (341 bp). *(L = 100bp ladder; lanes 2-10 = S. aureus)*

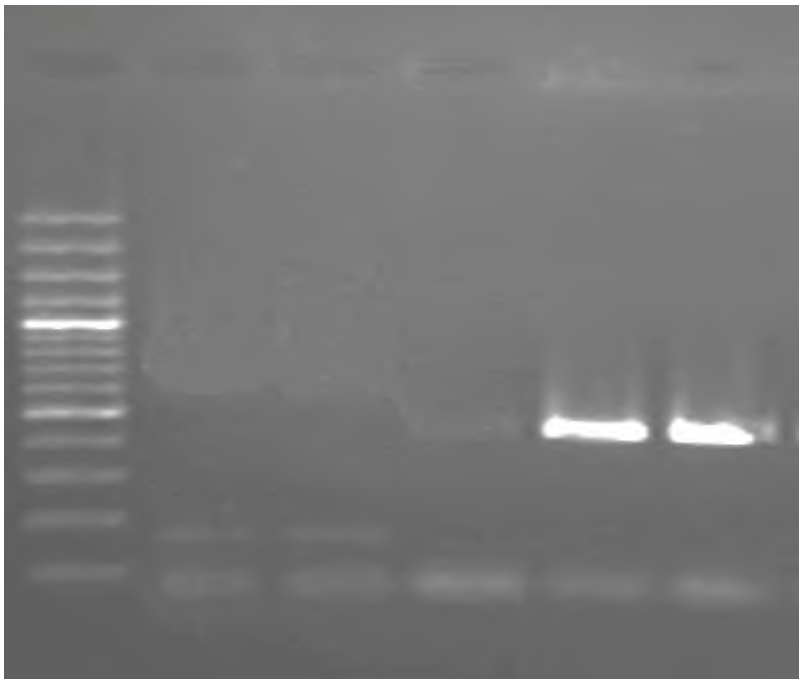

Figure 3. Gel representation of amplified *dfrG* (405 bp). *(L = 100bp ladder; lanes 2-5 = 85, 94a, 97, 100 (S. aureus); Lane 6 = 22a (S. epidermidis))*

Figure 4. Gel representation of amplified bla_{SHV} (768 bp) and bla_{TEM} (857 bp). *(L = 100bp ladder; 89b = P. aeruginosa, 80b =Shigella species, 37b = K. pneumoniae, 76b = E. coli)*

DISCUSSION

This study found bacterial contaminants in 91% of samples obtained from public transportation door handles and armrests, which was consistent with the findings of Otter & French (2009), who found bacterial isolates in 95% of samples taken. The increase in bacterial contamination seen in this study could be related to frequent contact between passengers' palm skin and the most frequently touched surfaces of public transit. Despite these surfaces being non-porous and unsuitable for microbial growth, a considerable number of microbes have been found on hand-touch surfaces in buses, trains, mobile phones, door handles, and computer keyboards (Yeh *et al*., 2011; Choudhary *et al*., 2016). Several factors contribute to the high number of bacteria on public transport, including frequent skin contact brought about by frequent use, crowdedness, lack of routine bus cleaning, lax public cleanliness standards, and passengers' lack of information. Thus, transportation through exposed surfaces represents a means by which passengers may become infected with the germs besides other routes such as food consumption (Choudhary *et al*., 2016).

This study found that *S. aureus, S. epidermidis, E. coli, Klebsiella* species, and *P. aeruginosa* were present on the door handles and armrests of public transport. Nwankwo *et al*. (2023) also reported similar results including the presence of *Streptococcus faecalis, Enterobacter* species, *Micrococcus* species, and *Bacillus* species which were not isolated in this study. *S. aureus* was the most predominant isolate in this study with a prevalence of 49.2% which was higher than the 8% reported by Otter and French (2009) whereas *Bacillus* species was the most often isolated species (20.5%) reported by Nwankwo *et al*. (2023). Hand-touch sites could get contaminated with staphylococci and may be sources of bacterial transmission between humans, potentially serving as a reservoir for community-associated methicillin-resistant *S. aureus* (CA-MRSA) in high-incidence areas (Otter and French, 2009).

The proportion of Gram-negative isolates (22.2%) found in this study was lower than that of Gram-positives (77.8%), which is consistent with the work of Kahsay *et al*. (2019), who found a prevalence of 18.2% in Gram-positives but differs from a report from Nigeria, which found the highest prevalence (57.5%) of Gram-negative bacteria (Nwankwo *et al*., 2023). This study also isolated *Shigella* and *Salmonella* species in agreement with the report by Choudhary *et al*. (2016). Kahsay *et al*. (2019) isolated *E. coli* on hand-touch surfaces of public buses, however, they were unable to identify common enteric pathogens such as *Salmonella* and *Shigella* species. The presence of enteric organisms such as *E. coli, Klebsiella* species, *Shigella*, and *Salmonella* species on touch surfaces of public transport in this

study is worrisome because these isolates are the most prevalent agents of gastrointestinal illnesses in people. The presence of enteric pathogens on touch surfaces for a significant amount of time indicates fecal-oral transmission and indicates a lack of sufficient hygiene management (Choudhary *et al*., 2016).

Antibiotic resistance has become a rising concern around the world (Olaniran, Adeleke, Donia, Shahid, & Bokhari, 2021; WHO, 2021). It was observed in this study that 11 (39.3%) and 20 (20.4%) of Gram-negative and Gram-positive isolates, respectively were multidrug resistant. Multidrug resistance was defined as resistance to at least one agent in three or more classes of antibiotics (Magiorakos *et al*., 2012). The isolates' patterns of resistance to test antibiotics foretell the establishment of serious illnesses once the individuals become infected (Choudhary *et al*., 2016). This study found that a significant percentage of *S. aureus* (56.5%) was resistant to cefoxitin, but Kahsay *et al*. (2019) observed a lower resistance rate of 31.5% to cefoxitin, which necessarily means resistant to methicillin (Fernandes, Fernandes, & Collignon, 2005). Choudhary *et al*. (2016) also documented methicillin-resistant *S. aureus* in samples taken from public transport. Co-trimoxazole (trimethoprim and sulfamethoxazole combination) is an effective antibacterial for the treatment of skin and soft tissue infections caused by community-associated methicillin-resistant *S. aureus* (Montravers & Eckmann, 2021). This study revealed a 28.6% ciprofloxacin resistance rate against *E. coli* from touch surfaces of public transport, but Kahsay *et al*. (2019) reported a 37.5% ciprofloxacin resistance rate. Imipenem, meropenem, ciprofloxacin, and amikacin were effective against Gram-negative isolates in this study.

The presence of *dfrG* gene in *S. aureus* has been documented (Reeve *et al*., 2016). The highest frequency of *dfrG* genes (55%) responsible for trimethoprim resistance in *Staphylococcus* species was also observed in this study. Nurjadi *et al*. (2014) demonstrated that the *dfrG* gene is widespread and the frequently observed genetic source of trimethoprim resistance in MSSA and MRSA from sub-Saharan Africa. The presence of *dfrG* and *dfrA* genes was found in 100% and 13.3% MRSA, respectively (Rosato *et al*., 2020). Moreover, Coelho *et al*. (2017) reported a higher prevalence of *dfrG* gene (78%) compared with the *dfrA* gene (19%) in *S. aureus* isolates from African countries. Shittu *et al*. (2011) documented the absence of the *dfrA* gene in trimethoprim-resistant *S. aureus* isolates and suggested that mutation of the dihydrofolate reductase is responsible for resistance. In another study, trimethoprim resistance was linked to the presence of *dfrG* and *dfrA* genes in *S. aureus* (Rosato *et al*., 2020).

The presence of *dfr* genes in Gram-negative bacteria has been linked with class 1 integrons (Grape, Motakefi, Pavuluri, & Kahlmeter, 2007). Class 1 integrons were discovered to be a major genetic basis of trimethoprim resistance in Gram-negative bacteria, and the presence of *dfrA* has been attributable to the horizontal transfer of class 1 integrons via conjugative plasmids (Yu, Lee, Kang, Yeong, 2004; Domínguez *et al*., 2019). The relationship between *dfr* genes and mobile genetic elements like plasmids and integrons is crucial to understanding why trimethoprim resistance is increasingly evolving, and spreading (Domínguez *et al*., 2019).

Even though this study found a low incidence of MDR Gram-negative isolates, 75% of them have ESBL genes. ESBL genes have been found in Gram-negative isolates from a variety of sources, including pathological specimens, hospital devices, and surroundings (Atata *et al*., 2010; Olaniran, Adeleke, Donia, Shahid, & Bokhari, 2021). Furthermore, the proximity of the Isale-Oko motor park to the teaching hospital could contribute to the spread of multidrug-resistant strains, as most patients visiting the hospital will, in some way, get to the garage to board a vehicle. This could lead to the spread of community-acquired infection.

CONCLUSION

The findings reveal that public tricycles and buses can serve as a reservoir for the propagation of potentially harmful bacteria. The movement of people from the hospital environment to the motor park may be the cause of the higher levels of antibiotic resistance seen in this study when compared to previous studies. The detection of multidrug-resistant strains carrying antibiotic-resistant genes is worrisome. Therefore, frequent handwashing after exiting public transport and regular disinfection of public vehicles is highly recommended to curtail the spread of infectious pathogens.

Peer-review: Externally peer-reviewed.

Author Contributions: Conception/Design of Study- O.B.F., T.I.F.; Data Acquisition- M.E.M., O.B.O.; Data Analysis/Interpretation- O.B.F., T.I.F., M.E.M., O.B.O.; Drafting Manuscript- O.B.F., M.E.M.; Critical Revision of Manuscript- O.B.F., T.I.F., O.B.O.; Final Approval and Accountability- O.B.F., T.I.F., M.E.M., O.B.O.

Conflict of Interest: The authors have no conflict of interest to declare.

Financial Disclosure: The authors declared no financial support.

ORCID IDs of the authors

Oluwatoyin B. Famojuro	0000-0001-7206-3762
Tayo I. Famojuro	0000-0001-6218-3189
Monioluwa E. Mayungbe	0009-0004-2701-7440
Oluremi B. Oluwatobi	0000-0002-4614-1736

REFERENCES

Allcock, S., Young, E.H., Holmes, M., Gurdasani, D., Dougan, G., Sandhu, M.S., ... Török, M.E. (2017). Antimicrobial resistance in human populations: challenges and opportunities. *Global Health Epidemiology and Genomics*, 10(2): Article e4. http://dx.doi.org/10.1017/gheg.2017.4

Argudın, M.A., Tenhagen, B.A., Fetsch, A., Sachsenro¨der, J., Ka¨sbohrer, A., Schroeter, A., ... Guerra, B. (2011). Virulence and resistance determinants of German *Staphylococcus aureus* ST398 isolates from nonhuman sources. *Applied Environmental Microbiology*, 77, 3052–3060. http://dx.doi.org/10.1128/AEM.02260-10.

Ashgar, S.S. &El-Said, H.M. (2012). Pathogenic bacteria associated with different public environmental sites in Mecca City. *Open Journal of Medical Microbiology*, 2, 133–137. http://dx.doi.org/10.4236/ojmm.2012.24020

Atata, R.F., Ibrahim, Y.K.E., Olurinola, P.F., Giwa, A., Akanbi, A.A. & Sani, A.A. (2010). Clinical bacterial isolates from a hospital environment as agents of surgical wound nosocomial infections. *Journal of Pharmacy and Bioresources*, 7(2), 146-155 http://dx.doi.org/10.4314/jpb.v7i2.15

Bauer, A.W., Kirby, W.M., Sherris, J.C. & Turck, M. (1966). Antibiotic susceptibility testing by a standardized single disk method. *American Journal of Clinical Pathology*,45(4), 493-496.

Bhatta, D.R., Hamal, D., Shrestha, R. Hosuru Subramanya, S., Baral, N., Singh, R.K., ... Gokhale, S. (2018). Bacterial contamination of frequently touched objects in a tertiary care hospital of Pokhara, Nepal: how safe are our hands? *Antimicrobial Resistance and Infection Contro*,. 7, 97. http://dx.doi.org/10.1186/s13756-018-0385-2

Birteksöz Tan, A.S. & Erdoğdu G. (2017). Microbiological burden of public transport vehicles. *Istanbul Journal of Pharmacy*, 47(2), 52-56. http://dx.doi.org/10.5152/IstanbulJPharm.2017.008

Cave, R., Cole, J. & Mkrtchyan, H.V. (2021). Surveillance and prevalence of antimicrobial resistant bacteria from public settings within urban built environments: Challenges and opportunities for hygiene and infection control. *Environment International*, 157: Article 106836. http://dx.doi.org/10.1016/j.envint.2021.106836.

Cheesbrough, M. (2006). District Laboratory Practice in Tropical Countries. Part 2, 2nd Edition, Cambridge University Press Publication, South Africa.

Chowdhury, T., Mahmud, A., Barua, A., Khalil, M.D.I., Chowdhury, R., Ahamed, F. & Dhar, K. (2016). Bacterial contamination on hand touch surfaces of public buses in Chittagong city, Bangladesh. *Journal of Environmental Science, Toxicology and Food Technology*, 10(4), 48–55. http://dx.doi.org/ 10.9790/2402-1004034855

Clinical and Laboratory Standards Institute (CLSI), (2022). Performance Standards for Antimicrobial Susceptibility Testing, 32nd Edition.

Coelho, C., de Lencastre, H. & Aires-de-Sousa, M. (2017). Frequent occurrence of trimethoprim-sulfamethoxazole hetero-resistant Staphylococcus aureus isolates in different African countries. *European Journal of Clinical Microbiology and Infectious Diseases*, 36, 1243–1252. http://dx.doi.org/ 10.1007/s10096-017-2915-x

Domínguez, M., Miranda, C.D., Fuentes, O., de la Fuente, M., Godoy, F.A., Bello-Toledo, H & González-Rocha, G. (2019). Occurrence of Transferable Integrons and sul and dfr Genes among Sulfonamide-and/or Trimethoprim-Resistant Bacteria Isolated from Chilean Salmonid Farms. *Frontiers in Microbiology*, 10, 748. http://dx.doi.org/ 10.3389/fmicb.2019.00748

Dutka-Malen, S., Evers, S. & Courvalin, P. (1995). Detection of glycopeptide resistance genotypes and identification to the species level of clinically relevant enterococci by PCR. *Journal of Clinical Microbiology*, 33(1), 24-27. http://dx.doi.org/10.1128/jcm.33.1.24-27.1995

Edelstein, M., Pimkin, M., Edelstein. I. & Stratchounski, L. (2003). Prevalence and molecular epidemiology of CTX-M extended-spectrum β-lactamase -producing *Escherichia coli* and *Klebsiella pneumoniae* in Russian hospitals. *Antimicrobial Agents Chemotherapy*, 47: 3724–3732.

Fernandes, C.J., Fernandes, L.A. & Collignon, P. (2005). Cefoxitin resistance as a surrogate marker for the detection of methicillin-resistant *Staphylococcus aureus*. *Journal of Antimicrobial Chemotherapy*, 55(4), 506-510. http://dx.doi.org/10.1093/jac/dki052

Furuya, H. (2007). Risk of transmission of airborne infection during train commute based on a mathematical model. *Environmental Health Preventive Medicine*, 12, 78–83. http://dx.doi.org/10.1007/BF02898153

Grape, M., Motakefi, A., Pavuluri, S. & Kahlmeter, G. (2007). Standard and real-time multiplex PCR methods for detection of trimethoprim resistance dfr genes in large collections of bacteria. *Clinical Microbiology and Infection*, 13, 1112–1118. http://dx.doi.org/ 10.1111/j.1469-0691.2007.01807.x.

Guimera, R., Mossa, S., Turtschi, A. & Amara, L.A.N. (2005). The worldwide air transportation network: anomalous centrality, community structure, and cities' global roles. *Proceedings of the National Academy of Sciences of the United States of America*, 102, 7794–7799. http://dx.doi.org/10.1073/pnas.0407994102

Kahsay, A.G., Asgedom, S.W. & Weldetinsaa, H.L. (2019). Enteric bacteria, methicillin-resistant *S. aureus* and antimicrobial susceptibility patterns from buses surfaces in Mekelle city, Tigray, Ethiopia. *BMC Research Notes*, 12, 337. http://dx.doi.org/10.1186/s13104-019-4366-4371

Magiorakos, A.-P., Srinivasan, A., Carey, R.B., Carmeli, Y., Falagas, M.E.C.G., Giske, C.G., ... Monnet, D.L. (2012). Multidrug-resistant, extensively drug-resistant and pandrug-resistant bacteria: an international expert proposal for interim standard definitions for acquired resistance. *Clinical Microbiology and Infection*, 18(3), 268-281. http://dx.doi.org/10.1111/j.1469-0691.2011.03570.x.

Maynard, C., Fairbrother, J.M., Bekal, S., Sanschagrin, F., Levesque, R.C., Brousseau, R., ... Harel, J. (2003). Antimicrobial resistance genes in enterotoxigenic *Escherichia coli* O149:K91 isolates obtained over a 23-year period from pigs. *Antimicrobial Agents Chemotherapy*, 47(10), 3214-3221. http://dx.doi.org/10.1128/AAC.47.10.3214-3221.2003

Montravers, P. & Eckmann, C. (2021). Cotrimoxazole and clindamycin in skin and soft tissue infections. *Current Opinion in Infectious Diseases*, 34(2), 63-71. http://dx.doi.org/10.1097/QCO.0000000000000698

Muley, D., Shahin, M., Dias C. & Abdullah, M. (2020). Role of Transport during Outbreak of Infectious Diseases: Evidence from the Past. *Sustainability*, 12, 7367. http://dx.doi.org/https://doi.org/10.3390/su12187367

Nurjadi, D., Olalekan, A.O., Layer, F., Shittu, A.O., Alabi, A., Ghebremedhin B., ... Zanger, P. (2014). Emergence of trimethoprim resistance gene *dfrG* in *Staphylococcus aureus* causing human infection and colonization in sub-Saharan Africa and its import to Europe. *Journal of Antimicrobial Chemotherapy*, 69, 2361–2368. http://dx.doi.org/10.1093/jac/dku174.

Nwankwo, E.O., Okey-kalu, E.U. & Eze F.A. (2023). Bacterial Contamination of Door Handles of Commercial Buses in Umuahia Metropolis Abia State. *Suan*

Sunandha Science and Technology Journal, 10(1), 54-61. http://dx.doi.org/https://doi.org/10.53848/ssstj.v10i1.414

Olaniran, O.B., Adeleke, O.E., Donia, A., Shahid, R. & Bokhari, H. (2021). Incidence and Molecular Characterization of Carbapenemase Genes in Association with Multidrug-Resistant Clinical Isolates of *Pseudomonas aeruginosa* from Tertiary Healthcare Facilities in Southwest Nigeria. Current Microbiology, 79(1), 27. http://dx.doi.org/10.1007/s00284-021-02706-3

Otter, J.A. & French, G.L. (2009). Bacterial contamination on touch surfaces in the public transport system and in public areas of a hospital in London. *Letters in Applied Microbiology*, 49(6), 803-807. http://dx.doi.org/10.1111/j.1472-765X.2009.02728.x

Reeve, S.M., Scocchera, E.W., G-Dayanadan, N., Keshipeddy, S., Krucinska, J., Hajian, B., Ferreira, J., Nailor, M., Aeschlimann, J., Wright, D.L.. . . ..Anderson, A.C. (2016). MRSA isolates from United States hospitals carry dfrG and dfrK resistance genes and succumb to propargyl-linked antifolates. *Cell Chemical Biology*, 23(12), 1458-1467. http://dx.doi.org/10.1016/j.chembiol.2016.11.007.

Rodrigue, J-P, (2020) *The Geography of Transport Systems*, Fifth Edition, London: Routledge. 456 pages. ISBN: 978-0-367-36463-2. https://doi.org/10.4324/9780429346323.‘

Rossato, A.M., Primon-Barros, M., Rocha, L.D.L., Reiter, K.C., Dias, C.A.G. & d’Azevedo, P.A. (2020). Resistance profile to antimicrobial agents in methicillin-resistant *Staphylococcus aureus* isolated from hospitals in South Brazil between 2014-2019. *Revista da Sociedade Brasileira de Medicina Tropical*, 53, Article e20200431. http://dx.doi.org/10.1590/0037-8682-0431-2020.

Rusin, P., Maxwell, S. & Gerba, C. (2002). Comparative surface-to-hand and fingertip-to-mouth transfer efficiency of gram-positive bacteria, gram-negative bacteria and phage. *Journal of Applied Microbiology*, 93, 585–592. http://dx.doi.org/10.1046/j.1365-2672.2002.01734.x

Shittu, A.O., Okon, K., Adesida, S., Oyedara, O., Witte, W., Strommenger, B., . . . Nübel, U. (2011). Antibiotic resistance and molecular epidemiology of *Staphylococcus aureus* in Nigeria. *BMC Microbiology*, 11, 92. http://dx.doi.org/ 10.1186/1471-2180-11-92

Tatem, A.J., Rogers, D.J. & Hay, S.I. (2006). Global Transport Networks and Infectious Disease Spread. *Advances in Parasitology*, 62, 293–343. http://dx.doi.org/ 10.1016/S0065-308X(05)62009-X

World Health Organization (WHO) 2021. Antimicrobial resistance. Downloaded on March 8, 2023. https://www.who.int/news-room/fact-sheets/detail/antimicrobial-resistance

World Health Organization, (2020). Updated WHO recommendations for international traffic in relation to COVID-19 outbreak. Downloaded on March 8, 2023. https://www.who.int/news-room/articles-detail/updated-who-recommendations-for-international-traffic-in-relation-to-covid-19-outbreak

Yeh, P.J., Simon, D.M., Millar, J.A., Alexander, H.F. & Franklin, D. (2011). A diversity of Antibiotic-resistant *Staphylococcus* spp. in a Public Transportation System. *Public Health and Research Perspectives*, 2(3), 202-209. http://dx.doi.org/10.1016/j.phrp.2011.11.047

Yu, H.S., Lee, J.C., Kang, H.Y. & Yeong, Y.S. (2004). Prevalence of dfr genes associated with integrons and dissemination of dfrA17 among urinary isolates of *Escherichia coli* in Korea. *Journal of Antimicrobial Chemotherapy*, 53(3), 445-450. http://dx.doi.org/ 10.1093/jac/dkh097

How cite this article

Famojuro, O.B., Famojuro, T.I., Mayungbe, M.E., & Oluwatobi, O.B. (2024). Detection of antibiotic resistance genes in bacterial isolates from most touched surfaces of public transports in Sagamu, Ogun state, Nigeria. *İstanbul Journal of Pharmacy, 54*(2), 144–153. DOI: 10.26650/IstanbulJPharm.2024.1362394

İstanbul Journal of Pharmacy
Istanbul J Pharm2024, 54 (2): 154–164
DOI: 10.26650/IstanbulJPharm.2024.1071442

Original Article

Comparison of polyphenolic content, radical scavenging activity, and mineral concentrations of *Cuscuta monogyna* VAHL on different host plants

Nazım Şekeroğlu[1], Gülten Korkmaz Yaşar[2], Ufuk Koca Çalışkan[3,4], Ceylan Dönmez[5], Sevgi Gezici[6], Faruk Özkutlu[7]

[1] Gaziantep University, Faculty of Arts and Sciences, Department of Biology, Gaziantep, Türkiye
[2] Kilis 7 Aralik University, Advanced Technology Application and Research Center, Kilis, Türkiye
[3] Gazi University, Faculty of Pharmacy, Deparment of Pharmacognosy, Ankara, Türkiye
[4] Düzce University, Faculty of Pharmacy, Deparment of Pharmacognosy, Düzce, Türkiye
[5] Selçuk University, Faculty of Pharmacy, Deparment of Pharmacognosy, Konya, Türkiye
[6] Gaziantep University, Faculty of Medicine, Gaziantep, Türkiye
[7] Ordu University, Faculty of Agriculture, Department of Soil Science, Ordu, Türkiye

ABSTRACT

Background and Aims: *Cuscuta* sp. (Dodder), known as "Ikşut", is a parasitic herbaceous plant that negatively affects the yield and quality of cultivated crops; however, it has been used as an ancient medicinal plant for curing liver problems for centuries in the southeastern part of Turkey. The aim of this study was to investigate the total phenolic and flavonoid contents and mineral compositions of *Cuscuta monogyna* Vahl. subsp. *monogyna* Vahl. (CMM) grown on different host plants, along with their antioxidant activity, and to compare the host plant parts and their collected dodders.

Methods: In this study, dodders were collected from host plants, including vineyardolive, pomegranate, green pepper, and liquorice in Turkey. The dodders were removed from their hosts before the drying process. Mineral contents were determined by Inductively Coupled Plasma Atomic Optical Spectroscopy (ICP-OES), and phytochemical contents were identified by chromatography. The total polyphenolic compositions and antioxidant activities were determined spectrophotometrically.

Results: Because of the phenolic contents in the host plants and dodders, a significant variation was observed, with values ranging from 5.175% to 35.238%.. Different plant extracts and their varied dilutions had radical scavenging activity on 2.2-diphenyl-1-picrylhydrazyl in the ranges of 57.78 - 95.87%. Variations in mineral compositions were also determined in the dodders and their host plants.

Conclusion: Mutualist or semi-parasitic plant communities share many phytochemical compounds and thus have the potential to exhibit similar activities. With regard to the obtained results, the chemical composition and pharmacological activities of dodder plants are closely related to their host plants.

Keywords: *Cuscuta* sp, dodder, host plant, antioxidant, mineral content, polyphenolic

INTRODUCTION

Cuscuta is a climbing-parasitic plant genus that is also generally known as 'Dodder'. It is a non-chlorophyll and leafless-flowering herbaceous plant that absorbs water, mineral matter, and photosynthetic substances by releasing these haustoriums into the wrapping of the host plant. However, being harmful parasites, they have ecological significance as keystone plant species for biocontrol (Li et al., 2015; Ahmad, Tandon, Xuan, & Nooreen, 2017; Ho & Costea, 2018).

Cuscuta species, which are important parasitic plants for agricultural production and traditional folk medicine in Turkey, are known as 'Ikşut' in Mardin region, and named as 'bostan-bozan, canavarotu, bagbozan, cinsacı, eftimon, gelinsaçı, kızıl-sarmaşık and seytansacı' in other regions (Baytop, 1997).

Dodders have a wide range of distribution by nearly 200 species almost all around the world, and 10 different species of them are widely distributed in Turkey (Davis, Mill, & Tan, 1965 Costea, García, & Stefanović, 2015). In Anatolia, three different parasitic species of dodder, including *Cuscuta campestris* Yunck., *C. approximata* Bab., and *C. monogyna* Vahl., were found on common cropped plants (Nemli, 1986). Additionally,

Corresponding Author: Ceylan Dönmez **E-mail:** akaceylan@gmail.com, ceylan.donmez@selcuk.edu.tr
Submitted: 11.02.2022 • **Revision Requested:** 21.10.2023 • **Last Revision Received:** 21.03.2024 • **Accepted:** 21.03.2024

C. arvensis has been observed on sugar beet, onion, clover, and other vegetables. These are parasitic crop-damaging plants which causes economically 50 - 90% yield loss in cultivated fields throughout the world. Furthermore, it was found that *Cuscuta* species were mostly damaged to plants such as clover, tomato, carrot, onion, and pepper (Lanini & Kogan, 2005).

In addition to being a harmful parasite, dodder has been prepared as an infusion or maceration for new-born mothers (one or two waterglass) and rarely infants in very small quantities (2-3 teaspoons) in traditional folk medicine in Mardin District in Turkey. In traditional uses, the dried plants are cleaned by passing through cold water, and the tea is prepared in warm water for about one night at room temperature with its lid closed by maceration. Then, the macerated tea is drunk by the mother without sweetener such as sugar or honey. The duration of treatment (3-4 glasses of water per day) is approximately 1 month before and after birth (Şekeroğlu, Koca, & Meraler, 2012).

It has been reported that the flowering branches of *C. europaea* L. have urinary enhancing, laxative, spasmolytic, and kolagogic effects (Baytop, 1999). While its seeds have been mostly used in aphrodisiac recipes in China, herba has been used in western countries to treat different ailments in folk medicine for centuries. Seeds of *C. chinensis* Lam. have also been used to treat liver and kidney problems, improve sexual function, prevent eye complaints such as blurred vision and fatigue; and to prevent clinical ageing (Zheng, Dong, & She, 1998).

According to previous reports, *C. chinensis* was found to possess anticancer, immunostimulant, and antioxidant properties (Nisa, Akbar, Tariq, & Hussain, 1986; Bao, Wang, Fang, & Li, 2002; Umehara et al., 2004). Furthermore, glycosides of *C. chinensis* have been shown anti-ageing and memory-enhancing effects by inducing PC12 cell differentiation (Jian-Hui, Bo, Yong-Ming, & Li-Jia, 2003). Detailed investigations revealed that *C. chinensis* seeds contain one trisaccharide and four new glycosidic acids, acetic acid, propionic acid, methylbutyric acid, tiglic acid, convolvulinic acid, and jalapinolic acid, in the ester-insoluble resin glycoside-like fraction (Du, Kohinata, Kawasaki, Guo, & Miyahara, 1998). Studies on *C. japonica*'s polar extract have shown that the active components are caffeoylquinic acid and caffeoylvinylate derivatives (Oh, Kang, Lee, & Lee, 2002). Subsequent studies have revealed that the methanolic extract of *C. reflexa* has strong antioxidant potential (Pal, Mandal, Senthilkumar, & Padhiari, 2006); and ethylacetate and methanol extracts of *C. chinensis* have antibacterial properties (Yen, Wu, Lin, Cham, & Lin, 2008); and also major components of *C. japonica* have antihypertensive effects (Oh et al., 2002). In addition, studies have shown that the glycoprotein of *C. europea* has an immunostimulant effect (Stanilova, Zhelev, & Dobreva, 2000), the ethanolic extract of *C. chinensis* has hepatoprotective activity (Yen, Wu, Lin, & Lin, 2007), and the methanolic extract of *C. reflexa* has an ovarian steroidogenesis suppressant effect (Gupta, Mazumder, Pal, & Bhattacharya, 2003). Hepatoprotective effects of methanolic extract and anti-inflammatory and analgesic effects of both ethanolic and aqueous extracts of *C. arvensis* were determined in mice in our previous studies (Koca, Küpeli-Akkol, & Sekeroglu, 2011; Koca-Caliskan et al., 2018). Although biological studies of the extracts obtained from *C. arvensis* and other *Cuscuta* species have been performed, no phytochemical studies have been conducted on C. arvensis except in our study in Turkey. Previous studies have been conducted to elucidate the phytochemical content of different *Cuscuta* species, and flavonoids, lignins, quinic acid, and polysaccharides were determined, particularly in *C. chinensis* (Du et al., 1998; Wang, Fang, Ge, & Li, 2000; Ye, Li, Yan, Liu, & Ji,, 2002; Ye, Yan, & Guo 2005). Thus, this study was assumed to be the first report to determine antioxidant activity, chemical and polyphenolic contents, as well as mineral compositions of *C. monogyna* VAHL subsp. *monogyna* VAHL collected from different host plants and evaluate each plant by comparing the plants and their dodders to each other.

MATERIAL AND METHOD

Plant materials

Cuscuta monogyna VAHL subsp. *monogyna* VAHL along with their hosts used as materials in this study were supplied from the agricultural production areas and natural flora of Kilis and Gaziantep, located in the southeastern part of Turkey. *Capsicum annuum* L. (green pepper) was collected from Bulamaçlı Village of Kilis in September; *Vitis vinifera* L. (vineyard) and *Olea europea* L. (olive) were collected from Akçabağlar Village of Kilis in July; *and Punica granatum* L. (pomegranate) and *Glycyrrhiza glabra* L. (liquorice) were collected from Nizip District of Gaziantep in July 2014 (Figure 1).

Cuscuta species, which naturally grows on garden plants in Kilis and Gaziantep provinces, were identified as "*Cuscuta monogyna* VAHL subsp. *monogyna* VAHL" by Prof. Dr. Nazim Sekeroglu, and the herbarium specimens were kept with KHB-79 code in the Herbarium of Kilis 7 Aralik University, Department of Biology.

Chemicals

Chemicals used in the analyses were gallic acid, 2.2-diphenyl-1-picrylhydrazyl (DPPH), ferric chloride, butylated hydroxy anisole (BHA), trichloroacetic acid (TCA), acetic acid, quercetin, potassium ferricyanide, sodium phosphate, sodium carbonate, methanol, ethanol, aluminium chloride purchased from Merck® (Darmastadt, Germany), ascorbic acid from Jt Baker, and Sigma (St. Louis, MO, USA).

Fig. 1A.

Fig. 1B.

Figure 1. A. *Cuscuta monogyna* VAHL subsp. monogyna VAHL, **B.** Dodder on different host plants such as vineyard, olive, liquorice, pomegranate, and green pepper

Preparation of extracts and extraction of plants

Cuscuta species and their host plants were separated, cleaned, dried, and powdered. Each plant sample (7-15 g) was mixed with a ten-fold methanol as solvent (about 100 mL), and they were held for 24 h at room temperature by shaking. At the end of the shaking period, the mixture was filtered with filter paper, and the same procedure was repeated twice by adding solvent to the wet plant again, and the solvents were then evaporated in rotavator. The following chemical analyses were performed on the dried extracts.

Determination of the total phenolic compounds

The total phenolic contents of 15 different extracts were determined by using Folin-Ciocalteau method (Singleton & Rossi, 1965) with minor modifications (Şenol, Şekeroğlu, Gezici, Kilic, Orhan, 2018; Gezici & Sekeroglu, 2019). According to the calibration curve, the total phenolic concentration was calculated as gallic acid equivalents using the absorbance of the samples at 765 nm.

Determination of the total flavonoids

To determine the total flavonoids, 2 mg mL^{-1} of each extract sample and the reference quercetin solutions were mixed with 75% EtOH, 10% $AlCl_3$, 1M sodium acetate and 2,800 µL distilled water separately. All procedures and reagents were the same as those described in our previous publication (Gezici & Sekeroglu, 2019). According to the calibration curves, total flavonoids were calculated as quercetin equivalents using the absorbance of the samples at 415 nm (Woisky & Salatino, 1998).

Determination of the radical scavenging activity

The method of diphenyl picrylhydrazyl (DPPH) was utilised to determine *the in vitro* radical scavenging activity (Blois, 1958; Lee, Chung, Chang, & Lee, 2007). The extracts were prepared in methanol with different concentrations in the range of 1 mg/mL^{-1}, 0.5 mg/mL^{-1}, 0.25 mg/mL^{-1}, 0.125 mg/mL^{-1} to 0.0625 mg/mL^{-1}, and butylated hydroxy anisole (BHA) was used as a reference. 1 mL of each extract and BHA were mixed with 2 mL of DPPH (0.1mM in 70 % methanol) and incubated for 30 min in the dark at room temperature, and their absorbances were measured at 517 nm. The antiradical activity was calculated as follows;

Scavenging activity (%) = (1- A1/A0) x 100
[A0: absorbance of control; A1: absorbance of sample]

Thin-layer chromatography

Chloroform and methanolic extracts (0.05 g) were dissolved in 5 mL of methanol. An ultrasonic bath was used to ensure complete dissolution of the extracts. On the aluminium plate, 80 µL of each extract was applied as a 0.5-cm-long line. The Chloroform: Methanol: Water (61: 32: 7) solvent system drifted up to 10 cm. The fluorescent stains were examined under ultraviolet light at 254 and 366 nm and marked. The revelator was then sprayed and exposed for 5 min at 120°C. The stains were disambiguated after this period.

Determination of the Concentration of Minerals

Preparation of the samples

The dodder, separated from the host plants, was washed with pure water and dried in the shade for 72 h. The plant material was dried again for 48 h at 70°C, and 2 mL of distilled water, 2 mL of H_2O_2 (30%) (Merck®, Darmastadt, Germany), and 4 mL of HNO_3 (65%) (Merck®, Darmastadt, Germany) were added to 0.2 g of the samples. The mixture was burned for 5 min at 200°C in a microwave (HP-500 CEM MARS 5 crop, Matthews NC, USA).

These incinerated samples were cooled to room temperature and filtered with a blue band filter paper containing pure water until the volume reached 25 mL. The extracts were stored at 4°C in polyethylene boxes until ICP-OES analysis. For accuracy, the analysis was repeated three times for each plant sample using standard reference samples (Corn bran, Standard Reference Material, 1547) supplied by NIST (International Institute of Standards and Technology). Read errors in the results of analysis were determined to be below 1% compared with the reference samples.

Preparation of the Standards

The polyethylene and glass materials used in the study were washed with 2-4% HCI before being passed through pure water three times. Merck® standards (R1 and R2 groups) were used as references. Cd, Cu, Fe, Mn, Zn, and HNO_3 were used in the analyses at a concentration of 1% in 1000 mg per stock solution.

Conditions of the ICP-OES Device

The ICP-OES device, supported by a magnetic field, atomised and stimulated in the sample, is a high-temperature plasma technique. Light is sent to the detector at the selected wavelength, and the light intensity is determined. According to the analytical method, the wavelengths of Al, B, Ca, Cd, Co, Fe, K, Mg, Mn, Mo, Na, Ni, Pb, S, and Zn were 396.152, 208.889, 370.602, 214.439, 2390.786, 238.204, 404.721, 383.829, 257.610, 203.846, 588.995, 216.555, 220.353, 181.972, and 213.857 nm, respectively. The cadmium concentration was found 0.1 µg/mL with ICAP-OES (Inductively Coupled Argon Plasma-Optical Emmision Spectrometer) U-5000 AT + Ultrasonic Nebuliser at 214.438 nm wavelength.

Statistical Analysis

The experiments were carried out in triplicate, and all the data are presented as the detected values ± standard deviation values (mean ± SD) for total amounts of phenolic and flavonoid substances for *Cuscuta* species and their host plants. The DPPH free radical scavenging activity of *Cuscuta* species and their host plants is given as a percentage of inhibition.

RESULTS AND DISCUSSION

Determination of the total phenolic compounds

Total phenolic compounds were determined from methanolic extracts of *Cuscuta* species and their host plants. The total amounts of the phenolics varied in a wide range from 5.175% to 35.237% (Table 1). As presented in Table 1, the total phenolic content also showed variations depending on the host plants and their used parts. As the highest total phenolic content was found in the liquorice leaf, the lowest value was determined in the pepper branches.

Considering the extracts prepared from Cuscuta species by their host plants; the highest value for total phenolic content was found in the dodder grown on liquorice. The lowest total phenolic content was determined in the extracts obtained from dodders on pepper plants. According to different hosts, the total phenolic contents in dodder extracts could be classified from higher levels to lowest values as liquorice, vineyard, pomegranate, olive, and pepper, respectively.

The amounts of total phenolic substances in the leaves of host plants (liquorice, vineyard and pomegranate) were higher than those in the branches of these plants and their parasites. The total amount of phenolic compound emerged in the highest value in the extract of olive's branch, while the lowest value in the olive leaf extract despite the total phenolic content differing partially in the pepper.

When the phenolic content of *C. reflexa* and *C. europea* plants collected from different hosts (*Acacia nilotica, Acacia nilotica, Lycium barbarum, Azadirachta indica, Calotropis procera* and *Ziziphus jujuba*) was examined, the highest value was found to be 189.68 (mg/100g) in the methanolic extract of *C. europea* obtained from *Ziziphus jujuba* host plants and the lowest value was 97.68 (mg/100g) in the methanolic extract of *C. europea* collected from *Calotropis procera* host plant (Perveen, Hussain Bukhari, Qurat-Ul-Ain, Kousar, & Rehman, 2013).

Determination of the total flavonoid compounds

Total flavonoid compounds were determined in the methanolic extracts of *Cuscuta* species and their host plants. The total amount of flavonoid compounds varied between 0.308% and 15.731% (Table1). The highest total phenolic content was found in the vineyard leaf compared with that of the others.

According to the data given in Table 1, the total phenolic content was found to be the highest value in vineyard leaves by comparing that of the other samples investigated. On the other hand, the lowest total flavonoid content was detected in the *Cuscuta* extracts obtained from the pomegranate branches (0.308

Table 1. Total amounts of phenolic and flavanoid substances of *Cuscuta* species and their host plants

Host plants	Parts of the plant	Total phenolic subtances (%)[a,b]	Total flavonoid subtances (%)[b,c]
Liquorice	Leaf	35.238 ± 1.096	7.638 ± 0.694
	Branch	11.438 ± 0.247	0.812 ± 0.145
	Dodder	27.138 ± 0.141	3.158 ± 0.183
Vineyard	Leaf	33.363 ± 0.282	15.731 ± 0.318
	Branch	25.713 ± 0.919	3.301 ± 0.694
	Dodder	26.388 ± 0.035	5.797 ± 0.463
Olive	Leaf	14.138 ± 0.494	2.667 ± 0.048
	Branch	29.013 ± 1.025	4.106 ± 0.019
	Dodder	19.700 ± 1.007	4.419 ± 0.019
Green pepper	Leaf	5.175 ± 0.265	4.297 ± 0.135
	Branch	6.180 ± 0.017	1.945 ± 0.068
	Dodder	7.237 ± 0.141	2.933 ± 0.135
Pomegranate	Leaf	14.100 ± 0.583	1.917 ± 0.087
	Branch	28.175 ± 0.583	0.308 ± 0.068
	Dodder	23.600 ± 1.361	2.845 ± 0.106

[a] mg equivalent of gallic acid (GAE) per g of extract.
[b] SD: Standard deviation (n=3).
[c] mg equivalent of quercetin (QE) per g of extract.

± 0.068), followed by liquorice (0.812 ± 0.145). The variation in the total flavonoid content of the host plant parts varied considerably. The highest values were found in the leaves of vineyard (15.731 ± 0.318), which is followed by liquorice and peppers (7.638 ± 0.694 and 4.297 ± 0.135, respectively). Although there is limited host plant-dodder comparison in terms of flavonoid content, there are studies evaluating the flavonoid content of different *Cuscuta* spp. seeds. In one study, it was shown that 80% methanolic extract of *C. reflexa* seed contains high flavonoids (Noureen et al., 2018). In a study examining *C. campestris* seeds, which are the hosts of thyme, basil, and onion, the highest flavonoid content was found in onion (Ramezan et al., 2023).

DPPH Free Radical Scavenging Activity

The DPPH free radical scavenging activity of methanolic extracts of *Cuscuta* species and their host plants was determined as a concentration-dependent variable (Table 2). The highest free radical scavenging activity was found at 1 mg/mL^{-1}dose of extract obtained from dodder on olive, whereas the lowest activity was found at 0.125 mg/mL^{-1}dose of extract prepared from dodder on pepper.

It was determined that the free radical scavenging activity of extracts obtained from *Cuscuta* species and their host plant's parts showed variation in accordance with doses of the extracts. As seen in Table 2, the highest antioxidant capacity was found in the olive, whereas the lowest effect was found in the pepper at 1 mg/mL^{-1} concentration.

Even though a remarkable variation was not observed among the extracts obtained from different host plants and their parts, extracts of *Cuscuta* species from the olive, liquorice, and vineyard showed higher DPPH scavenging activity than the others, even at lower concentrations. When antioxidant capacities of dodder were examined according to host plants, it was stated from high DPPH inhibition to low as olive'dodder>vineyard' dodder ≥ pomegranate' dodder ≥ liquorice' dodder >pepper' dodder.

In our study, the highest activity was found in the concentration of 1 mg/mL^{-1}solution of branch of olive and liquorice at 95.56%, and the lowest activity was found in the concentration of 0.125 mg/mL^{-1}in the leaf of pepper at 87.30% among the plant parts. The highest antioxidant activity was detected in the branches of each host plant, except for pepper. It is observed that the host plants and dodders have the highest activity at a dose of 1 mg/mL^{-1}and the lowest activity at a dose of 0.125 mg/mL^{-1}. The data obtained from the presented work were found to be in agreement with results reported by Koca et al. (2011) previously. Yen et al. (2007) also reported that ethanolic extracts of *Cuscuta chinensis* had hepatoprotective properties because of their high antioxidant capacities. Methanolic and n-hexane extracts of *C. reflexa* and *C. europea* from different host plants had different antioxidant capacities as DPPH (Perveen et al., 2013).

Thin-layer chromatography

Thin layer chromatography allows comparison of plants and hosts in terms of their phytochemical content. Because of this preliminary study, by ultraviolet spectroscopy, bluish-greenish and dark fluorescence belong to flavonoids or coumarin; and the red fluorescence at the upper part belongs to chlorophyll. After the vanillin-sulphuric acid revelator, which is used to di-

Table 2. DPPH free radical scavenging activity of *Cuscuta* species and their host plants

***Cuscuta* parts of the host plants**	**1** mg/mL^{-1}	**0.5** mg/mL^{-1}	**0.25** mg/mL^{-1}	**0.125** mg/mL^{-1}	**0.0625** mg/mL^{-1}
VL (Vineyard Leaf)	93.65 ± 0.03	87.94 ± 0.19	87.84 ± 0.12	87.62 ± 0.21	53.55 ± 0.31
VB (Vineyard Branch)	94.94 ±0.06	94.60 ± 0.06	94.29 ± 0.09	93.65 ± 0.04	72.99 ± 0.11
VD (Vineyard Dodder)	94.60 ±0.05	94.29 ± 0.08	94.19 ± 0.08	94.09 ± 0.05	67.77 ± 0.24
GPL (Green Pepper Leaf)	92.70 ± 0.05	92.06 ± 0.13	90.48 ± 0.05	87.30 ± 0.14	37.60 ± 0.36
GPB (Green Pepper Branch)	90.16 ± 0.11	87.94 ± 0.17	79.37 ± 0.25	75.24 ± 0.18	22.59 ± 0.45
GPD (Green Pepper Dodder)	93.33 ± 0.04	88.25 ± 0.21	80.32 ± 0.17	57.78 ± 0.29	40.76 ± 0.27
LL (Liquorice Leaf)	94.29 ± 0.07	93.65 ± 0.09	93.33 ± 0.06	93.02 ± 0.05	54.50 ± 0.27
LB (Liquorice Branch)	95.56 ± 0.08	94.29 ± 0.05	93.97 ± 0.03	92.38 ± 0.07	75.04 ± 0.10
LD (Liquorice Dodder)	94.60 ± 0.03	93.97 ± 0.10	93.65 ± 0.05	93.33 ± 0.03	56.08 ± 0.26
PL (Pomegranate Leaf)	94.60 ± 0.02	93.65 ± 0.07	93.02 ± 0.05	91.43 ± 0.08	56.08 ± 0.21
PB (Pomegranate Branch)	95.24 ± 0.05	94.60 ± 0.05	93.65 ± 0.08	91.11 ± 0.06	75.20 ± 0.14
PD (Pomegranate Dodder)	94.60 ± 0.04	93.97 ± 0.06	87.30 ± 0.12	86.67 ± 0.11	42.97 ± 0.13
OL (Olive Leaf)	95.24 ± 0.09	94.60 ± 0.07	94.29 ± 0.08	93.97 ± 0.03	82.46 ± 0.09
OB (Olive Branch)	95.56 ± 0.09	93.97 ± 0.09	93.65 ± 0.04	88.57 ± 0.05	82.46 ± 0.07
OD (Olive Dodder)	95.87 ± 0.04	95.60 ± 0.05	94.60 ± 0.09	93.65 ± 0.07	75.20 ± 0.14
BHA[b]	94.29 ± 0.07	93.65 ±0.03	92.70 ± 0.04	89.21 ± 0.09	87.68 ± 0.11

[a] Values are presented as percentages of inhibition
[b] Butylated hydroxy anisole; commercial standard

agnose metabolites such as steroids, highly structured alcohols, phenols, volatile oils, and terpenic compounds, was sprayed, it is thought that the pink purple spots belong to diterpenes, the yellowish spots belong to flavonoids or other phenolic compounds; orange colours belong to alkaloids or iridoid. It has been observed that compounds thought to be flavonoid derivatives are more concentrated in the host plant, olive, grape and green pepper, and are not taken up as much in dodder. On the contrary, it is thought that terpenic compounds are found more in cuscuta, which is a semi-parasitic plant, according to the TLC plate results (Figure 2).

Mineral Analysis

The amounts of 14 different minerals including aluminium, boron, calcium, cadmium, copper, iron, potassium, magnesium, manganese, sodium, nickel, phosphorus, sulphur, and zinc, were determined in the leaves, branches, and dodders of green pepper, grape, liquorice, pomegranate, and olive plants, and *Cuscuta* species on these plants. The mineral contents of *Cuscuta* species and their host plants were summarised in Table 3.

The aluminium (Al) contents of plants showed a wide variation between 28 and 747 mg/kg. The highest value was determined in the leaves of vineyard and the lowest value was determined in the branches of pomegranate according to plant parts. Aluminium concentrations of dodder samples collected from different plant species ranged from 152 to 285 mg/kg. The highest aluminium content was found in the pomegranate dodder, and the lowest value was found in the liquorice dodder. It was determined that the boron (B) minerals of *Cuscuta* species and parts of their host plants were in the range of 16-92 mg/kg in this study (Table 3). The amount of boron in the plant parts was found in the lowest branches of the pepper, and the

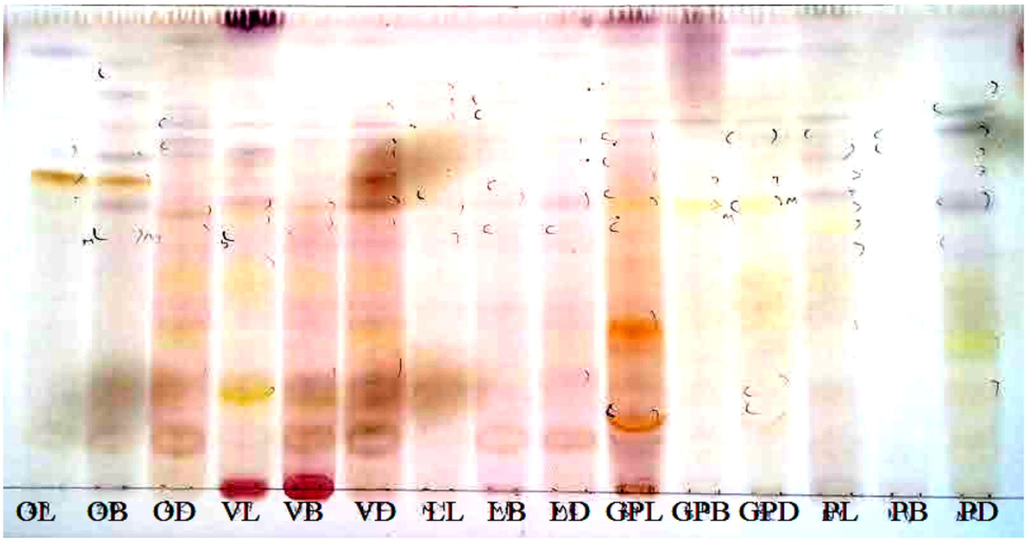

Olive Leaf (OL), Olive Branch (OB), Olive Dodder (OD), Vineyard Leaf (VL), Vineyard Branch (VB), Vineyard Dodder (VD), Liquorice Leaf (LL), Liquorice Branch (LB), Liquorice Dodder (LD), Green Pepper Leaf (GPL), Green Pepper Branch (GPB), Green Pepper Dodder (GPD), Pomegranate Leaf (PL), Pomegranate Branch (PB), and Pomegranate Dodder (PD).

Figure 2. Plate appearance after vanillin-sulphuric acid revelator spraying

Table 3. Mineral values of *Cuscuta* species and their host plants (mg/kg)

Cuscuta/ Plant[a]	Minerals (mg/kg)[b]													
	Al	**B**	**Ca**	**Cd**	**Cu**	**Fe**	**K**	**Mg**	**Mn**	**Na**	**Ni**	**P**	**S**	**Zn**
VL	747 ± 66	48 ± 1.3	33237 ± 658	0.07 ± 0.00	3.88 ± 0.05	140 ± 5.8	3817 ± 298	6205 ± 231	63.1 ± 2.0	208 ± 8.0	5.09 ± 0.30	1025 ± 98	1527 ± 65	16.3 ± 2.80
VB	117 ± 6	25 ± 0.8	8979 ± 203	0.17 ± 0.02	6.49 ± 0.02	139 ± 4.1	8694 ± 245	2350 ± 125	19.6 ± 0.8	214 ± 8.1	1.04 ± 0.10	773 ± 42	746 ± 47	21.9 ± 3.70
VD	206 ± 14	43 ± 2.1	3847 ± 125	0.02 ± 0.00	4.83 ± 0.06	220 ± 6.3	11508 ± 356	1043 ± 98	10.4 ± 0.3	129 ± 5.2	1.29 ± 0.20	990 ± 65	784 ± 32	3.9 ± 0.50
GPL	563 ± 42	92 ± 3.3	32868 ± 496	0.44 ± 0.07	22.76 ± 2.10	151 ± 3.0	26458 ± 375	1050 ± 88	132.1 ± 26	109 ± 2.5	10.01 ± 0.80	1776 ± 47	6568 ± 84	19.9 ± 0.40
GPB	277 ± 8	16 ± 0.4	9260 ± 236	0.18 ± 0.05	8.48 ± 0.08	265 ± 2.7	17314 ± 425	2350 ± 159	16.7 ± 0.8	121 ± 7.0	3.70 ± 0.10	662 ± 66	3018 ± 29	5.0 ± 0.90
GPD	157 ± 12	12 ± 0.5	3311 ± 125	0.09 ± 0.03	9.37 ± 1.10	190 ± 3.2	24721 ± 541	2445 ± 287	15.9 ± 1.4	118 ± 3.2	4.22 ± 0.30	2465 ± 75	2237 ± 54	13.9 ± 2.60
LL	268 ± 15	32 ± 2.3	17789 ± 326	0.05 ± 0.00	4.01 ± 0.02	237 ± 2.6	12524 ± 453	2644 ± 178	61.5 ± 1.4	74 ± 0.4	2.91 ± 0.40	785 ± 37	2044 ± 49	12.8 ± 1.80
LB	65 ± 5	16 ± 1.1	14045 ± 287	0.01 ± 0.00	3.10 ± 0.02	68 ± 0.8	8451 ± 125	1217 ± 101	12.7 ± 2.8	101 ± 0.9	1.62 ± 0.10	441 ± 24	881 ± 37	8.6 ± 0.50
LD	152 ± 11	26 ± 0.6	5115 ± 106	0.03 ± 0.00	4.50 ± 0.06	157 ± 2.4	13864 ± 264	1048 ± 76	19.3 ± 3.2	59 ± 0.8	4.22 ± 0.60	1208 ± 41	913 ± 19	15.3 ± 1.20
PL	145 ± 7	26 ± 0.8	17385 ± 456	0.05 ± 0.00	4.57 ± 0.01	147 ± 1.1	18351 ± 279	2434 ± 245	19.4 ± 1.1	48 ± 1.3	2.18 ± 0.30	1463 ± 32	1428 ± 47	19.3 ± 3.40
PB	28 ± 3	20 ± 0.5	10771 ± 258	0.01 ± 0.00	5.44 ± 0.02	32 ± 0.2	7332 ± 357	893 ± 65	8.6 ± 0.5	63 ± 1.1	1.69 ± 0.30	1092 ± 71	596 ± 39	18.1 ± 3.80
PD	285 ± 9	97 ± 2.5	4074 ± 125	0.06 ± 0.01	7.43 ± 0.04	217 ± 3.4	23173 ± 519	1226 ± 98	14.6 ± 0.7	57 ± 0.9	3.80 ± 0.20	2965 ± 59	1546 ± 40	19.4 ± 2.60
OL	645 ± 38	23 ± 0.2	16477 ± 546	0.05 ± 0.01	5.32 ± 0.03	55 ± 0.9	12176 ± 129	2123 ± 106	67.2 ± 3.7	129 ± 3.0	6.34 ± 0.70	1000 ± 47	1432 ± 41	11.7 ± 2.00
OB	83 ± 5	23 ± 0.2	6715 ± 312	0.02 ± 0.00	6.93 ± 0.02	87 ± 0.4	11750 ± 264	6205 ± 231	12.4 ± 0.8	153 ± 2.0	0.83 ± 0.10	845 ± 28	548 ± 38	7.8 ± 1.40
OD	282 ± 11	37 ± 0.4	3608 ± 211	0.03 ± 0.00	7.48 ± 0.03	145 ± 1.9	13233 ± 340	2350 ± 125	15.0 ± 1.0	164 ± 5.6	2.24 ± 0.40	1076 ± 54	834 ± 17	8.2 ± 1.00

[a] Vineyard Leaf (VL), Vineyard Branch (VB), Vineyard Dodder (VD), Green Pepper Leaf (GPL), Green Pepper Branch (GPB), Green Pepper Dodder (GPD), Liquorice Leaf (LL), Liquorice Branch (LB), Liquorice Dodder (LD), Pomegranate Leaf (PL), Pomegranate Branch (PB), Pomegranate Dodder (PD); Olive Leaf (OL), Olive Branch (OB), Olive Dodder (OD).
[b] Values are expressed as means ± standard deviation.

highest in the leaves of the green pepper. The boron minerals in the *Cuscuta* species, which are full parasites that grow on host plants, range from 12 to 97 mg/kg.

It was found that the highest boron value was in *Cuscuta* sp. collected from green pepper, and the lowest boron value was in *Cuscuta* sp. collected from pomegranate.

The amount of calcium (Ca) showed a variance in the range of 6715-33237 mg/kg (Table 3). The highest calcium value was observed in the leaf of the vineyard, whereas the lowest value was found in the olive branch. Calcium found in the dodders showed variance in the range of 3311-5115 mg/kg. As the lowest value was found in the green pepper dodder, the highest amount of calcium was found in the liquorice dodder.

Heavy metal cadmium (Cd), which limits plant growth, blocks and slows down the physiological processes of plants, and reduces their productivity, was determined in host plants and their dodders. Higher doses and long-term exposure to cadmium can cause plant death (Temmerman, Bouma, Govers, & Lauwaet, 2005; Marschner, 1995). World Health Organisation (WHO) explained that the limit value of Cd for medicinal plants

is 0.300 mg/kg (Şekeroğlu, Ozkutlu, Kara, & Ozguven, 2008). In parts of the plant, the highest value of cadmium was found to be 0.44 mg/kg in green pepper's leaf and the lowest value was found to be 0.01 mg/kg in pomegranate's leaf. While the lowest value (0.03 mg/kg) was found in the liquorice's dodder and in the olive's dodder, the highest value (0.09 mg/kg) was found in the green pepper's dodder (Table 3).

Copper (Cu) mineral in the dodder on host plants was determined to be in the range of 4.50–9.37 mg/kg. While the highest value was found in the green pepper'dodder; the lowest value was found in the liquorice dodder. In host plants, copper was found in the range of 3.10-22.76 mg/kg (Table 3). It is stated that the lowest amount was observed in the branch of liquorice, and the highest amount in the green pepper's leaf.

Iron (Fe) in plants is one of the important elements required for chlorophyll synthesis. Iron acts not only as a cofactor for peroxidase and some other enzymes but also in the content of ferrodoxin and cytochromes (Ozen and Onay, 2007). The iron mineral content in the dodders varied in the range of 145-220 mg/kg. As the highest iron value was found in the vineyard dodder, the lowest value was determined in the olive dodder. In the host plants, the iron mineral content varied from 32 to 265 mg/kg over a wide range. Among the host plants, the highest iron content was in the branch of green pepper, whereas the lowest iron content was in the branch of pomegranate (Table 3). It can be seen that the iron values obtained in this study are considerably lower than those in previous studies. Although it varies according to different parts of the plant, it is estimated that the low iron ratio is caused by the genetic structure and growth conditions of the plant. It plays a role in the opening and closing of plant stomata, the synthesis of starch, the activation of some enzymes, and the regulation of osmotic pressure (Basgel & Erdemoglu, 2006).

The content of potassium (K) ranged from 3817 to 26458 mg/kg in the plant parts. While the highest value was found in the green pepper's leaf, the lowest value was found in the vineyard's leaf. It was found that the highest potassium value (24701 mg/kg) was in the green pepper's dodder, and the lowest potassium value (11508 mg/kg) was found in the vineyard's dodder (Table 3). The potassium values determined in this study are in agreement with the results of previous studies on this base (Sekeroglu, Ozkutlu, Deveci, Dede, & Yilmaz,, 2006; Koca, Özkutlu, Şekeroğlu, 2009; Sekeroglu, Ozkutlu, & Kilic, 2017).

Magnesium (Mg) is an essential element in the basic structure of chlorophyll and is necessary for the synthesis of many enzymes and proteins (Ozen & Onay, 2007). Magnesium content varied from 837 to 2445 mg/kg in the present study (Table 3). The highest value was found in green pepper plants and the lowest value in olive plants. Magnesium values obtained from parts of the plant showed variance in the range of 893-6205 mg/kg. The branch of pomegranate had the lowest magnesium content, whereas the leaf of vineyard had the highest magnesium mineral content. The detected magnesium values in the analyzed plant samples were in the normal ranges declared by FAO/WHO (1993) and WHO (1999), and these values are similar to those reported in previous studies (Akgunlu et al,, 2016; Sekeroglu et al., 2017). Manganese (Mn) is important for photosynthesis and necessary for electron transfer (Özen and Onay, 2007). While the highest value (132.1 mg/kg) was found in the green pepper leaf, the lowest value (8.6 mg/kg) was found in the pomegranate branch. It was determined that the highest manganese value (19.3 mg/kg) in the liquorice' dodder, the lowest manganese value (10.4 mg/kg) in the vineyard's dodder (Table 3). Similar results were reported for investigated medicinal and aromatic plants by Sekeroglu et al. (2006) and Basgel and Erdemoglu (2006).

With regard to host plants, the amount of sodium (Na) mineral was found the highest (214 mg/kg) in the leaf of vineyard, which was found the lowest (48 mg/kg) in the leaf of pomegranate. In addition, the highest sodium value (164 mg/kg) was observed in the olive dodder, whereas the lowest sodium value (57 mg/kg) was observed in the pomegranate dodder. Sodium values obtained in this study were similar to those reported for different plants in previous studies (Akgunlu et al., 2016). Lower or higher values obtained in some plants are thought to be due to genetic structures, growth conditions, and different parts of the plants (Ozkutlu, Kara, & Şekeroğlu, 2007; Sekeroglu et al., 2006).

As for nickel (Ni), it helps to provide the absorption of iron and the germination of seeds of plants. It was found that the highest Ni value (4.22 mg/kg) in the green pepper dodder and liquorice dodder, and the lowest Ni value (1.29 mg/kg) was found in the vineyard dodder. In host plant parts, the amount of Ni mineral was identified as the highest (10.01 mg/kg) in the leaf of green pepper and the lowest (0.83 mg/kg) in the branch of olive. According to a report released by FAO/WHO, the permitted Ni limit for edible parts of plants is 1.63 mg/kg (FAO/WHO, 1984). Our results showed that the detected Ni levels were lower in wild crops and their hosts. When an agricultural system with chemicals is applied, Ni contents may increase by chemical uptake.

In the host plant's parts, the amount of phosphorus (P) mineral was found the highest (1776 mg/kg) in the leaf of green pepper, and that was the lowest (441 mg/kg) in the branch of liquorice. Furthermore, the highest P mineral value (2965 mg/kg) was determined in the pomegranate dodder, which was found to be the lowest (990 mg/kg) in the vineyard dodder. According to the analysis results, the highest P mineral values were detected in the leaves of the host plants and in the pomegranate dodder. According to sulphur (S) mineral content, it was found to be the highest with a value of 2237 mg/kg in the green pepper's dodder. In host plant parts, the amount of S mineral was determined to be the highest (6568 mg/kg) in the leaf of green pepper and the lowest (548 mg/kg) in the branch of

olive (Table 3). As previously reported, the sulphur source can be absorbed by plants as the elemental sulphur, SO_4^{-2} ions, SO_2 gas, and mineral matter contained in organic substances. This mineral plays a role in the composition of plant proteins, in the formation of chlorophyll, and in the content of some vitamins (Sekeroglu et al., 2018).

Zinc (Zn) plays an important role in pollen formation and auxin synthesis. It also preserves the ribosome structure (Özen and Onay, 2007). The amount of Zn mineral was found in the range of 3.9-19.4 mg/kg in the dodder collected from the host plants. The highest Zn mineral value was determined in the pomegranate's dodder, when the lowest Zn value was found in the vineyard's dodder. With respect to host plant parts, the amount of Zn mineral was observed the highest (21.9 mg/kg) in the branch of vineyard and that was the lowest (5.0 mg/kg) in the branch of green pepper (Table 3).

According to the analysis results, the mineral concentrations of the dodders and their host plants were highly variable. This variation could be explained by the amount of minerals reaching the plant body and tissues.. Moreover, this variability could result in the genetic structure and ecological and growing conditions of the investigated plants. Dodder mineral compositions are directly related to their host plants behaviour.

CONCLUSIONS

However, there has been a significant variation in the total polyphenolic contents of the extracts of *Cuscuta monogyna* VAHL subsp. *monogyna* VAHL plant parts and their host plants. The total amount of phenolic substance was observed to be the highest in the leaf of liquorice extract, which was closely followed by the leaf of vineyard, and the total amount of flavonoids was also determined to be the highest in the leaf of vineyard extract. According to the antioxidant capacity, almost all the extracts obtained from the host plants were found to have remarkable radical scavenging activities on DPPH. As for the thin layer chromatographic method, the general chemical profiles in terms of secondary metabolites, phenolic and terpenic compounds, especially flavonoids of dodders and host plants, were similar. In addition to the determination of the general chemical profiles, the morphogenetic variability of Al, B, Ca, Cd, Cu, Fe, K, Mg, Mn, Na, Ni, P, S, and Zn minerals was determined in this study.

It was concluded that the chemical content of *Cuscuta* species and its biological activity are closely related to the host plant because of parasitism. Despite its harmful effect on the parasitic direction, the results obtained from our laboratory studies could offer a positive scientific insight to obtain the desired and effective compounds from the plant. To the best of our knowledge, this is the first assessment conducted on *Cuscuta* species to reveal their interactions with host plants in Turkey

Viscum album L., which although semi-parasitic, has significant biological activity and phytochemical content, inspired this study. This preliminary study comparing the parasitic *Cuscuta* species with the host plant is considered to be a guide for future research. Further studies on different host plants and *Cuscuta* species are required.

Peer-review: Externally peer-reviewed.

Author Contributions: Conception/Design of Study- G.K.Y., N.Ş.; Data Acquisition- G.K.Y., C.D., U.K.Ç.; Data Analysis/Interpretation- G.K.Y., C.D.; Drafting Manuscript- S.G.; Critical Revision of Manuscript- N.Ş.; Final Approval and Accountability- G.K.Y., C.D., U.K.Ç., S.G., N.Ş., F.Ö.

Conflict of Interest: The authors have no conflict of interest to declare.

Financial Disclosure: The authors declared no financial support.

ORCID IDs of the authors

Nazım Şekeroğlu	0000-0002-0630-0106
Gülten Korkmaz Yaşar	0000-0002-7714-6118
Ufuk Koca Çalışkan	0000-0002-5216-7588
Ceylan Dönmez	0000-0002-8005-4425
Sevgi Gezici	0000-0002-4856-0221
Faruk Özkutlu	0000-0002-8651-3346

REFERENCES

Ahmad, A., Tandon, S., Xuan, T. D., & Nooreen, Z. (2017). A review on phytoconstituents and biological activities of *Cuscuta* species. *Biomedicine & Pharmacotherapy, 92*, 772-795.

Akgunlu, S., Sekeroglu, N., Koca-Caliskan, U., Ozkutlu, F., Ozcelik, B., Kulak, M., & Gezici, S. (2016). Research on selected wild edible vegetables: Mineral content and antimicrobial potentials. *Annals of Phytomedicine-An International Journal, 5*(2), 50-57.

Bao, X., Wang, Z., Fang, J., & Li, X. (2002). Structural features of an immunostimulating and antioxidant acidic polysaccharide from the seeds of *Cuscuta chinensis. Planta Medica, 68*(03), 237-243.

Başgel, S. & Erdemoğlu, S. B., (2006). Determination of mineral and trace elements in some medicinal herbs and their infusions consumed in Turkey. *Science of the Total Environment, 359*, 82-89.

Baytop, T. (1997). *Turkish Plant Names Dictionary* (pp.578). Istanbul: Turkey Language Society Publications.

Baytop, T. (1999). *Herbal Treatments in Turkey (From Past to Today)* (pp.372). Istanbul: Istanbul University Publications.

Blois, M. S. (1958). Antioxidant determinations by the use of a stable free radical. *Nature, 181*(4617), 1199.

Costea, M., García, M. A., & Stefanović, S. (2015). A phylogenetically based infrageneric classification of the parasitic plant genus *Cuscuta* (dodders, Convolvulaceae). *Systematic Botany, 40*(1), 269-285.

Davis, P. H., Mill, R. R., & Tan, K. (1965). *Flora of Turkey and the East Aegean Islands*. Vol. 1-9. Edinburgh: Edinburgh University Press.

Du, X. M., Kohinata, K., Kawasaki, T., Guo, Y. T., & Miyahara, K. (1998). Components of the ether-insoluble resin glycoside-like fraction from *Cuscuta chinensis. Phytochemistry, 48*(5), 843-850.

FAO/WHO, (1984). Food and Agriculture Organization/World Health Organization. Contaminants. In codex Alimentarius, Vol. XVII, Edition 1. Codex Alimentarius Commission, Rome.

FAO/WHO, (1993). Joint FAO/WHO Food Standards Programme. Codex Alimentarius Commission, 20th Session. 28 June to 7 July 1993. WHO, Geneva.

Gezici, S., & Sekeroglu, N. (2019). Neuroprotective potential and phytochemical composition of acorn fruits. *Industrial Crops and Products, 128*, 13-17.

Gupta, M., Mazumder, U. K., Pal, D. K., Bhattacharya, S. (2003). Anti-steroidogenic activity of methanolic extract of *Cuscuta reflexa* roxb. stem and *Corchorus olitorius* Linn. seed in mouse ovary. *Indian Journal of Experimental Biology, 41*(6), 641-644.

Ho, A., Costea, M. (2018). Diversity, evolution and taxonomic significance of fruit in *Cuscuta* (dodder, Convolvulaceae); the evolutionary advantages of indehiscence. *Perspectives in plant ecology, evolution and systematics, 32*, 1-17.

Jian-Hui, L., Bo, J., Yong-Ming, B., & Li-Jia, A. (2003). Effect of Cuscuta chinensis glycoside on the neuronal differentiation of rat pheochromocytoma PC12 cells. *International Journal of Developmental Neuroscience, 21*(5), 277-281.

Koca, U., Küpeli-Akkol, E., & Sekeroglu, N. (2011). Evaluation of in vivo and in vitro biological activities of different extracts of *Cuscuta arvensis. Natural product communications, 6*(10), 1433-1436.

Koca, U., Özkutlu, F., Şekeroğlu, N., 2009. Mineral composition of *Arnebia densiflora* (Nordm.) Ledeb. An endemic medicinal plant from Turkey. Biomed, 4, 51-56.

Koca-Caliskan, U., Yilmaz, I., Taslidere, A., Yalcin, F. N., Aka, C., & Sekeroglu, N. (2018). Cuscuta arvensis Beyr "Dodder": *In Vivo* Hepatoprotective Effects Against Acetaminophen-Induced Hepatotoxicity in Rats. *Journal of medicinal food, 21*(6), 625-631.

Lanini, W. T., & Kogan, M. (2005). Biology and management of *Cuscuta* in crops. *Ciencia e Investigación Agraria, 32*(3), 127-141.

Lee, J., Chung, H., Chang, P. S., & Lee, J. (2007). Development of a method predicting the oxidative stability of edible oils using 2, 2-diphenyl-1-picrylhydrazyl (DPPH). *Food chemistry, 103*(2), 662-669.

Li, J., Yang, B., Yan, Q., Zhang, J., Yan, M., & Li, M. (2015). Effects of a native parasitic plant on an exotic invader decrease with increasing host age. *AoB Plants, 7*,1-10.

Marschner, H. (1995). *Mineral Nutrition of Plants*. London: Academic Press.

Nemli, Y. (1986). Dodder species in the crop fields in Anatolia (*Cuscuta* spp.); Investigation of their distrubitions and hosts – *Ege University Agricultural Faculty Journal, 23*(3),11-21.

Nisa, M., Akbar, S., Tariq, M., & Hussain, Z. (1986). Effect of *Cuscuta chinensis* water extract on 7, 12-dimethylbenz [a] anthracene-induced skin papillomas and carcinomas in mice. *Journal of ethnopharmacology, 18*(1), 21-31.

Noureen, S., Noreen, S., Ghumman, S. A., Batool, F., Arshad, M., Noreen, F., Ishtiaq, U., & Bukhari, S. N. A. (2018). Seeds of giant dodder (*Cuscuta reflexa*) as a function of extract procedure and solvent nature. *Notulae Botanicae Horti Agrobotanici Cluj-Napoca, 46*(2), 653-662.

Oh, H., Kang, D. G., Lee, S., & Lee, H. S. (2002). Angiotensin converting enzyme inhibitors from *Cuscuta japonica* Choisy. *Journal of ethnopharmacology, 83*(1-2), 105-108.

Ozen, H. C., Onay, A. (2007). Plant Physiology, Book, ISBN 978-605-395-017-2, Nobel Publishing House, First Press, PP. 29-30, Ankara

Ozkutlu, F., Kara, S. M., & Şekeroğlu, N. (2007). Determination of mineral and trace elements in some spices cultivated in Turkey. In *International Symposium on Medicinal and Nutraceutical Plants, 756*, 321-328.

Pal, D. K., Mandal, M., Senthilkumar, G. P., & Padhiari, A. (2006). Antibacterial activity of *Cuscuta reflexa* stem and *Corchorus olitorius* seed. *Fitoterapia, 77*(7-8), 589-591.

Perveen, S., Hussain Bukhari, I., Qurat-Ul-Ain, Kousar, S., & Rehman, J., (2013). Antimicrobial, antioxidant and minerals evaluation of *Cuscuta europea* and *Cuscuta reflexa* collected from different hosts and exploring their role as functional attribute. *International Research Journal of Pharmaceutical and Applied Sciences, 3*(5), 43-49.

Ramezan, D., Farrokhzad, Y., Zargar, M., Stybayev, G., Kipshakbayeva, G., & Baitelenova, A. (2023). An Insight into *Cuscuta campestris* as a Medicinal Plant: Phytochemical Variation of *Cuscuta campestris* with Various Host Plants. *Agriculture, 13*(4), 770.

Sekeroglu, N., Karaoglan, M., Gezici, S., Kulak, M., Ozkutlu, F., Kacar, O., & Gul, F. (2018). Variation in the composition of the essential oils, hypericin and mineral elements in aerial parts, stem and flower of *Hypericum capitatum* (CHOISY) growing in Turkey with oxidative DNA damage protective activity. *Journal of Pharmaceutical Research, 17*(2), 67-77.

Sekeroglu, N., Ozkutlu, F., & Kilic, E. (2017). Mineral composition of acorn coffees. *Indian Journal of Pharmaceutical Education and Research, 51*, 136-143.

Sekeroglu, N., Ozkutlu, F., Deveci, M., Dede, O., & Yilmaz, N. (2006). Evaluation of some wild plants aspect of their nutritional values used as vegetable in eastern Black Sea region of Turkey. *Asian Journal of Plant Sciences, 5*(2), 185-189.

Singleton, V.L., & Rossi, J.A. (1965). Colorimetry of total phenolics with phosphomolybdic-phosphotungstic acid reagents. *American Journal of Enology and Viticulture, 16*, 144-158.

Stanilova, S. A., Zhelev, Z. D., & Dobreva, Z. G. (2000). Preliminary studies on the immunomodulatory effect of the C3 binding glycoprotein isolated from *Cuscuta europea. International journal of immunopharmacology, 22*(1), 15-24.

Şekeroğlu, N., Koca, U., & Meraler, S. A. (2012). Geleneksel Bir Halk İlacı: İkşut. *Yüzüncü Yıl Üniversitesi Tarım Bilimleri Dergisi, 22*(1), 235-243.

Şekeroğlu, N., Ozkutlu, F., Kara S.M., & Ozguven, M. (2008). Determining of cadmium and micronutrients in medicinal plants from Turkey. *Journal of the Science of Food and Agriculture, 88*, 86-90.

Şenol, F.S., Şekeroğlu, N., Gezici, S., Kilic, E., Orhan, İ.E., (2018). Neuroprotective potential of the fruit (acorn) from *Quercus coccifera* L. *Turkish Journal of Agriculture and Forestry, 42*, 82-87.

Temmerman, S., Bouma, T. J, Govers, G., & Lauwaet D. (2005). Flow paths of water and sediment in a tidal marsh: Relations with marsh developmental stage and tidal inundation height. *Estuaries, 28*(3), 338 – 352.

Umehara, K., Nemoto, K., Ohkubo, T., Miyase, T., Degawa, M., & Noguchi, H. (2004). Isolation of a new 15-membered macrocyclic glycolipid lactone, Cuscutic Resinoside a from the seeds of *Cuscuta chinensis*: a stimulator of breast cancer cell proliferation.

Planta medica, 70(04), 299-304.

Wang, Z, Fang, J.N., Ge, D.L, & Li, X.Y. (2000). Chemical characterization and immunological activities of an acidic polysaccharide isolated from the seeds of *Cuscuta chinensis* Lam. *Acta Pharmacologica Sinica, 21*, 1136–1140.

WHO, (1999). World Health Organization, Monographs on Selected Medicinal Plants, vol. 1. WHO, Geneva.

Woisky, R.G., & Salatino, A. (1998). Analysis of propolis: some parameters and procedures for chemical quality control. *Journal of Apicultural Research, 3* (7), 99-105.

Ye, M., Li, Y., Yan, Y., Liu, H., & Ji, X. (2002). Determination of flavonoids in Semen Cuscutae by RP-HPLC. *Journal of Pharmaceutical and Biomedical Analysis, 28*, 621–628.

Ye, M., Yan, Y., & Guo, D.A. (2005). Characterization of phenolic compounds in the Chinese herbal drug TuSi-Zi by liquid chromatography coupled to electrospray ionization mass spectrometry. *Rapid Communications in Mass Spectrometry, 19*(11), 1469–1484.

Yen, F. L., Wu, T. H., Lin, L. T., & Lin, C. C. (2007). Hepatoprotective and antioxidant effects of *Cuscuta chinensis* against acetaminophen-induced hepatotoxicity in rats. *Journal of Ethnopharmacology, 111*(1), 123-128.

Yen, F.L., Wu, T.H., Lin, L.T., Cham, T.M., & Lin, C.C. (2008). Concordance between antioxidant activities and flavonol contents in different extracts and fractions of *Cuscuta chinensis. Food Chemistry, 108*, 455–462.

Zheng, H.Z., Dong, Z.H., & She, J. (1998). *Modern Study of Traditional Chinese Medicine*, first edition. China: Beijing Xue Yuan Press of the People's Repubic of China, Beijing.

How cite this article

Şekeroğlu, N., Korkmaz Yaşar, G., Koca Çalışkan, U., Dönmez, C., & Gezici, S., & Özkutlu, F. (2024). Comparison of polyphenolic content, radical scavenging activity, and mineral concentrations of Cuscuta monogyna VAHL on different host plants. *İstanbul Journal of Pharmacy, 54*(2), 154–164. DOI: 10.26650/IstanbulJPharm.2024.1071442

İstanbul Journal of Pharmacy
Istanbul J Pharm2024, 54 (2): 165–174
DOI: 10.26650/IstanbulJPharm.2024.1313743

Original Article

Comparative examination of phenolic content, flavonoid content, and antioxidant efficacy of *Chenopodium album* L. and *Chenopodium pumilio* R. Br.

Firdose R. Kolar[1], Sidanand V. Kambhar[2], Vaishali S. Kamble[3], Azharuddin B. Daphedar[1]

[1]Karnataka State Akkamahadevi Women's University, Department of Botany, Vijayapura (Karnataka), India.
[2]Government of Karnataka, Department of Collegiate Education, Department of Botany Government First Grade College, Raibag, Belagavi (Karnataka), India
[3]Mudhoji College, Department of Botany, Phaltan (Maharashtra), India

ABSTRACT

Background and Aims: Traditional indigenous system of medicine employed many *Chenopodium* species to treat a wide range of ailments. Therefore, the current study aims to evaluate the phenolic content, flavonoid content, and antioxidant capacity of the species *Chenopodium album* and *Chenopodium pumilio.*

Methods: Phenolics and flavonoid content were quantified using spectrophotometric techniques. The antioxidant activity of *Chenopodium* extracts was evaluated by assaying ferric reducing antioxidant power, 1,1-diphenyl-2-picrylhydrazyl (DPPH) free radical scavenging activity, phosphomolybdenum reducing power, ferrous ion chelating activity, hydrogen peroxide radical scavenging activity, hydroxyl radical scavenging activity, deoxyribose degradation activity, and β-carotene bleaching activity.

Results: In *C. album* and *C. pumilio*, total phenolic concentration was 17.5–23.8 and 13.3–25.3 mg tannic acid equivalent/g, respectively, and flavonoid content was 0.21–0.85 mg and 0.10–0.89 mg quercetin equivalent/g, respectively. Thus, *C. pumilio* had a higher content of phenolics and flavonoids than *C. album*. However, comparison of extracts in different solvents showed that ethanolic and aqueous extracts exhibited higher phenolics and flavonoid content than other solvent systems. The antioxidant capability of the species, determined by antioxidant assays, varied with the species evaluated and the solvents used for extraction. Remarkably, the correlation coefficient of different antioxidant assays with the phenolics and flavonoid content in both species showed discrepancy.

Conclusion: Ethanolic and aqueous extracts of the *Chenopodium* species studied had higher phenolics, flavonoids, and free radical scavenging activity than methanolic and acetonic extracts. The ethanolic and aqueous extracts of the studied species provide a potential source of antioxidants for drug formulation.

Keywords: *Chenopodium*; phenolics; flavonoids; free radicals; reducing power; correlation

INTRODUCTION

The genus *Chenopodium* includes numerous species of annual or perennial herbaceous plants that have worldwide distribution. *Chenopodium* comprises 250 species, of which only 21 are confined to India, which can be grown as aromatic and nonaromatic herbs (Fuentes-Bazan, Mansion, & Borsch, 2012). Several species of the genus *Chenopodium* have high medicinal value, with antibacterial, antifungal, antidiaphoretic, and antiasthmatic properties. Therefore, it has been documented as folk medicine in indigenous systems of medicine. Since ancient times, people in South America have prepared infusions from the leaves and seeds of *C. ambrosioides* (Mexican tea, Indian worm seed), considering it to be the best remedy for intestinal parasites. Similar infusions have been used in various countries. In Europe, infusions are used against pectoralis and nervous affections. In Brazil, infusions are effective in relieving flatulence, excessive sweating, anemia, cough, and chronic obstructive pulmonary diseases. In New Mexico, the seeds of *C. ambrosioides* are used as an abortifacient with low toxicity (Conway & Slocumb, 1979). In Madagascar and La Reunion, the juice of the plant is consumed undiluted or as a decoction in milk or water as an effective vermifuge (Yadav, Vasudeva, Singh, & Sharma, 2007). *Chenopodium album* L. improves appetite, fights intestinal worms, helps in bowel movement, acts as a diuretic, etc. It is useful in nausea, vomiting, abdominal pain, and eye diseases. A fine dusting powder from the leaves of *C.*

Corresponding Author: Firdose R. Kolar **E-mail:** firdose.kousar@gmail.com
Submitted: 27.06.2023 • **Revision Requested:** 14.11.2023 • **Last Revision Received:** 06.03.2024 • **Accepted:** 21.03.2024

album is applied over the external genitals of children to avoid skin irritation. Traditional ayurvedic medicine has indicated its use in various skin diseases, burns, wrinkles, etc. (Karwani & Sisodia, 2015). The therapeutic qualities of *Chenopodium* species have increased interest in research related to its phytochemistry, ethnopharmacology, and pharmacology. In this study, we examined the phenolic content, flavonoid content, and antioxidant potential of *C. album* and *C. pumilio*.

MATERIALS AND METHODS

Specimen collection

Samples of *C. album* and *C. pumilio* were collected from the premises of Karnataka State Akkamahadevi Women's University, Vijayapura. Dr. Sidanand V. Kambhar verified the authenticity of the plants. The herbaria voucher specimens and the herbaria for the species' (*C. album*: KSAWUV-159; *C. pumilio*: KSAWUV-160) were prepared and deposited in the Department of Botany, Karnataka State Akkamahadevi Women's University, Vijayapura (Karnataka).

Preparation of extracts

The whole plant (aerial part and root) was used for extraction. Deionized water, methanol, ethanol, and acetone were used as solvents to prepare the extracts on a dry weight basis. A mortar and pestle was used to homogenize 5 g of dried material in 25 mL of deionized water. The resultant extract was mixed well, shaken for 5–10 min, left on a rotary shaker for 24 h, and centrifuged for 14 min at 10,000 rpm. The supernatant was collected in a test tube, and the residue was centrifuged using 25 mL of solvent to extract remaining material. The supernatants were pooled and mixed with deionized water to a final volume of 50 mL. The same procedure was used to prepare extracts in different solvents. All the extracts were stored at 4°C, and 1% (v/v) extracts were used to quantify phenolics and flavonoids and evaluate antioxidant activity.

Total phenolic content

Total phenolic content in the plant samples was estimated by using the method of Gutierrez and Navarro (2010). The assay mixture was prepared by mixing 0.125 mL of sample extract with 0.125 mL of Folin–Ciocalteu reagent and 1.25 mL of saturated Na_2CO_3 solution. This was followed by incubation for 90 min at room temperature (25±2 °C), and optical density was measured at 760 nm. All the samples were analyzed in triplicate, and mean absorbance was measured. Based on the absorbance of standard tannic acid, a calibration curve was prepared (10–100 µg/mL, R^2 = 0.99). The results were expressed as mg tannic acid equivalent (TAE) per gram dry weight.

Total flavonoid content

Total flavonoid content of the plant samples was analyzed according to the spectrophotometric method (Basniwal et al., 2009). The assay mixture was prepared by incubating plant extract (1.5 mL) with 2 % methanolic $AlCl_3$ (1.5 mL) for 10 min at room temperature. Optical density was recorded at 420 nm. All the samples were analyzed in triplicate. Mean absorbance was recorded, and a calibration curve was plotted using standard quercetin (10–100 µg/mL, R^2 = 0.99). The final results were expressed as mg quercetin equivalent (QE) per gram dry weight.

Ferric reducing antioxidant power assay

The reducing power of the plant extracts was estimated using an advanced assay developed by Pulido et al. (2000). The assay mixture was prepared by mixing 100 µL of plant extract with 3 mL of ferric reducing antioxidant power (FRAP) assay reagent. The FRAP reagent contains one volume of 10 mM 2,4,6-Tripyridyl-S-triazine (TPTZ) solution, one volume of 20 mM $FeCl_3.6H_2O$, and ten volumes of 300 mM sodium acetate buffer (pH 3.6). The reaction mixture was incubated for 15 min at 37°C, and absorbance was recorded at 595 nm. A standard curve was obtained, utilizing an aqueous solution of ascorbic acid (10–100 µg/mL, R^2 = 0.98). The reducing ability of the extract was estimated as mg ascorbic acid equivalent (AAE) per gram dry weight.

DPPH free radical scavenging assay

The scavenging ability of 1,1-diphenyl-2-picrylhydrazyl (DPPH) free radical in the plant extract was evaluated following the assay devised by Aquino et al. (2001). To prepare the assay mixture, plant extract (25 µL) was mixed with 25 mM DPPH solution (3 mL). The reaction mixture was incubated in the dark for 20 min at room temperature, and optical density was recorded at 515 nm against a blank. The following equation was used to calculate radical scavenging activity, and the results were measured as percent inhibition of DPPH radical.

$$\text{DPPH free radical scavenging activity (\%)} = A0 - A1/A0 \times 100$$

Where, A0 is the absorbance of the DPPH radical without sample and A1 is the absorbance of the DPPH radical with sample.

Phosphomolybdenum reducing power assay

The reducing power of the extracts was evaluated using the phosphomolybdenum reduction assay, according to Prieto et al. (1999). The reaction mixture was prepared by mixing 0.3 mL of sample with 3 mL of reagent. The reagent contained 28 mM sodium phosphate, 4 mM ammonium molybdate, and 0.6

M sulfuric acid. The tubes containing the reaction mixture were sealed with aluminum foil, incubated for 90 min at 95°C, and cooled. Absorbance was measured at 965 nm against a blank. A standard curve was plotted using ascorbic acid (10–100 µg/mL, R^2 = 0.98). On the basis of absorbance values, the reducing ability of the extracts was measured and represented as AAE per gram dry weight.

Ferrous ion chelating activity

The ability of the sample extracts to chelate ferrous ions was analyzed by using the assay developed by Chew, Goh, & Lim, (2009). An aliquot was incubated with 2 mM $FeCl_2$ (100 µL) and 5 mM ferrozine (300 µL) for 10 min. Optical density was recorded at 562 nm. Percent chelating activity of the sample extract was measured by using the formula of inhibition percentage as applied for DPPH free radical scavenging activity.

Hydrogen peroxide radical scavenging activity

The titration method was adopted to analyze hydrogen peroxide scavenging activity (Zhao et al., 2006). The assay mixture was prepared by mixing 200 µL of 40 mM H_2O_2, 200 µL of the test compound, 200 µL of 3 % ammonium molybdate, 200 µL of 2 M H_2SO_4, and 1.4 mL of 1.8 M KI. The reaction mixture was titrated against 5.09 mM NaS_2O_3 until color changed from yellow to colorless. The following formula was used to assess ability to scavenge hydrogen peroxide.

Hydrogen peroxide scavenging activity (%)
= [(Vc - Vs)/Vc] × 100

Where, Vc and Vs are control and samples volumes, respectively.

Hydroxyl radical scavenging activity

To measure hydroxyl radical scavenging activity, 1.5 mL of extract was mixed with 2.4 mL of 0.2 M phosphate buffer (pH 7.8), 0.06 mL of $FeCl_3$ (1.0 mM), and 0.09 mL of 1,10- phenanthroline (1 mM) (Fadda, Barberis, & Sanna, 2018). Oxidation was initiated by adding 0.15 mL of hydrogen peroxide (0.17 M). The reaction mixture was incubated at room temperature for 5 min, and absorbance was recorded at 560 nm with a spectrophotometer. Hydroxyl radical scavenging activity was measured using the formula applied for DPPH free radical scavenging activity.

Deoxyribose degradation assay

Deoxyribose degradation ability of the extracts was determined by the assay devised by Cheng & Chang, (2003). The reaction mixtures were prepared by mixing 50 µL of deoxyribose (50 mM), 300 µL of phosphate buffer (0.2 M, pH 7.4), 50 µL of Na2EDTA (1 mM), 50 µL of FeCl3 (3.2 mM), and 50 µL of H_2O_2 (50 mM). Then 50 µL of ascorbic acid (1.8 mM) was added to the reaction mixture, and final volume was made up by adding 800 µL buffer. This was followed by incubation at 50°C for 20 min. The reaction was completed by adding 250 µL of trichloroacetic acid (10 %, w/w). Then, the reaction mixture was incubated with 150 µL of thiobarbituric acid (5 %) in 1.25 % aqueous NaOH at 105 °C in an oven for 15 min, which led to color change, and cooled. Absorbance was recorded at 530 nm against a blank (buffer). Inhibition of deoxyribose degradation was calculated in percentage using the same formula applied for DPPH free radical scavenging activity.

β-carotene bleaching assay

The β-carotene bleaching assay was conducted to determine antioxidant activity in the sample (Prieto, Rodríguez-Amado, Vázquez, & Murado, 2012). The assay mixture was prepared by adding 1 mL of β carotene solution (0.2 mg/mL chloroform) in a round bottom flask (50 mL) with 20 µL of linoleic acid and 200 µL of Tween 20 (100 %). The mixture was placed on a rotary evaporator for 10 min at 40°C to evaporate excess chloroform. Distilled water was added gradually with a burette to agitate the mixture into forming an emulsion. Then 3 mL of emulsion was mixed thoroughly with 200 µL of sample in a test tube, placed in a water bath for 2 h at 50°C, and cooled. Absorbance was recorded at 470 nm at two different times—immediately after preparation (t = 0 min) and after 2 h against a blank. All the aliquots were analyzed in triplicate. Total antioxidant activity was measured by using the following equation:

$$BBA\% = 1 - \frac{A1_{(t=0)} - A1_{(t=120)}}{A0_{(t=0)} - A0_{(t=120)}} \times 100$$

where:
BBA % is percent β-carotene bleaching activity
A1 (t = 0) is absorbance of test sample at time 0
A1 (t = 120) is absorbance of test sample after 2 h
A0 (t = 0) is absorbance of the control at time 0
A0 (t = 120) is absorbance of the control after 2 h

Statistical analysis

All experiments were conducted three times, and the results were analyzed and displayed as mean ± standard deviation. Statistical analysis was performed using MS Excel and GraphPad InStat 3 software. *P* value <0.05 was considered statistically significant.

RESULTS AND DISCUSSION

Phenolics and flavonoid content

In flowering plants, phenolics and flavonoid are the most important antioxidants, because they adsorb and neutralize

free radicals (Tungmunnithum, Thongboonyou, Pholboon, & Yangsabai, 2018). Therefore, the total content of phenolics and flavonoids in different extracts of two *Chenopodium* species (*C. album* and *C. pumilio*) was assessed. The quantity of total phenolics is expressed as mg TAE/g of sample and the quantity of total flavonoids as mg QE/g of sample (Table 1). The results revealed that the amount of phenolics greatly varied among the two taxa of the genus Chenopodium, i.e., *C. album* and *C. pumilio*. *C. album* showed the maximum amount of total phenolics in the ethanolic extract (23.8 mg TAE/g) and the lowest in the methanolic extract (14.9 mg TAE/g). Similarly, *C. pumilio* exhibited the highest phenolic content in the aqueous extract (25.3 mg TAE/g) and the lowest in the acetonic extract (13.3 mg TAE/g). Significantly high results were found for phenolic content in this order: ethanol > aqueous > acetone > methanol for *C. album* and aqueous > ethanol > methanol > acetone for *C. pumilio*. Water, ethanol, methanol, acetone, and their aqueous mixes are the most commonly used solvents for phenolic extraction (Michiels, Kevers, Pincemail, Defraigne, & Dommes, 2012). According to Huang, Ou, Hampsch-Woodill, Flanagan, & Deemer (2002), the antioxidant properties of plants are primarily attributed to phenolic chemicals, which are categorized as hydrophilic antioxidants. This could explain our findings that water and ethanol were the most effective extraction solvents. This might have resulted from interactions (hydrogen bonds) between the solvent and polar sites of the antioxidants, which improved the solvation of the chemicals found in Chenopodium species.

C. album and *C. pumilio* showed significant variation in flavonoid content with the solvents. Among the solvents, ethanolic and aqueous extracts showed the highest amounts of total flavonoids in *C. album* (0.89 mg QE/g) and *C. pumilio* (0.85 mg QE /g), respectively (Table 1). The content in different solvents was in this order: ethanol > methanol > aqueous > acetone for *C. album* and aqueous > ethanol > methanol > acetone for *C. pumilio*. Comparatively, *C. pumilio* exhibited a greater amount of TFC than *C. album*. When the phenolic and flavonoid content of different species was compared, *C. pumilio* had higher total phenolic and flavonoid content than *C. album*. According to Repo-Carrasco-Valencia et al. (2010), the polyphenol content of the Chenopodiaceae is high, with phenolics and flavonoids derivatives acting as radical scavengers. However, our findings contradict those of Repo-Carrasco-Valencia. There are reports that are consistent with our findings, according to which phenolic derivatives in plants have higher antioxidant potencies, because they neutralize lipid free radicals or prevent the breakdown of H_2O_2 (Cai, Luo, Sun, & Corke, 2004; Pitchaon, Suttajit, & Pongsawatmani, 2007). Thus, although the concentration of phenolics and flavonoids varies among species, they are both potent antioxidants that can scavenge free radicals (Muflihah, Gollavelli, & Ling, 2021).There is a direct correlation between the antioxidant activity of plants and their phenolic or flavonoid content (Joshi, Deepa, & Sharma., 2022).

FRAP assay

The reduction potential of *Chenopodium* species assessed by the FRAP assay revealed that the reducing power of both plants is significantly high, and highest activity is exhibited by the ethanolic extract of C. album (37.5 mg AAE/g) and aqueous extract of *C. pumilio* (37.9 mg AAE/g). *C. pumilio* had higher ferric reducing activity than *C. album* (Table 2). The reduction potential of the studied *Chenopodium* species is supported by data from earlier studies on other medicinal plants. Antioxidants found in plants were responsible for ferric reducing antioxidant properties (Rajurkar and Hande, 2011, Fernandes et al., 2016, Al-Laith, Alkhuzai, & Freije, 2019). The reason for this is the extract's ability to donate hydrogen atoms through cleaving (Marimuthu, Balakrishnan, & Nair, 2013). The plant primarily contains phenolic composites with redox properties, which enable them to function as singlet oxygen quenchers, reducing agents, and hydrogen donors. The determination of antioxidant potential was significantly influenced by this reduction potential. The phenolics and flavonoid compounds of the investigated Chenopodium species may be responsible for their reduction potential.

DPPH free radical scavenging activity

The DPPH free radical scavenging ability of the extracts was established in the following order: ethanol > methanol > aqueous > acetone for *C. album* and aqueous > ethanol > methanol > acetone for *C. pumilio*. *C. album* showed highest DPPH scavenging activity in the ethanolic extract (96.7 %), and *C. pumilio* exhibited the highest DPPH scavenging activity in the aqueous extract (90.6 %). The study indicated that all the extracts acted as potent hydrogen donors; they might serve as free radical scavengers and primary antioxidants. The DPPH radicals show a biphasic response to many plant-derived antioxidants. Numerous phytochemicals are present in plant extracts, and plant extracts with different phytochemicals may also show different biological activity (Molole, Gure, & Abdissa, 2022). Because of the combination of antioxidants present, plant extracts may be more reactive against DPPH radicals. Based on the findings, it is perceived that both species exhibited stable DPPH free radical scavenging activity and that the antioxidant radicals present in sample extracts may have contributed to this capacity. Although the DPPH free radical scavenging activity of *C. album* and other Chenopodium species has been investigated (Nowak, Szewczyk, Gawlik-Dziki, Rzymowska, & Komsta, 2016), the results of various studies can be difficult to compare because different experimental conditions are used in each study (Hirose et al., 2010). However, when comparing scavenging activity of *C. album* reported by Adedapo, Jimoh, & Afolayan (2011), the methanolic and acetonic extracts demonstrated the highest

Table 1. Total phenolics and flavonoid content of *Chenopodium album* and *Chenopodium pumilio*.

Species	Solvents	Total phenolic content (mg TAE/g dw)	Total flavonoid content (mg QE/g dw)
C. album	Aqueous	19.8±0.04	0.31±0.09
	Ethanol	23.8±0.06	0.85±0.06
	Methanol	14.9±0.10	0.37±0.07
	Acetone	17.5±0.12	0.21±0.01
C. pumilio	Aqueous	25.3±0.10	0.89±0.07
	Ethanol	15.6±0.09	0.31±0.06
	Methanol	15.1±0.10	0.15±0.01
	Acetone	13.3±0.07	0.10±0.03

Values are expressed as mean ± SD of triplicate measurements.
mg TAE/g **dw**: milligram tannic acid equivalent per gram **dry weight**.
mg QE/g **dw**: milligram quercetin equivalent per gram **dry weight**.

Table 2. Ferric reducing antioxidant power and DPPH free radical scavenging activity of *Chenopodium album* and *Chenopodium pumilio.*

Species	Solvents	Ferric reducing antioxidant power (mg AAE/g dw)	DPPH free radical scavenging activity (%)
C. album	Aqueous	20.6±0.15	79.6±0.07
	Ethanol	37.5±0.11	96.7±0.11
	Methanol	18.5±0.19	91.5±0.09
	Acetone	17.1±0.13	74.3±0.11
C. pumilio	Aqueous	37.9±0.08	90.6±0.11
	Ethanol	23.2±0.40	86.1±0.09
	Methanol	20.5±0.08	75.5±0.19
	Acetone	15.2±0.30	53.4±0.11

Values are expressed as mean ± SD of triplicate measurements.
mg AAE /g dw : milli gram ascorbic acid equivalent per gram dry weight.
% - percentage inhibition per gram dry weight.

activity, whereas the aqueous extract demonstrated the lowest scavenging activity.

Phosphomolybdenum reducing power

The reducing ability of the extracts could be considered a significant indicator of their potential as antioxidants (Eshwarappa, Iyer, Subbaramaiah, Richard, & Dhananjaya, 2014). The increasing amount of total antioxidant activity is directly proportional to the reducing power of the extracts. The phosphomolybdenum reducing power of the studied *Chenopodium* species varied with respect to different solvents and was found to be in the order ethanol > aqueous > methanol > acetone for *C. album* and aqueous > methanol > ethanol > acetone for *C. pumilio* (Table 3). Reducing power was lowest for acetone extracts in both *Chenopodium* species. *C. pumilio* (43.3 mg AAE/g) exhibited the highest reductive ability compared with *C. album* (34.7 mg AAE/g). Numerous studies have demonstrated a correlation between antioxidant activity and the ability of bioactive compounds to donate electrons (Gupta, Maurya, Agarwal, Kushwaha, & Kumar, 2016; Kolar, Kambhar, Chavana, Kadam, & Nadaf, 2021). The reducing power of *Chenopodium* species' chemical components reported may allow them to function as primary and secondary antioxidants by acting as electron donors and reducing the oxidized intermediates of lipid peroxidation.

Ferrous ion chelating activity

The Fe^{2+} chelating activities of the extracts were in the following order: ethanol > aqueous > methanol > acetone in *C. album* and aqueous > ethanol > methanol > acetone in C. pumilio (Table 3). According to the results, metal chelating activity was highest in the ethanolic extract of *C. album* (97.0 %) and aqueous extract of C. pumilio (65.4 %). Therefore, it was suggested that the Fe^{2+} chelating effects of *C. album* and *C. pumilio* could help in protecting against free radical damage. The oxidative degradation of lipids can be controlled by reducing metal

Table 3. Phosphomolybdenum reducing power and ferrous ion chelating activity of *Chenopodium album* and *Chenopodium pumilio.*

Species	Solvents	Phosphomolybdenum reducing power (mg AAE/g dw)	Ferrous ion chelating activity (%)
C. album	Aqueous	33.8±0.80	92.6±1.12
	Ethanol	34.7±0.12	97.0±0.68
	Methanol	27.5±0.09	57.9±0.93
	Acetone	22.5±0.64	44.6±1.36
C. pumilio	Aqueous	43.3±0.39	65.4±1.79
	Ethanol	34.4±0.17	61.4±0.89
	Methanol	36.5±0.32	59.1±0.89
	Acetone	20.6±0.10	56.9±1.61

Values are expressed as mean ± SD of triplicate measurements.
mg AAE /g dw: milli gram ascorbic acid equivalent per gram dry weight.
% - percentage inhibition per gram dry weight.

concentration through the metal chelating capacity of the compound (Gulcin, & Alwasel, 2022). The chelators have more affinity for metal; therefore, the chelating agents form covalent bonds with metal ions. Therefore, chelating agents are considered secondary antioxidants. They can reduce and stabilize metal ion oxidation (Sahat, Ibrahim, & Alsaid, 2015). Our data revealed that the phytocompounds in the extracts demonstrated strong ability toward iron binding, and the antioxidant action may be owed to its iron-binding ability.

Hydrogen peroxide radical scavenging activity

Both *Chenopodium* species showed effective scavenging activity for hydrogen peroxide. The activity for *C. album* follows the order ethanol > aqueous > methanol > acetone, and that for *C. pumilio* follows the order aqueous > methanol > ethanol > acetone. Highest activity was recorded for the aqueous extract of *C. pumilio* (66.6 %) and the ethanolic extract of *C. album* (53.3 %). Several dietetic polyphenols, such as catechin, quercetin, caffeic acid, and gallic acid, are main components of plant-based foods, especially fruits and vegetables. High amounts of hydrogen peroxide in plant and animal cells may cause oxidative stress, and extremely high concentrations may lead to cell death. Dietary polyphenols establish a protective shield against cell damage in mammalian and bacterial cells (Saffoon et al., 2014). On the basis of these results, phenolic and flavonoid compounds of *Chenopodium* species are involved in quenching H_2O_2, and hence, show significant hydrogen peroxide radical scavenging activity.

Hydroxyl radical scavenging activity

Antioxidant activity is comparable to hydroxyl radical scavenging activity. In our study, ethanolic and aqueous extracts exhibited the highest hydroxyl radical scavenging activity in *C. album* (74.4 %) and *C. pumilio* (78.5 %), respectively (Table 4). Hydroxyl radicals are highly reactive and have a short half-life; hence, they can damage all three important classes of biological molecules, including nucleic acids, proteins, and lipids (Das & Roychoudhury, 2014). The initiation of lipid peroxidation is carried out by radicals. This process is completed by taking hydrogen atoms from unsaturated fatty acids. As a result, one of a living body's most efficient defense against numerous diseases is the elimination of hydroxyl radicals. The *Chenopodium* species studied exhibited effective hydroxyl radical scavenging activity. Hence, it can act against various diseases by removing hydroxyl radicals.

Deoxyribose degradation activity

The deoxyribose degradation test showed that the *Chenopodium* species were effective in neutralizing OH radicals, where percentage inhibition followed the order ethanol > aqueous > methanol > acetone for *C. album* and aqueous > methanol > ethanol > acetone for *C. pumilio* (Table 5). The ethanolic and aqueous extracts exhibited the highest degradation activity in *C. album* (89.6 %) and *C. pumilio* (57.0 %), respectively. *C. album* is more potent at degrading deoxyribose than *C. pumilio*. The low intensity of red color indicated that antioxidant activity is comparable to hydroxyl radical scavenging activity (Gulcin, Berashvili, & Gepdiremen, 2005). The result showed that degradation of deoxyribose was prevented due to the addition of fractions of *Chenopodium* in the reaction mixture. Moreover, it helped initiate scavenging of hydroxyl radicals.

β-carotene bleaching activity

The ability of *Chenopodium* species to bleach β-carotene differed depending on the species and solvent type. The ethanolic and aqueous extracts of *C. album* (91.7 %) and *C. pumilio* (93.1%) had the highest β-carotene bleaching activity, respectively (Table 5). The order of activity for *C. album* is ethanol > aqueous > acetone > methanol, whereas the sequence for *C.*

Table 4. Hydrogen peroxide radical scavenging activity and hydroxyl radical scavenging activity of *Chenopodium album* and *Chenopodium pumilio.*

Species	Solvents	Hydrogen peroxide radical scavenging activity (%)	Hydroxyl radical scavenging activity (%)
C. album	Aqueous	48.5±1.05	67.5±1.04
	Ethanol	53.3±1.34	74.4±1.38
	Methanol	47.8±1.05	62.3±1.11
	Acetone	40.5±1.46	55.5±1.36
C. pumilio	Aqueous	66.6±1.15	78.5±0.98
	Ethanol	57.3±0.99	71.8±0.68
	Methanol	61.9±1.55	58.8±1.06
	Acetone	57.1±1.40	60.3±1.36

Values are expressed as mean ± SD of triplicate measurements.
% - percentage inhibition per gram dry weight.

Table 5. Deoxyribose degradation and β- Carotene bleaching activity of *Chenopodium album* and *Chenopodium pumilio.*

Species	Solvents	Deoxyribose degradation activity (%)	β- Carotene bleaching activity (%)
C. album	Aqueous	80.4±0.67	89.3±1.05
	Ethanol	89.6±1.10	91.7±0.94
	Methanol	74.9±0.97	82.8±0.77
	Acetone	57.8±0.67	85.4±0.62
C. pumilio	Aqueous	57.0±0.91	93.1±0.60
	Ethanol	44.5±0.59	82.5±1.03
	Methanol	53.2±1.08	87.7±1.25
	Acetone	37.4±0.64	78.4±1.16

Values are expressed as mean ± SD of triplicate measurements.
% - percentage inhibition per gram dry weight.

Table 6. Regression coefficients (r^2 value) for antioxidant activity assessed by different methods and the relative influence of antioxidant components.

Species		FRAP	DPPH	PMR	FC	HPS	HRS	DD	β- CB
C. album	**TPC**	0.783	0.125	0.522	0.648	0.406	0.637	0.443	0.951
	TFC	0.957	0.728	0.449	0.445	0.717	0.735	0.652	0.464
C. pumilio	**TPC**	0.968	0.296	0.620	0.877	0.793	0.704	0.584	0.794
	TFC	0.967	0.531	0.570	0.912	0.666	0.821	0.474	0.691

TPC = Total phenolic content; TFC = Total flavonoid content; FRAP = Ferric reducing antioxidant power; DPPH = DPPH free radical scavenging activity; PMR= Phosphomolybdenum reduction; FC=Ferrous ion chelation; HPS: Hydrogen Peroxide Scavenging; HRS: Hydroxyl Radical Scavenging; DD=Dexyribose degradation; β- CB= β- Carotene bleaching activity.

Table 7. ANOVA for antioxidant activity among different extracts by different antioxidant assays of two *Chenopodium* species.

Antioxidant assays	df	MS	*P*
FRAP	1	1.110	0.916
DPPH	1	5.661	0.628
PMR	1	33.17	0.491
FC	1	304.0	0.379
HPS	1	348.6	0.008
HRS	1	11.66	0.709
DD	1	11.90	0.013
β- CB	1	7.566	0.622

FRAP = Ferric reducing antioxidant power; DPPH = DPPH Radical scavenging; PMR= Phosphomolybdenum reduction; FC=Ferrous ion chelation; HPS: Hydrogen Peroxide Scavenging; HRS: Hydroxyl Radical Scavenging; DD=Dexyribose degradation; β- CB= β- Carotene bleaching activity.

pumilio is aqueous > methanol > ethanol > acetone. Compared to methanolic and acetone extracts, the β carotene bleaching inhibitory activity was relatively higher in ethanolic and aqueous extracts. The amount of bleaching is reduced by antioxidants in plants, which neutralize the linoleic hydroperoxyl free radicals produced (Kulisic et al., 2004). As a result, the antioxidant activity of the sample extracts influences the rate at which β-carotene degrades. The findings indicate that the extracts of *Chenopodium* species studied could prevent β-carotene from bleaching, making them effective antioxidants.

Correlation between phytochemical constituents and antioxidant activity

The relationship of the phytocompounds with the antioxidant ability of the plants examined was determined (Table 6). Phenolic content displayed a significant correlation with most of the antioxidant tests, such as ferric reducing antioxidant power ($r = 0.783$) and β-carotene bleaching activity ($r = 0.951$) in C. album, and with ferric reducing antioxidant power ($r = 0.968$), ferrous ion chelation ($r = 0.877$) and β-carotene bleaching activity ($r = 0.794$) in *C. pumilio*. Similarly, the flavonoid content of C. album indicated a good correlation with antioxidant assays, such as ferric reducing antioxidant power ($r = 0.957$), DPPH free radical scavenging activity ($r = 0.728$), hydrogen peroxide scavenging activity ($r = 0.728$), and hydroxyl radical scavenging activity ($r = 0.735$). The flavonoid content of *C. pumilio* revealed a significant correlation with ferric reducing antioxidant power ($r = 0.967$), ferrous ion chelation ($r = 0.912$) and hydroxyl radical scavenging activity ($r = 0.821$). The remaining assays exhibited average correlation in both species. The antioxidant capacity of different extracts shows great variation in results, probably due to factors such as genetics, agro-technical practices, and environmental circumstances, which have great impact on the presence of phenolics and flavonoid compounds. Several reports have indicated that antioxidant activity and phenols correlate directly (Aryal et al., 2009; Muflihah, Gollavelli, & Ling, 2021; Alnsour, Issa, Awwad, Albals, & Al-Momani, 2022). The inconsistencies observed in the correlation in this study explained that different plants are rich in different specialized metabolites; therefore, it is difficult to consider which is predominant. The literature reviews showed a discrepancy in the correlation of phytochemical constituents with antioxidant activity. This inconsistency is due to variations in the representation and elucidation of results, methodology used, and evaluation of interfering substances, such as ascorbic acid, saccharides, and carotenoids. Moreover, the antioxidant activity of an extract can fluctuate due to many factors, such as the method of mixture preparation, antioxidant solubility, oxidation state, pH, and type of oxidation-prone substrate (Alvarez-Jubete, Wijngaard, Arendt, & Gallagher, 2010).

ANOVA was used to evaluate significantly mean differences amid the different solvent extracts of *Chenopodium* species, and a significant difference was confirmed at the $P < 0.05$ level in different assays (Table 7). The examined plant extracts had promising antioxidant and free radical scavenging activity.

This study has some limitations. Instead of analyzing pure chemicals, the studies were performed on extracts and fractions. From the perspective of single molecule-based medicine, they are inconclusive, although they offer highly valuable insights into the use of plant-based medicine in chronic conditions. The results of the *in vitro* tests performed in this work must be validated *in vivo*.

CONCLUSION

The results of this study demonstrated the presence of flavonoids, phenolics, and antioxidant activity in the two *Chenopodium* species. Based on the results, in various test procedures, all the solvent extracts of both the species showed varying levels of antioxidant activity. A sufficient quantity of flavonoids and phenolics was present, which accounts for the observed antioxidant efficiency. When compared with other solvent extracts, aqueous and ethanolic extracts showed the highest concentrations of phenolics and flavonoids and the strongest antioxidant activity. Therefore, aqueous and ethanolic extracts of *C. album* and *C. pumilio* can be utilized as readily available sources of natural antioxidants. Further studies on the role of these antioxidants are warranted. The purification, separation, and identification of active compounds, as well as their function in disease prevention, must be evaluated.

Peer-review: Externally peer-reviewed.

Author Contributions: Conception/Design of Study- F.R.K.; Data Acquisition- F.R.K., S.V.K.; Data Analysis/Interpretation- F.V.K., V.S.K.; Drafting Manuscript- F.R.K., A.B.D.; Critical Revision of Manuscript- F.R.K., A.B.D.; Final Approval and Accountability- F.R.K., S.V.K., V.S.K., A.B.D.

Conflict of Interest: The authors have no conflict of interest to declare.

Financial Disclosure: The authors declared no financial support.

Acknowledgments: The Karnataka State Akkamahadevi Women's University, Vijayapura administration is appreciated by the authors for providing the laboratory and characterization facilities. We appreciate Dr. Babu R. L.'s unwavering encouragement and support.

ORCID IDs of the authors

Firdose R. Kolar	0000-0001-7482-8802
Sidanand V. Kambhar	0000-0002-1701-0892
Vaishali S. Kamble	0009-0001-1237-1736
Azharuddin B. Daphedar	0000-0001-7824-3035

REFERENCES

Adedapo A., Jimoh F., Afolayan A. (2011). Comparison of the nutritive value and biological activities of the acetone, methanol and water extracts of the leaves of *Biden spilosa* and *Chenopodium album. Acta Poloniae Pharmaceutica Drug Research, 68*, 83–92.

Al-Laith, A.A., Alkhuzai, J., & Freije, A. (2019). Assessment of antioxidant activities of three wild medicinal plants from Bahrain. *Arabian Journal of Chemistry, 12* (8), 2365-2371. https://doi.org/10.1016/j.arabjc.2015.03.004.

Alnsour, L., Issa, R., Awwad, S., Albals, D., & Al-Momani, I. (2022). Quantification of total phenols and antioxidants in coffee samples of different origins and evaluation of the effect of degree of roasting on their levels. *Molecules, 28*, 27(5):1591. https://doi.org/10.3390/molecules27051591.

Alvarez-Jubete, L., Wijngaard, H., Arendt, E. K., & Gallagher, E. (2010). Polyphenol composition and in vitro antioxidant activity of amaranth, quinoa buckwheat and wheat as affected by sprouting and baking. *Food Chemistry, 119* (2), 770-778. https://doi.org/10.1016/j.foodchem.2009.07.032.

Aquino, R., Morelli, S., Lauro, M. R., Abdo, S., Saija, A., & Tomaino, A. (2001). Phenolic constituents and antioxidant activity of an extract of *Anthurium versicolor* leaves. *Journal of Natural Products, 64*(8), 1019-23. https://doi.org/10.1021/np0101245.

Aryal, S., Baniya, M. K., Danekhu, K., Kunwar, P., Gurung, R., & Koirala, N. (2019). Total phenolic content, flavonoid content and antioxidant potential of wild vegetables from western Nepal. *Plants* (Basel), 8(4), 96. https://doi.org/10.3390/plants8040096.

Basniwal, P. K., Suthar, M., Rathore, G. S., Gupta, R., Kumar, V., Pareek, A., & Jain D. (2009). In-vitro antioxidant activity of hot aqueous extract of *Helicteres isora* Linn. fruits. Natural Product Radiance, 8, 483–7.

Cai. Y. Z., Luo, Q., Sun, M., & Corke, H. (2004). Antioxidant activity and phenolic compounds of 112 traditional Chinese medicinal plants associated with anticancer. *Life Science, 74*, 2157-2184. https://doi.org/10.1016/j.lfs.2003.09.047.

Cheng, Z., Li, Y., & Chang, W. (2003). Kinetic deoxyribose degradation assay and its application in assessing the antioxidant activities of phenolic compounds in a Fenton-type reaction system. *Analytica Chimica Acta, 478*(1), 129-137. https://doi.org/10.1016/S0003-2670(02)01435-6.

Chew, Y.L., Goh J.K., & Lim Y.Y. (2009). Assessment of in-vitro antioxidant capacity and polyphenolic composition of selected medicinal herbs from Leguminosae family in Peninsular Malaysia. *Food Chemistry, 116*, 13–18. https://doi.org/10.1016/j.foodchem.2009.01.091.

Conway, G. A., & Slocumb J. C. (1979). Plants used as abortifacients and emmenagogues by Spanish New Mexicans. *Journal of Ethnopharmacology, 1*(3), 241-261. https://doi.org/10.1016/s0378-8741(79)80014-8.

Das, K., & Roychoudhury, A. (2014). Reactive oxygen species (ROS) and response of antioxidants as ROS-scavengers during environmental stress in plants. *Frontiers in Environmental Science,* 2, 53. https://doi.org/10.3389/fenvs.2014.00053

Eshwarappa, R. S., Iyer, R. S., Subbaramaiah, S. R., Richard, S. A., & Dhananjaya, B. L. (2014). Antioxidant activity of *Syzygium cumini* leaf gall extracts. *Bioimpacts, 4*(2), 101-7. https://doi.org/10.5681/bi.2014.018

Fadda A., Barberis A., & Sanna D. (2018). Influence of pH, buffers and role of quinolinic acid, a novel iron chelating agent, in the determination of hydroxyl radical scavenging activity of plant extracts by Electron Paramagnetic Resonance (EPR). *Food Chemistry, 240*,174–182. https://doi.org/10.1016/j.foodchem.2017.07.076.

Fernandes, R. P., Trindade, M. A., Tonin, F. G., Lima, C. G., Pugine, S. M., Munekata, P. E., Lorenzo, J. M., & de Melo M. P. (2016). Evaluation of antioxidant capacity of 13 plant extracts by three different methods: cluster analyses applied for selection of the natural extracts with higher antioxidant capacity to replace synthetic antioxidant in lamb burgers. *Journal of Food Science and Technology, 53*(1), 451-60. https://doi.org/10.1007/s13197-015-1994-x.

Fuentes-Bazan, S., Mansion, G., & Borsch, T. (2012). Towards a species level tree of the globally diverse genus *Chenopodium* (Chenopodiaceae). *Molecular Phylogenetics and Evolution, 62*, 359–374. https://doi.org/10.1016/j.ympev.2011.10.006.

Gulcin, İ., & Alwasel, S. H. (2022). Metal Ions, Metal Chelators and Metal Chelating Assay as Antioxidant Method. *Processes, 10*(1), 132. https://doi.org/10.3390/pr10010132.

Gulcin, I., Berashvili, D., & Gepdiremen, A. (2005). Antiradical and antioxidant activity of total anthocyanins from Perilla pankinensis decne. Journal of Ethnopharmacology, 101, 287–293. https://doi.org/10.1016/j.jep.2005.05.006.

Gupta, K., Maurya, S., Agarwal, S., Kushwaha, A., & Kumar, R. (2016). Antioxidant assessment of extracts obtained through hot extraction process. *Cell and Molecular Biology, 62* (3), 129. https://doi.org/10.4172/1165-158X.1000129.

Gutierrez, R. M., & Navarro, Y. T. (2010). Antioxidant and hepatoprotective effects of the methanol extract of the leaves of *Satureja macrostema. Pharmacognosy Magazine, 6*,125–31. https://doi.org/10.4103/0973-1296.62901.

Hirose, Y., Fujta T., Ishii T., & Ueno N. (2010). Antioxidative properties and flavonoids composition of *Chenopodium* quinoa seeds cultivated in Japan. *Food Chemistry, 119*, 1300–1306. https://doi.org/10.1016/j.foodchem.2009.09.008

Huang, D., Ou, B., Hampsch-Woodill, M., Flanagan, J. A., & Deemer, E. K. (2002). Development and validation of oxygen radical absorbance capacity assay for lipophilic antioxidants using randomly methylated beta-cyclodextrin as the solubility enhancer. *Journal of Agriculture and Food Chemistry, 50*, 1815-1821. https://doi.org/10.1021/jf0113732.

Joshi, T., Deepa, P. R., & Sharma, P. K. (2022). Effect of different proportions of phenolics on antioxidant potential: Pointers for bioactive Synergy/Antagonism in foods and nutraceuticals. *Proceedings of the National Academy of Sciences, India Section* B. 92, 939–946. https://doi.org/10.1007/s40011-022-01396-6.

Karwani, G. & Sisodia, S. S. (2015). *Chenopodium album* Linn (Bathua): A review of potential therapeutic applications. *International Journal of Chemical and Pharmaceutical Analysis, 2*(4), 1-5. https://doi.org/10.1007/s13197-014-1553-x.

Kolar, F. R., Kambhar, S. V., Chavana, M., Kadam, S. & Nadaf P. (2021). Disparities of phytochemical constituents and antioxidant activities of some Indigofera species. *Israel Journal of Plant Sciences, 68* (1-2), 151-160. https://doi.org/10.1163/22238980-bja10025.

Kulisic, T., Radonic, A., Katalinic, V. & Milos, M. (2004). Use of different methods for testing antioxidative activity of oregano essential oil. *Food Chemistry, 85*, 633–640. https://doi.org/10.1016/j.foodchem.2003.07.024.

Marimuthu, S., Balakrishnan, P., & Nair, S. (2013). Phytochemical investigation and radical scavenging activities of Melia azedarach and its DNA protective effect in cultured lymphocytes. *Pharmaceutical Biology*, 51(10), 1331–1340. https://doi.org/10.3109/13880209.2013.791323.

Michiels, J. A., Kevers, C., Pincemail, J., Defraigne, J. O., & Dommes, J. (2012). Extraction conditions can greatly influence antioxidant

capacity assays in plant food matrices. *Food Chemistry, 130*, 986-993. https://doi.org/10.1016/j.foodchem.2011.07.117.

Mololе, G. J., Gure, A., & Abdissa, N. (2022). Determination of total phenolic content and antioxidant activity of *Commiphora mollis* (Oliv.) Engl. resin. BMC Chemistry, 25, 16(1):48. https://doi.org/10.1186/s13065-022-00841-x.

Muflihah, Y. M., Gollavelli, G., & Ling, Y. C. (2021). Correlation study of antioxidant activity with phenolic and flavonoid compounds in 12 Indonesian indigenous herbs. *Antioxidants* (Basel), 27, 10(10):1530. https://doi.org/10.3390/antiox10101530.

Nowak, R., Szewczyk, K., Gawlik-Dziki, U., Rzymowska, J., & Komsta, Ł. (2016). Antioxidative and cytotoxic potential of some *Chenopodium* L. species growing in Poland. *Saudi Journal of Biological Sciences, 23* (1), 15-23. https://doi.org/10.1016/j.sjbs.2015.01.017.

Pitchaon, M., Suttajit, M., & Pongsawatmani, R. (2007). Assessment of phenolic content and free radical scavenging capacity of some Thai indigenous plants. *Food Chemistry, 100*, 1409-1418. https://doi.org/10.1016/j.foodchem.2005.11.032.

Prieto, M. A., Rodríguez-Amado, I., Vázquez, J. A., & Murado, M. A. (2012). β-carotene assay revisited. Application to characterize and quantify antioxidant and prooxidant activities in a microplate. *Journal of Agricultural and Food Chemistry, 60* (36), 8983-8993. https://doi.org/10.1021/jf302218g.

Prieto, P., Pineda, M., & Aguilar, M. (1999). Spectrophotometric quantitation of antioxidant capacity through the formation of a phosphor molybdenum complex: specific application to the determination of vitamin E. *Analytical Biochemistry, 269*, 337–341. https://doi.org/10.1006/abio.1999.4019.

Pulido, R., Bravo, L., & Saura-Calixto, F. (2000). Antioxidant of dietary polyphenols as determined by a modified ferric reducing antioxidant power assay. *Journal of Agriculture and Food Chemistry, 46*, 3396-3402. https://doi.org/10.1021/jf9913458. PMID: 10956123. ,

Rajurkar, N. S., & Hande, S. M. (2011). Estimation of phytochemical content and antioxidant activity of some selected traditional Indian medicinal plants. *Indian Journal of Pharmaceutical Sciences. 73*(2), 146-51.https://doi.org/10.4103/0250-474x.91574.

Repo-Carrasco-Valencia, R., Hellström Pihlava, J. M., & Mattila, P.H. (2010). Flavonoids and other phenolic compounds in Andean indigenous grains: Quinoa *(Chenopodium quinoa), Kañiwa (Chenopodium pallidicaule)* and Kiwicha *(Amaranthus caudatus). Food Chemistry, 120*(1), 128-133. https://doi.org/10.1016/j.foodchem.2009.09.087.

Saffoon, N., Uddin, R., Subhan, N., Hossain, H., Reza, H. M., & Alam M. A. (2014). *In vitro* anti-oxidant activity and HPLC-DAD system based phenolic content analysis of *Codiaeum variegatum* found in Bangladesh. *Advanced Pharmaceutical Bulletin. 4* (Suppl 2), 533-541.https://doi.org/10.5681/apb.2014.079.

Sahat A. A., Ibrahim A. Y., & Alsaid M. S. (2015). Antioxidant capacity and phenolic content of seven Saudi Arabian medicinal herbs traditionally used in Saudi Arabia. *Indian Journal of Traditional Knowledge, 1*(1), 28-35.

Talcott, S.T., Howard, L.R., & Brenes, C.H. (2000). Antioxidant changes and sensory properties of carrot puree processed with or without periderm tissue. *Journal of Agricultural and Food Chemistry, 48*, 1315–1321. https://doi.org/10.1021/jf9910178

Tungmunnithum, D., Thongboonyou, A., Pholboon, A., & Yangsabai, A. (2018). Flavonoids and other phenolic compounds from medicinal plants for pharmaceutical and medical aspects: An overview. *Medicines* (Basel), 25, 5(3):93. https://doi.org/10.3390/medicines5030093.

Yadav, N., Vasudeva, N., Singh, S., & Sharma, S. K. (2007). Medicinal properties of genus *Chenopodium* Linn. *Natural Product Radiance, 6*(2), 131-134.

Zhao, G. R., Xiang, Z. J., Ye, T. X., Yuan, Y. J., & Guo, Z. X. (2006). Antioxidant activities of *Salvia miltiorrhiza* and *Panax notoginseng*. Food Chemistry, 99, 767-774. . https://doi.org/10.1016/j.foodchem.2005.09.002.,

How to cite this article

Kolar, F.R., Kambhar, S.V., Kamble, V.S., Daphedar, A.B. (2024). Comparative examination of phenolic content, flavonoid content, and antioxidant efficacy of Chenopodium album L. and Chenopodium pumilio R. Br.. *İstanbul Journal of Pharmacy, 54*(2), 165–174. DOI: 10.26650/IstanbulJPharm.2024.1313743

İstanbul Journal of Pharmacy
Istanbul J Pharm2024, 54 (2): 175–181
DOI: 10.26650/IstanbulJPharm.2024.1248393

Original Article

Compositions of the essential oils and antimicrobial activities of the rediscovered Turkish endemic *Salvia freyniana* and *Salvia quezelii* (Lamiaceae)

Ayla Kaya[1], Gözde Öztürk[2], Süleyman Doğu[3], Betül Demirci[2]

[1]Anadolu University, Faculty of Pharmacy, Department of Pharmaceutical Botany, Eskişehir, Türkiye
[2]Anadolu University, Faculty of Pharmacy, Department of Pharmacognosy, Eskişehir, Türkiye
[3]Necmettin Erbakan University Meram Vocational School, Department of Medical and Aromatic Plants, Konya, Türkiye

ABSTRACT

Background and Aims: This study aims to determine the chemical compositions and antibacterial activity of the rediscovered Turkish endemic *Salvia freyniana* Bornm. and *Salvia quezelii* Hedge & Afzal-Rafii.

Methods: The study simultaneously uses gas chromatography (GC-FID) and gas chromatography-mass spectrometry (GC-MS) systems, to analyze the hydrodistilled essential oils of *S. freyniana* and *S. quezelii*. The study examines the antibacterial activity of *Salvia* essential oils against the human pathogens *Escherichia coli* ATCC 8739, *Staphylococcus aureus* ATCC 6538, *Pseudomonas aeruginosa* ATCC B888, and *Salmonella typhimurium* ATCC 13311 and evaluates the oils' minimum inhibitory concentrations (MIC).

Results: The major components were found as 1,8-cineole (21.9%), β-pinene (14.2%), camphor (8.7%), α-pinene (8.0%), and valeranone (7.0%) for *S. freyniana* and limonene (20.8%), pinocamphone (11.4%), α-pinene (10.6%), camphor (9.1%), β-pinene (7.5%), camphene (7.1%) and isopinocamphone (6.7%) for *S. quezelii*. *S. typhimurium* was inhibited at a concentration of 5 mg/mL by both essential oils, with a MIC value of 5 mg/mL being found against *S. aureus* by *S. freyniana*. The other tested samples show rather moderate inhibitory effects (20 mg/mL).

Conclusion: To the best of this study's knowledge, this is the first report to show the antimicrobial activity of the essential oils of *S. freyniana* and *S. quezelii*.

Keywords: antibacterial activity, GC-FID, GC-MS, *Salvia freyniana, Salvia quezelii*, rediscovery

INTRODUCTION

The genus *Salvia* L. is one of the largest members of the Lamiaceae family (tribe: Mentheae) and contains approximately 1000 species spread all over the world (Harley et al., 2004). Türkiye is a main center of diversity for the genus in Asia, which is represented by 99 species, 52 of which are endemic to Türkiye (Hedge, 1982; Celep, Kahraman, Atalay & Dogan, 2014).

Most of the species from the genus *Salvia* have medicinal significance, as they produce many useful natural constituents including terpenes and flavonoids. Some of the essential oils and phenolic compounds of plants belonging to this genus possess a long list of medicinal uses for being spasmolytic, antiseptic, and/or astringent, and they have also shown excellent antimicrobial activity and antioxidant capacity, with some used as anticancer agents or having a hypoglycemic effect (Kelen & Tepe, 2008; Kintzios, 2000; Tepe, Daferara, Sökmen, Sökmen & Polissiou, 2005; Khalil & Zheng-Guo, 2011). Some *Salvia* species are also used as flavoring agents in perfumery and cosmetics. Many wild-growing *Salvia* species are also used in the traditional medicine of different nations in place of sage or as an adulteration (Bisset & Wichtl, 2001). Chemical compounds and biological activities in the essential oils of some *Salvia* species have been reported in Türkiye (Demirci, Başer & Tümen, 2002; Başer, 2002; Demirci, Başer, Yıldız & Bahçecioglu, 2003; Kaya, Demirci & Başer, 2003; Kaya, Demirci & Başer 2009; Karik, Sağlam, Kürkçüoğlu & Başer, 2011; Kaya, Dinç, Doğu & Demirci, 2017).

S. freyniana Bornm. (Figure 1) is, an endemic, perennial suffruticose herb with a woody rootstock whose stems ascend to erect at 15-35 cm. Its leaves are pinnatisect. Inflorescence is

Corresponding Author: Gözde Öztürk **E-mail:** gozde_ozturk@anadolu.edu.tr
Submitted: 06.02.2023 • **Revision Requested:** 26.10.2023 • **Last Revision Received:** 02.04.2024 • **Accepted:** 02.04.2024

racemose. The calyx is campanulate at 7-11 mm, and its corolla is lilac-blue with a white center (Bagherpour, Celep, Doğan & Kahraman, 2009).

Figure 1. *Salvia freyniana* Bornm

S. quezelii Hedge & Afzal-Rafii (Figure 2) is an endemic perennial herb with a woody rootstock. Stems are procumbent-ascending at 6-45 cm, and its leaves are pinnate. The inflorescence is few-flowered at 5–35 cm. The calyx is green, and the corolla is white cream-colored (Celep et al., 2014).

Figure 2. *Salvia quezelii Hedge and Afzal-Rafii*

The specimens of *S. freyniana* were first collected and described from Yenipazar in Yozgat Province by Bornmueller in 1892. Later, it was rediscovered by Bagherpour, Celep, Doğan & Kahraman (2006), who gave a detailed account of the morphological and pollen-mericarp micromorphological characteristics of S. freyniana (Bagherpour, Celep, Doğan & Kahraman, 2009).

The specimens of *S. quezelii* were first collected from Mersin in 1931 by Eig and Zohary and then collected again from Namrun in Mersin Province (formerly Içel) as a type specimen by Quezel in 1970. Later, a population of *S. quezelii* was rediscovered between Anamur and Ermenek by Celep et al. in 2009, who gave a detailed account of the morphological, anatomical, pollen, mericarp, myxocarpy, and trichome micromorphological characteristics of the little-known *S. quezelii* (Celep et al., 2014). *S. freyniana* is known as *göl şalba* in Türkiye, while *S. quezelii* is known as *limon adaçayı* (Güner, Aslan, Ekim, Vural, & Babaç, 2012).

A literature search revealed no reference to any previous work on the essential oils of *S. freyniana* and *S. quezelii*. This study reports for the first time on the chemical constituents of the essential oils and the antimicrobial activity of the rediscovered *S. freyniana* and *S. quezelii*.

MATERIALS AND METHODS

Materials

Salvia freyniana and *Salvia quezelii* samples were collected during their flowering period (June, 2018) from Türkiye's Yozgat Province (Büyükören village of Yenipazarı municipality, 1000-1250 m) and Mersin Province (Km 40 on Ermenek road in Anamur municipality, 1050 m,), respectively. Voucher specimens were deposited in the herbarium of the Faculty of Education of Necmettin Erbakan University in Konya, Türkiye (NEÜ Herb.). The essential oils from air-dried plant materials were isolated by hydrodistillation for 3 h using a Clevenger-type apparatus. The obtained oils were dried over anhydrous sodium sulfate and stored at +4°C in the dark until analyzed and tested.

Analysis of volatile components

The processes for the gas chromatography-flame ionization detection (GC-FID) and gas chromatography-mass spectrometry (GC-MS) analyses were performed with reference to Demirci, Yusufoglu, Tabanca, Temel, Bernier, Agramonte, Alqasoumi, Al-Rehaily, Başer, & Demirci, (2017).

Antibacterial activity assay

The microorganisms' strains used for the evaluation of antibacterial activity were obtained from the American Type Culture Collection (ATCC) in lyophilized form. Mueller-Hilton Agar

(MHA) was used as a medium for growing the bacterial strains. The prepared media were stored at +4°C for a maximum of 2 weeks. Their purity was controlled, and the microorganisms stored in 15% glycerol solution at -85°C were inoculated into the prepared media and allowed to multiply by incubating in a bacteriological incubator at 37°C for 24 h.

The antibacterial activity of both essential oils was evaluated by broth microdilution assay according to a modified Clinical and Laboratory Standards Institute (2006) method, as previously described. Gram-negative strains (*Escherichia coli* ATCC 8739, *Pseudomonas aeruginosa* ATCC B888, and *Salmonella typhimurium* ATCC 13311) and a Gram-positive strain (*Staphylococcus aureus* ATCC 6538) were used as the standard test microorganisms. The essential oils (20-0.01 mg/mL) were dissolved in sterile dimethyl sulfoxide (DMSO) for the initial stock solution. 100 µL of essential oil was applied to 96-well microplates, and 2-fold serial dilutions were then performed. Strains were incubated in Mueller-Hinton Broth (MHB) overnight at 37°C for 24h. After the dilutions, 50 µL aliquots of turbidometrically adjusted microorganisms were inoculated (10^5-10^6 CFU/mL) onto the plates. After incubation at 37°C for 24 h, the first well was treated with 20 µL of resazurin, which ensured the minimum inhibitory concentrations (MIC) where the lowest concentration of the samples prevented visible growth was present on all microplate wells. The standard antibiotic ciprofloxacin (2.5-0.1 µg/ml) was used as the standard control. Solvent and microbial controls were also added to the assay plate. Antibacterial assays were repeated at least three times for all test samples (CLSI, 2006).

RESULTS AND DISCUSSION

The water-distilled essential oils from the aerial parts of *S. freyniana* and *S. quezelii* were characterized using GC-FID and GC-MS. The compounds identified from the essential oils along with their relative percentages are listed in Table 1. Totals of 64 and 55 compounds were identified from the respective essential oils of *S. freyniana* and *S. quezelii*, representing 99.1% and 98.9% of their respective oils. Oil components can be grouped under six main chemical classes: monoterpene hydrocarbons, oxygenated monoterpenes, sesquiterpene hydrocarbons, oxygenated sesquiterpenes, fatty acids, and others. The oils of the *S. freyniana* and *S. quezelii* are characterized by a high content of monoterpene hydrocarbons (35.1% and 51.0%, respectively) and oxygenated monoterpenes (40.1 % and 44.3% respectively). The major components were found as 1,8-cineole (21.9%), β-pinene (14.2%), camphor (8.7%), α-pinene (8.0%), and valeranone (7.0%) for *S. freyniana* and limonene (20.8%), pinocamphone (11.4%), α-pinene (10.6%), camphor (9.1%), β-pinene (7.5%), camphene (7.1%), and isopinocamphone (6.7%) for *S. quezelii*.

According to the results in Table 1, oxygenated monoterpenes are present in almost equal amounts in the oils of *S. freyniana* and *S. quezelii*, while *S. quezelii* is characterized by a high content of monoterpene hydrocarbons in its oil. However, some important differences were found regarding the constituents of the oils. As can be seen in Table 1, *S. freyniana* is characterized by high oxygenated sesquiterpenes content in its oil.

The essential oil composition of the 64 *Salvia* taxa from Türkiye has already been studied, with monoterpene hydrocarbons (Group 1), oxygenated monoterpenes (Group 2), sesquiterpene hydrocarbons (Group 3), oxygenated sesquiterpenes (Group 4), and phenylpropanoid (Group 5) being reported as the main groups of the constituents in the *Salvia* taxa's essential oils (Başer, 2002). According to the current study's results, *S. freyniana* and *S. quezelii* have many monoterpene hydrocarbons and oxygenated monoterpenes. As such, they can be categorized into the first and second groups, respectively.

The study has examined the antibacterial activity of *Salvia* essential oils against *E. coli* ATCC 8739, *S. aureus* ATCC 6538, *P. aeruginosa* ATCC B888, and *S. typhimurium* ATCC 13311. S. aureus and *S. typhimurium* were inhibited at a concentration of 5 µg/ml by *S. freyniana* as the best performance among the tested samples. In addition, *S. typhimurium* was inhibited at a concentration of 5 µg/ml by *S. quezelii* essential oil. The other tested samples showed rather moderate inhibitory effects. The comparative results are given in Table 2.

Table 1. The composition of the essential oils of *Salvia freyniana* and *Salvia quezelii*

RRI[a]	Compound	*S. frey.* %[b]	*S. quez.* %	IM[d]
1014	Tricyclene	0.2	0.3	MS
1032	*a*-Pinene	**8.0**	**10.6**	RRI, MS[e]
1035	*a*-Thujene	1.0	-	MS
1072	*a*-Fenchene	-	0.2	RRI, MS
1076	Camphene	**3.8**	**7.1**	RRI, MS
1118	*b*-Pinene	**14.2**	**7.5**	RRI, MS
1132	Sabinene	1.9	-	RRI, MS
1159	*d-3*-Carene	-	0.1	MS
1174	Myrcene	0.7	0.8	RRI, MS
1188	*a*-Terpinene	0.2	0.1	RRI, MS
1203	Limonene	2.3	**20.8**	RRI, MS
1213	1,8-Cineole	**21.9**	-	RRI, MS
1218	*b*-Phellandrene	-	0.6	RRI, MS
1246	(*Z*)-*b*-Ocimene	tr[c]	-	MS
1255	*g*-Terpinene	0.6	-	RRI, MS
1266	(*E*)-*b*-Ocimene	0.1	-	MS
1280	*p*-Cymene	2.0	2.9	RRI, MS
1290	Terpinolene	0.1	-	RRI, MS
1400	Nonanal	tr	-	MS
1406	*a*-Fenchone	-	tr	RRI, MS
1450	*trans*-Linalool oxide (*Furanoid*)	-	tr	MS
1452	1-Octen-3-ol	0.2	0.2	MS
1466	*a*-Cubebene	tr	-	RRI, MS
1474	*trans*-Sabinene hydrate	0.4	-	MS
1478	*cis*-Linalool oxide (*Furanoid*)	-	tr	MS
1493	*a*-Ylangene	-	0.3	MS
1497	*a*-Copaene	0.2	0.3	RRI, MS
1499	*a*-Campholene aldehyde	0.1	0.1	MS
1532	Camphor	**8.7**	**9.1**	RRI, MS
1535	*b*-Bourbonene	0.6	-	MS
1536	Pinocamphone	-	**11.4**	RRI, MS
1553	Linalool	0.2	0.6	RRI, MS
1556	*cis*-Sabinene hydrate	0.4	-	MS
1562	Isopinocamphone	-	**6.7**	MS
1571	*trans-p*-Menth-2-en-1-ol	0.1	-	MS
1586	Pinocarvone	0.3	0.4	RRI, MS

Table 1. Continued

1591	Bornyl acetate	4.2	1.1	RRI, MS
1597	*b*-Copaene	0.1	-	MS
1598	Camphene hydrate	-	0.3	MS
1601	Nopinone	-	0.1	MS
1611	Terpinen-4-ol	0.6	1.9	RRI, MS
1612	*b*-Caryophyllene	1.2	0.2	RRI, MS
1617	6,9-Guaiadiene	0.7	-	MS
1639	*trans*-*p*-Mentha-2,8-dien-1-ol	-	0.2	MS
1648	Myrtenal	0.4	1.5	MS
1661	*trans*-Pinocarvyl acetate	-	0.2	RRI, MS
1668	(*Z*)-*b*-Farnesene	2.2	-	MS
1670	*trans*-Pinocarveol	0.4	3.5	RRI, MS
1683	*trans*-Verbenol	0.4	-	RRI, MS
1704	Myrtenyl acetate	-	1.5	MS
1704	*g*-Muurolene	0.2	tr	MS
1706	*a*-Terpineol	0.3	1.9	RRI, MS
1719	Borneol	0.9	2.0	RRI, MS
1726	Germacrene D	0.3	-	MS
1740	*a*-Muurolene	-	0.2	MS
1741	*b*-Bisabolene	0.2	-	RRI, MS
1751	Carvone	-	0.1	RRI, MS
1755	Bicyclogermacrene	0.3	-	MS
1773	*d*-Cadinene	0.2	0.2	MS
1776	*g*-Cadinene	0.2	0.1	MS
1804	Myrtenol	0.5	1.3	MS
1845	*trans*-Carveol	0.3	0.1	RRI, MS
1849	Calamenene	tr	0.5	MS
1882	*cis*-Carveol	-	0.2	RRI, MS
1896	*cis*-*p*-Mentha-1(7),8-diene-2-ol	-	0.2	MS
1900	*epi*-Cubebol	0.1	-	MS
1941	*a*-Calacorene	-	0.1	MS
1957	Cubebol	0.1	-	MS
2001	Isocaryophyllene oxide	0.3	-	MS
2008	Caryophyllene oxide	6.1	0.1	RRI, MS
2029	Perilla alcohol	-	0.1	MS
2071	Humulene epoxide-II	0.4	-	MS
2104	Viridiflorol	0.7	-	MS
2131	Hexahydrofarnesyl acetone	0.6	-	MS

Table 1. Continued

2145	Valeranone	**7.0**	-	MS
2173	6-*epi*-Cubenol	-	0.5	MS
2187	T-Cadinol	0.3	0.1	MS
2192	Nonanoic acid	0.1	-	RRI, MS
2250	*a*-Eudesmol	-	tr	MS
2255	*a*-Cadinol	0.1	0.2	MS
2256	Cadalene	-	0.4	MS
2278	Torilenol	0.1	-	MS
2324	Caryophylla-2(12),6(13)-dien-5*a*-ol (=*Caryophylladienol II*)	0.4	-	MS
2392	Caryophylla-2(12),6-dien-5*b*-ol (=*Caryophyllenol II*)	0.6	-	MS
2503	Dodecanoic acid	0.1	-	RRI, MS
2670	Tetradecanoic acid	0.1	-	RRI, MS
2931	Hexadecanoic acid	0.2	-	RRI, MS
	Monoterpene Hydrocarbons	35.1	51.0	
	Oxygenated Monoterpenes	40.1	44.3	
	Sesquiterpene Hydrocarbons	6.4	2.3	
	Oxygenated Sesquiterpenes	16.2	1.0	
	Fatty acids	0.5	-	
	Others	0.8	0.3	
	Oil Yield (%)	0.5	0.98	
	Total	**99.1**	**98.9**	

[a] Relative retention indices calculated against *n*-alkanes; [b] Percentages calculated from FID data; [c] Trace (< 0.1 %); [d] Identification method based on the relative retention indices (RRI) of authentic compounds on the HP Innowax column and/or mass spectra (MS) identified based on computer matching of MS[e] with those of the Wiley and MassFinder libraries and comparison with literature data.

Table 2. MIC values (μg/ml)

	***E. coli* ATCC 8739**	***S. aureus* ATCC 6538**	***P. aeruginosa* ATCC B888**	***S. typhimurium* ATCC 13311**
***S. freyniana* essential oil**	20	5	20	5
***S. quezelii* essential oil**	20	10	20	5
Ciprofloxacin	0.1	0.1	0.1	0.1

CONCLUSION

When comparing the literature, no study is found regarding the antimicrobial activities of the essential oils of *S. freyniana* and *S. quezelii*. To the best of this study's knowledge, this is the first report to show the antimicrobial activity of the essential oils of *S. freyniana* and *S. quezelii*. More in detail evaluations on biological activity both on in vitro and in vivo levels are needed to exhaust the potential of essential oils from *S. freyniana* and *S. quezelii*. Further work is ongoing.

Peer-review: Externally peer-reviewed.

Author Contributions: Conception/Design of Study- A.K., G.Ö., B.D.; Data Acquisition- G.Ö., B.D.; Data Analysis/Interpretation- A.K., G.Ö., B.D.; Drafting Manuscript- A.K., G.Ö.; Critical Revision of Manuscript- A.K., G.Ö., B.D., S.D.; Final Approval and Accountability- A.K., G.Ö., B.D., S.D.

Conflict of Interest: The authors have no conflict of interest to declare.

Financial Disclosure: The authors declared no financial support.

ORCID IDs of the authors

Ayla Kaya 0000-0002-7598-7132
Gözde Öztürk 0000-0002-3998-8859
Süleyman Doğu 0000-0002-5352-9288
Betül Demirci 0000-0003-2343-746X

REFERENCES

Bagherpour, S., Celep, F., Doğan, M., & Kahraman, A. (2009). Rediscovery of *Salvia freyniana* Bornm. (Lamiaceae), a critically endangered species in Turkey. *Bangladesh Journal of Botany, 38(2)*, 189-191. https://doi.org/10.3329/bjb.v38i2.5146.

Başer, K.H.C. (2002). Aromatic biodiversity among the flowering plant taxa of Turkey. *Pure and Applied Chemistry, 74 (4)*, 527–545. https://doi.org/10.1351/pac200274040527.

Bisset, N., & Wichtl, M. (2001). *Herbal drugs and phytopharmaceuticals*. London: CRC.

Celep, F., Kahraman, A., Atalay, Z., & Dogan, M. (2014). Morphology, anatomy, palynology, mericarp and trichome micromorphology of the rediscovered Turkish endemic *Salvia quezelii* (Lamiaceae) and their taxonomic implications. *Plant Systematics and Evolution, 300(9)*, 1945-1958. https://doi.org/10.1007/s00606-014-1020-1.

CLSI (2006). Methods for dilution antimicrobial susceptibility tests for bacteria that grow aerobically; approved standard, M7-A7, Clinical and Laboratory Standards Institute.

Demirci, B., Başer, K.H.C., & Tümen, G. (2002). Composition of the essential oil of *Salvia aramiensis* Rech. fil. growing in Turkey. *Flavour and Fragrance Journal, 17*, 23-25. https://doi.org/10.1002/ffj.1027.

Demirci, B., Başer, K.H.C., Yıldız, B., & Bahçecioglu, Z. (2003). Composition of the essential oils of six endemic *Salvia* species from Turkey, *Flavour and Fragrance Journal, 18*, 116-121. https://doi.org/10.1002/ffj.1173

Demirci, B., Yusufoglu, H.S., Tabanca, N., Temel, H.E., Bernier, U.R., Agramonte, N.M., Alqasoumi, S.A., Al-Rehaily, A.J., Başer, K.H.C., & Demirci, F. (2017). *Rhanterium epapposum* Oliv. essential oil: Chemical composition and antimicrobial, insect-repellent and anticholinesterase activities, *Saudi Pharmaceutical Journal, 25(5)*, 703-708. https://doi.org/10.1016/j.jsps.2016.10.009.

Güner, A., Aslan, S., Ekim, T., Vural, M., & Babaç, M. (2012). *Türkiye Bitkileri Listesi (Damarlı Bitkiler)*. İstanbul, Turkey: Nezahat Gökyiğit Botanik Bahçesi ve Flora Araştırmaları Derneği Yayını,

Harley, R.M., Atkins, S., Budantsey, A.L., Cantino, P.D., Conn, B.J., Grayer, R., Harley, M. M., de Kok, R., Krestovskaja, T., Morales, R., Paton, A. J., Ryding, O., & T. Upson (2004). Labiatae. In Kadereit JW (Eds.), *The families and genera of vascular plants*. (pp. 167-275). Berlin Heidelberg: Springer.

Karik, U., Sağlam, A.C., Kürkçüoğlu, M., & Başer, K.H.C. (2011). Compositions of the essential oils of *Salvia fruticosa* Mill. populations in the flora of Marmara region. *Planta Medica, 77(12)*, 1302-1302. https://doi.org/10.1055/s-0031-1282368.

Kaya, A., Başer, K.H.C., & Demirci, B. (2009). Composition of essential oil of endemic *Salvia wiedemannii* from Turkey. *Chemistry of Natural Compound, 45*, 552-553.

Kaya, A., Demirci, B., & Başer, K.H.C. (2003). Glandular trichomes and essential oils of *Salvia glutinosa* L. *South African Journal of Botany, 69 (3)*, 422–427.

Kaya, A., Dinç, M., Doğu, S., & Demirci, B. (2017). Compositions of essential oils of *Salvia adenophylla, Salvia pilifera* and *Salvia viscosa* in Turkey. *Journal of Essential Oil Research, 29 (3)*, 233–239. https://doi.org./10.1080/10412905.2016.1216901.

Kelen, M., & Tepe, B. (2008). Chemical composition, antioxidant and antimicrobial properties of the essential oils of three Salvia species from Turkish flora. *Bioresource Technology, 99*, 4096-4104. https://doi.org/10.1016/j.biortech.2007.09.002.

Khalil, R., & Zheng-Guo, L. (2011). Antimicrobial activity of essential oil of *Salvia officinalis* L. collected in Syria. *African Journal of Biotechnology, 10(42)*, 8397-8402. https://doi.org/10.5897/AJB10.2615.

Kintzios, S.E. (2000). *Sage: the genus Salvia*. Australia: Canada Harwood academic Publisher.

McLafferty, F.W., Stauffer, D.B. (1989). The Wiley/NBS Registry of Mass Spectral Data, New York, USA: J Wiley and Sons.

Tepe, B., Daferara, D., Sökmen, A., Sökmen, M., & Polissiou, M. (2005). Antimicrobial and antioxidant activities of the essential oil and various extracts of *Salvia tomentosa* Miller (Lamiaceae). *Food Chemistry, 90 (3)*, 333-340.

How cite this article

Kaya, A., Öztürk, G., Doğu, S., & Demirci, B. (2024). Compositions of the essential oils and antimicrobial activities of the rediscovered Turkish endemic Salvia freyniana and Salvia quezelii (Lamiaceae). *İstanbul Journal of Pharmacy, 54*(2), 175–181. DOI: 10.26650/IstanbulJPharm.2024.1248393

İstanbul Journal of Pharmacy
Istanbul J Pharm2024, 54 (2): 182–188
DOI: 10.26650/IstanbulJPharm.2024.1036392

Original Article

Determining the fatty acid composition and antioxidant activities of *Centaurea virgata* Lam.

Burcu Sümer Tüzün[1], Tuğçe Fafal[1], Bijen Kıvçak[1]

[1]Ege University, Faculty of Pharmacy, Department of Pharmacognosy, İzmir, Türkiye

ABSTRACT

Background and Aims: *Centaurea* is a significant widespread genus in the *Asteraceae* family. Türkiye has 194 species, of which 118 are endemic. Free radicals can alter lipids, proteins, and DNA and trigger many diseases. However, a person with an insufficient immune system needs outside assistance to scavenge free radicals. Antioxidants protect the body from oxidative stress by scavenging free radicals. Fats are also very important because they contain fat-soluble vitamins, form lipoproteins with proteins, and affect health. Fatty acids serve as part of molecules in cells or alone as building blocks of cell membranes. They also promote energy and signaling molecules. Polyunsaturated fatty acids (PUFAs) have significant antioxidant activity. Studies are found showing PUFAs to be able to be used as a preservative in foods. These effects are due to phenolic hydroxyl groups. The aim of the current study is to evaluate the fatty acid profile of *C. virgata* to determine the fatty acid content and examine the antioxidant activities related to major fatty acids.

Methods: Gas chromatography Mass Spectrometry (GC/MS) analyses were carried out to determine the fatty acid content. Furthermore, the *in vitro* antioxidant activities of methanol extract were determined using DPPH (2, 2'-Diphenyl-1-picrylhydrazyl) and ABTS (2,2'-Azino-bis (3-ethylbenzothiazoline-6-sulfonic acid) diammonium salt) radical scavenging and the reducing power assay methods. The program IBM SPSS Statistics (ver. 25) was used to evaluate antioxidant activities.

Results: *C. virgata*'s major components were found to be palmitic acid (30.13%), oleic acid (9.17%), and linoleic acid (11.64%). The DPPH results indicated the IC_{50} value of the methanol extract to be 378.86 ± 0.60 µg/mL, while ABTS was found to be 19.38 ± 0.49 µg/mL. The results from the reducing power assay found the absorbance of ascorbic acid to be 0.55 at a 100 µg/mL concentration and it measure 0.12 in *C. virgata*.

Conclusion: According to the evaluation results, harmony is seen to exist between the groups regarding the activities.

Keywords: ABTS, *Centaurea*, DPPH, Fatty acid, GC-MS

INTRODUCTION

The genus *Centaurea* is one of the most significant extensive genii of the *Asteraceae* family. *Centaurea* is predominantly distributed in Western Asia and the Mediterranean region and is common in the Southwest, Central Anatolian, and Eastern Anatolian regions of Türkiye. *Centaurea* is also known as the largest genus after *Astragalus* and *Verbascum* in Türkiye and has more than 700 species worldwide (Zengin et al., 2019). Türkiye has 194 species, of which118 are endemic (Albayrak, Atasagun & Aksoy, 2017).

Centaurea is a genus known to have significant potential in both conventional systems and drug development (Zengin et al., 2018). It has traditionally been used for asthma, abdominal pain, headache, hemorrhoids, diarrhea, rheumatoid arthritis, and stomach, as well as for its antipyretic, astringent, and antibacterial effects (Albayrak et al., 2017; Baytop, 1999; Köse, İşçan et al., 2016; Zengin et al., 2019b).

The genus contains intensely phenolic structures and flavonoids, in addition to sesquiterpene lactones, lignans, and alkaloids that are occasionally seen. The genus shows a wide variety of biological activities with its rich chemical content, with studies having observed antioxidant, antimicrobial, antiproliferative, hepatoprotective, anti-inflammatory, antiulcerogenic, antiplasmodial, and enzyme inhibitor activities in *Centaurea* species (Boğa et al., 2016; Köse et al., 2016).

Free radicals are formed by the body as a result of metabolic reactions. Free radicals can alter lipids, proteins, and DNA and trigger many diseases. The control of this production is provided by the endogenous and exogenous systems. However,

Corresponding Author: Burcu Sümer Tüzün **E-mail:** burcusmer@gmail.com
Submitted: 14.12.2021 • **Revision Requested:** 19.05.2022 • **Last Revision Received:** 10.03.2023 • **Accepted:** 29.05.2023

when produced in excess, the immune system may be insufficient to scavenge these free radicals. In such cases, external assistance is needed to scavenge them. The oxidative stress caused by overproduction can cause neurodegenerative disorders, atherosclerosis, cancer, hypertension, aging, and similar diseases. Antioxidants protect the body from oxidative stress by scavenging free radicals. Plants also contain phytochemical antioxidants such as phenolic substances that act as powerful natural antioxidants (Köse et al., 2016; Zengin et al., 2011).

An important relationship is known to exist between a person's nutritional habits and disease. Carbohydrates, proteins, and fats are essential for the survival of all living organisms. Fats are made up of glycerol and fatty acids and are an important essential ingredient for their high energy and for being highly suitable for storage. While glycerol is the same in every plant, fatty acids occur differently in each plant. In addition to being a source of energy, fats are very important because they contain fat-soluble vitamins, form lipoproteins with proteins, and affect health. Saturated fatty acids increase the rate of fat in the blood and low density lipoprotein (LDL) levels and are also effective in the formation of insulin resistance. Unsaturated fatty acids are known as important sources of prostaglandins that increase the amount of high density lipoproteins (HDLs), which have protective properties against cardiovascular diseases, inflammatory diseases, and cancer (NRC, 1989; Ros& Mataix, 2006).

This study aims to determine the fatty acid content of *Centaurea virgata* Lam. and to examine its *in-vitro* antioxidant activities related to major fatty acids.

MATERIALS AND METHODS

Plant Collection

The aerial parts of *C. virgata* Lam. were collected from the Harput district in Elazığ in 2014. These were registered under No. 1461 in the herbarium of Ege University Faculty of Pharmacy, Department of Pharmacognosy.

Plant Extraction

The aerial parts of *C. virgata* Lam were dried in the shade at room temperature and then ground into fine powder with the help of a mill. Methanol extract was prepared by continuous shaking and maceration 5 g of the fine powder in 100 mL of methanol. The study then investigated the antioxidant activities of the prepared extract after filtration and evaporation of the solvents.

Fatty Acid Analysis

40 g of the powdered plant was extracted with petroleum ether in a Soxhlet extractor at 60ºC for 6 h. It was first saponified with 0.5 N NaOH. It was then treated with 14% boron trifluoride-methanol complex and n-heptane mixed with a saturated solution of NaCl to achieve phase separation. The oily part that was obtained forms the part to be analyzed in gas chromatography (GC; UPAC, 1979; Yıldırım et al., 2009). The GC operating conditions are given in Table 3. GC analysis was performed in three parallels.

GC/MS Analysis

Hewlett-Packard (HP) Agilent 6890 N Gas Chromatograph was used and equipped with a flame ionization detector (FID). It was fitted to the Supelco SP-2380 Phased Silica Capillary Column (60 m*0.25 mm, 0.2 µm). Injector temperature was 250°C and detector temperature was 260°C. After waiting 5 min at 140°C, the temperature was then raised to 240°C in 3°C increments. Helium was used as the carrier gas at a flow rate of 41.33 cm/sec. Total run time was set for 70 min. Fatty acids were identified by comparing the mass spectra and retention time to standard values (Supelco Component FAME mix and NIST 11 and WILEY 7 commercial mass spectral libraries). Quantification was performed by internal standard mass and relative percentage of GC. The results were determined as Mean ± SD.

Antioxidant Activities

2, 2'-Diphenyl-1-picrylhydrazyl assay (DPPH)

1 mL from each of the extracts prepared at concentrations between 100-1000 µg/mL was taken and mixed with 4 mL of DPPH solution. After incubating for 30 min at room temperature, the absorbance at 517 nm was measured. Higher absorbance indicates less activity. Ascorbic acid was used as the standard (Esmaeili & Sonboli, 2010). Experiments were performed in three parallels.

$$I(\%) = 100\, x\, (A_0 - A_S)/(A_0) \quad (1)$$

A_0 (absorbance of control)
A_S (absorbance of sample)
I (inhibition)

Reducing Power Assay

According to Oyaizu (1986), 1.25 mL of the 0.2 M sodium phosphate buffer (pH 6.6) and 1.25 mL of a 1% potassium ferricyanide mixture were added to 50, 100, and 200 µg/mL of each extract. The mixture was incubated using the LAB-LINE MaxQ6000 instrument at 50ºC for 20 min. After incubation, 1.25 mL of 10% trichloroacetic acid and 0.5 mL of 1% $FeCl_3$ were added. All the mixtures' absorbance values were measured at 700 nm (Oyaizu, 1986). Ascorbic acid was used as the control [23]. Experiments were performed in three parallels.

2,2'-Azino-Bis-(3-Ethylbenzothiazoline-6-Sulfonic) Acid (ABTS) Radical Scavenging Assay

1 mL from each of the methanol extracts prepared at concentrations between 100-1000 µg/mL was taken, and 3 ml of ethanol and 1 mL of ABTS radical solution were added to it. After 6 min, the absorbance at 734 nm was measured against the blank (ABTS solution and ethanol mixture without the extract). α-tocopherol was used as the standard (Çelik, 2011). The experiments were performed in three parallels. Calculated according to Eq 1.

Statistical Analysis

All results are expressed as Mean ± SD. Analysis of variance was also performed, and significant differences between means were determined using Duncan's multiple range tests at a significance level of $p < 0.05$ in IBM SPSS (ver. 25).

RESULTS AND DISCUSSION

The fatty acid content of *C. virgata* Lam. was determined, with Table 1 showing the results. Accordingly, the major fatty acids of *C. virgata* Lam. have been determined as palmitic acid (30.13%), oleic acid (9.17%) and linoleic acid (11.64%). 43.50% of these are saturated fatty acids. Palmitic acid (hexadecanoic acid) constitutes the largest part of the saturated fatty acids at 30.13%, followed by heneicosanoic acid and myristic acid. Palmitic and myristic acid have an important role in the acylation of membrane proteins, which are important in fixing proteins to the plasma membrane. A positive relationship is known to exist for myristic and palmitic acid concentrations with type 2 diabetes and to be inversely proportional to that of pentadecanoic and heptadecanoic acids, which are odd-numbered saturated fatty acids. Still, myristic and palmitic acid are present in small amounts in the plant being researched here. Saturated fatty acids are known to stimulate inflammation (i.e., NF-kB). Because NF-kB has an immunomodulatory role, it being stimulated has great significance; NF-kB is important for designing treatments that can prevent or minimize acute inflammatory damage associated with critical illness. Monounsaturated fatty acids (MUFA) comprise 15.98% of *C. virgata* Lam., with oleic acid being the most prevalent here. Oleic acid is generally known for its LDL cholesterol lowering effect. It has no effect on HDL, has a slight anti-inflammatory effect, and also regulates insulin. Polyunsaturated fatty acids (PUFA) comprise 19.96% of *C. virgata* Lam. with linoleic acid being the most prevalent here. Linoleic acid is one of the basic building blocks of membrane phospholipids and is also an important component of ceramides, especially those in the skin. It provides skin integrity and prevents water loss and is also an important cholesterol lowering agent. It has little effect on inflammation. PUFAs have significant antioxidant activity. Studies are found to have shown it can be used as a preservative in foods. These effects are due to the phenolic hydroxyl groups (Cakmakci & Kahyaoglu, 2012; Neitzel, 2010).

Various studies have occurred on the fatty acid content and antioxidant activities of the extracts in the genus *Centaurea*. Tekeli et al.'s (2011) study identified the fatty acid compositions of *Centaurea balsamita, C. calolepis, C. carduiformis, C. cariensis* subsp. *maculiceps, C. cariensis* subsp. *microlepis*, and *C. iberica*, with C 18:2 6 linoleic acid, C 16:0 palmitic acid, C 18:3 3 linolenic acid, and C 18:1 oleic acid generally being found as major components in all these species. They also found polyunsaturated fatty acids to occur more than saturated and monosaturated fatty acids. For *Centaurea balsamita, C. calolepis, C. carduiformis, C. cariensis* subsp. *maculiceps, C. cariensis* subsp. *microlepis*, and *C. iberica* PUFA values are given as 55.10%, 50.25%, 51.41%, 41.02%, 46.18% and 58.80% respectively. Erdoğan et al.'s (2014) study investigated the fatty acid profiles for *C. behen, C. saligna, C. depressa, C. urvillei* subsp. *urvillei, C. urvillei* subsp. *hayekiana*, and *C. aggregata* subsp. *aggregata* plants collected from Elazig. The found the ratio of saturated fatty acids to vary between 24.61%-50.92%, of monosaturated fatty acids to vary between 3.40%-37.96%, and of polyunsaturated fatty acids to vary between 2.21%-20.57%. They also found the most common fatty acids in all species to be palmitic acid C 16:0, oleic acid C 18:1 and linoleic acid C 18:1. Zengin et al. (2010) investigated the fatty acid profiles of *C. pulchella, C. patula*, and *C. tchihatcheffii* and identified 33 fatty acids in the plants. They found linoleic acid to be the most common fatty acid in *C. pulchella* and *C. tchihatcheffii* and alpha-linolenic acid to be the most common fatty acid in *C. patula*. Aktümsek et al. (2013) examined the fatty acid profiles of *C. pseudoscabiosa* subsp. *aratica, C. pulcherrima* var. *pulcherrima, C. salicifolia* subsp. *abbreviata*, and *C. babylonica* and detected the most common fatty acids as palmitic acid (23.38–30.49%) and linoleic acid (20.19–29.93%). Aktümsek et al. also examined the fatty acid contents of *C. kurdica, C. rigida, C. amanicola, C. cheirolopha*, and *C. ptosimopappoides* and determined palmitic, linoleic, oleic, and linolenic acids as the major components. Zengin et al. (2011) found *C. urvillei* subsp. *hayekiana* to contain high amounts of C 18:2 omega 6 (linoleic acid) and C 18:1 omega 9 (oleic acid). In the study of Ayaz et al.'s (2017) study examined the fatty acid profiles of 10 *Centaurea* species and found their most common fatty acids to be palmitic acid C16:0 (5.22-12.06%), oleic acid C18:1n9 (8.57-30.29%), and linoleic acid C18:2n6 (49.15-79.15%). (Janackovic et al. (2017) determined the fatty acid profiles of the cypselae part of *C. galicica* and *C. tomorosii*, identified 11 fatty acids, and found palmitic acid to have the highest concentration. Zengin et al.'s (2011) study determined the fatty acid profile and antioxidant properties of *C. kotschii* and identified the most prevalent fatty acid as α-linolenic acid.

Author Senatore et al.'s (2008) study examined the volatile components of *Centaurea* species and identified high amounts

Table 1. Fatty acid content of *C. virgata* Lam.(%)

Fatty Acids	*C. virgata*
C 4:0 (butyric acid)	-
C 6:0 (caproic acid)	0.13
C 8:0 (caprylic acid)	0.57
C 12:0 (lauric acid)	1.02
C 13:0 (tridecyclic acid)	0.28
C 14:0 (myristic acid)	3.75
C 15:0 (pentadecanoic acid)	0.18
C 16:0 (palmitic acid)	30.13
C 17:0 (heptadecanoic acid)	0.45
C 18:0 (stearic acid)	1.87
C 21:0 (heneicosanoic acid)	4.09
C 22:0 (behenic acid)	0.64
C 23:0 (trichosanoic acid)	0.39
C 24:0 (lignoceric acid)	-
∑SFA[b]	**43.50**
C 18:1 ω9 (Oleic acid)	9.17
C 20:1 ω9 (Gondoic acid)	6.81
C 24:1 ω9 (Nervonic acid)	-
∑MUFA[b]	**15.98**
C 18:2 ω6 (Linoleic acid)	11.64
C 18:3 ω6 (γ-linolenic acid)	1.78
C 20:3 ω3 (Eicosatrienoic acid)	4.98
C 20:5 ω3 (Eicosopenteanoic acid)	1.56
∑PUFA[b]	**19.96**

*C:D ratio (the total number of *carbon* atoms to the number of *carbon-carbon* double bonds)

of fatty acid content, with *C. nicaeensis* oil containing 66.4% fatty acids and hexadecanoic acid and 9-12-octadecadienoic acid being the most common. They found the *C. parlatoris* plant oil to contain 22% fatty acids, with the highest amount being 18.1% hexadecanoic acid. Finally, . solstitialis subsp *schouwii* oil was found to contain 43.6% fatty acids and their esters, with hexadecanoic acid (29.4%) being the main component. Formisano et al.'s (2008) study examined endemic *Centaurea* plants and observed *C. amanicola* to be characterized by high amounts of caryophyllene oxide (12%) and caryophyllene (5.4%) and *C. consanguinea* to have germakren B (8.3%) and caryophyllene oxide (7.3%). Finally, they found a high amount os sesquiterpene inthe *C. ptosimopappa* plant, the concentrations were quite low, with only β-ödesmol is high. Lazari et al. (2000)examined the volatile components of *C. pelia, C. thessola*, and *C. zuccariana* and observed the plants to contain 31.9%, 13%, and 17.3% fatty acids, respectively, with hexadecanoic acid being the most common in all three plants. It was also observeda composition of 32.5% fatty acids in the volatile components of *C. sipthorpii*, with hexadecanoic acid again being determined as the most common, and additionally investigated the fatty acid contents and antioxidant activities of *C. iberica, C. urvillei* ssp. *hayekiana*, and *C. urvillei* ssp. *nimrodis* (Taştan et al. 2017). Oleic acid was major for three of the speciesIn the end, when evaluating all the results, the components that were found to be most common are compatible with the literature, with the most common saturated fatty acid being palmitic acid. Various fatty acid and antioxidant activity studies on *C. virgata* collected from different places have occurred. The current research has evaluated the similarity *C. virgata* collected from Elazig has with C. virgata collected from elsewhere. A study (Tekeli et al., 2013) on C. virgata collected from Konya showed the most common fatty acids that were found to be linoleic (29.15%), palmitic (28.41%), oleic (9.04%), and *α*-linoleic (21.33%) acids. These results also differ from the current study regarding the amounts and most common components, this difference is considered to be due to the growing conditions. The most common fatty acids in the *Centaurea virgata* Ayaz et al. (2017) collected from Gümüşhane were found as palmitic (5.75%), oleic (18.40%), and linoleic (62.99%) acids. Meanwhile the current study found the same substances to be the most common in the species collected from Elazig, though the amounts were found to be quite different. The reason for the change in the amount of content is thought to be region-based (Çelik, 2011).

Table 2. Antioxidant activity results for *C. virgata* Lam.

	DPPH (IC_{50} µg/mL)	ABTS (IC_{50} µg/mL)
CVM	378.86±0.60	19.38±0.49
Ascorbic acid	4.68±0.21	-
Trolox	-	18.22±1.15

CVM = MeOH extract of *C. virgata* Lam.

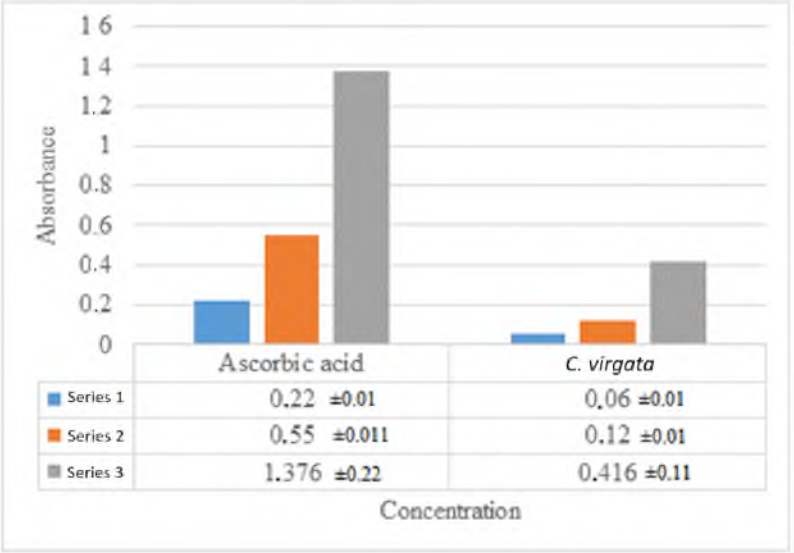

Figure 1. Reducing Power Results of the *C. virgata* Lam.

Table 2 and Figure show the results regarding the antioxidant activities, with the results appearing statistically significant at $p \leq 0.05$. The study evaluated DPPH, FRAP, and CUPRAC antioxidant activities and obtained respective values of 135.56 µmol TE/ 100 g dw, 57.63 µmol TE/ 100 g, and 68.19 µmol TE/ 100 g. The data indicate the *C. virgata* to have antioxidant effects similar to the *C. virgata* collected from Gümüşhane (see Ayaz et al., 2017), but at different levels. *C. kotschii* was investigated for its antioxidant potential. The current study has observed the antioxidant properties to be at a significant level. The IC_{50} value of the extract in the DPPH assay was determined as 37.09 g/mL. The extract exhibits a 65.22% linoleic oxidation in the beta-carotene/linoleic acid system. The amount of total phenolic content and total antioxidant capacity were detected as 36.52 mg gallic acid equivalent (GAE) per gram and 74.93 mg ascorbic acid equivalent (AE) per gram, respectively (Zengin et al., 2011). Zengin et al. (2010) had also investigated the antioxidant activities of the methanol extracts from *C. pulchella, C. patula*, and *C. tchihatcheffii*, and their results determined all of these to show antioxidant activity, with *C. pulchella* being the most active. Aktümsek et al. (2013) had investigated the antioxidant activities of *C. pseudoscabiosa* subsp. *aratica, C. pulcherrima* var. *pulcherrima, C. salicifolia* subsp. *abbreviata*, and *C. babylonica* and found *C. pulcherrima* var. *pulcherrima* to be the most active extract. Aktümsek et al. (2011) also identified the antioxidant activities of *C. kurdica, C. rigida, C. amanicola, C. cheirolopha*, and *C. ptosimopappoides* and found them to all have antioxidant activity.

CONCLUSION

In conclusion, the plants of the genus *Centaurea* and *C. virgata* Lam. have been the subject of much research because of their fatty acid content and antioxidant activities, which are known to be significant. However, no previous research could be found on the fatty acid and antioxidant activities of *C. virgata* collected from the Elazığ region. After evaluating the results, differences were determined to be present in the amounts and types of fatty acids, as well as in antioxidant activities, all due to effects such as growing and climatic conditions as well as soil richness.

According to this research, *C. virgata* can be considered an important source of antioxidants and fatty acids.

Peer-review: Externally peer-reviewed.

Author Contributions: Conception/Design of Study- B.S.T., T.F., B.K.; Data Acquisition- B.S.T., T.F., B.K.; Data Analysis/Interpretation- B.S.T., T.F., B.K.; Drafting Manuscript- B.S.T.; Critical Revision of Manuscript- B.S.T., B.K.; Final Approval and Accountability- B.S.T., T.F., B.K.

Conflict of Interest: The authors have no conflict of interest to declare.

Financial Disclosure: The authors declared no financial support.

ORCID IDs of the authors

Burcu Sümer Tüzün 0000-0002-9194-3447
Tuğçe Fafal 0000-0002-7445-5855
Bijen Kıvçak 0000-0001-7645-1930

REFERENCES

Aktumsek, A., Zengin, G., Guler, G.O., Cakmak, Y.S. & Duran, A. (2011). Screening for in vitro antioxidant capacities and fatty acid profiles of five *Centaurea* L. species from Turkey flora. *Food Chemistry and Toxicology, 49*, 2914-2920. [CrossRef]

Aktumsek, A., Zengin, G., Guler, G.O., Cakmak, Y.S. & Duran, A. (2013). Assesment of the antioxidant potential and fatty acid composition of four *Centaurea* L. taxa from Turkey. *Food Chemistry, 141*, 91-97. [CrossRef]

Albayrak, S., Atasagun, B., Aksoy, A. (2017). Comparison of phenolic components and biological activities of two *Centaurea* sp. obtained by three extraction techniques", Asian *Asian Pasidic Journal of Tropical Medicine, 10(6)*, 599-606. [CrossRef]

Ayaz, F.A., Özcan, M, Kurt, A., Karayiğit, B., Ozogul, Y., Glew, R. & Ozogul F. (2017). Fatty acid composition and antioxidant capacity of cypselas in *Centaurea* s.l. taxa (*Asteraceae, Cardueae*) from NE Anatolia. *South African Journal of Botany, 112*, 474- 482. [CrossRef]

Baytop, T. (1999). Therapy with medicinal plants in Turkey, Past and Present, second ed., Nobel Tıp Basımevi, Istanbul, Turkey.

Boğa, M., Alkan, H., Ertaş, A., Oral, E.V., Yılmaz, M.A., Yeşil, Y.. . . & Kolak, U. (2016). Phytochemical profile and some biological activities of three *Centaurea* species from Turkey. *Tropical Journal of Pharmaceutical Research, 15 (9)*, 1865-1875. [CrossRef]

Çelik, S.E. (2011). Farklı tür, karışım ve çözücü ortamlarına uygulanabilen modifiye Cuprac antioksidan kapasite ölçümleri. İstanbul Üniversitesi, Fen bilimleri Enstitüsü.

Erdogan, T., Gonenc, T., Cakilcioglu, U. & Kivcak, B. (2014). Fatty acid composition of the aerial parts of some *Centaurea* species in Elazıg, Turkey. *Tropical Journal of Pharmaecutical Research, 13(4)*, 613-616. [CrossRef]

Esmaeili, M.A. & Sonboli, A. (2010). Antioxidant, free radical scavenging activities of *Salvia branchyantha* and its protective effect against oxidative cell injury. *Food Chemistry and Toxicology, 48*, 846-853. [CrossRef]

Janackovic, P., Gavrilovic, M., Vujisic, L., Matevski, V. & Marin, P.D. (2017). Fatty acid composition of the cypcelae of two endemic *Centaurea* species (Asteraceae). *Botanical Serbica, 41 (1)*, 3-9. [CrossRef]

Köse, Y.B., İşçan, G., Göger, F., Akalın, G., Demirci, B. & Başer, K.H.C. (2016). Chemical composition and biological activity of *Centaurea baseri*: New species from Turkey. *Chemical Biodiversity, 13*, 1369 –1379. [CrossRef]

Lazari, D., Skaltsa H., Constantinidis, T. (2000). Volatile constituents of *Centaurea pelia* DC., C. *thessala* Hausskn. subsp. *drakiensis* (Freyn & Sint.) Georg. and *C. zuccariniana* DC. from Greece. *Flavour and Fragrance Journal, 15(1)*, 7- 11.

National Research Council (US) Comittee on Diet and Health. (1989). Diet and Health: Implications for Reducing Chronic Disease Risk. National Academies Press. Fats and Other Lipids. Hard copy version at National Academies Press, Washington DC.

Oyaizu, M. (1986). Studies on product of browning reaction prepared from glucose amine. *The Japanese Journal of Nutrition and Dietetics, 44*, 307. [CrossRef]

Ros, E. & Mataix, J. (2006) Fatty acid composition of nuts- implications for cardiovascular health. *British Journal of Nursing, 96 (2)*, 29-35. [CrossRef]

Senatore, F., Formisano, C., Raio, A., Bellone G. & Bruno M. (2008). Volatile components from flower-heads of *Centaurea nicaeensis* All., *C. parlatoris* Helder and *C. solstitialis* L. ssp. *schouwii* (DC.) Dostál growing wild in southern Italy and their biological activity. *Natural Product Research, 22(10)*, 825- 832. [CrossRef]

Tastan, P., Tuzun, B., Kivcak, B. & Fafal T. Fatty acids and antioxidant capacities of three *Centaurea* L. species. J Pharm Res. *Article in Press*.

Tekeli, Y., Zengin, G., Aktümsek, A., Sezgin, M. & Torlak, E. (2011). Antibacterial activities of extracts from twelve *Centaurea* species from Turkey. *Archieves of Biological Sciences, 63(3)*, 685-690. [CrossRef]

UPAC. (1979). Standards methods for analysis of oils, fats and derivatives. 6th ed., Pergamon Press, Oxford, 59-66.

Yıldırım, N., Sunar, S., Agar, G., Bozarı, S.& Aksakal, O. (2009). Biochemical and molecular characterization of some *Centaurea* species growing in the Eastern Anatolia region of Turkey. *Biochemical Genetics, 47*, 850-859. [CrossRef]

Zengin, G., Aktümsek, A., Güler, G.Ö., Çakmak, Y.S.& Yıldıztugay, E. (2011). Antioxidant properties of methanolic extract and fatty acid composition of *Centaurea urvillei* DC. subsp. *hayekiana* Wagenitz. *Records of Natural Products, 5 (2)*, 123-132.

Zengin, G., Çakmak, Y.S., Guler, G.O. & Aktumsek, A. (2010). *In vitro* antioxidant capacities and fatty acid compositions of three *Centaurea* species collected from Central Anatolia region of Turkey. *Food Chemistry and Toxicology, 48*, 2368-2341. [CrossRef]

Zengin, G., Guler, G.O., Cakmak, Y.S. & Aktumsek, A. (2011). Antioxidant capacity and fatty acid profile of *Centaurea kotschyi* (Boiss.& Heldr.) Hayek var. *persica* (Boiss.) Wagenitz from Turkey. *Grasas Y Acaites, 62 (1)*, 90- 95. [CrossRef]

Zengin, G., L-lorent-Martinez, E., Sinan, K.I., Yıldıztugay, E., Picot-Allain, C.&Mahomoodally, M.F. (2019a). Chemical profiling of *Centaurea bornmuelleri* Hausskn. aerial parts by HPLC-MS/MS and their pharmaceutical effects: From nature to novel perspectives. *Journal of Pharmaceutical and Biomedical Analysis, 174*, 406-413. [CrossRef]

Zengin, G., Zheleva-Dimitrovab, D., Gevrenovab, R., Aktumsek, A., Sinan, K.I. & Mahomood, M.F. (2019b). A comparative assess-

ment of the LC-MS profiles and cluster analysis of four *Centaurea* species from Turkey. *Biocatalysis Agricultural Biotechnology, 20 (2019)*, 10189. [CrossRef]

Zengin, G., Zhelava-Dimitrova, D., Gevrenova, R., Nedialkov, P, Mocan, A. . . .& Ciric, A. (2018). Identification of phenolic components via LC-MS analysis and biological activities of two *Centaurea* species: *Centaurea drabifolia* subsp. *drabifolia* and *Centaurea lycopifolia. Journal of Pharmaceutical and Biomedical Analysis, 149*, 436- 441. [CrossRef]

How cite this article

Sümer Tüzün, B., Fafal, T., & Kıvçak, B. (2024). Determining the fatty acid composition and antioxidant activities of Centaurea virgata Lam.. *İstanbul Journal of Pharmacy, 54*(2), 182–188. DOI: 10.26650/IstanbulJPharm.2024.1036392

İstanbul Journal of Pharmacy
Istanbul J Pharm2024, 54 (2): 189–194
DOI: 10.26650/IstanbulJPharm.2024.1417841

Original Article

Comparison of the inhibition of *Candida spp.* biofilm formation by quorum-sensing molecules, farnesol and tyrosol with amphotericin B

Müzeyyen Aydın[1,2], Mayram Hacıoğlu[2], Neşe İnan[3]

[1]İstanbul University Institute of Health Sciences İstanbul, Türkiye
[2]İstanbul University, Faculty of Pharmacy, Department of Pharmaceutical Microbiology, İstanbul, Türkiye
[3]Dr. Abdurrahman Yurtaslan Ankara Oncology Hospital, Medical Microbiology Laboratory, Ankara, Türkiye

ABSTRACT

Background and Aims: Quorum sensing is a mechanism of cell-to-cell communication for controlling virulence and the biofilm formation of microorganisms. Due to this new treatment requiring approaches for biofilm-related infections, this study aims to examine the biofilm formation properties of both *Candida albicans* and non-albicans (NAC) strains and to compare the effects of the quorum-sensing molecules (QSMs) farnesol and tyrosol with the widely used antifungal agent amphotericin B with regard to biofilm attachment and biofilm formation.

Methods: Biofilm formation of 57 nonrepeat clinical isolates of *Candida spp*. (36 *C. albicans* and 21 NAC) was assessed through the crystal violet technique. Farnesol (300 µM), tyrosol (80 µM), and amphotericin B (4 µg/ml) were evaluated against biofilm attachment and biofilm formation (plates incubated 2, 4, 6 and 24 h).

Results: All isolates displayed biofilm-forming capabilities. *C. albicans* demonstrated mostly weak biofilm formation (42.2%), whereas the NAC species showed strong biofilm formation (52.38%). Depending on the stage at which they were added, farnesol and tyrosol significantly inhibited the biofilm formation of *C. albicans* and NAC species, especially at 6 h, which is the early stage of biofilm development. Unfortunately, QSM activity decreased at 24 h. In addition, amphotericin B showed a stronger inhibitory effect than the QSMs at all time points studied, with up to 60% inhibition being observed.

Conclusion: QSMs can significantly inhibit biofilm development in both *C. albicans* and NAC species depending on the stage when they are added, especially in the early stages of biofilm formation.

Keywords: *Candida spp*., biofilm, quorum sensing, farnesol, tyrosol, amphotericin B

INTRODUCTION

Recent years have seen a notable increase in the prevalence of human fungal infections, particularly *Candida* infections which include invasive candidiasis, oropharyngeal/oral candidiasis, and vulvovaginal candidiasis. The main contributing factors have been the Acquired Immune Deficiency Syndrome epidemic, an increasingly aging population, an increase in immunocompromised patient numbers, and also the increased use of indwelling medical devices (Silva et al., 2012). While *Candida albicans* is the most commonly isolated *Candida* species among humans (representing over 80% of all candidiasis cases in humans), the prevalence of infections due to non-albicans *Candida* (NAC) species such as *Candida tropicalis, Candida glabrata, Candida parapsilosis, Candida krusei*, and *Candida kefyr* over the last two decades has increased significantly (Chin, Lee, Rusliza, & Chong, 2016; Silva et al., 2012).

Although *Candida* species are present on the mucosal membranes and skin of normal individuals, they can cause infection under specific circumstances. The most important step in the *Candida* infection is the adhesion to host surfaces, as this is necessary for initial colonization and can lead to the organism's persistence. Adherence is considered critical for establishing disease. Additionally, *Candida* species have also have the ability to attach to the surfaces of medical equipment and develop biofilms (Malinovská, Čonková, & Váczi, 2023; Silva et al., 2012). Biofilms are organized communities of microorganisms that adhere to a surface or interface and are surrounded by a self-produced exopolymeric matrix. Microorganisms predominantly exist as biofilms in the natural environment or within human systems. Biofilms are estimated to be associated with 80% of microbial infections in humans and in the natural environment (Brackman & Coenye, 2015). Systemic mycoses, for which *Candida* is responsible in 90% of cases, are strongly as-

Corresponding Author: Müzeyyen Aydın **E-mail:** muzeyyenaydin151@gmail.com
Submitted: 12.01.2024 • **Revision Requested:** 12.03.2024 • **Last Revision Received:** 25.03.2024 • **Accepted:** 26.03.2024

sociated with biofilm formation. According to recent statistics, systemic mycoses unfortunately result in approximately 1.6 million human deaths each year (Malinovská et al., 2023; Nami, Aghebati-Maleki, Morovati, & Aghebati Maleki, 2019). In addition, the mortality rate for *Candida*-related bloodstream infections is 37.9%. Of these, 70.0% are due to biofilm-related infections (Atiencia-Carrera, Cabezas-Mera, Tejera, & Machado, 2022).

Quorum sensing (QS) is a mechanism of cell-to-cell communication for controlling virulence and biofilm formation and occurs through the continuous release and monitoring of hormone-like molecules known as autoinducers, or quorum-sensing molecules (QSMs; Albuquerque & Casadevall, 2012).

QS regulation was first discovered in bacteria in the 1960s and 1970s during studies of genetic competence in *Streptococcus pneumoniae* and bioluminescence in marine *Vibrio* species. Until farnesol was discovered as a QSM in *C. albicans*, QS in eukaryotic organisms had been unknown. Since then, studies have shown a large number of structurally distinct fungal QSMs, such as tyrosine (tyrosol), phenylalanine (phenylethanol), and tryptophan (tryptophol), that are responsible for a variety of properties in evolutionarily divergent fungi (Albuquerque & Casadevall, 2012; Tian, Ding, Ke, & Wang, 2021).

Although its concentration and production are highest in *C. albicans*, the first eukaryotic QSM (i.e., farnesol) is able to be secreted by eight *Candida* under different conditions: *C. albicans, C. tropicalis, C. parapsilosis, C. kefyr, C. krusei, C. glabrata, Candida dubliniensis* and *Candida guilliermondii* (Weber, Sohr, Schulz, Fleischhacker, & Ruhnke, 2008). Farnesol is involved in inhibiting hypha formation and in regulating various physiological processes, including filamentation, drug efflux, and apoptosis. Farnesol has also been shown to be able to reversibly inhibit biofilm formation without blocking the elongation of pre-existing hyphae (De Sordi & Mühlschlegel, 2009; Rodrigues & Černáková, 2020).

Tyrosol is the another major QSM secreted by *C. albicans* and is released into the culture medium continuously as the organism grows. Tyrosol reduces the duration of the lag phase of growth and stimulates filamentation and biofilm formation during the early steps of biofilm development (1-6 h). Therefore, its effects are particularly strong during the early and intermediate periods of biofilm formation (Albuquerque & Casadevall, 2012; Rodrigues & Černáková, 2020).

New treatment approaches are well known to be required for biofilm-associated infections, which are notoriously difficult to treat. Additionally, eradicating mature biofilms is a challenging task. This study investigates the biofilm formation properties of both *C. albicans* and NAC strains and compares the effects of two important QSMs (i.e., farnesol and tyrosol) on the biofilm formation of these strains with that of amphotericin B.

MATERIALS AND METHODS

Fungal isolates

A total of 57 *Candida* spp. (nonrepeat), including 36 *C. albicans* and 21 NAC species (6 *C. glabrata*, 6 *C. tropicalis*, 5 *C. parapsilosis*, 2 *C. famata*, 1 *C. kefyr*, and 1 *C. krusei*) contained in various clinical samples from blood, urine, vagina, ear, esophagus, sputum, endotracheal aspirate, and wounds were submitted to the Synevo Laboratories Ankara Central Laboratory in Türkiye (2021-2022). The Vitek 2 (BioMerieux, France) and CHROMagar *Candida* (BioMerieux, France) systems were used to identify the strains. Each isolate was grown on Sabouraud dextrose agar (SDA, Merck) to ensure viability before analysis.

QSMs and Amphotericin B

The QSMs of farnesol and tyrosol were used in respective 300 and 80 μM concentrations in the experiments and were purchased from Sigma-Aldrich. Amphotericin B (4 μg/ml) was kindly provided by the manufacturer, and stock solutions were prepared from dry powders in water and stored frozen at -80°C; the frozen solutions were used within 6 months. The antimicrobial concentrations that were used are based in part on those used in previous studies and the closest toxic concentrations (Hacioglu, Haciosmanoglu, Birteksoz-Tan, Bozkurt-Guzel, & Savage, 2019b; Katragkou et al., 2015; Shanmughapriya, Sornakumari, Lency, Kavitha, & Natarajaseenivasan, 2014).

Biofilm formation

Biofilms were formed in microtiter plate wells using clinical isolates of *C. albicans* and NAC species according to the protocol of Ramage, Vande, Wickes, & Lopez-Ribot (2001). Overnight cultures of isolates from 24-h growth on yeast extract-peptone-dextrose agar (Sigma-Aldrich) were inoculated into yeast extract-peptone-dextrose broth (YPDB, Sigma-Aldrich) and incubated overnight at 37°C on an orbital shaker. Cultures were centrifuged (3000 rpm for 5-10 min), rinsed twice with sterile phosphate-buffered saline (PBS) and resuspended in YPDB at a cell density equivalent to 1×10^6 cells/mL. For biofilm formation, 100 μL of the standardized cell suspension was carefully pipetted into the selected wells of sterile flat-bottomed 96-well polystyrene tissue culture plates (Greiner Bio-One, Germany) and incubated at 37°C for 24 h. After incubation, the waste medium was gently aspirated, and non-adherent cells were removed by washing the biofilms three times with sterile PBS.

Quantification of biofilm formation

Biofilm formation of the clinical isolates of *C. albicans* and NAC species was assessed using the crystal violet technique as described by Djordjevic, Wiedmann, & McLandsborough

(2002) and Hacioglu, Tan, Dosler, Inan, & Otuk (2018). In brief, after the formation of the biofilm, each well was washed twice with 200 ml of PBS and air dried. Each washed well was then stained for 45 min with 100 ml of 0.4% aqueous crystal violet solution. These wells were then washed four times again with sterile PBS and instantly distained with 200 ml of 95% ethanol. After 45 min 100 ml of the distaining solution was transferred to a new well. The amount of crystal violet staining in the distaining solution was measured using a microtiter plate reader (Bio-Rad Novapath, California, USA) at 595 nm. In order to reduce background interference, the negative controls' absorbance values (containing no cells) were removed from the values of the test wells. Biofilm formation was measured in triplicate for each isolate using the wild-type strain of *C. albicans* (SC 5314) as the strong biofilm producer. Weak, moderate, and strong biofilm formation were defined as follows:

OD (optical density) (isolate) ≤ OD (negative control) = negative biofilm formation;

OD (negative control) ≤ OD (isolate) ≤ 2xOD (negative control) = weak biofilm formation;

2xOD (negative control) ≤ OD (isolate) ≤ 4xOD (negative control) = moderate biofilm formation;

4xOD (negative control) ≤ OD (isolate) = strong biofilm formation (Oyardi, Hacioglu, Yilmaz, Inan, & Bırteksoz Tan, 2023)

Inhibition of biofilm attachment and biofilm formation

Overnight cultures of isolates were prepared in YPDB so as to result in a cell density equivalent to 1×10^6 cells/mL. The clinical isolates of the *C. albicans* and NAC species were added to each well of tissue culture microtitration plates (96 wells) containing the QSMs and amphotericin B. Positive controls with no antimicrobials and negative controls with no cells were also added. Plates were incubated at 37°C for 2, 4, 6, and 24 h. After incubation, the wells were washed twice with PBS, and the optical density (OD) was read spectrophotometrically at 450 nm using a microplate reader (Bio-Rad Novapath, California, USA; Bozkurt-Guzel, Hacioglu, & Savage, 2018).

RESULTS

Biofilm formation assay

All isolates displayed biofilm-forming capabilities. In particular, *C. albicans* demonstrated mostly weak biofilm formation (42.2%), whereas the NAC species showed strong biofilm formation (52.38%). The results are shown in Table 1.

Effects of QSMs and amphotericin B on *C. albicans* biofilm attachment and biofilm formation

Although the inhibition of adhesion and biofilm formation rates was time-dependent, the range of percentage inhibition rates (%) for farnesol and tyrosol was found to be between 3.18 and 31.13 for farnesol and between -5.31 and 12.65 for tyrosol. Both QSMs showed the highest inhibitory effect at 6 h, while their activity decreased at 24 h. Amphotericin B showed a stronger inhibitory effect than the QSMs for all time points studied (Figure 1a).

Effects of QSMs and amphotericin B on NAC biofilm attachment and biofilm formation

The time-dependent inhibition rates (%) of farnesol and tyrosol respectively ranged between -3.47 and 20.78 and between -2.47 and 9.59. Farnesol was more effective than tyrosol except at time zero. The most potent antimicrobial agent with up to 60% inhibition rates was found to be amphotericin B (Figure 1b).

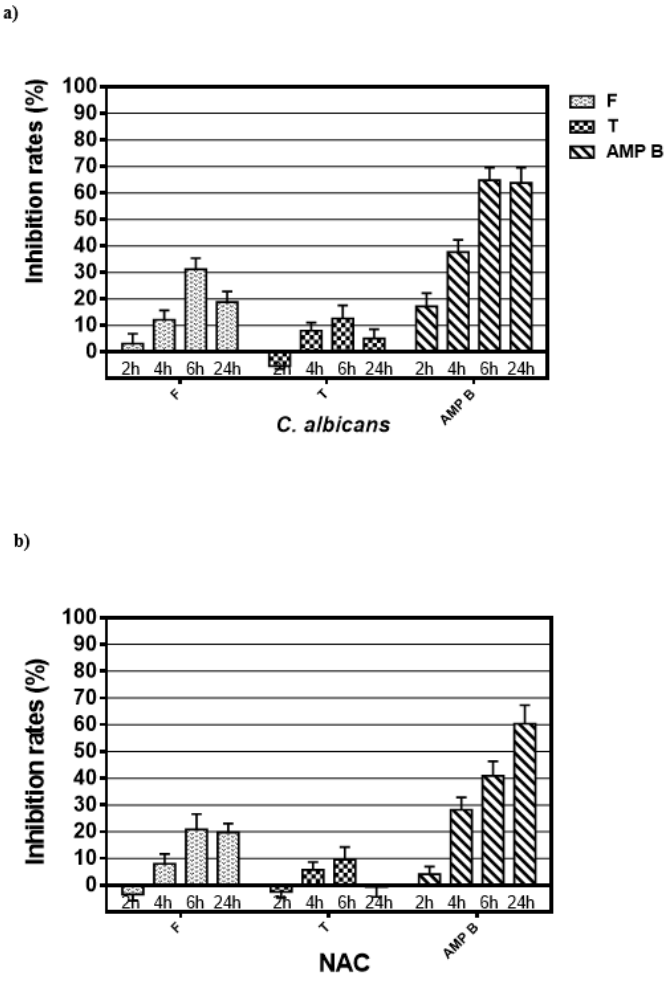

Figure 1. Effects of QSMs and amphotericin B on *Candida spp*. biofilm attachment and biofilm formation. a) *C. albicans* b) NAC. Inoculums were incubated for 2, 4, 6 and 24 hat 37°C. Four wells were used for each agent, and each experiment was performed with at least two independent tests. The error bars indicate the standard deviations.
F = farnesol; T = tyrosol; AMP B = amphotericin B

Table 1. Biofilm formation rates of isolates

	Biofilm formation capabilities (%)		
Strains	**Strong**	**Moderate**	**Weak**
***C. albicans* (n=36)**	22.2 (n=8)	30.55 (n=11)	42.2 (n=17)
NAC (n=21)	52.38 (n=11)	28.57 (n=6)	19.04 (n=4)
C. glabrata (n=6)	50 (n=3)	33.3 (n=2)	16.6 (n=1)
C. tropicalis (n=6)	50 (n=3)	-	50 (n=3)
C. parapsilosis (n=5)	60 (n=3)	40 (n=2)	-
C. famata (n=2)	50 (n=1)	50 (n=1)	-
C. kefyr (n=1)	100 (n=1)	-	-
C. krusei (n=1)	-	100 (n=1)	-

DISCUSSION

Candida is an opportunistic yeast genus and is the fourth most common cause of hospital-acquired bloodstream infections. It is responsible for 90% of systemic mycoses, with around 70% of candidemia being closely related to biofilm formation. These infections cause approximately 1.6 million human deaths each year. *Candida* biofilms can be seen on both living surfaces such as mucous membranes, organs, and blood vessels, as well as on non-living surfaces such as medical devices (e.g., medical catheters contact lenses, cardiovascular implants, pacemakers, shunts; Atiencia-Carrera et al., 2022; Malinovská et al., 2023). Biofilms are well known for being able to lead to significant resistance to antifungal agents. Therefore, a pressing need exists for novel agents that target biofilm and that operate through unique mechanisms such as QSMs. For this purpose, the aim of the present study has been to investigate the biofilm formation properties of both *C. albicans* and NAC species and to compare the effects of two important QSMs (i.e., farnesol and tyrosol) against amphotericin B regarding biofilm formation.

The study's results demonstrate all of the isolates to have produced biofilms; however, the NAC strains showed stronger biofilm formation rates (52.38%) than the *C. albicans* strains (22.2%). Previous studies have shown *Candida* isolates from different clinical materials to be able to form biofilms at different rates. One study observed biofilm formation in 92% of *C. albicans* isolates (n=77), and 100% of NAC species (n=16) that had been isolated from vulvovaginal candidiasis patients showing the ability to form biofilms (Hacioglu, Guzel, Savage, & Tan, 2019a). Atiencia-Carrera et al. (2022) investigated the rate, type, and antifungal resistance of *Candida* biofilms among hospitalized patients for the years 1995 and 2020. According to their results, the low, intermediate, and high biofilm rates were 36.2%, 18.9%, and 35%, respectively, with *C. tropicalis* being the predominant species in high biofilm formation (67.5%) and *C. krusei* and *C. glabrata* being the second and third most common strong biofilm producers among the *Candida* species.

In line with emerging areas of research focusing on the prevention of microorganisms' adherence and biofilm development, the present study has investigated farnesol and tyrosol's and amphotericin B's ability to inhibit biofilm attachment and biofilm formation in the clinical isolates of *C. albicans* and NAC species.

Although biofilm formation is a process present in all *Candida* species, which is able to form a biofilm in 38-72 h, this formation is influenced by several factors and varies significantly from species to species (Malinovská et al., 2023). *C. albicans* biofilm formation has been characterized by three stages of development: 1) adhesion of the yeast cells (early stage: 0–11 h), 2) yeast cell differentiation into hyphal cells (intermediate stage: 12–30 h), and 3) matrix increase (maturation stage: 31–72 h; Atriwal et al., 2021; Tobudic, Kratzer, Lassnigg, & Boucherit, 2012). According to the current study's results regarding *C. albicans*, inhibition rates for farnesol and tyrosol were respectively found to be 31.13% and 12.65% at 6 h, which is the early stage of biofilm development. Unfortunately, these QSMs' activity decreased at 24 h.

C. albicans biofilms exhibit a heterogeneous structure comprised of cells, hyphae, and pseudohyphae enclosed by an extracellular matrix (ECM) material. The ECM provides a structural support for adhesion between biofilm cells and biotic or abiotic surfaces. It also acts as a barrier between the biofilm cells and the surrounding environment. Among the NAC species, *C. glabrata* is not polymorphic, does not form true hyphae or pseudohyphae, and has a biofilm consisting of yeast cells in a multilayered organization (i.e., cell clusters). The biofilms of *C. tropicalis* and *C. parapsilosis* have a biofilm structure consisting of yeasts and pseudohyphae surrounded by a minimal ECM with low carbohydrate and protein content (Cavalheiro & Teixeira, 2018; Malinovská et al., 2023). The present study

found the QSMs of farnesol and tyrosol to inhibit biofilm attachment of NAC species at 20.78% and 9.59%, respectively at 6 h.

The QSMs of farnesol and tyrosol work together in the fungal life cycle to aid fungal adhesion, proliferation, filamentation, and dispersal. Farnesol prevents hyphae formation and inhibits biofilm formation when added at beginning of biofilm formation, whereas tyrosol stimulates hyphal formation, particularly in the early and intermediate stages of biofilm formation (Cordeiro et al., 2015; Fourie & Pohl, 2019). The current study's results have also confirmed farnesol to be able to significantly inhibit biofilm formation when added at the early stages of biofilm formation, whereas tyrosol promoted biofilm growth. The biofilm inhibition rates for tyrosol at 2 h were -5.31% and -2.47% respectively for both the *C. albicans* and NAC species. However, tyrosol showed biofilm inhibition at 4 and 6 h for both *C. albicans* and NAC species. According to Sebaa, Boucherit-Otmani, & Courtois (2019), farnesol at 3 mM and tyrosol at 20 mM showed stronger inhibition when added at the beginning of biofilm formation (>50% and >80% inhibition, respectively) than when added to preformed biofilms (<10% and <40% inhibition, respectively). Other studies have also shown farnesol and tyrosol to be able to be effective against *Candida* biofilms, depending on the concentration and stage when they are added (Alem, Oteef, Flowers, & Douglas, 2006; Yapıcı, Gürsu, & Dağ, 2021).

The polyene antifungal agent amphotericin B is widely used in the treatment of invasive fungal infections, such as candidiasis and biofilm infections and is considered to be the most reliable and widest spectrum treatment against these types of infections (Hamill, 2013; Touil, Boucherit-Otmani, & Boucherit, 2018). The current study found amphotericin B to show a stronger inhibitory effect than the QSMs at all time points studied, with up to 60% inhibition. Another study investigated the inhibition of biofilm formation for 23 clinical *Candida* isolates (10 *C. krusei* and 13 *C. tropicalis*) using amphotericin B, tyrosol, and the combination of the two. The inhibition of biofilm by amphotericin B or tyrosol was shown to be concentration dependent, with a 50% reduction at 4 µg/ml and 80 µM, respectively (Shanmughapriya et al., 2014).

In conclusion, the QSMs of farnesol and tyrosol work together to regulate fungal morphology, especially with regard to biofilms. The study's results show these QSMs to be able to significantly inhibit biofilm formation in both *C. albicans* and NAC species, depending on the stage when they are added and especially during the early stages of biofilm formation. The antibiofilm activity of QSMs may be of interest for developing new antifungal strategies due to the clinical importance of *Candida* biofilm infections.

Peer-review: Externally peer-reviewed.

Author Contributions: Conception/Design of Study- M.A., M.H., N.İ.; Data Acquisition- M.A., M.H., N.İ.; Data Analysis/Interpretation- M.A., M.H., N.İ.; Drafting Manuscript- M.A., M.H., N.İ.; Critical Revision of Manuscript- M.H., N.İ.; Final Approval and Accountability- M.A., M.H., N.İ.

Conflict of Interest: The authors have no conflict of interest to declare.

Financial Disclosure: This work was supported by the Research Fund of Istanbul University [project number 34926].

ORCID IDs of the authors

Müzeyyen Aydın 0000-0002-8082-9470
Mayram Hacıoğlu 0000-0003-0823-631X
Neşe İnan 0000-0002-1559-6244

REFERENCES

Albuquerque, P., & Casadevall, A. (2012). Quorum sensing in fungi–a review. *Medical Mycology*, 50(4), 337-345. doi:10.3109/13693786.2011.652201

Alem, M. A., Oteef, M. D., Flowers, T. H., & Douglas, L. J. (2006). Production of tyrosol by Candida albicans biofilms and its role in quorum sensing and biofilm development. *Eukaryotic Cell*, 5(10), 1770-1779. https://doi.org/10.1128/EC.00219-06

Atiencia-Carrera, M. B., Cabezas-Mera, F. S., Tejera, E., & Machado, A. (2022). Prevalence of biofilms in Candida spp. bloodstream infections: A meta-analysis. *PLoS One*, 17(2), e0263522. https://doi.org/10.1371/journal.pone.0263522

Atriwal, T., Azeem, K., Husain, F. M., Hussain, A., Khan, M. N., Alajmi, M. F., & Abid, M. (2021). Mechanistic understanding of Candida albicans biofilm formation and approaches for its inhibition. *Frontiers in Microbiology*, 12, 638609. https://doi.org/10.3389/fmicb.2021.638609

Bozkurt-Guzel, C., Hacioglu, M., & Savage, P. B. (2018). Investigation of the in vitro antifungal and antibiofilm activities of ceragenins CSA-8, CSA-13, CSA-44, CSA-131, and CSA-138 against Candida species. *Diagnostic Microbiology and Infectious Disease*, 91(4), 324-330. https://doi.org/10.1016/j.diagmicrobio.2018.03.014

Brackman, G., & Coenye, T. (2015). Quorum sensing inhibitors as anti-biofilm agents. *Current Pharmaceutical Design*, 21(1), 5-11. https://doi.org/10.2174/1381612820666140905114627

Cavalheiro, M., & Teixeira, M. C. (2018). Candida biofilms: threats, challenges, and promising strategies. *Frontiers in Medicine*, 5, 28. https://doi.org/10.3389/fmed.2018.00028

Chin, V. K., Lee, T. Y., Rusliza, B., & Chong, P. P. (2016). Dissecting Candida albicans infection from the perspective of C. albicans virulence and omics approaches on host–pathogen interaction: a review. *International Journal of Molecular Sciences*, 17(10), 1643. https://doi.org/10.3390/ijms17101643

Cordeiro, R. D. A., Teixeira, C. E., Brilhante, R. S., Castelo-Branco, D. S., Alencar, L. P., de Oliveira, J. S., ... & Rocha,

M. F. (2015). Exogenous tyrosol inhibits planktonic cells and biofilms of Candida species and enhances their susceptibility to antifungals. *FEMS Yeast Research*, 15(4), fov012. https://doi.org/10.1093/femsyr/fov012

De Sordi, L., & Mühlschlegel, F. A. (2009). Quorum sensing and fungal–bacterial interactions in Candida albicans: a communicative network regulating microbial coexistence and virulence. *FEMS Yeast Research*, 9(7), 990-999. https://doi.org/10.1111/j.1567-1364.2009.00573.x

Djordjevic, D., Wiedmann, M., & McLandsborough, L. A. (2002). Microtiter plate assay for assessment of Listeria monocytogenes biofilm formation. *Applied and Environmental Microbiology*, 68(6), 2950-2958. doi:10.1128/AEM.68.6.2950-2958.2002

Fourie, R., & Pohl, C. H. (2019). Beyond antagonism: the interaction between Candida species and Pseudomonas aeruginosa. Journal of Fungi, 5(2), 34. https://doi.org/10.3390/jof5020034

Hacioglu, M., Tan, A. S. B., Dosler, S., Inan, N., & Otuk, G. (2018). In vitro activities of antifungals alone and in combination with tigecycline against *Candida albicans* biofilms. PeerJ, 6, e5263. https://doi.org/10.7717/peerj.5263

Hacioglu, M., Guzel, C. B., Savage, P. B., & Tan, A. S. B. (2019a). Antifungal susceptibilities, in vitro production of virulence factors and activities of ceragenins against *Candida* spp. isolated from vulvovaginal candidiasis. *Medical Mycology*, 57(3), 291-299. https://doi.org/10.1093/mmy/myy023

Hacioglu, M., Haciosmanoglu, E., Birteksoz-Tan, A. S., Bozkurt-Guzel, C., & Savage, P. B. (2019b). Effects of ceragenins and conventional antimicrobials on *Candida albicans* and *Staphylococcus aureus* mono and multispecies biofilms. *Diagnostic Microbiology and Infectious Disease*, 95(3), 114863. https://doi.org/10.1016/j.diagmicrobio.2019.06.014

Hamill, R. J. (2013). Amphotericin B formulations: a comparative review of efficacy and toxicity. *Drugs*, 73, 919-934. https://doi.org/10.1007/s40265- 013-0069-4

Katragkou, A., McCarthy, M., Alexander, E. L., Antachopoulos, C., Meletiadis, J., Jabra-Rizk, M. A., ... & Walsh, T. J. (2015). In vitro interactions between farnesol and fluconazole, amphotericin B or micafungin against Candida albicans biofilms. *Journal of Antimicrobial Chemotherapy*, 70(2), 470-478. https://doi.org/10.1093/jac/dku374

Malinovská, Z., Čonková, E., & Váczi, P. (2023). Biofilm Formation in medically important Candida species. *Journal of Fungi*, 9(10), 955. https://doi.org/10.3390/jof9100955

Nami, S., Aghebati-Maleki, A., Morovati, H., & Aghebati-Maleki, L. (2019). Current antifungal drugs and immunotherapeutic approaches as promising strategies to treatment of fungal diseases. *Biomedicine & Pharmacotherapy*, 110, 857-868. https://doi.org/10.1016/j.biopha.2018.12.009

Oyardi, O., Hacioglu, M., Yilmaz, F.N., Inan, N., & Birteksoz Tan, A.S. (2023). Antibiotic susceptibility and biofilm formation of multi-drug resistant Gram-negative bacteria. *Istanbul Journal of Pharmacy*, 53(1), 45-50. doi: 10.26650/IstanbulJPharm.2023.1156339

Ramage, G., Vande Walle, K., Wickes, B. L., & Lopez-Ribot, J. L. (2001). Standardized method for in vitro antifungal susceptibility testing of *Candida albicans biofilms. Antimicrobial Agents and Chemotherapy*, 45(9), 2475-2479. https://doi.org/10.1128/aac.45.9.2475-2479.2001

Rodrigues, C. F., & Černáková, L. (2020). Farnesol and tyrosol: secondary metabolites with a crucial quorum-sensing role in *Candida* biofilm development. Genes, 11(4), 444. https://doi.org/10.3390/genes11040444

Sebaa, S., Boucherit-Otmani, Z., & Courtois, P. (2019). Effects of tyrosol and farnesol on Candida albicans biofilm. *Molecular Medicine Reports*, 19(4), 3201-3209. https://doi.org/10.3892/mmr.2019.9981

Shanmughapriya, S., Sornakumari, H., Lency, A., Kavitha, S., & Natarajaseenivasan, K. (2014). Synergistic effect of amphotericin B and tyrosol on biofilm formed by Candida krusei and Candida tropicalis from intrauterine device users. *Medical Mycology*, 52(8), 853-861. https://doi.org/10.1093/mmy/myu046

Silva, S., Negri, M., Henriques, M., Oliveira, R., Williams, D. W., & Azeredo, J. (2012). Candida glabrata, Candida parapsilosis and Candida tropicalis: biology, epidemiology, pathogenicity and antifungal resistance. *FEMS Microbiology Reviews*, 36(2), 288-305. https://doi.org/10.1111/j.1574-6976.2011.00278.x

Tian, X., Ding, H., Ke, W., & Wang, L. (2021). Quorum sensing in fungal species. *Annual Review of Microbiology*, 75, 449-469. https://doi.org/10.1146/annurev-micro-060321-045510

Tobudic, S., Kratzer, C., Lassnigg, A., & Presterl, E. (2012). Antifungal susceptibility of Candida albicans in biofilms. *Mycoses*, 55(3), 199-204. https://doi.org/10.1111/j.1439-0507.2011.02076.x

Touil, H. F. Z., Boucherit-Otmani, Z., & Boucherit, K. (2018). In vitro activity of antifungal combinations against planktonic and sessile cells of Candida albicans isolated from medical devices in an intensive care department. *Journal de Mycologie Medicale*, 28(3), 414-418. https://doi.org/10.1016/j.mycmed.2018.06.008

Weber, K., Sohr, R., Schulz, B., Fleischhacker, M., & Ruhnke, M. (2008). Secretion of E, E-farnesol and biofilm formation in eight different Candida species. *Antimicrobial Agents and Chemotherapy*, 52(5), 1859-1861. https://doi.org/10.1128/AAC.01646-07

Yapıcı, M., Gürsu, B. Y., & Dağ, İ. (2021). In vitro antibiofilm efficacy of farnesol against Candida species. *International Microbiology*, 24(2), 251-262. https://doi.org/10.1007/s10123-021-00162-4

How cite this article

Aydın, M., Hacıoğlu, M., & İnan, N. (2024). Comparison of the inhibition of *Candida spp.* biofilm formation by quorum-sensing molecules, farnesol and tyrosol with amphotericin B *İstanbul Journal of Pharmacy, 54*(2), 189–194. DOI: 10.26650/IstanbulJPharm.2024.1417841

İstanbul Journal of Pharmacy
Istanbul J Pharm2024, 54 (2): 195–204
DOI: 10.26650/IstanbulJPharm.2024.1322171

Original Article

Anti-inflammatory activity of a novel lectin isolated from *Pleurotus eryngii* var. *ferulae* mushroom*

Thoiba Mogahid Hussein Seliman[1], Gülsüm Altıparmak Ülbegi[1], Nurten Özsoy[1], Hevidar Alp Kavlo[2], Pınar Aksoy Sağırlı[1]

[1]İstanbul University, Faculty of Pharmacy, Department of Biochemistry, Istanbul, Türkiye
[2]Munzur University, Tunceli Vocational School, Department of Food Process, Tunceli, Türkiye
*This study was accepted as a Biochemistry Master thesis within the scope of the İstanbul University Faculty of Pharmacy Biochemistry Master Program in 2021.

ABSTRACT

Background and Aims: *Pleurotus* species are edible mushrooms with important economic and medicinal value. Many pharmacological properties of these species, such as anticancer, immunomodulating, and anti-inflammatory activities, have been attributed to lectin. The aim of this study was to purify a novel lectin from *Pleurotus eryngii* var. *ferulae* (PEFL) and investigate its anti-inflammatory activity.

Methods: PEFL was purified by 80% ammonium sulphate fractionation, diethylaminoethyl (DEAE)-Sepharose-4B anion exchange, and Sephadex G-100 gel filtration chromatography. The molar mass of the purified lectin was determined by sodium dodecyl sulphate-polyacrylamide gel electrophoresis (SDS-PAGE) under denaturing conditions. Inhibition of lectin-induced haemagglutination by several carbohydrates and one glycoprotein (ovalbumin) was also performed using the haemagglutination inhibition activity test. The anti-inflammatory effect of PEFL was tested in a lipopolysaccharide (LPS)-induced inflammation model in mouse macrophage cells (RAW 264.7). The levels of prostaglandin (PG)-E2, tumour necrosis factor-alpha (TNF-α), interleukin-1-beta (IL-1β), interleukin-6 (IL-6), interleukin-10 (IL-10), and interferon-gamma (IFN-γ) were determined using enzyme-linked immunosorbent assay (ELISA) kits. Furthermore, the expression of nitric oxide synthase (iNOS) and cyclooxygenase-2 (COX-2) was estimated by western blot analysis.

Results: PEFL was obtained in 16% yield. The specific activity of PEFL was calculated as 1280 haemagglutinating units (HU)/mg protein and was inhibited only by D-galactose. The molecular weight was determined to be 46 kDa. PEFL showed an anti-inflammatory effect by reducing the production of pro-inflammatory PGs through COX-2 inhibition, as well as reducing iNOS expression. Furthermore, our findings reported that PEFL has a protective effect on inflammation by decreasing the production of pro-inflammatory cytokines and increasing the production of the anti-inflammatory cytokine (IL-10).

Conclusion: The results suggest that PEFL can be considered as a potential therapeutic agent in the development of new therapeutic strategies for inflammatory diseases.

Keywords: Cytokines, Lectin, Lipopolysaccharide, Mushroom, *Pleurotus eryngii* var. *ferulae*, RAW 264.7 macrophage

INTRODUCTION

In recent years, lectins have begun to be investigated more extensively because it is understood that these proteins are invaluable tools for the structural and functional examination of complex carbohydrates, especially glycoproteins, specific drug targeting, bioadhesion applications, diagnostics, and cancer therapy (Santos et al., 2014; Dan, Liu & Ng, 2015). It has been discovered that lectins play a role as recognition molecules in many biological events such as signal transduction, regulation of glycoprotein synthesis and intracellular trafficking, cancer and metastasis, attachment of infecting agents to host cells, directing leukocytes to inflammation sites, immunomodulation, and regulation of cell growth and apoptosis (Sharon & Lis, 2004; Muramoto, 2017; Coelho et al., 2017).

Today, scientific researches are focussed on drug production from pure substances obtained from natural sources. Mushrooms have been used as food for centuries as well as medicine for the treatment of many diseases. Mushrooms can be considered as a healthy food, rich in polysaccharides, proteins, and other functional components with many bioactivities that

Corresponding Author: Thoiba Mogahid Hussein Seliman **E-mail:** thwiiiban.m@gmail.com
Submitted: 04.07.2023 • **Revision Requested:** 07.11.2023 • **Last Revision Received:** 29.04.2024 • **Accepted:** 29.04.2024

increase immunity, reduce the risk of cancer, prevent the proliferation of tumour cells, and protect the nervous system. Overall, the spectrum of beneficial effects of mushrooms is heterogeneous, and it has been suggested that mushrooms can be consumed daily as one of the best acceptable nutraceutical foods (Ma et al., 2018).

Lectins isolated from medicinal mushrooms are used in the prevention and treatment of many diseases, and scientific studies on this subject have been increasing rapidly all over the world. It has been reported that lectins isolated from mushrooms have mitogenic, antiviral, antitumor, immunomodulatory, and anti-HIV-1 reverse transcriptase activities (Singh, Bhari & Kaur, 2010; Hassan, Rouf, Tiralongo, May & Tiralongo, 2015). Medicinal mushroom lectins can be considered as potential therapeutic agents in the development of new therapeutic strategies for various cancers and inflammatory diseases because of their anti-inflammatory and immunomodulatory effects (Lull, Wichers & Savelkoul, 2005; Muszyńska, Grzywacz-Kisielewska, Kała & Gdula-Argasińska, 2018). Many mushroom lectins have been reported to date. Lectins from higher fungi have been reviewed by Guillot and Konska (1997) and Wang, Ng, and Ooi (1998). Singh et al. (2010) published a comprehensive review of 336 mushroom lectins. A complete list of lectins identified in mushrooms and their carbohydrate and/or glycoprotein specificity was provided by Hassan et al. (2015).

Pleurotus species are edible mushrooms with important economic and medicinal value (Khan & Tania, 2012). Studies have reported that *Pleurotus* species have antitumor, antioxidant, antiviral, antibacterial, hypocholesterolemic, hypoglycaemic, immunomodulatory, and anti-HIV-1 reverse transcriptase effects and reduce blood pressure and blood lipid levels (Li, Liu, Wang & Ng, 2008; Patel, Naraian & Singh, 2012; Anjana & Savita, 2017). In addition, their antiviral activities against severe acute respiratory syndrome coronavirus 2 (SARS-CoV-2) have been recently investigated (Elhusseiny et al., 2022).

Pleurotus eryngii (DC. ex Fr.) Quel. var. *ferulae* Lanzi (PEF) is an edible mushroom of the family Pleurotaceae and the order Agaricales (Jo et al., 2019). PEF is frequently consumed and distributed in the Eastern Anatolia Region of Turkey (Akyüz & Kırbağ, 2007). PEF extracts have been reported to have antioxidant (Hu, Lien, Hsieh, Wang, & Chang, 2009), antiatherosclerotic (Mori, Kobayashi, Tomita, Inatomi & Ikeda, 2008; Choi, Kim, Kim & Kim, 2017), antitumor, and immunostimulatory (Choi, Cha, Kang & Lee, 2004; Yuan et al., 2017a; Sun, Hu & Li, 2017) effects.

New sources should be explored to isolate novel lectins with potential therapeutic properties. The aim of this study was to elucidate the anti-inflammatory activity of lectin purified to homogeneity from PEF mushroom.

MATERIALS AND METHODS

Materials and Chemicals

A glass column (Pharmacia Fine Chemicals, Upsala, Sweden), diethylaminoethyl (DEAE)-Sepharose ion exchange resin (DCL6B100, Sigma-Aldrich, St. Louis, MO, USA), and Sephadex G-100 (17-0061-01, Pharmacia) were used during the purification processes. RAW 264.7 mouse macrophage cells (ATCC TIB-71) were obtained from the American Type Culture Collection. Dulbecco's Modified Eagle Medium (DMEM) (319-005 CL, Wisent, Montreal, QC, Canada), penicillin-streptomycin (450-201-EL, Wisent, Montreal, QC, Canada) and fetal bovine serum (FBS) (FBS-11A, Capricorn, Ebsdorfergrund, Germany) were used for cell culture. All ELISA kits were obtained from Thermo-Invitrogen (Carlsbad, CA, USA). Anti-iNOS (ab15323, Abcam Cambridge, MA, USA), anti-COX-2 (NB100-689SS, Novus Bio, Littleton, CO, USA), anti-beta-actin (MO1263, BOSTER, Beijing, China), anti-rabbit IgG H&L (HRP) (ab205718, Abcam Cambridge, MA, USA), anti-mouse IgG (HRP) (sc-2005, Santa Cruz, CA, USA) antibodies and protein ladder (LC5615, Thermo-Invitrogen, Carlsbad, CA, USA) were used for western blot analysis. Lipopolysaccharide (LPS) (L2654), bicinchoninic acid (BCA) kit (BCA1), and phenazine methosulfate (PMS) (P9625) were obtained from Sigma (St. Louis, MO, USA), and 3-(4,5-dimethylthiazol-2-yl)-5-(3-carboxymethoxyphenyl)-2-(4-sulfophenyl)-2H-tetrazolium (MTS) (G1112) was obtained from Promega (Madison, WI, USA).

Mushroom material

PEF mushrooms were collected and dried by Dr. Hevidar Alp at Munzur University, Tunceli Province, Turkey, in April-May-June 2020. The identification of the species was performed by Prof. Dr. Abdulnasır Yıldız from Dicle University, Faculty of Science, Department of Biology, Turkey.

Purification of lectin from *Pleurotus eryngii* var. *ferulae* (PEFL)

30 g of dried PEF were crushed with a blender until it became a powder, and then incubated overnight with 500 mL PBS (phosphate-buffered saline), pH 7.4, in a refrigerator. The supernatant was collected by centrifugation at 10,000 rpm for 20 min in a refrigerated centrifuge to obtain the crude extract. Proteins in the crude extract were precipitated by the addition of $(NH_4)_2SO_4$ to 80% saturation. The precipitate, which was obtained by centrifugation at 10,000 rpm for 20 min at 4°C, was dissolved in PBS. After centrifugation at 10,000 rpm for 10 min to remove unabsorbed materials, the supernatant was named the 80% NH_4SO_4 fraction and dialysed against the same buffer, and then applied to a DEAE-Sepharose-4B (1x15 cm) pre-equilibrated with 6 mM PBS. The column was eluted with

a linear gradient from 25 to 1000 mM NaCl in PBS. The fractions were collected in 1 mL volumes at a flow rate of 30 mL/h. The fraction showing haemagglutinating activity was concentrated by ultrafiltration through a Millipore CX-10 membrane with a stirred cell (model; Amicon, Inc., Beverly, Mass.) and dialysed against PBS. The concentrated and dialysed fraction was then applied to a Sephadex G-100 column, which had previously been equilibrated with 6 mM PBS and eluted with the same buffer at a flow rate of 30 mL/h. The elutes were collected in 1 mL fractions, assayed at 280 nm for protein content, and tested for haemagglutinating activity. The fraction with the highest haemagglutinating activity was concentrated and stored at -20°C for analysis.

Determination of the protein concentration

Protein concentration was determined by measuring at 280 nm and using the BCA kit. The BCA method was performed by optimising the kit protocol recommended by the manufacturer using bovine serum albumin as a standard.

Evaluation of the stability of the haemolysin activity in crude mushroom extract

To inhibit the haemolytic activity of haemolysin found in PEF, which causes the haemolysis of erythrocytes and prevents the interpretation of haemagglutination activity tests, 1 mL of crude extract was heated at 37°C and 50°C for 30 min, and the haemolytic activity was examined. In addition, serial dilutions of 50 mM Na_2CO_3, Na_3PO_4, $FeCl_2$, and $CuCl_2$ salt solutions were added to equal volumes of the crude extract in separate experiments to examine the effect of some salts on the haemolytic activity of PEF haemolysin.

Measurement of PEFL haemagglutinating activity

The test was performed by making serial 2-fold dilutions of PEFL solution in 0.9% NaCl solution using U-bottom microplates. To each well 25 µL of 4% human (A Rh+ blood group) erythrocyte suspension was added, and after incubation at room temperature for 30 min, haemagglutination was determined both visually and microscopically. Haemagglutination titre was expressed as the reciprocal of the dilution exhibiting detectable agglutination, according to Lis & Sharon (1972). The results were expressed as a haemagglutinating unit (HU), which is the minimum amount of sample capable of inducing agglutination. Specific activity was defined as the number of haemagglutinating units per mg of protein (HU/mg).

Haemagglutination inhibition test: determination of the specific carbohydrate unit of lectin

To investigate the inhibition of lectin-induced haemagglutination by several carbohydrates and one glycoprotein (ovalbumin) at different concentrations, the haemagglutinating inhibition test was performed in a manner similar to the haemagglutination test. Serial 2-fold dilutions of sugar samples were prepared in PBS and mixed with an equal volume (25 µL) of a PEFL solution containing four haemagglutination units. The mixture was incubated for 30 min at room temperature and then mixed with 25 µL of a 4% erythrocyte suspension.

Sodium dodecyl sulphate-polyacrylamide gel electrophoresis (SDS-PAGE)

The purity and molecular mass of the protein were determined by SDS-PAGE according to the Laemmli method (Laemmli, 1970) and visualised by 0.2% Coomassie blue R-250 staining. The molecular weight was determined by comparing the electrophoretic mobility of lectin with that of marker proteins from Invitrogen (LC5615).

Cell culture

RAW 264.7 cells (ATCC TIB-71) were cultured in DMEM supplemented with 10% FBS, 100 U/mL penicillin and 100 µg/mL streptomycin, followed by incubation under a humidified environment containing 5% CO_2 at 37°C. For enzyme-linked immunosorbent assay (ELISA) and western blot analysis, $3x10^6$ cells suspension was cultured in 100-mm Petri dishes and incubated for 24 h at 37°C and 5% CO_2. After incubation, cells were treated with different concentrations (100, 50, 25, 12.5, and 6.25 µg/mL) of PEFL and then stimulated with LPS (1 µg/mL) (Yoon et al., 2009) for 24 h. To determine the effect of LPS, one group of cells was treated with LPS only; as a negative control, non-treated cells with any LPS or lectin were used. All Petri dishes were incubated for a further 24 h in a 5% CO_2 incubator at 37°C. After incubation for 24 h, the cells were harvested and separated into two groups to be evaluated for cytokine production and western blot analysis.

Cytotoxic activity of PEFL in macrophages

RAW 264.7 cells ($2x10^4$) were seeded into 96-well plates and incubated overnight. The next day, PEFL was added to the wells at different concentrations (100, 50, 25, 12.5, and 6.25 µg/mL) and incubated for a further 24 h. After incubation, cell viability was assessed using the MTS assay according to the manufacturer's instructions. Briefly, 20 µL of MTS/PMS mixture was added and incubated for 2-4 h at 37°C. The absorbance was then read on the microplate reader device (Eon Biotek, Winooski, VT, USA) at 490 nm. Cell growth inhibition percentages were

calculated as Cell growth inhibition (%) = [1-(Absorbance of sample/Absorbance of control)]x100

Enzyme-linked immunosorbent assay (ELISA)

The harvested cells were sonicated by ultrasonic homogenizer (Art-MICCRA D-1, Heitersheim, Deutschland) with a 10-15 second interval, then centrifuged at 10,000 g for 5 min in a refrigerated centrifuge, and the supernatants were collected. Commercial ELISA kits were used for tumour necrosis factor-alpha (TNF-α), prostaglandin-E2 (PG-E2), interferon-gamma (IFN-γ), interleukin-1-beta (IL-1β), interleukin-6 (IL-6), and interleukin-10 (IL-10) levels determination, and the test was performed according to the manufacturer's instructions.

Western blot analysis

The harvested cells were washed with cold PBS and lysed in radioimmunoprecipitation assay buffer (50 mM Tris-HCl, pH 8.0, 150 mM NaCl, 1% Nonidet P-40, 0.5% sodium deoxycholate and 0.1% SDS). The samples were centrifuged at 24,000 g for 45 min in a refrigerated centrifuge at 4°C, and the supernatants were used to determine cyclooxygenase-2 (COX-2) and nitric oxide synthase (iNOS) protein levels by western blot analysis. For western blot analysis, an equal amount of cellular protein (20 µg/mL) was separated by SDS-PAGE. The separated proteins were transferred to a polyvinylidene difluoride membrane using the Trans-Blot Turbo™ transfer system (Bio-Rad, Hercules, CA, USA). The membrane was then blocked with 5% non-fat milk blocking buffer and consecutively incubated with primary antibodies [iNOS (1:500), COX-2 (1:20000), and beta-actin (1:10000)] and HRP-conjugated secondary antibodies [anti-mouse (1:10000) and anti-rabbit (1:20000)]. In the last step, the membrane was incubated with a chemiluminescent substrate for 5 min and visualised by the imaging system (Vilber Lourmat, Fusion FX5, Marne-la-Vallée, France).

Statistical analysis

The data are presented as mean ± standard deviation. GraphPad Prism 9 (GraphPad Software, La Jolla, CA, USA) and SPSS 20.0 (SPSS Inc, Chicago, IL, USA) were used to evaluate the differences between the tested items. A p-value of <0.05 was set as the limit of significance.

RESULTS

Purification of lectin from *Pleurotus eryngii* var. *ferulae* (PEFL)

Elution of the PEFL active 80% ammonium sulphate fraction through a DEAE-Sepharose-4B column with a stepwise NaCl gradient resulted in the appearance of four protein peaks, with one peak showing haemagglutinating activity (eluted with PBS containing 0.2 M NaCl) (Figure 1). The peak with haemagglutinating activity was further purified by gel filtration chromatography on Sephadex G-100. The chromatogram showed one peak with haemagglutinating activity, as shown in Figure 2.

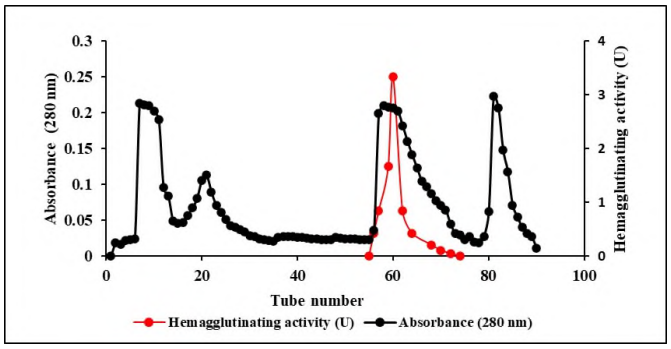

Figure 1. DEAE-Sepharose-4B ion exchange chromatography elution profile of the 80% ammonium sulfate fraction of PEF crude extract.
Column: 15 x 1 cm, sample volume: 12 mL (28.8 mg protein), flow rate: 1 mL/min, the lectin was eluted with a linear gradient of 0.25-1 M NaCl in 6 mM PBS buffer.

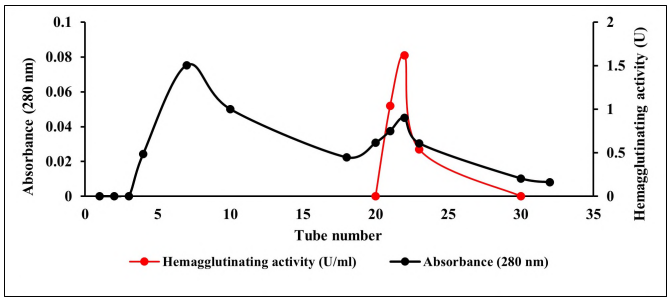

Figure 2. Elution profile of the elute obtained by DEAE-Sepharose-4B on the Sephadex G-100 column.
Column dimensions: 10 x 1 cm, sample volume 1.6 mL (5.4 mg protein), flow rate: 1 mL/min. Buffer used: 6 mM PBS.

PEFL was purified approximately 16-fold over the crude extract. The specific activity of the purified lectin was 1280 HU/mg. The results of the purification of PEFL are summarised in Table 1.

It examined the stability of the haemolysin activity in the crude mushroom extract. It was found that the haemolytic activity of the haemolysin was not inhibited by heating the crude extract at 30°C and 50°C for 30 min. Furthermore, it was observed that among all the salts examined, only Na_3PO_4 inhibited the haemolytic activity of the lectin at a concentration of 25 mM, but the haemolytic activity recovered after 30 min. The haemagglutinating activity of the lectin was determined within 30 min.

Among the glycoproteins and various carbohydrates tested, D-galactose was the only carbohydrate that could inhibit the haemagglutinating activity of PEFL (Table 2).

Table 1. Purification of PEFL (30 g powder).

Step	Volume (mL)	Protein (mg/mL)	Total protein (mg)	Haemagglutinating activity (HU)	Specific activity (HU/mg)	Purification fold
Crude extract	400	3.5	1400	112000	80	1
80% $(NH_4)_2SO_4$	12	2.4	28.8	4608.1	160	2
DEAE-Sepharose-4B	3.4	1.6	5.4	3481.2	644	8
Sephadex G-100	2	1	2	2560	1280	16

Table 2. Haemagglutination inhibition test of PEFL by various sugars and one glycoprotein (initial haemagglutinating activity is 4 haemagglutinating units).

Carbohydrate/glycoprotein	Concentration (mM)							
	100	50	25	12.5	6.25	3.12	1.56	0.78
D- Lactose	+	+	+	+	+	+	+	+
D- Glucosamine hydrochloride	+	+	+	+	+	+	+	+
Methyl-α-D-mannopyranoside	+	+	+	+	+	+	+	+
D- Fucose	+	+	+	+	+	+	+	+
D- Mannose	+	+	+	+	+	+	+	+
N-Acetyl-D-galacosamine	+	+	+	+	+	+	+	+
N-Acetyl-D-galactosamine	+	+	+	+	+	+	+	+
4-Nitrophenyl-β-D-glucopyranoside	+	+	+	+	+	+	+	+
4-Nitrophenyl-α-D-glucopyranoside	+	+	+	+	+	+	+	+
D- Raffinose	+	+	+	+	+	+	+	+
Ovalbumin	+	+	+	+	+	+	+	+
Maltose	+	+	+	+	+	+	+	+
D- Galactose	-	-	-	-	-	-	-	-

+: haemagglutinating activity; –: no haemagglutinating activity.

PEFL showed a single band with a molecular weight of 46 kDa determined by SDS–PAGE under denaturing conditions (Figure 3).

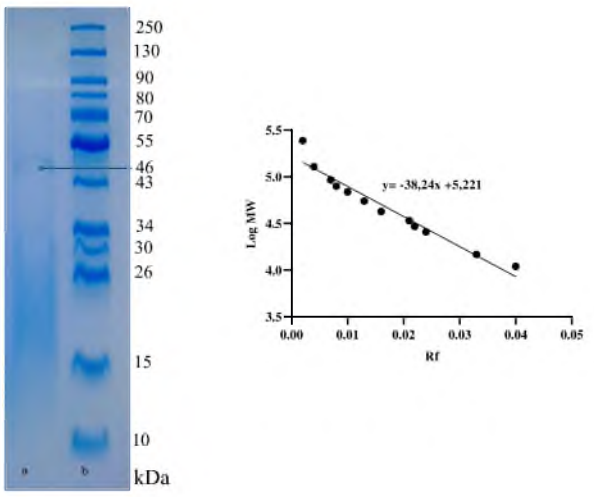

Figure 3. Molecular weight determination based on SDS-PAGE.
The monomeric subunit molecular weight of the lectin was calculated from the calibration curve and estimated to be 46 kDa as a single monomeric subunit using 10% SDS-PAGE (Coomassie blue stained). a) Sephadex G-100 chromatography output. b) Protein molecular mass ladder.

Cytotoxic activity of PEFL

To evaluate the cytotoxic effects of PEFL on macrophage cells, we examined macrophage cell growth inhibition in the presence of different concentrations of PEFL using the MTS assay. As shown in Figure 4, PEFL showed low cytotoxic activity at 100, 50, and 25 µg/mL and high cytotoxic activity at 200 µg/mL concentration. The remaining concentrations were non-toxic against macrophage cells.

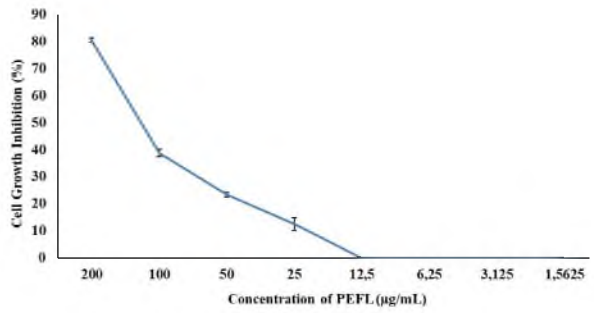

Figure 4. Effect of PEFL on cell growth inhibition in RAW 264.7 cells.
Data were expressed as mean ± standard deviation (n=3). Values represent cell growth inhibition (% inhibition) resulting from 24 h incubation with PEFL.

Anti-inflammatory effects of PEFL

Effect of PEFL on cytokine profile

The anti-inflammatory effects of PEFL were tested on lipopolysaccharide (LPS)-induced inflammation in RAW 264.7 macrophages. In the LPS-treated group, prostaglandin-E2 (PG-E2) and cytokine levels were significantly ($p < 0.05$) higher than those in the control group. It was observed a significant reduction in PG-E2, tumour necrosis factor-alpha (TNF-α), interleukin-1-beta (IL-1β), interleukin-6 (IL-6), and interferon-gamma (IFN-γ) levels, as well as a significant increase in interleukin-10 (IL-10) levels in the LPS+PEFL treated groups ($p < 0.05$), compared with the only LPS treated group (Figure 5). No inhibitory effects were detected at concentrations of 12.5 and 6.25 µg/mL.

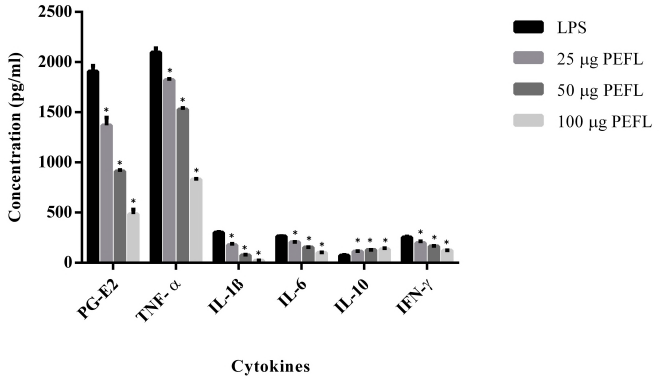

Figure 5. Cytokines levels in the supernatants of cell groups (Mean ± standard deviation). * p<0.05

Western blot analysis

In western blot analysis, nitric oxide synthase (iNOS) and cyclooxygenase-2 (COX-2) were markedly expressed in the LPS-treated groups, whereas in the LPS+PEFL-treated groups, PEFL significantly inhibited the expression of these proteins in a concentration-dependent manner. iNOS protein expression was 100% inhibited by the application of PEFL at concentrations of 100 µg/mL and 50 µg/mL. Furthermore, inhibition of 61.81% was observed even at the lowest concentration (6.25 µg/mL). Considering the COX-2 protein level, it was determined that COX-2 protein expression decreased by 69.4% and 5.94% after the application of PEFL at concentrations of 100 µg/mL and 25 µg/mL, respectively (Figure 6).

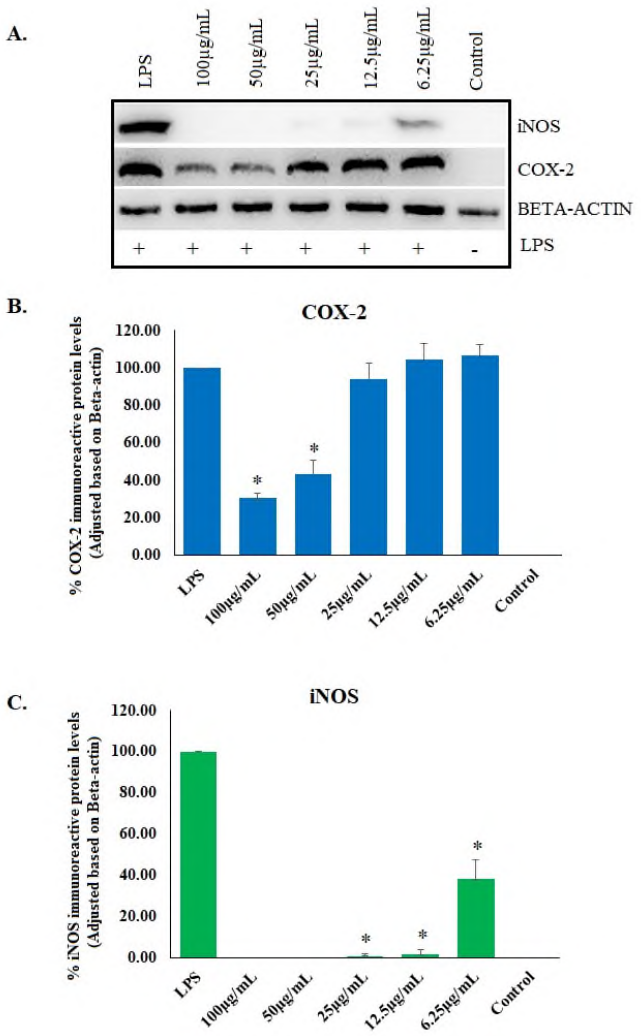

Figure 6. The effects of PEFL on iNOS and COX-2 protein expressions in LPS-induced RAW 264.7 cells.
A: The effects of different doses of PEFL on iNOS and COX-2 protein expressions in a model of LPS-induced inflammation (LPS 1 µg/mL).
B: Effect of PEFL on COX-2 protein expression in a model of LPS-induced inflammation. * p<0.05
C: Effect of PEFL on iNOS protein expression in a model of LPS-induced inflammation. * p<0.05

DISCUSSION

There is an increasing interest in lectins because of their unique carbohydrate-binding properties. The ability of lectins to specifically bind to glycoconjugates present on the cell surface has made them essential tools in diverse applications. Taking advantage of this specific interaction, it is possible to design drugs to combat many diseases such as infection, inflammation, and cancer (Coelho et al., 2017). Lectins have been obtained from different sources such as mammalian tissues, viruses, bacteria, insects, plant seeds and roots, and fungi (Hassan et al., 2015). Mushrooms are a rich source of lectins (Singh et al., 2010). It is well established that many mushroom-

extracted compounds are commonly used as immunomodulators or biological response modifiers (Zaidman, Yassin, Mahajna & Wasser, 2005).

The present study was based on the findings of Yuan et al. (2017b), in which four different protein fractions (DE1, DE2, DE3, and DE4) were obtained from *Pleurotus eryngii* and a protein (named PEP) with anti-inflammatory properties was isolated from the DE3 fraction. These results suggest that one of these four fractions may be lectin. In view of the importance of lectins, the present investigation was undertaken to purify a lectin from *Pleurotus eryngii* var. *ferulae* (PEFL) using a three-step procedure of $(NH_4)_2SO_4$ precipitation, ion exchange chromatography on DEAE-Sepharose-4B, followed by gel filtration chromatography on a Sephadex G-100 column. In addition, our results were in agreement with the work of Xu et al. (2014), who isolated and purified a D-galactose-specific lectin with strong proliferative and haemagglutination activity against mouse splenocytes from *P. ferulae* extract by applying 75% (NH4)2SO4 precipitation, DEAE-cellulose ion exchange, and Sepharose-6B affinity chromatography. A novel lectin with potent antitumor, mitogenic, and HIV-1 reverse transcriptase inhibitory activities from fresh fruiting bodies of the edible mushroom *P. citrinopileatus* (Li et al., 2008) and an N-acetylglucosamine-specific lectin from fresh sclerotia of the edible mushroom *P. tuber-regium* (Wang & Ng, 2003) were isolated using similar protocols.

The lectin's haemagglutinating activity underwent a decline because of the presence of haemolysin (Ngai & Ng, 2006; Shibata et al., 2010), which caused haemolysis of erythrocytes and prevented determination of haemagglutinating activity of the lectin. Lectins isolated from *Pleurotus* species have been identified with varying sugar specificities towards melibiose, galactose, lactose, raffinose, (*P. ostreatus*), inulin, maltose, ortho-nitrophenyl-β-D-galactopyranoside, ortho/para-nitrophenyl-β-D-glucopyranoside (*P. citrinopileatus*), N-acetylglucosamine (*P. tuber-regium*), N-acetylgalactosamine (*P. serotinus*), lactose (*P. spodoleucus*), methyl-α-D-galactoside, galactosamine, mannosamine, asialofetuin (PEL) (*P. eous*), and asialo-mucin (*P. cornucopiae*) (Hassan et al., 2015). The D-galactose specificity of the pure lectin obtained in this study was similar to that of lectin isolated from *P. ostreatus*.

The molecular weights of fungal lectins vary between 12 and 68 kDa (Singh et al., 2015). The lectin isolated from the fresh fruit body of *P. ostreatus* was reported to be a heterodimer, with molecular weights of 40 and 41 kDa for each subunit (Wang, Gao & Ng, 2000). The lectins of *P. citrinopileatus* (Li et al., 2008) and *P. tuber-regium* (Wang & Ng, 2003) were reported to be homodimers with a subunit molecular mass of 32 kDa. The molecular weight of the lectin from *P. ferulae* was determined to be 35 kDa and was found to be a homodimer with a subunit molecular mass of 17.5 kDa (Xu et al., 2014). In this study, the monomeric subunit molecular weight of PEFL was estimated to be 46 kDa, which is similar to that of *P. ostreatus* lectin.

Lectins have attracted attention because of their mitogenic, antitumor, antiproliferative, and immunomodulatory activities. Owing to their specificity in binding to surface receptors, certain lectins are potent immunomodulators (Zaidman et al., 2005). It has been reported that lectins have anti-inflammatory effects by decreasing the secretion of pro-inflammatory cytokines through I-kappa-B (IkB)/nuclear factor kappa B (NF-κB) transduction and increasing the production of anti-inflammatory cytokines (Coelho et al., 2017). In addition, it has been reported that they show anti-inflammatory effects by reducing the production of proinflammatory prostaglandins (PG) through the inhibition of cyclooxygenase-2 (COX-2) whose expression is frequently increased in many premalignant tissues and malignant tumours. It has been observed that lectins reduce the secretion of proinflammatory cytokines by suppressing the increased expression of induced nitric oxide synthase (iNOS) during inflammatory processes (Muszyńska et al., 2018).

There are several reports of *Pleurotus* extracts showing anti-inflammatory activities. The methanolic extract of *P. florida* was found to reduce carrageenan-induced and formalin-induced paw acute inflammation in mice (Jose, Ajith & Janardhanan, 2004). Jedinak, Dudhgaonkar, Wu, Simon, & Sliva (2011) reported that *P. ostreatus* concentrate demonstrates its anti-inflammatory effect by inhibiting lipopolysaccharide (LPS)-induced interleukin-6 (IL-6), interleukin-12, prostaglandin-E2 (PG-E2), and nitric oxide (NO) production and modulating the downstream regulation of iNOS and COX-2 expression via the suppression of NF-κB activation in RAW 264.7 cells. Tanaka, Nishimura, Sato, Sato, and Nishihira (2016) found that oyster mushroom extract stimulates macrophages by interferon-gamma (IFN-γ) which results in the activation of the immune system.

Nowadays, the researches are focussed on the isolation and characterisation of the pure active constituents of mushrooms, including mainly polysaccharides (in particular β-D-glucans), polysaccharopeptides (Lull et al., 2005) and proteins like lectins, fungal immunomodulatory proteins, among others (Motta, Gershwin & Selmi, 2021), which demonstrate immunomodulatory activities. An insoluble beta-glucan (pleuran) isolated from *P. ostreatus* was reported to suppress inflammation in a model of acute colitis in rats (Bobek, Nosálová & Cerná, 2001). The extract and polysaccharide isolated from *P. ostreatus* were reported to be effective in stimulating natural killer cells cytotoxic effect with induction of IFN-γ against lung and breast cancer cells, enhanced in the presence of interleukin-2 (El-Deeb et al., 2019). The anti-inflammatory effect of glucan isolated from *P. pulmonaris* was examined by acetic acid-induced writhing reaction in mice, which is a typical model to measure inflammatory pain, and it was observed that the glucan

inhibits leukocyte migration to damaged tissues (Smiderle et al., 2008). Minato, Laan, van Die & Mizuno (2019) reported that the *P. citrinopileatus* polysaccharide can inhibit the secretion of pro-inflammatory cytokines and chemokines in LPS/IFNγ activated macrophages and promote the expression of the anti-inflammatory cytokine interleukin-10.

Some immunomodulator compounds have been isolated from *P. eryngii*. A glycosphingolipid isolated from *P. eryngii* induces the secretion of IFN-γ and interleukin-4 from T cells (Nozaki et al., 2008). Sun et al. (2017) showed that a polypeptide isolated from *P. eryngii* mycelium is a good antioxidant with antitumor and immunostimulatory activities. In another study (Yuan et al., 2017b), a protein (PEP) isolated from P. eryngii showed strong anti-inflammatory effects by inhibiting pro-inflammatory mediators, including NO, interleukin-1-beta, and IL-6, and deactivating NF-κB and mitogen-activated protein kinase pathways. Although there is a possibility that the protein is a lectin, the study has not provided any explanation regarding this anti-inflammatory protein being a lectin. Therefore, there are currently no reports on the anti-inflammatory effectiveness of lectins isolated from *Pleurotus* species. In the present study, a lectin with potent anti-inflammatory activity that may be used as a prospective immunotherapeutic molecule in the treatment of some immunodeficiency diseases was isolated and purified to homogeneity from *P. eryngii* crude extract. Our study was in agreement with other studies showing that edible mushrooms possess anti-inflammatory activity (Muszyńska et al., 2018).

CONCLUSION

It was concluded that PEFL may play a role in the regulation of the inflammatory process by suppressing COX-2 and iNOS expressions and reducing the production of pro-inflammatory cytokines. Moreover, because of its anti-inflammatory and immunomodulatory effects, it can be considered as a potential therapeutic agent in the development of new therapeutic strategies for various cancers and inflammatory diseases. The present study is the first to show that the anti-inflammatory effect of *P. eryngii* is due to its lectin.

Peer-review: Externally peer-reviewed.

Author Contributions: Conception/Design of Study- T.M.H.S., N.O., P.A.S., G.A.U., H.A.K..; Data Acquisition- T.M.H.S., N.O. G.A.U.; Data Analysis/Interpretation- T.M.H.S., N.O., P.A.S., G.A.U.; Drafting Manuscript- T.M.H.S.; Critical Revision of Manuscript- T.M.H.S., N.O., P.A.S., G.A.U., H.A.K.; Final Approval and Accountability- T.M.H.S., N.O., P.A.S., G.A.U., H.A.K.

Conflict of Interest: The authors have no conflict of interest to declare.

Financial Disclosure: This study was funded by the Scientific Research Projects Coordination Unit of Istanbul University. Project number: 37626.

ORCID IDs of the authors

Thoiba Mogahid Hussein Seliman	0000-0002-9193-1833
Gülsüm Altıparmak Ülbegi	0000-0002-2585-1931
Nurten Özsoy	0000-0002-2419-9128
Hevidar Alp Kavlo	0000-0001-9167-5844
Pınar Aksoy Sağırlı	0000-0002-9432-3163

REFERENCES

Akyüz, M. & Kırbağ, S. (2007). Ülkemizde sebze ve meyvelerin yanı sıra alternatif besin kaynağı: yabani mantar (*Pleurotus eryngii* var. *ferulae*). *Artvin Çoruh Üniversitesi Orman Fakültesi Dergisi* 8(1), 26-36. http://ofd.artvin.edu.tr/download/article-file/25715

Anjana, S.H. & Savita, J.A. (2017). Oyster mushroom: answer to human ailments. Asian *Journal of Pharmaceutical and Clinical Research*, 10(4), 24-27. https://doi.org/10.22159/ajpcr.2017.v10i4.16867

Bobek, P., Nosálová, V. & Cerná, S. (2001). Effect of pleuran (beta-glucan from *Pleurotus ostreatus*) in diet or drinking fluid on colitis in rats. Nahrung, 45(5), 360-363. https://doi.org/10.1002/1521-3803(20011001)45:5<360::AID-FOOD360>3.0.CO;2-C

Choi, D. B., Cha, W. S., Kang, S. H. & Lee, B. R. (2004). Effect of *Pleurotus ferulae* extracts on viability of human lung cancer and cervical cancer cell lines. *Biotechnology and Bioprocess Engineering*, 9, 356-361. https://doi.org/10.1007/BF02933057

Choi, J.H., Kim, D.W., Kim, S., & Kim, S.J. (2017). In vitro antioxidant and in vivo hypolipidemic effects of the king oyster culinary-medicinal mushroom, *Pleurotus eryngii* var. *ferulae* DDL01 (Agaricomycetes), in rats with high-fat diet–induced fatty liver and hyperlipidemia. *International Journal of Medicinal Mushrooms*, 19(2), 107-119. https://doi.org/10.1615/IntJMedMushrooms.v19.i2.20

Coelho, L.C.B.B., Silva, P.M.S., Lima, V.L.M., Pontual, E.V., Paiva, P.M.G., Napoleão,T.H. & Correia, M.T.S. (2017). Lectins, interconnecting proteins with biotechnological/pharmacological and therapeutic applications. *Evidence-Based Complementary and Alternative Medicine*, 1594074, 1-22. http://dx.doi.org/10.1155/2017/1594074

Dan, X., Liu, W. & Ng, T.B. (2015). Development and applications of lectins as biological tools in biomedi-

cal research. *Medicinal Research Reviews*, 36(2), 221-247. https://doi.org/10.1002/med.21363

El-Deeb, N.M., El-Adawi, H.I., El-Wahab, A.E.A., Haddad, A.M., El Enshasy, H.A.,He, Y.- W. & Davis, K.R. (2019). Modulation of NKG2D, KIR2DL and cytokine production by *Pleurotus ostreatus* glucan enhances natural killer cell cytotoxicity toward cancer cells. *Frontiers in Cell Developmental Biology*, 7, 165. https://doi.org/10.3389/fcell.2019.00165.

Elhusseiny, S.M., El-Mahdy, T.S., Elleboudy, N.S., Yahia, I.S., Farag, M.M., Ismail, N.S., Yassien, M.A. & Aboshanab, K.M. (2022). In vitro anti SARS-CoV-2 activity and docking analysis of *Pleurotus ostreatus, Lentinula edodes and Agaricus bisporus* edible mushrooms. *Infection and Drug Resistance*, 15, 3459-3475. https://doi.org/10.2147/IDR.S362823

Guillot, J. & Konska, G. (1997). Lectins in higher fungi. *Biochemical Systematics and Ecology*, 25, 203-230. https://doi.org/10.1016/S0305-1978(96)00110-X

Hassan, M.A.A., Rouf, R., Tiralongo, E., May, T.W. & Tiralongo, J. (2015). Mushroom lectins: Specificity, structure and bioactivity relevant to human disease. *International Journal of Molecular Sciences*, 16(4), 7802-7838. https://doi.org/10.3390/ijms16047802

Hu, S.H., Lien, J.L., Hsieh, S.L., Wang, J.C. & Chang, S.J. (2009). Antioxidant and antigenotoxicity activities of extracts from liquid submerged culture of culinary-medicinal ferula oyster mushroom, *Pleurotus eryngii* (DC.) Quel. var. *ferulae* (Lanzi) Sacc. (Agaricomycetideae). *International Journal of Medicinal Mushrooms*, 11(4), 395-408. https://doi.org/10.1615/IntJMedMushr.v11.i4.60

Jedinak, A., Dudhgaonkar, S., Wu, Q.L., Simon, J. & Sliva, D. (2011). Anti-inflammatory activity of edible oyster mushroom is mediated through the inhibition of NF-κB and AP-1 signaling. *Nutrition Journal*, 10, 1-10. https://doi.org/10.1186/1475-2891-10-52

Jo, K.-J., Ghim, J., Kim, J., Lee, H., Lee, T. G., Kim, J.-I., Kim, Y., Byun, J.W., Min, B.S., Son, J.S., Shim, S.G., Cheon, W.J. & Ryu, S.H. (2019). Water extract of *Pleurotus eryngii* var. *ferulae* prevents high-fat diet-induced obesity by inhibiting pancreatic lipase. *Journal of Medicinal Food*, 22(2), 178-185. https://doi.org/10.1089/jmf.2018.4255

Jose, N., Ajith, T.A. & Janardhanan, K.K. (2004). Methanol extract of the oyster mushroom, *Pleurotus florida*, inhibits inflammation and platelet aggregation. *Phytotherapy Research*, 18(1), 43-46. https://doi.org/10.1002/ptr.1355

Khan, M.A. & Tania, M. (2012). Nutritional and medicinal importance of Pleurotus mushroom: An overview. *Food Reviews International*, 28(3), 313-329. https://doi.org/10.1080/87559129.2011.637267

Laemmli, U.K. (1970). Cleavage of structural proteins during the assembly of the head of bacteriophage T4. *Nature*, 227, 680-685. https://doi.org/10.1038/227680a0

Li, Y. R., Liu, Q. H., Wang, H. X. & Ng, T. B. (2008). A novel lectin with potent antitumor, mitogenic and HIV-1 reverse transcriptase inhibitory activities from the edible mushroom *Pleurotus citrinopileatus. Biochimica et Biophysica Acta (BBA)-General Subjects*, 1780(1), 51-57. https://doi.org/10.1016/j.bbagen.2007.09.004

Lis, H. & Sharon, N. (1972). Soybean (*Glycine max*) agglutinin. *Methods in Enzymology*, 28, 360-365. https://doi.org/10.1016/0076-6879(72)28046-6

Lull, C., Wichers, H.J. & Savelkoul, H.F.J. (2005). Antiinflammatory and immunomodulating properties of fungal metabolites. *Mediators of Inflammation*, 2005(2), 63-80. https://doi.org/10.1155/MI.2005.63

Ma, G., Yang, W., Zhao, L., Pei, F., Fang, D. & Hu, Q. (2018). A critical review on the health promoting effects of mushrooms nutraceuticals. *Food Science and Human Wellness*, 7, 125-133. https://doi.org/10.1016/j.fshw.2018.05.002

Minato, K.-i., Laan, L.C., van Die, I. & Mizuno, M. (2019). *Pleurotus citrinopileatus* polysaccharide stimulates anti-inflammatory properties during monocyte-to-macrophage differentiation. *International Journal of Biological Macromolecules*, 122, 705-712. https://doi.org/10.1016/j.ijbiomac.2018.10.157.

Mori, K., Kobayashi, C., Tomita, T., Inatomi, S. & Ikeda, M. (2008). Antiatherosclerotic effect of the edible mushrooms *Pleurotus eryngii* (Eringi), *Grifola frondosa* (Maitake), and *Hypsizygus marmoreus* (Bunashimeji) in apolipoprotein E–deficient mice. *Nutrition Research*, 28(5), 335-342. https://doi.org/10.1016/j.nutres.2008.03.010

Motta, F., Gershwin, M.E. & Selmi, C. (2021). Mushrooms and immunity. *Journal of Autoimmunity*, 117, 102576. https://doi.org/10.1016/j.jaut.2020.102576

Muramoto, K. (2017). Lectins as bioactive proteins in foods and feeds. *Food Science and Technology Research*, 23(4), 487-494. https://doi.org/ 10.3136/fstr.23.487

Muszyńska, B., Grzywacz-Kisielewska, A., Kała, K. & Gdula-Argasińska, J. (2018). Anti-inflammatory properties of edible mushrooms: A review. *Food Chemistry*, 243, 373-381. https://doi.org/10.1016/j.foodchem.2017.09.149

Ngai, P.H. & Ng, T.B. (2006). A hemolysin from the mushroom *Pleurotus eryngii. Applied Microbiology and Biotechnology*, 72, 1185-1191. https://doi.org/10.1007/s00253-006-0406-6

Nozaki, H., Itonori, S., Sugita, M., Nakamura, K., Ohba, K., Suzuki, A. & Kushi, Y. (2008). Mushroom acidic glycosphingolipid induction of cytokine secretion from murine T cells and proliferation of NK1.1 alpha/beta TCR-double positive cells in vitro. *Biochemical and Biophysical Research Communications*, 373, 435-439. https://doi.org/10.1016/j.bbrc.2008.06.047.

Patel, Y., Naraian, R. & Singh, V.K. (2012). Medicinal properties of *Pleurotus* species (oyster mushroom): A review. *World Journal of Fungal and Plant Biology*, 3(1), 1-12. https://doi.org/10.5829/idosi.wjfpb.2012.3.1.303

Santos, A.F.S., da Silva, M.D.C., Napoleão, T.H., Paiva, P.M.G., Correia, S. & Coelho, L.C.B.B. (2014). Lectins: Function, structure, biological properties and potential applications. *Current Topics in Peptide & Protein Research*, 15, 41-62. https://doi.org/10.1016/j.carres.2021.108367

Sharon, N. & Lis, H. (1972). Lectins: cell-agglutinating and sugar-specific proteins. *Science*, 177, 949-958. https://doi.org/10.1126/science.177.4053.949

Sharon, N. & Lis, H. (2004). History of lectins: From hemagglutinins to biological recognition molecules. *Glycobiology*, 14, 53R-62R. https://doi.org/10.1093/glycob/cwh122

Shibata, T., Kudou, M., Hoshi, Y., Kudo, A., Nanashima, N. & Miyairi, K. (2010). Isolation and characterization of a novel two-component hemolysin, erylysin A and B, from an edible mushroom, *Pleurotus eryngii. Toxicon*, 56(8), 1436-1442. https://doi.org/10.1016/j.toxicon.2010.08.010

Singh, R. S., Bhari, R. & Kaur, H. P. (2010). Mushroom lectins: current status and future perspectives. *Critical Reviews in Biotechnology*, 30(2), 99-126. https://doi.org/10.3109/07388550903365048

Singh, S.S., Wang, H., Chan, Y.S., Pan, W., Dan, X., Yin, C.M., Akkouh, O. & Ng, T.B. (2015). Lectins from edible mushrooms. *Molecules*, 20, 446-469. https://doi.org/10.3390/molecules20010446

Smiderle, F.R., Olsen, L.M., Carbonero, E.R., Baggio, C.H., Freitas, C.S., Marcon, R., Santos, A.R.S., Gorin, P.A.J., Iacomini, M.

(2008). Anti-inflammatory and analgesic properties in a rodent model of a (1–>3),(1–>6)-linked beta-glucan isolated from *Pleurotus pulmonarius. European Journal of Pharmacology*, 597(1-3), 86-91. https://doi.org/10.1016/j.ejphar.2008.08.028

Sun, Y., Hu, X., & Li, W. (2017). Antioxidant, antitumor and immunostimulatory activities of the polypeptide from Pleurotus eryngii mycelium. *International Journal of Biological Macromolecules*, 97, 323-330. https://doi.org/10.1016/j.ijbiomac.2017.01.043

Tanaka, A., Nishimura, M., Sato, Y., Sato, H. & Nishihira, J. (2016). Enhancement of the Th1-phenotype immune system by the intake of oyster mushroom (Tamogitake) extract in a double-blind, placebo-controlled study. *Journal of Traditional and Complementary Medicine*, 6, 424-430. https://doi.org/10.1016/j.jtcme.2015.11.004

Wang, H., Ng, T.B. & Ooi, V.E.C. (1998). Lectins from mushrooms. *Mycolocigal Research*, 102 (8), 897-906. https://doi.org/10.1017/S0953756298006200

Wang, H., Gao, J. & Ng, T.B. (2000). A new lectin with highly potent antihepatoma and antisarcoma activities from the oyster mushroom *Pleurotus ostreatus. Biochemical and Biophyical Research Communications*, 275, 810-816. https://doi.org/10.1006/bbrc.2000.3373

Wang, H. & Ng. T.B. (2003). Isolation of a novel N-acetylglucosamine-specific lectin from fresh sclerotia of the edible mushroom *Pleurotus tuber-regium. Protein Expression and Purification*, 29(2), 156-160. https://doi.org/10.1016/S1046-5928(03)00059-7

Xu, C.-J., Wang, Y.-X., Niu, B.-N., Liu, B., Li, Y.-B., Wang, X.-M. & Lu, S.-L. (2014). Isolation and characterization of a novel lectin with mitogenic activity from *Pleurotus ferulae. Pakistan Journal of Pharmaceutical Sciences*, 27 (4), 983-989.

Yoon, S.-B., Lee, Y.- J., Park, S.-K., Kim, H.-C., Bae, H., Kim, H. M., Ko, S.-G., Choi, H.Y., Oh, M.S. & Park, W. (2009). Anti-inflammatory effects of *Scutellaria baicalensis* water extract on LPS-activated RAW 264.7 macrophages. *Journal of Ethnopharmacology*, 125(2), 286-290. https://doi.org/10.1016/j.jep.2009.06.027

Yuan, B., Ma, Ning, Zhao, L., Zhao, E., Gao, Z., Wang, W., Song, M., Zhang, G., Hu, Q. & Xiao, H. (2017a). In vitro and in vivo inhibitory effects of a *Pleurotus eryngii* protein on colon cancer cells. *Food and Function*, 8, 3553-3562. https://doi.org/10.1039/c7fo00895c

Yuan, B., Zhao, L., Rakariyatham, K., Han, Y., Gao, Z., Kimatu, B.M., Hu, Q. & Xiao, H. (2017b). Isolation of a novel bioactive protein from an edible mushroom *Pleurotus eryngii* and its inflammatory potential. *Food and Function*, 8, 2175-2183. http://dx.doi.org/10.1039/c7fo00244k

Zaidman, B.-Z., Yassin, M., Mahajna, J. & Wasser, S.P. (2005). Medicinal mushroom modulators of molecular targets as cancer therapeutics. *Applied Microbiology and Biotechnology*, 67, 453-468. http://dx.doi.org/10.1007/s00253-004-1787-z

How cite this article

Seliman, T.M.H., Altıparmak Ülbegi, G.., Özsoy, N., Alp Kavlo, H., Aksoy Sağırlı, P. (2024). Anti-inflammatory activity of a novel lectin isolated from *Pleurotus eryngii* var. *ferulae* mushroom. *İstanbul Journal of Pharmacy, 54*(2), 195–204. DOI: 10.26650/IstanbulJPharm.2024.1322171

İstanbul Journal of Pharmacy
Istanbul J Pharm2024, 54 (2): 205–214
DOI: 10.26650/IstanbulJPharm.2024.1399961

Original Article

In silico analysis to predict the carcinogenicity and mutagenicity of a group of triazole fungicides

Mine Çağlayan[1]

[1]Biruni University, Faculty of Pharmacy, Pharmaceutical Toxicology Department, İstanbul, Türkiye

ABSTRACT

Background and Aims: Fungicides, particularly triazoles, are of global concern for pesticide contamination because of their widespread use. This study focuses on estimating the carcinogenicity and mutagenicity of 15 commonly used triazole fungicides.

Methods: *In silico* prediction tools such as ProTox-II, Toxtree, Lazar, and VEGA were used to predict mutagenicity and carcinogenicity.

Results: All compounds were predicted to be "non-mutagenic" by ProTox-II, Toxtree, and Lazar. However, the CONSENSUS of VEGA identified epoxiconazole and prothioconazole as "mutagenic." Regarding carcinogenicity predictions, ProTox-II indicated non-carcinogenicity for all compounds, whereas Toxtree and VEGA (ISS) raised structural alerts for 10 compounds. In addition, Lazar predicted carcinogenicity for tebuconazole, paclobutrazol, and penconazole. It is worth noting that the results exhibit variable reliability, emphasising the need for further investigation and validation.

Conclusion: *In silico* tools proved valuable for predicting the toxicity of triazole fungicides, emphasising the need for additional data. Although the study categorises compounds as non-mutagenic, some exhibit structural alerts for potential carcinogenicity. This strategic approach contributes to pesticide risk assessment by highlighting the role of computational models in advancing our understanding of the health impacts associated with pesticide exposure.

Keywords: Carcinogenicity, genotoxicity, *in silico*, mutagenicity, triazole fungicides

INTRODUCTION

Pesticide contamination in the environment and food is a major issue in global agriculture (Li et al., 2022). Fungicides, particularly azoles (triazoles, imidazoles), are widely used worldwide for pesticide control and to enhance agricultural productivity. Azoles, such as triazoles, are the most commonly used antifungals because of their broad-spectrum activity and high efficiency (Rjiba-Touati et al., 2022a). Numerous conazoles, a category of fungicides, are used in the management of fungal infections and the prevention of fungal proliferation in diverse crops. This leads to their introduction into the ecosystem, with the potential for accumulation in living organisms (Perdichizzi et al., 2014). Triazole fungicides, which are pivotal in hindering fungal ergosterol biosynthesis, play a crucial economic role in crops (Filipov & Lawrence, 2001). The prevalent use of triazole pesticides has generated concerns regarding environmental contamination and food safety (Li et al., 2022).

Alterations in agricultural methodologies and the adoption of intensive farming practices have notably elevated the use of pesticides (Camilo-Cotrim et al., 2022). In 2019, it was estimated that 2 million tonnes of pesticides were used globally annually (Sharma et al., 2019).

Because of the capacity of triazole compounds to impede oestrogen/androgen biosynthesis, extended exposure is under suspicion for potentially inducing diverse disorders in both humans and animals (Hamdi et al., 2022). Studies underscore the diverse cytotoxic and genotoxic impacts of these fungicides across different biological systems, emphasising the importance of understanding their potential risks in various environmental and health contexts (Ben Othmène et al., 2020; Hamdi et al., 2022; Macar, 2021; Rjiba-Touati et al., 2022a; Rjiba-Touati et al., 2022b). Kahle et al. (2008) showed that commonly used azole fungicides are widely available and are continuously released into the aquatic environment. Furthermore, higher octanol-water partition coefficients for propiconazole and tebuconazole (log Kow 3.7) indicate the bioaccumulation potential of these substances (Kahle et al., 2008). In addition, triazole fungicides can accumulate in aquatic organisms, leading to toxic effects on reproduction and embryonic development (Wang et al., 2023).

Corresponding Author: Mine Çağlayan **E-mail:** mcaglayan@biruni.ed.tr
Submitted: 04.12.2023 • **Revision Requested:** 21.12.2023 • **Last Revision Received:** 18.01.2024 • **Accepted:** 18.01.2024

Despite widespread use, toxicity assessments for most triazole fungicides are limited to legal regulations, and comprehensive data evaluating their biological effects are lacking. Data addressing potential adverse effects during development are even more limited (Filipov & Lawrence, 2001).

The rise in hazardous chemical release raises concerns about its impact on living organisms and ecosystems. Genotoxic and mutagenic effects, causing genetic damage and affecting future generations, are particularly worrisome. Consequently, genotoxicity and mutagenicity analyses are needed to ensure environmental quality (Leme & Marin-Morales, 2009).

In the computational domain, there are models that predict bacterial mutagenicity, which serve as an indirect indication of whether a construct acts as an electrophile or has the potential to transform into an electrophile (Benigni & Bossa, 2011). These models effectively anticipate the mutagenic potential of a structure, and their utilisation has gained acceptance as a substitute for the Ames test in assessing mutagenicity. The U.S. The Food and Drug Administration (FDA) Centre has introduced rodent carcinogenicity (Quantitative) Structure-Activity Relationship ((Q)SAR) models through the VEGA Hub, designed to predict the carcinogenic potential of chemicals in rodents (Tice et al., 2021).

This study aims to prioritise 15 triazole fungicides (Figure 1) based on *in silico* predictions, providing a foundation for future investigations. Given the increasing release of hazardous chemicals into the environment, understanding their potential genotoxic and mutagenic effects is crucial. This study explores computational models for predicting bacterial mutagenicity, offering insights into the potential carcinogenicity of these compounds.

MATERIALS AND METHODS

Chemical structures of the fungicides

The molecular structures of bromuconazole, diniconazole, epoxiconazole, fenbuconazole, flutriafol, hexaconazole, enilconazole/imazalil, metconazole, myclobutanil, paclobutrazol, penconazole, prothioconazole, tebuconazole, triticonazole, and uniconazole were inserted to run the analysis using the Simplified Molecular Input Line Entry Specification (SMILES) system, according to the PubChem canonical SMILES in (Table 1).

In silico predictions

Mutagenicity and Carcinogenicity

Mutagenicity is an important toxicological endpoint for chemical risk assessment. Structural alert (SA) refers to the molecular structure associated with adverse outcomes or toxicological endpoints. In the context of mutagenicity, SA includes molecular functions or substructures linked to the mutagenic activity of chemical compounds. Mutagenicity tests include in vitro tests such as the Ames test, primarily using bacterial and mammalian systems such as *Salmonella typhimurium*. For mutagenicity in this study, ProTox-II, Toxtree version 2.6.13, Lazar version 1.4.2, and VEGA version 1.2.3 mutagenicity (Ames) models (CEASAR, ISS, SarPy-IRFMN, and CONSENSUS) were used for prediction analyses. The ProTox-II web server includes molecular similarity and machine learning models for various toxicity endpoints. The prediction scheme of ProTox-II is classified according to different toxicity levels such as toxicological endpoints (such as mutagenicity, carcino-toxicity). Toxtree predicts various toxic hazards using structured rules that can predict toxic hazards by applying a decision tree approach. A decision tree for carcinogenicity and mutagenicity prediction by discriminant analysis and structural rules based on in vitro mutagenicity (Ames test) alerts by the ISS, published in the Benigni 2008 document. Vega is a prediction model covering human toxicity predictions, including mutagenicity and carcinogenicity models. Within the VEGA platform, the CAESAR and Benigni/Bossa computer models are implemented for mutagenicity and carcinogenicity (Benigni & Bossa, 2006; Benigni & Bossa, 2008; Mombelli & Devillers, 2010). Lazar predicts toxicological endpoints such as mutagenicity and mouse, rat, and rodent carcinogenicity. Lazar uses the random forest algorithm in R's Caret package to build local QSAR models. In all applications, canonical SMILES representations of the compounds are used as input. Toxtree indicates SA, whereas ProTox-II and VEGA models determine mutagenicity as positive/negative. The CONSENSUS approach categorises compounds as "possibly mutagenic" or "non-mutagenic" (Bhat and Chatterjee, 2021).

During the process of loading the chemical structures in SMILES format into the programmes we used in our study, the structures in each programme were carefully examined separately. No inconsistencies were detected in this study. To validate our approach, we entered and validated the canonical SMILES codes of the fungicides in Table 1 into the programmes. This validation process increases the reliability of our findings and demonstrates the accuracy of our study.

Carcinogenicity

Carcinogenicity, the potential to cause cancer, can result from genotoxic or non-genotoxic pathways. In this study, carcinogenicity predictions were made using the ProTox-II web server, Toxtree version 2.6.13, Lazar version 1.4.2, and VEGA version 1.2.3 carcinogenicity models (CAESAR and ISS). While ProTox-II and Lazar predict whether a compound is carcinogenic, CAESAR provides additional information. Toxtree has a decision tree for predicting carcinogenicity through discriminant analysis and structural rules based on those published in Benigni 2013.

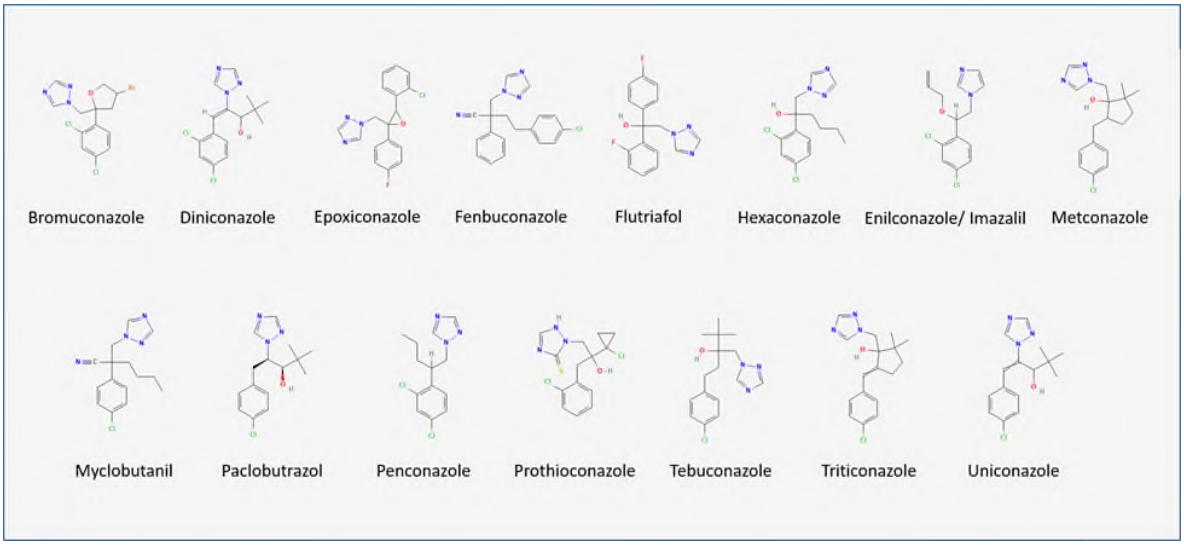

Figure 1. Chemical structures of a group of triazole fungicides.

Table 1. Chemical structures of a group of triazole fungicides.

Chemical Name	CAS number	Log Kow[1]	Molecular weight (g/mol)	Canonical SMILES
Bromuconazole	116255-48-2	3.24	377.1	(C3NCN(CC1(CC(CO1)BR)C2CCC(CC2CL)CL)N3
Diniconazole	83657-24-3	-	326.2	CC(C)(C)C(C(=CC1=C(C=C(C=C1)Cl)Cl)N2C=NC=N2)O
Epoxiconazole	106325-08-0	-	329.8	C1=CC=C(C(=C1)C2C(O2)(CN3C=NC=N3)C4=CC=C(C=C4)F)Cl
Fenbuconazole	114369-43-6	-	336.8	C1=CC=C(C=C1)C(CCC2=CC=C(C=C2)Cl)(CN3C=NC=N3)C#N
Flutriafol	76674-21-0	-	301.29	C1=CC=C(C(=C1)C(CN2C=NC=N2)(C3=CC=C(C=C3)F)O)F
Hexaconazole	79983-71-4	-	314.2	CCCCC(CN1C=NC=N1)(C2=C(C=C(C=C2)Cl)Cl)O
Enilconazole/imazalil	35554-44-0	3.82 (pH 9.2 buffer)	297.2	C=CCOC(CN1C=CN=C1)C2=C(C=C(C=C2)Cl)Cl
Metconazole	125116-23-6	-	319.8	CC1(CCC(C1(CN2C=NC=N2)O)CC3=CC=C(C=C3)Cl)C
Myclobutanil	88671-89-0	2.94	288.77	CCCCC(CN1C=NC=N1)(C#N)C2=CC=C(C=C2)Cl
Paclobutrazol	76738-62-0	-	293.79	C1CC1(C(CC2=CC=CC=C2Cl)(CN3C(=S)N=CN3)O)Cl
Penconazole	66246-88-6	-	284.18	CCCC(CN1C=NC=N1)C2=C(C=C(C=C2)Cl)Cl
Prothioconazole	178928-70-6	4.05 (unbuffered, 20 °C), 4.16 (pH 4), 3.82 (pH 7), 2.00 (pH 9)	344.3	SC1CC1(C(CC2=CC=CC=C2Cl)(CN3C(=S)N=CN3)O)Cl
Tebuconazole	107534-96-3	3.7	307.82	CC(C)(C)C(CCC1=CC=C(C=C1)Cl)(CN2C=NC=N2)O
Triticonazole	131983-72-7	3.29 at 20 °C	317.8	CC1(CCC(=CC2=CC=C(C=C2)Cl)C1(CN3C=NC=N3)O)C
Uniconazole	83657-22-1	-	291.77	CC(C)(C)C(C(=CC1=CC=C(C=C1)Cl)N2C=NC=N2)O

[1] Log Kow: Logarithm of the octanol-water partition coefficient.

Considering the results obtained from VEGA, a value greater than zero was considered consensus for the applicability domain of all models. For the overall assessment, consensus was accepted and the compound was labelled as "probably

carcinogenic" if two or more applications predicted positive carcinogenicity, whereas the compound was labelled as "not carcinogenic" if two or more applications predicted negative carcinogenicity (Bhat, & Chatterjee, 2021).

RESULTS

Mutagenicity

Based on the consensus of results from three prediction tools (ProTox-II, Toxtree, and Lazar), all compounds were classified as “non-mutagenic,” as shown in Tables 2, 3, and 4, respectively. These three prediction tools consistently demonstrated the absence of mutagenic potential in the evaluated compounds. However, in the predictions derived from VEGA, all compounds exhibited different levels of safety, ranging from low to moderate. According to the VEGA CONSENSUS model, consensus mutagenicity scores ranged from 0 to 0.3. Although VEGA detected mutagenicity in 2 (epoxiconazole and prothioconazole) out of 15 compounds (13.3%) according to the CONSENSUS model (Table 5). For epoxiconazole, one of the two compounds detected as mutagenic by VEGA, both the "mutagenic" and "non-mutagenic" consensus scores were equal (50%). This finding is due to the result of the Predicted Consensus Mutagen activity, where the model indicates mutagenicity with the same scores for both the mutagenic and non-mutagenic categories (both scores are 0.15).

Carcinogenicity

ProTox-II assessed all compounds as "non-carcinogenic" with probability values ranging from 0.56 to 0.62 (Table 2). According to SA, Toxtree predicted that all compounds fall into High-Class III. Toxtree and VEGA (ISS model) predicted SA for genotoxic carcinogenicity for 1 (epoxiconazole) out of 15 compounds and non-genotoxic carcinogenicity for 10 out of 15 compounds (66.7%). In 9 of 15 compounds (60%), the most frequently observed SA was predicted to be monohalogenated benzene. Again, n-alkyl carboxylic SA was observed in 26.7% of the compounds. (Table 3). Lazar predicted that fenbuconazole and penconazole are carcinogenic in rats and that paclobutrazol is carcinogenic in mice and rodents, but this model warned that this prediction "may be outside the domain of predictability with a similarity threshold < 0.5" (Table 4).

The VEGA results demonstrated varying levels of reliability, with approximately 26.7% of compounds exhibiting relatively lower reliability and approximately 20% displaying middle levels of reliability. Notably, for 8 out of 15 compounds (53,3%), the caesar result on VEGA indicated that "the predicted compound is outside the applicability domain of the model." The chemical compound under evaluation falls outside the range of compounds for which the model is considered reliable. (Table 5). In the context of predictive models, the applicability domain refers to the specific conditions or characteristics under which a model is expected to provide accurate and reliable predictions. Further investigation and validation, possibly using additional experimental data or domain-specific knowledge, are recommended to assess the reliability of the model’s prediction of carcinogenicity in this particular case.

DISCUSSION

Epidemiological studies consistently associate pesticide exposure with an elevated risk of cancer, as supported by various literature reviews highlighting a positive correlation between pesticide exposure and cancer development (Mostafalou & Abdollahi, 2017; Varghese et al., 2020). The assessment of the risk of specific chemical substances heavily relies on the availability of experimental toxicological data and adequate exposure information. Unfortunately, in numerous instances, such data are either insufficient or entirely unavailable, making a reliable risk assessment nearly unattainable. Over the past decades, (Q)SAR models have emerged as valuable tools for predicting toxic properties (Chen et al., 2022; Kianpour et al., 2021; Wang et al., 2022).

In this study, *in silico* tools were employed to predict the toxicity of several triazole fungicide compounds, with a primary focus on mutagenicity and carcinogenicity, which are considered the most crucial endpoints. According to our toxicity assessment, two compounds (epoxiconazole and prothioconazole) were found to be mutagenic based on VEGA’s *in silico* mutagenicity prediction (CONSENSUS). However, it is noteworthy that other *in silico* tools used in this study, including Toxtree, ProTox-II, and Lazar, classified all assessed compounds, including epoxiconazole and prothioconazole, as non-mutagenic. Additionally, using three *in silico* carcinogenicity prediction models (Toxtree and VEGA (ISS)), 10 compounds—diniconazole, epoxiconazole, fenbuconazolemetconazole, myclobutanil, paclobutrazol, prothioconazole, tebuconazole, triticonazole, and uniconazole—were indicated as potentially carcinogenic.

Holečková et al. (2013) reported that most of the experimental data suggest that the mutagenic properties of the pesticide are questionable. In addition, the genotoxic effects of commercial forms commonly used in agriculture are greater than the genotoxic effects of individual compounds. While conazoles are not considered classical mutagens because they do not give positive results in short-term mutagenicity tests such as Ames (Šiviková et al., 2018), a study has shown that stereoisomers of difenoconazole can cause liver injuries, mutagenicity and skin sensitisation (Gridan et al., 2019). Our study revealed that all compounds were classified as non-mutagenic. However, VEGA detected mutagenicity in two compounds, namely epoxiconazole and prothioconazole.

The results of our carcinogenicity study reflect some findings of previous studies. Epoxiconazole showed cytotoxic effects,

Table 2. ProTox-II mutagenicity and carcinogenicity predictions.

Triazole Fungicides	Octanol/water partition coefficient (logP)	Prediction of Carcinogenicity	Prediction of Mutagenicity	Predicted Toxicity Class	Prediction accuracy
Bromuconazole	3.66	Inactive	Inactive	4	100%
Diniconazole	3.99	Inactive	Inactive	4	100%
Epoxiconazole	3.74	Inactive	Inactive	4	68.07%
Fenbuconazole	4.03	Inactive	Inactive	4	100%
Flutriafol	2.49	Inactive	Inactive	3	100%
Hexaconazole	3.66	Inactive	Inactive	4	100%
Enilconazole/imazalil	4.13	Inactive	Inactive	3	100%
Metconazole	3.34	Inactive	Inactive	4	100%
Myclobutanil	3.58	Inactive	Inactive	4	100%
Paclobutrazol	3.12	Inactive	Inactive	4	100%
Penconazole	4.17	Inactive	Inactive	5	100%
Prothioconazole	3.34	Inactive	Inactive	4	100%
Tebuconazole	3.34	Inactive	Inactive	4	100%
Triticonazole	3.57	Inactive	Inactive	4	68.07%
Uniconazole	3.34	Inactive	Inactive	4	100%

Table 3. Toxtree mutagenicity and carcinogenicity predictions.

Trizole Fungicides	Genotoxic carcinogenicity	Non-genotoxic carcinogenicity	Mutagenicity by ISS
Bromuconazole	Negative	Negative	No
Diniconazole	Negative	SA for nongenotoxic carcinogenicity QSA41_nogen.substituted n-alkylcarboxylic acids	No
Epoxiconazole	SA for genotoxic carcinogenicity QSA7_gen. Epoxides and aziridines	SA for nongenotoxic carcinogenicity QSA31a_nogen. Halogenated benzene (Nongenotoxic carcinogens)	No
Fenbuconazole	Negative	SA for nongenotoxic carcinogenicity QSA31a_nogen. Halogenated benzene (Nongenotoxic carcinogens)	No
Flutriafol	Negative	Negative	No
Hexaconazole	Negative	Negative	No
Enilconazole/imazalil	Negative	Negative	No
Metconazole	Negative	SA for nongenotoxic carcinogenicity QSA31a_nogen. Halogenated benzene (Nongenotoxic carcinogens)	No
Myclobutanil	Negative	SA for nongenotoxic carcinogenicity QSA31a_nogen. Halogenated benzene (Nongenotoxic carcinogens)	No
Paclobutrazol	Negative	SA for nongenotoxic carcinogenicity QSA31a_nogen. Halogenated benzene (Nongenotoxic carcinogens) QSA41_nogen.substituted n-alkylcarboxylic acids	No
Penconazole	Negative	Negative	No
Prothioconazole	Negative	SA for nongenotoxic carcinogenicity QSA17_nogen. Thiocarbonyl (Nongenotoxic carcinogens) QSA31a_nogen. Halogenated benzene (Nongenotoxic carcinogens)	No
Tebuconazole	Negative	SA for nongenotoxic carcinogenicity QSA31a_nogen. Halogenated benzene (Nongenotoxic carcinogens) QSA41_nogen.substituted n-alkylcarboxylic acids	No
Triticonazole	Negative	SA for nongenotoxic carcinogenicity QSA31a_nogen. Halogenated benzene (Nongenotoxic carcinogens)	No
Uniconazole	Negative	SA for nongenotoxic carcinogenicity QSA31a_nogen. Halogenated benzene (Nongenotoxic carcinogens) QSA41_nogen.substituted n-alkylcarboxylic acids	No

Table 4. Lazar mutagenicity and carcinogenicity predictions.

Trizaole Fungicides	Carcinogenicity Prediction	Warning for Carcinogenicity	Mutagenicity Predictiton (*Salmonella typhimurium*)	Warning for Mutagenicity
Bromuconazole	(Mouse) Non-carcinogenic	Similarity threshold 0.2 < 0.5, prediction may be out of applicability domain.	Non-mutagenic	Similarity threshold 0.2 < 0.5, prediction may be out of applicability domain.
Diniconazole Flutriafol	(Mouse, rat) Cannot create prediction	Only one similar compound for threshold 0.2 in the training set (Threshold: 0.2).	Non-mutagenic	Similarity threshold 0.2 < 0.5, prediction may be out of applicability domain.
Epoxiconazole	(Mouse) Non-carcinogenic	Similarity threshold 0.2 < 0.5, prediction may be out of applicability domain.	Non-mutagenic	Similarity threshold 0.2 < 0.5, prediction may be out of applicability domain.
Fenbuconazole	(Mouse) Non-carcinogenic (Rat) Carcinogenic	Similarity threshold 0.2 < 0.5, prediction may be out of applicability domain.	Non-mutagenic	Similar to bioassay results
Hexaconazole Myclobutanil	(Mouse) non-Carcinogenic	Similarity threshold 0.2 < 0.5, prediction may be out of applicability domain.	Non-mutagenic	Similar to bioassay results
Enilconazole/imazalil	(Rodent) Non-carcinogenic	Similarity threshold 0.2 < 0.5, prediction may be out of applicability domain.	Non-mutagenic	Similar to bioassay results
Metconazole	(Mouse, rat) Cannot create prediction	Only one similar compound for threshold 0.2 in the training set (Threshold: 0.2).	Non-mutagenic	Similar to bioassay results
Paclobutrazol	(Mouse, rodent) Carcinogenic	Similarity threshold 0.2 < 0.5, prediction may be out of applicability domain.	Non-mutagenic	Similarity threshold 0.2 < 0.5, prediction may be out of applicability domain.
Penconazole	(Rat) Carcinogenic	Similarity threshold 0.2 < 0.5, prediction may be out of applicability domain.	Non-mutagenic	Similar to bioassay results
Prothioconazole	(Rat, rodent) Cannot create prediction	Only one similar compound for threshold 0.2 in the training set (Threshold: 0.2).	Non-mutagenic	Similar to bioassay results
Tebuconazole	(Mouse, rat) Cannot create prediction	Only one similar compound for threshold 0.2 in the training set (Threshold: 0.2).	Non-mutagenic	Similar to bioassay results
Triticonazole Uniconazole	(Mouse, rat, rodent)	Could not find similar substances for threshold 0.2 with experimental data in the training dataset.	Non-mutagenic	Similarity threshold 0.2 < 0.5, prediction may be out of applicability domain.

induced DNA damage through a caspase-dependent pathway, triggered apoptosis, and caused oxidative stress in PC12 rat pheochromocytoma cells (Hamdi et al., 2022). Furthermore, only the VEGA (CEASAR) prediction tool identified bromuconazole as a carcinogen in our study. Previous studies have shown that bromuconazole causes genotoxic damage and organ damage in rat liver and kidney tissues, possibly associated with impaired oxidative stress in these organs, supporting findings from different studies (Rjiba-Touati et al., 2022b). Furthermore, our research revealed that tebuconazole and myclobutanil are predicted to be non-genotoxic carcinogens in line with the consistent results of Toxtree and VEGA (ISS). Tebuconazole has been associated with genotoxicity in adult Danio rerio (Castro et al., 2018) and poses a potential carcinogenic risk to humans (Liu et al., 2016). Myclobutanil is a potential carcinogen (Shellenberger and Briggs, 1986).

In summary, the computer models utilised in this study exhibit adequacy in predicting crucial toxicological endpoints for health safety, including mutagenicity and carcinogenicity; however, their predictability is acknowledged to be less than fully reliable. Despite this limitation, this study introduces a strategic approach to harness *in silico* prediction tools for prioritisation purposes, presenting a valuable concept for future investigations.

Table 5. VEGA mutagenicity and carcinogenicity prediction models (CEASAR, ISS, SarPy and CONSENSUS).

VEGA Prediction Models	Predicted Carcinogen activity: Carcinogen	Predicted Carcinogen activity: NON-Carcinogen	Predicted Mutagen activity: Mutagenic	Predicted Mutagen activity: NON-Mutagenic
CEASAR	Bromuconazole** Epoxiconazole* Flutriafol** Hexaconazole** Metconazole* Prothioconazole* Triticonazole*	Diniconazole* Fenbuconazole** Enilconazole/imazalil* Myclobutanil* Paclobutrazol* Penconazole* Tebuconazole* Uniconazole*	Epoxiconazole* (Suspect Mutagenic, SA7 Epoxides and aziridines)	Bromuconazole** Diniconazole* Fenbuconazole* Flutriafol** Hexaconazole** Enilconazole/imazalil** Metconazole** Myclobutanil* Paclobutrazol* Penconazole** Prothioconazole* Tebuconazole** Triticonazole* Uniconazole*
ISS	Diniconazole* (SA41 Substituted n-alkylcarboxylic acids) Epoxiconazole* (SA7 Epoxides and aziridines; SA31a Halogenated benzene (Nongenotoxic carcinogens) Fenbuconazole* (SA31a Halogenated benzene (Nongenotoxic carcinogens) Metconazole* (SA31a Halogenated benzene (Nongenotoxic carcinogens) Myclobutanil* (SA31a Halogenated benzene (Nongenotoxic carcinogens) Paclobutrazol* SA31a Halogenated benzene (Nongenotoxic carcinogens); SA41 Substituted n-alkylcarboxylic acids) Prothioconazole** (SA17 Thiocarbonyl (Nongenotoxic carcinogens); SA31a Halogenated benzene (Nongenotoxic carcinogens) Tebuconazole** (SA31a Halogenated benzene (Nongenotoxic carcinogens); SA41 Substituted n-alkylcarboxylic acids) Triticonazole**	Bromuconazole* Flutriafol* Hexaconazole* Enilconazole/imazalil* Penconazole**	Epoxiconazole*	Bromuconazole* Diniconazole* Fenbuconazole* Flutriafol* Hexaconazole* Enilconazole/imazalil* Metconazole* Myclobutanil* Paclobutrazol* Penconazole* Prothioconazole* Tebuconazole* Triticonazole* Uniconazole*

Table 5. Continued

	(SA31a Halogenated benzene (Nongenotoxic carcinogens) Uniconazole* (SA31a Halogenated benzene (Nongenotoxic carcinogens); SA41 Substituted n-alkylcarboxylic acids)		
SarPy		Bromuconazole* Epoxiconazole* Prothioconazole**	Diniconazole** Fenbuconazole** Flutriafol** Hexaconazole** Enilconazole/imazalil** Metconazole** Myclobutanil** Paclobutrazol** Penconazole** Tebuconazole** Triticonazole* Uniconazole**
CONSENSUS (based on 4 models)		Epoxiconazole Prothioconazole	Bromuconazole Diniconazole Fenbuconazole Flutriafol Hexaconazole Enilconazole/imazalil Metconazole Myclobutanil Paclobutrazol Penconazole Tebuconazole Triticonazole Uniconazole

The reliability levels are indicated as follows: *Low reliability; **Moderate reliability.

CONCLUSION

In conclusion, our study underscores the invaluable role of *in silico* tools, such as (Q)SAR models, in predicting the toxic properties of triazole fungicide compounds. The prioritisation strategy proposed in this study, which combines multiple predictive models and emphasises the need for additional data, provides a valuable framework for future investigations in the field of pesticide risk assessment. It is crucial to recognise the inherent limitations and uncertainties in the current predictive capabilities and to continuously refine these tools for improved accuracy. Overall, this study contributes to the ongoing efforts to bridge the gap between traditional toxicological assessments and the evolving landscape of computational approaches, offering a strategic pathway for advancing our understanding of the health impacts associated with pesticide exposure.

Peer-review: Externally peer-reviewed.

Conflict of Interest: The author has no conflict of interest to declare.

Financial Disclosure: The author declared no financial support.

ORCID IDs of the authors

Mine Çağlayan 0000-0001-8910-0005

REFERENCES

Ben Othmène, Y., Hamdi, H., Annabi, E., Amara, I., Ben Salem, I., Neffati, F., Najjar, M. F., & Abid-Essefi, S. (2020). Tebuconazole induced cardiotoxicity in male adult rat. *Food and Chemical Toxicology : An International Journal Published for the British Industrial Biological Research Association, 137*, 111134. https://doi.org/10.1016/j.fct.2020.111134

Benigni, R., & Bossa, C. (2006). Structure-activity models of chemical carcinogens: state of the art, and new directions. *Annali Dell'istituto Superiore Di Sanita, 42*(2), 118–126.

Benigni, R., & Bossa, C. (2008). Structure alerts for carcinogenicity, and the Salmonella assay system: a novel insight through the chemical relational databases technology. *Mutation Research, 659*(3), 248–261. https://doi.org/10.1016/j.mrrev.2008.05.003

Benigni, R., & Bossa, C. (2011). Mechanisms of chemical carcinogenicity and mutagenicity: a review with implications for predictive toxicology. *Chemical Reviews, 111*(4), 2507-2536.

Benigni, R., Bossa, C., & Tcheremenskaia, O. (2013). Nongenotoxic carcinogenicity of chemicals: mechanisms of action and early recognition through a new set of structural alerts. *Chemical Reviews, 113*(5), 2940-57.

Bhat, V., & Chatterjee, J. (2021). The Use of In Silico Tools for the Toxicity Prediction of Potential Inhibitors of SARS-CoV-2. *Alternatives to laboratory Animals: ATLA, 49*(1-2), 22–32. https://doi.org/10.1177/02611929211008196

Castro, T. F. D., da Silva Souza, J. G., de Carvalho, A. F. S., de Lima Assis, I., Palmieri, M. J., Vieira, L. F. A., Marcussi, S., Machado, M. R. F., & Murgas, L. D. S. (2018). Anxiety-associated behavior and genotoxicity found in adult Danio rerio exposed to tebuconazole-based commercial product. *Environmental Toxicology and Pharmacology, 62*, 140–146. https://doi.org/10.1016/j.etap.2018.06.011.

Chen, Y., Dong, Y., Li, L., Jiao, J., Liu, S., & Zou, X. (2022). Toxicity Rank Order (TRO) As a New Approach for Toxicity Prediction by QSAR Models. *International Journal of Environmental Research and Public Health*, 20(1), 701. https://doi.org/10.3390/ijerph20010701

de Oliveira, L. A. B., Pacheco, H. P., & Scherer, R. (2016). Flutriafol and pyraclostrobin residues in Brazilian green coffees. *Food Chemistry, 190*, 60–63. https://doi.org/10.1016/j.foodchem.2015.05.035.

Filipov, N. M., & Lawrence, D. A. (2001). Developmental toxicity of a triazole fungicide: consideration of interorgan communication. *Toxicological Sciences : An Official Journal of The Society of Toxicology, 62*(2), 185–186. https://doi.org/10.1093/toxsci/62.2.185

h, I. M., Ciorsac, A. A., & Isvoran, A. (2019). Prediction of ADME-Tox properties and toxicological endpoints of triazole fungicides used for cereals protection. *ADMET & DMPK, 7*(3), 161–173. https://doi.org/10.5599/admet.668.

Hamdi, H., Rjiba-Touati, K., Ayed-Boussema, I., M'nassri, A., Chaabani, H., Rich, S., & Abid-Essefi, S. (2022). Epoxiconazole caused oxidative stress related DNA damage and apoptosis in PC12 rat Pheochromocytoma. Neurotoxicology, 89, 184–190. https://doi.org/10.1016/j.neuro.2022.02.003

Holečková, B., Šiviková, K., Dianovský, J., & Galdíková, M. (2013). Effect of triazole pesticide formulation on bovine culture cells. Journal of environmental science and health. Part. B, *Pesticides, Food Contaminants, and Agricultural Wastes, 48*(12), 1080–1088.

Jurašeková, Z., Jutková, A., Kožár, T., & Staničová, J. (2022). Vibrational characterization of the pesticide molecule Tebuconazole. Spectrochimica acta. Part A, *Molecular and Biomolecular Spectroscopy, 268*, 120629. https://doi.org/10.1016/j.saa.2021.120629.

Kahle, M., Buerge, I. J., Hauser, A., Müller, M. D., & Poiger, T. (2008). Azole fungicides: occurrence and fate in wastewater and surface waters. *Environmental Science & Technology, 42*(19), 7193–7200. https://doi.org/10.1021/es8009309

Kianpour, M., Mohammadinasab, E., & Isfahani, T. M. (2021). Prediction of Oral Acute Toxicity of Organophosphates Using QSAR Methods. *Current Computer-Aided Drug Design, 17*(1), 38–56. https://doi.org/10.2174/1573409916666191227093237

Leme, D. M., & Marin-Morales, M. A. (2009). Allium cepa test in environmental monitoring: a review on its application. *Mutation Research, 682*(1), 71–81. https://doi.org/10.1016/j.mrrev.2009.06.002

Li, Y., Nie, J., Zhang, J., Xu, G., Zhang, H., Liu, M., Gao, X., Shah, B. S. A., & Yin, N. (2022). Chiral fungicide penconazole: Absolute configuration, bioactivity, toxicity, and stereoselective degradation in apples. *The Science of the Total Environment, 808*, 152061. https://doi.org/10.1016/j.scitotenv.2021.152061

Liu, N., Dong, F., Xu, J., Liu, X., & Zheng, Y. (2016). Chiral bioaccumulation behavior of tebuconazole in the zebrafish (Danio rerio). *Ecotoxicology and Environmental Safety, 126*, 78-84.

Macar O. (2021). Multiple toxic effects of tetraconazole in Allium cepa L. meristematic cells. *Environmental Science and Pollution Research International, 28*(8), 10092–10099. https://doi.org/10.1007/s11356-020-11584-4

Mombelli, E., & Devillers, J. (2010). Evaluation of the OECD (Q)SAR Application Toolbox and Toxtree for predicting and profiling the carcinogenic potential of chemicals. *SAR and QSAR in Environmental Research, 21*(7-8), 731–752. https://doi.org/10.1080/1062936X.2010.528598

Mostafalou, S., & Abdollahi, M. (2017). *Pesticides: An Update of Human Exposure and Toxicity. Archives of Toxicology, 91*(2), 549–599. https://doi.org/10.1007/s00204-016-1849-x.

Perdichizzi, S., Mascolo, M. G., Silingardi, P., Morandi, E., Rotondo, F., Guerrini, A., Prete, L., Vaccari, M., & Colacci, A. (2014). Cancer-related genes transcriptionally induced by the fungicide penconazole. *Toxicology In Vitro : An International Journal Published in Association with BIBRA, 28*(1), 125–130. https://doi.org/10.1016/j.tiv.2013.06.006

Protox II Software, https://tox-new.charite.de/protox_II/ (accessed November 25, 2023).

Pubchem, "Bromuconazole." Retrieved from https://pubchem.ncbi.nlm.nih.gov/compound/3444 (accessed November 20, 2023).

Pubchem, "Diniconazole." Retrieved from https://pubchem.ncbi.nlm.nih.gov/compound/6436605 (accessed November 20, 2023).

Pubchem, "Enilconazole." Retrieved from https://pubchem.ncbi.nlm.nih.gov/compound/37175 (accessed November 20, 2023).

Pubchem, "Epiconazole." Retrieved from https://pubchem.ncbi.nlm.nih.gov/compound/3317081 (accessed November 20, 2023).

Pubchem, "Fenbuconazole." Retrieved from https://pubchem.ncbi.nlm.nih.gov/compound/86138 (accessed November 20, 2023).

Pubchem, "Flutriafol." Retrieved from https://pubchem.ncbi.nlm.nih.gov/compound/91727 (accessed November 20, 2023).

Pubchem, "Hexaconazole." Retrieved from https://pubchem.ncbi.nlm.nih.gov/compound/66461 (accessed November 20, 2023).

Pubchem, "Metconazole." Retrieved from https://pubchem.ncbi.nlm.nih.gov/compound/86210 (accessed November 20, 2023).

Pubchem, "Myclobutanil." Retrieved from https://pubchem.ncbi.nlm.nih.gov/compound/6336 (accessed November 20, 2023).

Pubchem, "Paclobutrazol." Retrieved from https://pubchem.ncbi.nlm.nih.gov/compound/158076 (accessed November 20, 2023).

Pubchem, "Penconazole." Retrieved from https://pubchem.ncbi.nlm.nih.gov/compound/91693 (accessed November 20, 2023).

Pubchem, "Prothioconazole." Retrieved from https://pubchem.ncbi.nlm.nih.gov/compound/6451142 (accessed November 20, 2023).

Pubchem, "Tebuconazole." Retrieved from https://pubchem.ncbi.nlm.nih.gov/compound/86102 (accessed November 20, 2023).

Pubchem, "Triticonazole." Retrieved from https://pubchem.ncbi.nlm.nih.gov/compound/6537961 (accessed November 20, 2023).

Pubchem, "Uniconazole." Retrieved from https://pubchem.ncbi.nlm.nih.gov/compound/6436604 (accessed November 20, 2023).

Rjiba-Touati, K., Ayed-Boussema, I., Hamdi, H., Azzebi, A., & Abid, S. (2022a). Bromuconazole fungicide induces cell cycle arrest and apoptotic cell death in cultured human colon carcinoma cells (HCT116) via oxidative stress process. *Biomarkers : Biochemical Indicators Of Exposure, Response, and Susceptibility to Chemicals, 27*(7), 659–670. https://doi.org/10.1080/1354750X.2022.2098378

Rjiba-Touati, K., Hamdi, H., M'nassri, A., Guedri, Y., Mokni, M., & Abid, S. (2022b). Bromuconazole Caused Genotoxicity And Hepatic and Renal Damage Via Oxidative Stress Process in Wistar Rats. *Environmental Science and Pollution Research International, 29*(10), 14111–14120. https://doi.org/10.1007/s11356-021-16091-8

Sharma, A., Kumar, V., Shahzad, B., Tanveer, M., Sidhu, G. P. S., Handa, N., Kohli, D. K., Yadav, P., Bali, A. S., Parihar, R. D., Dar, O. I., Singh, K., Jasroita, S., Bakshi, P., Ramakrishnan, M., Kumar, S., Bhardwaj, R., & Thukral, A. K. (2019). Worldwide pesticide usage and its impacts on ecosystem. *Sn Applied Sciences, 1*, 1-16.

Šiviková, K., Holečková, B., Schwarzbacherová, V., Galdíková, M., & Dianovský, J. (2018). Potential chromosome damage, cell-cycle kinetics/and apoptosis induced by epoxiconazole in bovine peripheral lymphocytes in vitro. *Chemosphere, 193*, 82–88. https://doi.org/10.1016/j.chemosphere.2017.11.008

Tice, R. R., Bassan, A., Amberg, A., Anger, L. T., Beal, M. A., Bellion, P., Benigni, R., Birmingham, J., Brigo, A., Bringezu, F., Ceriani, L., Crooks, I., Cross, K., Elespuru, R., Faulkner, D. M., Fortin, M. C., Fowler, P., Frericks, M., Gerets, H. H. J., Jahnke, G. D., . . . Myatt, G. J. (2021). In Silico Approaches In Carcinogenicity Hazard Assessment: Current Status and Future Needs. *Computational Toxicology (Amsterdam, Netherlands), 20*, 100191. https://doi.org/10.1016/j.comtox.2021.100191.

Toxtree Software, https://toxtree.sourceforge.net/ (accessed November 20, 2023).

Varghese, J. V., Sebastian, E. M., Iqbal, T., & Tom, A. A. (2020). Pesticide applicators and cancer: a systematic review. *Reviews On Environmental Health, 36*(4), 467–476. https://doi.org/10.1515/reveh-2020-0121

VEGA Hub Software, Retrieved from https://www.vegahub.eu/about-vegahub/ (accessed November 20, 2023).

Wang, Y., Ren, Y., Ning, X., Li, G., & Sang, N. (2023). Environmental exposure to triazole fungicide causes left-right asymmetry defects and contributes to abnormal heart development in zebrafish embryos by activating PPARγ-coupled Wnt/β-catenin signaling pathway. *The Science of the Total Environment, 859*(Pt 2), 160286. https://doi.org/10.1016/j.scitotenv.2022.160286

Wang, S., Zhang, X., Gui, B., Xu, X., Su, L., Zhao, Y. H., & Martyniuk, C. J. (2022). Comparison of modes of action between fish, cell and mitochondrial toxicity based on toxicity correlation, excess toxicity and QSAR for class-based compounds. *Toxicology, 470*, 153155. https://doi.org/10.1016/j.tox.2022.153155

Zhang, Z., Gao, B., He, Z., Li, L., Zhang, Q., Kaziem, A. E., & Wang, M. (2019). Stereoselective bioactivity of the chiral triazole fungicide prothioconazole and its metabolite. *Pesticide Biochemistry and Physiology, 160*, 112–118. https://doi.org/10.1016/j.pestbp.2019.07.012.

How cite this article

Çağlayan, M. (2024). *In silico* analysis to predict the carcinogenicity and mutagenicity of a group of triazole fungicides. *İstanbul Journal of Pharmacy, 54*(2), 205–214. DOI: 10.26650/IstanbulJPharm.2024.1399961

İstanbul Journal of Pharmacy
Istanbul J Pharm2024, 54 (2): 215–222
DOI: 10.26650/IstanbulJPharm.2024.1336667

Original Article

The proteasome inhibitor ixazomib targets epigenetic chromatin modification enzymes upregulated by m2c macrophage polarisation in lung cancer*

Elif Kaya Tilki[1], Selin Engür Öztürk[2]

[1]Anadolu University, Faculty of Pharmacy, Department of Pharmacology, Eskişehir, Türkiye
[2]Pamukkale University, Tavas Health Services Vocational School, Department of Pharmacy Services, Denizli, Türkiye
*The results of this study were previously presented as a poster at the 6th European Congress of Immunology.

ABSTRACT

Background and Aims: Poor prognosis in lung cancer is associated with tumor-associated macrophages (TAMs) that exhibit M2c-like behaviours that support multiple pathways in the tumour microenvironment. The interplay between epigenetic modifications and the ubiquitin-proteasome pathway involves three key mechanisms: regulation of epigenetic enzymes by ubiquitin, interaction between ubiquitin and epigenetic modifiers, and epigenetic silencing of critical genes involved in cellular processes. Therefore, we investigated the effects of ixazomib, a proteasome inhibitor, on gene expression changes in epigenetic chromatin modification enzymes in a co-culture of M2c macrophages and A549 lung cancer cells.

Methods: The IC_{50} concentration of ixazomib was determined to be 2.19 µM using a real-time cell analyser. THP-1 monocytes were polarised into M0 macrophages with 100 ng/mL phorbol 12-myristate 13-acetate (PMA), rested, and then exposed to 1 mM hydrocortisone to become M2c macrophages. A549 cells were seeded in the lower chamber of a co-culture plate. M2c macrophages were then co-cultured with A549 cells for 24 h with or without 2.19 µM ixazomib. After being isolated, mRNA was converted to cDNA and analysed using a gene panel with RT-PCR.

Results: The findings showed that 56 genes had exceptionally high expression levels (up to 1848-fold. Ixazomib downregulated these overexpressed genes.

Conclusion: Ixazomib effectively modulates the expression of genes involved in epigenetic chromatin modification in the lung cancer microenvironment, indicating its utility in lung cancer therapy. Further studies are needed to explore the combined use of epigenetic drugs and proteasome inhibitors.

Keywords: Macrophage, polarisation, epigenetics, ixazomib, lung cancer.

INTRODUCTION

Macrophages are functionally complex players in adaptive and innate immune responses to pathogens, tissue regeneration and development. Macrophages adopt a variety of polarisation states, which have been characterised as M1- and M2-polarized subtypes, to facilitate this. Understanding phenotypic heterogeneity and transcriptional regulation is important because in many disorders, macrophages have emerged as essential because of their essential phagocytic function in defence and homeostasis (Guerriero, 2018).

Tumour-associated macrophages (TAMs) can contribute up to half of the tumour mass and exert potent effects on metastatic processes and tumour growth. Poor clinical outcomes have been linked to high numbers of cells with macrophage-associated markers in several solid tumours (Hu et al., 2016). Among other types of cancer, M2-like macrophages outnumber M1-like macrophages in lung cancer (Zhang et al., 2011). Based on the features that stimulated their polarisation, M2 macrophages are further classified as M2a, M2b, and M2c. Poor prognosis is caused by macrophage acquisition of M2a- and M2c-like phenotypes in the microenvironment of lung cancer, which promote epithelial–mesenchymal transition, cell infiltration, and tumour growth. M1-like macrophages, on the other hand, cause less lung cancer cell proliferation, lower angiogenesis, and apoptosis (Atri, Guerfali, & Laouini, 2018).

Nearly all cellular processes, including cell cycle, gene transcription and translation, survival and apoptosis, cell

Corresponding Author: Elif Kaya Tilki **E-mail:** elif_kaya@anadolu.edu.tr
Submitted: 02.08.2023 • **Revision Requested:** 27.05.2024 • **Last Revision Received:** 07.06.2024 • **Accepted:** 29.06.2024

metabolism, and protein quality control, are dependent on the ubiquitin-proteasome pathway or partially modified transcription factors. Growing evidence indicates that the ubiquitin-proteasome system controls epigenetic changes. Recent studies have demonstrated that, in comparison to non-epigenetic regulatory mechanisms like genetic modifications or conventional signal transduction pathways, epigenetic regulation is equally important for practically both for pathological conditions like cancer and all biological processes (Yerlikaya, Kanbur, Stanley, & Tümer, 2021). Epigenetic regulation modifies gene function without modifying the DNA sequence. Chromatin conformation regulates the accessibility of DNA and thus the binding elements of transcription, gene expression, and phenotype. Closely packed chromatin, also known as heterochromatin, has poor DNA accessibility and is linked to gene silencing. On the other hand, open-chromatin conformation of DNA is easily accessible, facilitating transcription factor binding and gene expression (Baardman, Licht, De Winther, & Van den Bossche, 2015). A potential connection between the environment, metabolism, gene regulation, and the consequent macrophage polarisation state is made feasible by epigenetic enzymes using the metabolites created by cell metabolism (Van den Bossche, Neele, Hoeksema, & De Winther, 2014).

Ixazomib, a medication that is orally bioavailable and has a lower toxicity profile, has been designed to reversibly, selectively, and potently inhibit proteasomes (Xie, Wan, Liang, Zhang, & Jiang, 2019). Ixazomib is widely used for the treatment of multiple myeloma, a type of cancer that affects plasma cells in bone marrow. It is used in combination with lenalidomide and dexamethasone to treat relapsed or refractory multiple myeloma (Lee et al., 2024). Considering these findings, the effects of M2c macrophage polarisation on genes associated with epigenetic chromatin regulation in lung cancer and the therapeutic effect of ixazomib on this pathway were investigated.

MATERIAL AND METHODS

Cell Culture Studies

Human lung cancer A549 (ATCC® CCL-185TM) and human monocyte THP-1 (ATCC® TIB-202) cells were grown in RPMI-1640 growth media containing 10% foetal bovine serum (FBS) and 1% penicillin/streptomycin at 37 °C in a humid incubator containing 5% CO_2.

Proliferation assay using a real-time cell analysis system

By monitoring the impedance changes of linked cells and generating a cell index (CI) value, the real-time cell analysis system (RTCA DP) system continuously analyzes cell behaviour. Every hour during the experiment, the well impedance for each group and concentration was measured and converted into a CI value. Cell proliferation in A549 lung cancer cells was investigated, and the IC_{50} doses of ixazomib were calculated using this system.

The cells were seeded at a density of 1x104 cells per well on 16-well E-plates in 100 µL media for this purpose. After 24 h of incubation, the instrument was stopped, and the current medium was replaced with fresh medium containing ixazomib at several concentrations (100 nM, 1 µM, 10 µM and 20 µM). The xCELLigence RTCA DP Instrument (ACEA Biosciences, USA) was used to evaluate the impedance of each well every hour for 24 h. The assays were performed in 8 wells, and the average CI was calculated. The cell proliferation levels and IC_{50} of ixazomib were calculated according to the CI values using RTCA DP Software 1.2.1. (Dikmen, Canturk, Kaya-Tilki, & Engur, 2017).

Macrophage Polarisation and Co-Culture Studies

THP-1 human monocyte cells were polarised into M2c macrophages and co-cultured with A549 cells for 24 h before mRNA isolation for gene expression arrays. The steps followed during the polarisation from monocyte to M2c macrophages are described as follows:

THP-1 monocytes were incubated with 100 ng/mL PMA in 1% serum for 48 h to differentiate into M0 macrophages. After removing the PMA-containing medium, the cells were washed with phosphate-buffered saline (PBS) three times. The cells were then incubated in normal medium for 48 h to eliminate the effects of PMA. During PMA application, medium serum concentration was maintained at 1% to support differentiation (Chanput, Mes, & Wichers, 2014).

For M2c macrophage polarisation, firstly M0 macrophage cells were stained with Trypan blue solution and $2.5x10^5$ cells counted using a cell counter (Cedex XS®, Innovatis, USA) and plated into the 0.4 µm pore-sized upper chamber of the co-culture plate in serum-free medium. After 48 h, the rested cells were treated with 1 µM hydrocortisone containing serum-free medium and incubated for 72 h (Martinez, Sica, Mantovani, & Locati, 2008). Polarised macrophages were washed with PBS to eliminate remaining debris, and the cells were incubated in growth medium for another 24 h. Using BD Accury C6 flow cytometry, the expression of the cell surface markers CD-206 (M2) and CD163 (M2c) (BioLegend) was used to determine the macrophage subtypes. Macrophages M0 and M2c were imaged morphologically using a Leica DM inverted light microscope.

In accordance with this co-culture, 5x105 A549 cells were seeded into the lower chamber of a second 6-well plate and allowed to adhere the day before the co-culture. The upper chambers containing the M2c macrophages were placed into six-well plates containing A549 cells, and the two cell populations were co-cultured for 24 h with or without the addition of 2 µM ixazomib (24h IC_{50} concentration for A549 cells) (Engür-Öztürk & Dikmen, 2022). Untreated A549 cells were used as the control.

Isolation of mRNA and Real-Time Polymerase Chain Reaction (RT-PCR)

mRNA was isolated from cells co-cultured for 24 hours to investigate the interaction between the gene expression levels of epigenetic chromatin modification enzymes in M2c macrophages and A549 lung cancer cells. In this co-culture, 5×105 A549 cells were seeded into the lower chamber of a 6-well plate and allowed to adhere the day before co-culturing. The upper chambers containing M2c macrophages were then placed into the wells with A549 cells, and the two cell populations were co-cultured for 24 hours with or without the addition of 2 µM ixazomib, which is the 24-hour IC_{50} concentration for A549 cells. Untreated A549 cells served as the control.

mRNA isolation were carried out using the MagNA Pure Compact RNA Isolation Kit® (Catalogue No: 04802993001, Roche, Germany) in the MagNA Pure Compact System. The total mRNA concentrations of the samples were assessed using a NanoDrop 2000® (Thermo Fisher, USA) spectrophotometer at 260 and 280 nm. Using the Transcriptor High Fidelity cDNA Synthesis Kit® (Catalogue no. 05091284001, Roche, Germany), according to the manufacturer's instructions, 500 ng/µL of mRNA from each sample was converted to cDNA. Realtime Ready Custom Gene Panel 96 (Catalogue no. 100141919, Roche, Germany), which contains the enzymes responsible for epigenetic chromatin modification, was used to measure gene expression levels after cDNA samples were replicated using the PCR method. The internal housekeeping gene actin-beta (ACTB) was employed. Using the instrument's analytic software, the results were examined in relation to changes in amplification levels compared with the control group.

Statistical analysis

In Graphpad Prism 8.4.2, one-way ANOVA and Tukey's post hoc tests were used to examine the findings. The mean standard deviation (±) represents the average of three separate studies. *P* values ($P>0.05$ n.s, $P<0.05$*, $P<0.01$**, $P<0.001$***, and $P<0.0001$****) are used to indicate how significant the results are in relation to the control and M2c groups.

RESULTS

M2c Macrophage Polarisation

Macrophage polarisation, which is crucial for tissue repair and homeostasis preservation, is the process by which macrophages change into different functional phenotypes in response to particular microenvironmental stimuli and signals. According to cell surface markers, released cytokines, and biological roles, M2 macrophages are classified into subcategories (Yao, Xu, & Jin, 2019). As macrophages probe and move through their surrounding matrix, their morphology shifts, and changes in cell shape are linked to changes in cell function. As shown in Figure 1, in the presence of M2c-inducing cytokines, they transform morphologically from a round and flattened shape to one that is significantly more elongated (McWhorter, Wang, Nguyen, Chung, & Liu, 2013).

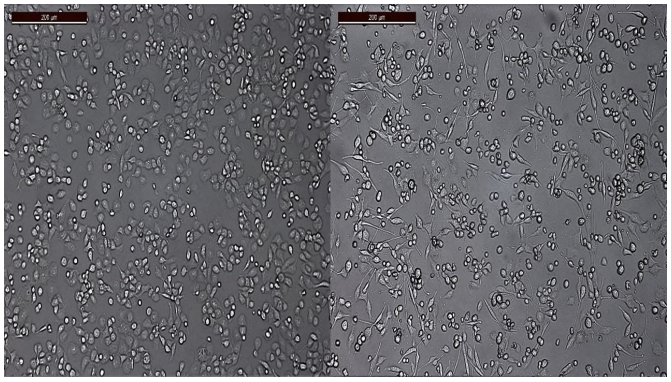

Figure 1. THP-1-origin macrophages (M0) (left) and M2c polarised macrophage (right) observed under a light microscope (10X).

Determination of Antiproliferative Effects of Ixazomib Using RTCA DP

The RTCA DP generates real-time data by gathering measurements at specified intervals over a period of days, indirectly detecting the cell number by measuring the electrical impedance (Dikmen et al., 2020). Real-time and time-dependent analyses of the IC_{50} concentrations of A549 lung cancer cells were performed using the RTCA DP system. The correct ixazomib concentrations for the xCELLigence system evaluation were selected using the WST-1 approach (data not shown). Ixazomib dose-dependently reduced the viability of A549 cells (Figure 2. In A549 lung cancer cells, the ixazomib IC_{50} value was calculated to be 2.45 µM at 24 h (Figure 3).

Determination of Gene Expression Levels of Epigenetic Chromatin Modification Enzymes

mRNA was isolated from cells co-cultured for 24 hours to examine the gene expression of epigenetic chromatin modification enzymes in M2c macrophages and A549 lung cancer cells. After co-culturing with or without 2 µM ixazomib, RT-PCR experiments were conducted to analyze the gene expression levels. Untreated A549 cells were used as the control.

The RT-PCR results revealed that 56 genes involved in epigenetic chromatin changes had incredibly high expression levels up to 1848-fold, including DNA methyl transferase (DNMT), histone deacetylase (HDAC), protein arginine specific methyl transferase (PRMT), ubiquitin conjugating (UBE), lysine demethylase (KDM), aurora kinase (AURK), mixed lineage leukaemia (MLL), and SET domain-containing (SETD) enzyme families (Table 1). Overexpressed genes were downregulated in the presence of the proteasome inhibitor ixazomib, except SETD5 and SETD6, which were increased by 3,84 and 870,69-fold, respectively.

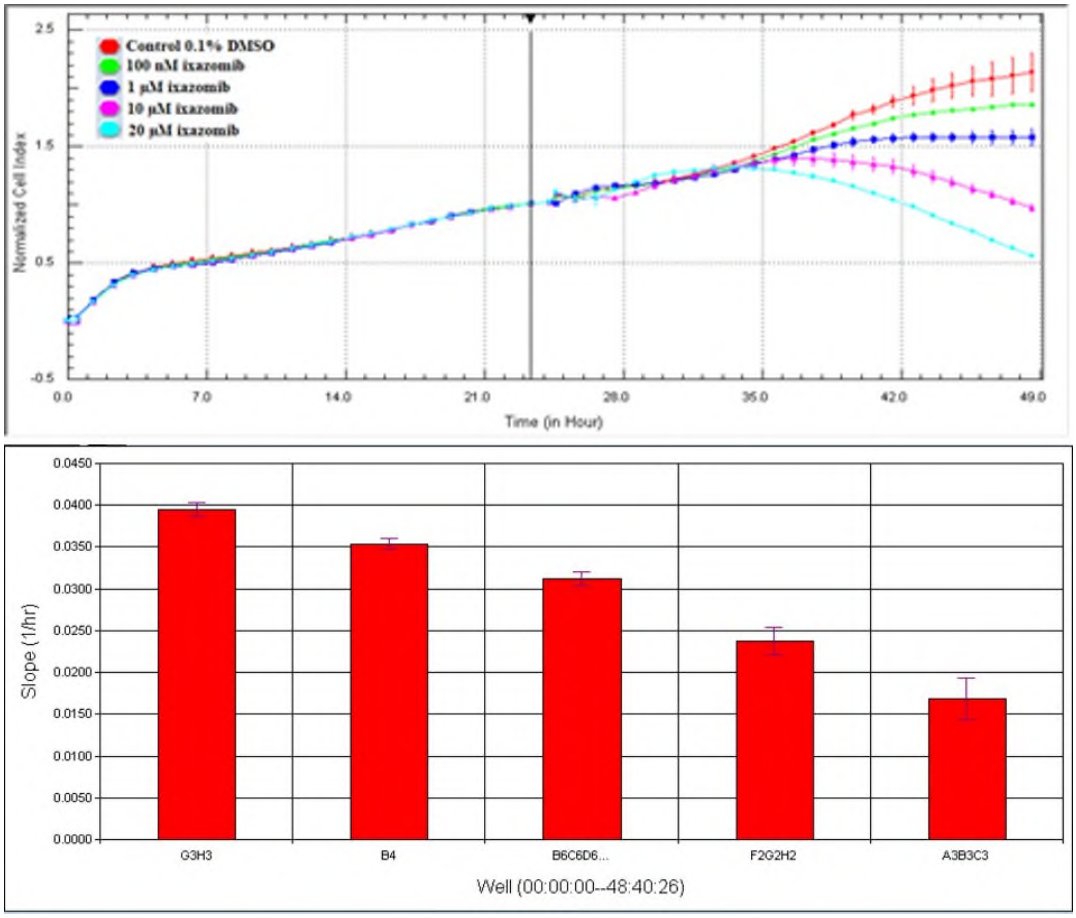

Figure 2. Real-time monitoring of the antiproliferative effects of ixazomib in A549 cells using RTCA DP Software 1.2.1 (n=8). (A) After 24 hours of incubation with ixazomib at various concentrations, real-time CI values were monitored to determine the IC_{50} value. (B) The slope graph is plotted according to the CI data from the 24th hour.

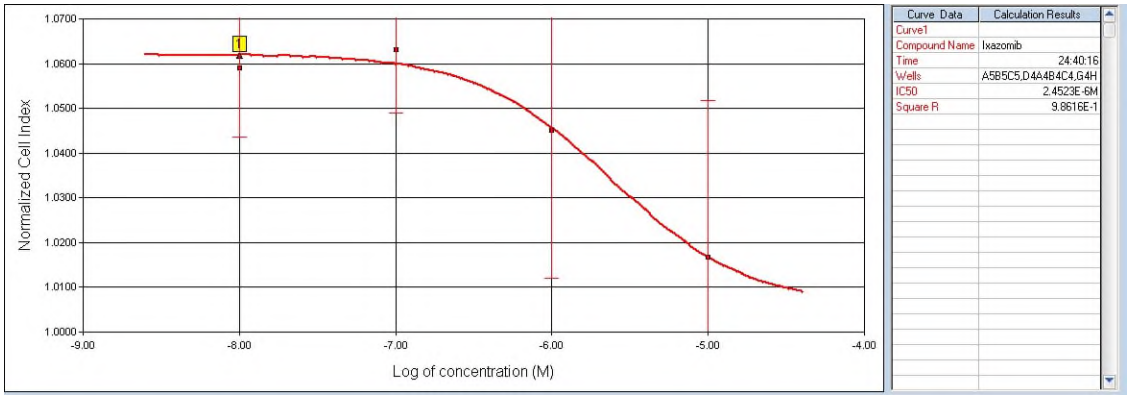

Figure 3. The IC_{50} concentration of ixazomib in A549 cells was determined using the dose-response curves of the cell index and RTCA DP Software 1.2.1 at 24 h (IC_{50}: 2.45 µM).

In the presence of M2c macrophages, HDAC enzymes, particularly HDAC4, were significantly upregulated, showing a remarkable 1848-fold increase in expression. Treatment with ixazomib resulted in a significant reduction (1112-fold) in HDAC4 expression. Additionally, UBE2A and UBE2B expression increased significantly in the presence of ixazomib but decreased substantially when ixazomib was present. The M2c-induced increase in the expression of DNMT1, DNMT3a, and DNMT3b was reversed in the presence of ixazomib. Furthermore, SETD6, which was activated in the presence of ixazomib, showed potential in suppressing inflammatory responses and influencing tumour suppression and anti-inflammatory responses through its effect on NF-κB signalling.

Table 1. Fold changes in the mRNA expression levels of epigenetic chromatin modification enzymes in M2c co-cultured A549 cells treated with or without 2 µM ixazomib.

Gene Name	Gene Symbol	Fold Change (Mean±Std. Deviation)		*P* value					
		M2c	**M2c+Ixazomib**	**Control vs. M2c**		**Control vs. M2c + ixazomib treatment**		**M2c vs. M2c + ixazomib**	
Aurora Kinase A	AURKA	6,24±0,1	0,52±0,2	<0,0001	****	0,052	ns	<0,0001	****
Aurora Kinase B	AURKB	2,91±0,2	0,16±0,06	0,0001	***	0,0112	*	<0,0001	****
ASH1 Like Histone Lysine Methyltransferase	ASH1L	2,17±0,4	0,45±0,05	0,0053	**	0,1153	ns	0,0007	***
Activating Transcription Factor 2	ATF2	20,19±0,06	2,96±0,3	<0,0001	****	0,0002	***	<0,0001	****
Coactivator-associated Arg1 methyltransferase 1	CARM1	5,55±0,3	0,62±0,3	<0,0001	****	0,4658	ns	<0,0001	****
CSRP2-binding protein	CSRP2BP	9,29±0,6	0,33±0,2	<0,0001	****	0,1674	ns	<0,0001	****
Disruptor of Telomeric Silencing 1-like	DOT1L	3,67±0,3	0,41±0,3	<0,0001	****	0,0824	ns	<0,0001	****
Dipeptidase 2	DPEP2	3,58±0,4	0,16±0,2	<0,0001	****	0,0156	*	<0,0001	****
DNA Methyltransferase 1	DNMT1	2,26±0,14	0,11±0,02	0,002	**	0,0114	*	0,0001	***
DNA Methyltransferase 3A	DNMT3A	64,71±1,3	0,1±0,03	<0,0001	****	0,381	ns	<0,0001	****
DNA Methyltransferase 3B	DNMT3B	15,27±1,1	0,41±0,37	<0,0001	****	0,6089	ns	<0,0001	****
Histone Deacetylase 1	HDAC1	40,02±1,59	8,5±0,27	<0,0001	****	0,0002	***	<0,0001	****
Histone Deacetylase 2	HDAC2	8,91±0,13	0,73±0,44	<0,0001	****	0,5397	ns	<0,0001	****
Histone Deacetylase 3	HDAC3	4,94±1,23	0,64±0,26	0,0014	**	0,8231	ns	0,0009	***
Histone Deacetylase 4	HDAC4	1848,02±1	1112,46±0,57	<0,0001	****	<0,0001	****	<0,0001	****
Histone Deacetylase 7	HDAC7	3,69±1,2	0,2±0,03	0,0125	*	0,2516	ns	0,0022	**
Histone Deacetylase 8	HDAC8	32,35±1,24	4,64±0,69	<0,0001	****	0,0069	**	<0,0001	****
Histone Deacetylase 10	HDAC10	7,13±0,96	1,27±0,17	<0,0001	****	0,9514	ns	<0,0001	****
Histone Deacetylase 11	HDAC11	3,09±0,17	0,2±0,09	<0,0001	****	0,0004	***	<0,0001	****
Histone Acetyltransferase 1	HAT1	10±0,87	1,02±0,45	<0,0001	****	0,9991	ns	<0,0001	****
Lysine Acetyltransferase 2B	KAT2B	9,97±1,13	0,38±0,14	<0,0001	****	0,5241	ns	<0,0001	****
Lysine Demethylase 1A	KDM1A	2,68±0,47	0,24±0,13	0,001	***	0,0428	*	0,0001	***
Lysine Demethylase 4A	KDM4A	13,01±1,17	2,75±0,47	<0,0001	****	0,0613	ns	<0,0001	****
Lysine Demethylase 4C	KDM4C	3,85±0,79	0,29±0,07	0,0007	***	0,2194	ns	0,0002	***
Lysine Demethylase 5C	KDM5C	2,77±0,45	1,09±0,22	0,0009	***	0,9286	ns	0,0011	**
Lysine Methyltransferase 2A	MLL	2,88±0,24	0,49±0,12	<0,0001	****	0,0166	*	<0,0001	****
Lysine Methyltransferase 2C	MLL3	12,99±0,18	0,1±0,08	<0,0001	****	0,0002	***	<0,0001	****
Lysine Methyltransferase 2E	MLL5	9,18±0,78	0,74±0,31	<0,0001	****	0,8059	ns	<0,0001	****
Myb Like, SWIRM, and MPN Domains 1	MYSM1	3,2±0,45	0,34±0,11	0,0002	***	0,0608	ns	<0,0001	****
Lysine Acetyltransferase 8	MYST1	11,72±1,1	1,85±0,23	<0,0001	****	0,3267	ns	<0,0001	****
Lysine Acetyltransferase 7	MYST2	5,88±0,47	2,26±0,58	<0,0001	****	0,0271	*	0,0001	***
Lysine Acetyltransferase 6A	MYST3	7,74±0,25	2,06±0,48	<0,0001	****	0,023	*	<0,0001	****
Lysine Acetyltransferase 6B	MYST4	2,4±0,2	0,27±0,04	0,0006	***	0,0153	*	<0,0001	****
Nuclear Receptor Co-activator 1	NCOA1	7,47±0,04	1,02±0,26	<0,0001	****	0,9859	ns	<0,0001	****
Nuclear Receptor Co-activator 3	NCOA3	5,08±1,01	0,53±0,14	0,0004	***	0,6318	ns	0,0002	***
Nuclear Receptor Co-activator 6	NCOA6	5,12±0,36	0,49±0,12	<0,0001	****	0,0668	ns	<0,0001	****
Nuclear Receptor-binding SET domain protein 1	NSD1	2,79±0,24	0,23±0,03	<0,0001	****	0,0018	**	<0,0001	****
P21 (RAC1) Activated Kinase 1	PAK1	2,15±0,42	0,38±0,16	0,0039	**	0,0601	ns	0,0004	***
Protein Arginine Methyltransferase 1	PRMT1	10,96±0,74	1,52±0,48	<0,0001	****	0,53	ns	<0,0001	****
Protein Arginine Methyltransferase 2	PRMT2	3,31±0,6	0,17±0,07	0,0005	***	0,0641	ns	<0,0001	****
Protein Arginine Methyltransferase 3	PRMT3	2,9±0,2	0,39±0,09	<0,0001	****	0,0041	**	<0,0001	****
Protein Arginine Methyltransferase 5	PRMT5	2,05±0,05	0,66±0,24	0,0003	***	0,0613	ns	<0,0001	****
Protein Arginine Methyltransferase 7	PRMT7	3,64±1,05	0,36±0,19	0,0048	**	0,4628	ns	0,0016	**
Ring Finger Protein 2	RNF2	2,3±0,3	0,17±0,03	0,0007	***	0,0072	**	<0,0001	****

Table 1. Continued

Ribosomal Protein S6 Kinase A3	RPS6KA3	4,79±0,78	0,42±0,22	0,0002	***	0,3536	ns	<0,0001	****
SET Domain Containing 1A	SETD1A	1,71±0,56	0,17±0,03	0,0892	ns	0,0514	ns	0,0032	**
SET Domain Containing 1B	SETD1B	6,2±0,4	0,65±0,11	<0,0001	****	0,2588	ns	<0,0001	****
SET Domain Containing 2	SETD2	2,22±0,22	0,39±0,22	0,0024	**	0,0548	ns	0,0003	***
SET Domain Containing B2	SETDB2	5,87±0,23	1,44±0,13	<0,0001	****	0,0684	ns	<0,0001	****
SET Domain Containing 3	SETD3	9,07±0,66	3,56±0,48	<0,0001	****	0,0015	**	<0,0001	****
SET Domain Containing 4	SETD4	5,6±0,3	0,91±0,27	<0,0001	****	0,9072	ns	<0,0001	****
SET Domain Containing 5	SETD5	0,94±0,04	3,84±0,13	0,7714	ns	<0,0001	****	<0,0001	****
SET Domain Containing 6	SETD6	0,06±0,03	870,69±0,76	0,0877	ns	<0,0001	****	<0,0001	****
SET Domain Containing 7	SETD7	0,69±0,05	0,1±0,03	<0,0001	****	<0,0001	****	<0,0001	****
SET Domain Containing 8	SETD8	10,41±0,62	6,51±0,28	<0,0001	****	<0,0001	****	<0,0001	****
SET and MYND Domains Containing 3	SMYD3	3,85±0,82	0,09±0,08	0,0008	***	0,1254	ns	0,0002	***
Suppressor Of Variegation 3-9 Homologue 1	SUV39H1	1,85±0,14	0,13±0,06	0,0001	***	0,0001	***	<0,0001	****
Lysine Methyltransferase 5B	SUV420H1	2,61±0,25	0,05±0,02	<0,0001	****	0,0005	***	<0,0001	****
Ubiquitin-Conjugating Enzyme E2 A	UBE2A	65,69±0,73	43,46±0,24	<0,0001	****	<0,0001	****	<0,0001	****
Ubiquitin-Conjugating Enzyme E2 B	UBE2B	5,02±0,49	0,59±0,16	<0,0001	****	0,3892	ns	<0,0001	****
Wolf-Hirschhorn Syndrome Candidate 1 (2019)	WHSC1	3,16±0,25	0,16±0,03	<0,0001	****	0,0043	**	<0,0001	****

DISCUSSION

Inflammatory processes and macrophage polarisation are necessary for cells to respond to microenvironmental changes and stimuli. Epigenetic pathways improve macrophage diversity and plasticity in order to defend the host from various threats. However, disorders are persistent because of maladaptive epigenetic modifications. As a result, the goal of pharmacological action is to convert a damaged epigenetic landscape into a healthy one. To identify harmful epigenetic signatures and predict disease vulnerability, the epigenetic landscapes of major immune cells should be screened.

Many HDAC isoenzymes are upregulated in various cancers. However, because of the complexity of the linked pathways, the complete mechanisms of action of HDACs have yet to be fully explored (Damaskos et al., 2018). According to our results, HDAC enzymes were dramatically upregulated in the presence of M2c macrophages. HDAC4, whose expression was increased 1848-fold between these enzymes, was the most striking result. Due to its participation in various biological processes, HDAC4 (a class IIa HDAC) has been identified as a significant enzyme in cancer pathogenesis (Jin et al., 2018). HDAC4 expression is not only related with tumour size in malignant thyroid lesions, but it also promotes tumour development in ovarian, colon, glioblastoma, and gastric cancer cells by inhibiting p21 expression (Zeng et al., 2016). In human A549 lung cancer cells, HDAC4 overexpression determines etoposide resistance via P-glycoprotein expression (Kaewpiboon et al., 2015). According to our findings, ixazomib treatment reduced HDAC4 expression by 1112-fold. This is an intriguing finding concerning the importance of combining epigenetic medications with cancer drugs for treating lung cancer, particularly in terms of preventing resistance.

One of the significant results was the upregulation of ubiquitin conjugating enzyme E2A (UBE2A) and UBE2B to 65.7- and 5-fold levels, respectively. In DNA damage-induced mutagenesis, mismatch repair, and gene silencing, UBE2A and UBE2B play crucial roles (Bruinsma et al., 2016). Both genes are members of the E2 family of ubiquitin-conjugating enzymes, which are essential for protein degradation via the ubiquitin proteasome pathway (UPP). The expression of these genes decreased to 45.5 and 0.6-fold, respectively, when ixazomib, a proteasome inhibitor, was present. In addition, abnormal DNMT activity plays a key role in the onset and development of malignancies, leading to the methylation of tumour suppressor genes (Robertson, 2001). DNMT1 is a maintenance enzyme that maintains the semi-methylation of the CpG dinucleotide in newly cloned DNA (Bestor, 1992). As a result, its role in the maintenance of methylation in the genomes of growing cells is critical. DNMT3a and DNMT3b are critical for *de novo* methylation and the establishment of a novel methylation state *in vivo* (Okano, Bell, Haber, & Li, 1999). In the presence of ixazomib, the increase in M2c-induced expression of these genes was eliminated.

Unlike M2c-activated genes, SETD6, which was activated in the presence of ixazomib in the gene panel, yielded some interesting findings. Numerous biological and pathological processes have been linked to the methylation of lysine residues in proteins, although many human protein lysine methyltransferase have unclear catalytic activity or substrate specificity. SETD6 was shown to be a methyltransferase that monomethylated the Lys310 position of the transcription factor linked with

the chromatin NF-kB subunit RelA. Through SETD6-mediated methylation, RelA was rendered inactive, and RelA-driven transcriptional pathways involved in the inflammatory response in primary immune cells were diminished (Levy et al., 2011). Because NF-κB signalling is connected to pathological inflammatory processes and cancer, SETD6 upregulation can be effective for a number of mechanisms through which protein methylation and chromatin regulation influence tumour suppression and anti-inflammatory responses.

CONCLUSION

In conclusion, our study highlights the significant impact of the interplay between M2c macrophages and lung cancer cells on the induction of a notable increase in gene expression within epigenetic pathways in the tumour microenvironment. Proteasome inhibitors are effective in alleviating these dysfunctions. Although proteasome inhibitors have primarily excelled in treating haematological malignancies, their potential in lung cancer treatment is noteworthy, particularly when combined with epigenetic therapies. However, it is essential to acknowledge that our study did not directly assess the effectiveness of combined epigenetic drugs and proteasome inhibitors. Further investigations are essential to explore the potential synergistic effects of combined therapy against lung cancer.

Peer-review: Externally peer-reviewed.

Author Contributions: Conception/Design of Study- E.K.T., S.E.Ö.; Data Acquisition- E.K.T., S.E.Ö.; Data Analysis/Interpretation- E.K.T., S.E.Ö.; Drafting Manuscript- E.K.T.; Critical Revision of Manuscript- S.E.Ö.; Final Approval and Accountability- E.K.T., S.E.Ö.

Conflicts of Interest: The authors have no conflict of interest to declare.

Financial Disclosure: The authors declared that this study has received no financial support.

ORCID IDs of the authors

Elif Kaya Tilki 0000-0003-2122-5324
Selin Engür Öztürk 0000-0003-1534-8117

REFERENCES

Atri, C., Guerfali, F.Z., & Laouini, D. (2018). Role of human macrophage polarization in inflammation during infectious diseases. *International Journal of Molecular Sciences,* 19(6), 1801.

Baardman, J., Licht, I., De Winther, M.P.J., & Van den Bossche, J. (2015). Metabolic–epigenetic crosstalk in macrophage activation. *Epigenomics*, 7(7), 1155–64.

Bestor, T.H. (1992). Activation of mammalian DNA methyltransferase by cleavage of a Zn binding regulatory domain. *The EMBO Journal, 11*(7), 2611–7.

Bruinsma, C. F., Savelberg, S. M., Kool, M. J., Jolfaei, M. A., Van Woerden, G. M., Baarends, W. M., & Elgersma, Y. (2016). An essential role for UBE2A/HR6A in learning and memory and mGLUR-dependent long-term depression. *Human molecular genetics*, 25(1), 1-8.

Chanput, W., Mes, J. J., & Wichers, H. J. (2014). THP-1 cell line: an in vitro cell model for immune modulation approach. *International immunopharmacology, 23*(1), 37-45.

Damaskos, C., Tomos, I., Garmpis, N., Karakatsani, A., Dimitroulis, D., Garmpi, A., ... & Tomos, P. (2018). Histone deacetylase inhibitors as a novel targeted therapy against non-small cell lung cancer: where are we now and what should we expect?. *Anticancer Research*, 38(1), 37-43.

Dikmen, M., Canturk, Z., Tilki, E. K., & Engur, S. (2017). Evaluation of antiangiogenic and antimetastatic Effects of Penicillium chrysogenum Secondary Metabolites. *Indian J Pharm Sci, 79*(1), 49-57.

Dikmen, M., Öztürk, S. E., Cantürk, Z., Ceylan, G., Karaduman, A. B., & Yamaç, M. (2020). Anticancer and antimetastatic activity of Hypomyces chrysospermus, a cosmopolitan parasite in different human cancer cells. *Molecular Biology Reports*, 47, 3765-3778.

Engür-Öztürk, S., & Dikmen, M. (2022). Proteasome inhibitor immunotherapy for the epithelial to mesenchymal transition: assessing the A549 lung cancer cell microenvironment and the role of M1, M2a and M2c 'hydrocortisone-polarised'macrophages. *Molecular Biology Reports*, 49(6), 4777-4793.

Guerriero, J. L. (2018). Macrophages: the road less traveled, changing anticancer therapy. *Trends in Molecular Medicine*, 24(5), 472-489.

Hu, Y., He, M. Y., Zhu, L. F., Yang, C. C., Zhou, M. L., Wang, Q., ... & Liu, L. K. (2016). Tumor-associated macrophages correlate with the clinicopathological features and poor outcomes via inducing epithelial to mesenchymal transition in oral squamous cell carcinoma. *Journal of Experimental & Clinical Cancer Research*, 35, 1-19.

Jin, K., Zhao, W., Xie, X., Pan, Y., Wang, K., & Zhang, H. (2018). MiR-520b restrains cell growth by targeting HDAC4 in lung cancer. *Thoracic cancer*, 9(10), 1249-1254.

Kaewpiboon, C., Srisuttee, R., Malilas, W., Moon, J., Oh, S., Jeong, H. G., ... & Chung, Y. H. (2015). Upregulation of Stat1-HDAC4 confers resistance to etoposide through enhanced multidrug resistance 1 expression in human A549 lung cancer cells. *Molecular Medicine Reports, 11*(3), 2315-2321.

Lee, H. C., Ramasamy, K., Macro, M., Davies, F. E., Abonour, R., van Rhee, F., ... & Leleu, X. (2024). Impact of prior lenalidomide or proteasome inhibitor exposure on the effectiveness of ixazomib–lenalidomide–dexamethasone for relapsed/refractory multiple myeloma: A pooled analysis from the INSURE study. *European Journal of Haematology*, 1-11.

Levy, D., Kuo, A. J., Chang, Y., Schaefer, U., Kitson, C., Cheung, P., ... & Gozani, O. (2011). Lysine methylation of the NF-κB subunit RelA by SETD6 couples activity of the histone methyltransferase GLP at chromatin to tonic repression of NF-κB signaling. *Nature Immunology, 12*(1), 29.

Lu, J., Cao, Q. I., Zheng, D., Sun, Y., Wang, C., Yu, X., ... & Wang, Y. (2013). Discrete functions of M2a and M2c macrophage subsets determine their relative efficacy in treating chronic kidney disease. *Kidney International*, 84(4), 745-755.

Martinez, F. O., Sica, A., Mantovani, A., & Locati, M. (2008). Macrophage activation and polarization. *Front biosci*, 13(13), 453-461.

McWhorter, F. Y., Wang, T., Nguyen, P., Chung, T., & Liu, W. F. (2013). Modulation of macrophage phenotype by cell shape. Pro-

ceedings of the National Academy of Sciences, 110(43), 17253-17258.

Okano, M., Bell, D. W., Haber, D. A., & Li, E. (1999). DNA methyltransferases Dnmt3a and Dnmt3b are essential for de novo methylation and mammalian development. *Cell*, 99(3), 247-257.

Robertson, K. D. (2001). DNA methylation, methyltransferases, and cancer. *Oncogene*, 20(24), 3139-3155.

Van den Bossche, J., Neele, A. E., Hoeksema, M. A., & De Winther, M. P. (2014). Macrophage polarization: the epigenetic point of view. *Current opinion in lipidology*, 25(5), 367-373. horyear-Author12007]aut

Xie, J., Wan, N., Liang, Z., Zhang, T., & Jiang, J. (2019). Ixazomib–the first oral proteasome inhibitor. *Leukemia & Lymphoma*, 60(3), 610-618.

Yao, Y., Xu, X. H., & Jin, L. (2019). Macrophage polarization in physiological and pathological pregnancy. *Frontiers in immunology*, 10, 434399.

Yerlikaya, A., Kanbur, E., Stanley, B. A., & Tümer, E. (2021). The ubiquitin-proteasome pathway and epigenetic modifications in cancer. *Anti-Cancer Agents in Medicinal Chemistry (Formerly Current Medicinal Chemistry-Anti-Cancer Agents)*, 21(1), 20-32.

Zeng, L. S., Yang, X. Z., Wen, Y. F., Mai, S. J., Wang, M. H., Zhang, M. Y., ... & Wang, H. Y. (2016). Overexpressed HDAC4 is associated with poor survival and promotes tumor progression in esophageal carcinoma. Aging (Albany NY), 8(6), 1236.

Zhang, B., Yao, G., Zhang, Y., Gao, J., Yang, B., Rao, Z., & Gao, J. (2011). M2-polarized tumor-associated macrophages are associated with poor prognoses resulting from accelerated lymphangiogenesis in lung adenocarcinoma. Clinics, 66(11), 1879-1886.

How cite this article

Kaya Tilki, E., & Engür Öztürk, S. (2024). The proteasome inhibitor ixazomib targets epigenetic chromatin modification enzymes upregulated by m2c macrophage polarisation in lung cancer. *İstanbul Journal of Pharmacy, 54*(2), 215–222. DOI:10.26650/IstanbulJPharm.2024.1336667

İstanbul Journal of Pharmacy
Istanbul J Pharm2024, 54 (2): 223–232
DOI: 10.26650/IstanbulJPharm.2024.1368223

Original Article

Development and validation of stability indicating HPLC method for favipiravir used in the treatment of the Covid-19 disease

Büşra Gülşen[1], Sıdıka Ertürk Toker[2]

[1]İstanbul University, Graduate School of Health Sciences, İstanbul, Türkiye
[2]İstanbul University, Faculty of Pharmacy, Department of Analytical Chemistry, İstanbul, Türkiye

ABSTRACT

Background and Aims: Favipiravir (FAV) is one of the active pharmaceutical ingredients used in the treatment of patients suffering from Covid-19. The epidemic started in 2019 and is still continuing all over the world. In this study, an analysis method was developed and validated for the simultaneous analysis of FAV and its degradation impurities.

Methods: The stationary phase of the developed method was determined using Kinetex® EVO C18 column and the mobile phase was pH 3.0 phosphate buffer:acetonitrile (90:10; v/v). Chromatographic separations were carried out at 30 °C column temperature and samples were monitored by a UV-Visible detector with a wavelength of 222 nm at 0.5 mL/min flow rate.

Results: Total analysis time was 25 minutes; FAV retention time was approximately 9 minutes. The retention times of major impurities formed under alkaline, acidic, oxidative conditions were observed at about 4, 5, 7 and,12 minutes (RRT 0.51, 0.54, 0.76, 1.31), respectively. According to the validation data, the linearity range was obtained as 0.030 – 0.750 µg/mL, the limit of quantitation and the limit of detection were 0.030 µg/mL and 0.010 µg/mL, respectively. Percentage relative standard deviation values obtained in intra-day and between day repeatability studies were determined as 0.17% and 0.28%, respectively, and the average recovery value was found to be 99.46%.

Conclusion: This validated method has been successfully applied to the determination of all possible degradation impurities of FAV that increase under stress conditions such as high temperature, humidity and photodegradation from tablet form. The developed HPLC method is extremely suitable for the routine analysis of this drug used in the treatment of the Covid-19 disease, especially in terms of speed and convenience.

Keywords: Covid-19, favipiravir, stability indicating method, HPLC, validation

INTRODUCTION

Favipiravir (FAV) is an antiviral drug whose chemical name is 6-fluoro-3-hydroxypyrazine-2-carboxamide (Figure 1). It was first approved in Japan in 2014 to treat pandemic influenza infections (Delong, Abdelnabi, & Neyts, 2018). This active ingredient has also been used in the treatment of Covid-19, a virus that first appeared in the Wuhan Province of China in December 2019 with respiratory symptoms such as fever, cough, and shortness of breath (Turkish Republic Ministry of Health, 2020).

FAV is an RNA-dependent RNA polymerase (RdRp) enzyme inhibitor, in addition to its anti-influenza virus activity, it has the ability to block the replication of flavi-, alpha-, filo-, bunya-, arena-, noro- and other RNA viruses (Drugbank, 2021; Baranovich et al., 2013). With these features, it was thought to have has fewer side effects than the combined drug group (Kiso et al., 2010; Watanabe et al., 2013).

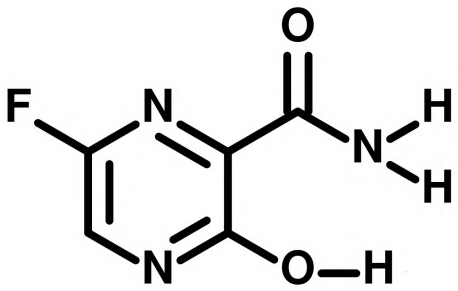

Figure 1. Chemical structure of FAV.

The first pharmaceutical preparation containing FAV is a

Corresponding Author: Sıdıka Ertürk Toker **E-mail:** serturk@istanbul.edu.tr
Submitted: 30.09.2023 • **Revision Requested:** 14.11.2023 • **Last Revision Received:** 19.01.2024 • **Accepted:** 22.01.2024

medicine in tablet form (Avigan® 200 mg Tablet) originating in Japan. This preparation is typically used only in new influenza virus outbreaks where other anti-influenza virus agents are not effective enough (Pharmaceuticals and Medical Devices Agency, 2014). FAV became one of the preferred options in the treatment of COVID-19 symptoms during the pandemic period, where fast and effective treatment was essential. It was used in our country as well as in some other countries. During the manufacturing of the drug products of FAV, well-developed and validated analytical methods are required to enable quicker and easier analysis to be made.

To date, HPLC methods (Cuiyan, Yuanyuan, Lichao, Yangjin, & Lei, 2015; Yegorova, Scrypynets, Leonenko, Umetskaya, & Voitiuk, 2020; Bulduk, 2020), – as well as spectrophotometric methods (Yegorova et al., 2020; Megahed, Habib, Hammad, & Kamal, 2020) and a Luminescence method (Yegorova et al., 2020) have been developed for the quantification of FAV in its tablet forms. Moreover, the Chinese patents (CN104914185A (Guangling et al., 2015) and CN104914185B (Guangling et al., 2016)) and the stability-indicating HPLC method (Ali et al., 2021) are available on FAV impurity determination in studies conducted so far. In the stability-indicating HPLC method published by Ali et al. (Ali et al., 2021), impurities were not identified one by one and the degradation results were not published in detail.

In this study, a new HPLC method was developed and validated for the simultaneous analysis of FAV and its degradation impurities. Furthermore, its applicability in pharmaceutical preparations has been proven with detailed degradation studies.

MATERIAL AND METHODS

Chemicals

Analytical grade Potassium Dihydrogen Phosphate, 85% Phosphoric Acid, 37% Hydrochloric Acid and Sodium Hydroxide were purchased from Merck (Germany). HPLC grade Acetonitrile and Methanol were purchased from J.T.Baker (United States); distilled water was used from Merck Millipore Milli-Q Advantage A10 Ultrapure water system (United States). FAV working standard was obtained from Zhejiang Hengkang Pharmaceutical Co., Ltd. (China). FAV 200 mg film-coated tablet (FAAR1-V-01, ARIS) and adjuvant (placebo) mixture were supplied from Ali Raif Pharmaceutical Company (Türkiye); Avigan 200 mg film-coated tablet was purchased from Toyama Chemical Co. Ltd. (Japan) as a reference product.

Solutions

10 mM phosphate buffer was prepared by dissolving 1.36 g of potassium dihydrogen phosphate in approximately 950 mL of distilled water and adjusting the pH to 3.0±0.05 with 85% phosphoric acid. The solution was then made up to 1 L of volume.

A mobile phase solution was prepared by combining 10 mM phosphate buffer and acetonitrile at a ratio of 90:10 (v/v). The mobile phase solution was also used as the dilution solution.

FAV stock solution was prepared by dissolving 25 mg FAV working standard in approximately 25 mL of dilution solution and then kept in an ultrasonic bath for 15 minutes. After dissolution was achieved, it was made up to 50 mL volume with the dilution solution (C_{FAV} : 0.5 mg/mL).

For preparing the standard solution 1/100 dilutions of the FAV stock solution and 1/10 dilutions of the 1/100 solution were made and the volumes were completed with the dilution solution each time (C_{FAV} : 0.0005 mg/mL).

For the sample solution 5 FAV 200 mg film-coated tablets were crushed in a mortar and powdered. Tablet powder (32.58 mg) equivalent to 25 mg FAV was weighed and transferred to a 50 mL volumetric flask. 25 mL of dilution solution was added to it and left in an ultrasonic bath for 15 minutes and made up to volume with dilution solution (C_{FAV} : 0.5 mg/mL). The placebo solution consisted of excipients was also prepared similarly to the sample solution.

All prepared solutions were filtered through a 0.45 µm membrane filter (Millipore®, Germany).

HPLC system

Two different types of HPLC columns and mobile phases were examined during the selection of the column and mobile phase. C18 (Kinetex EVO C18 ; 100Å, 250 x 4.6 mm, 5 µm) and C8 (Waters® XBridge C8; 250 x 4.6 mm, 5 µm) columns were used and the mobile phases were tested according to the physicochemical properties of FAV. The HPLC system, showing the best achieved results and the conditions in which trials were carried out, is shown in Table 1. The run time of the method was 25 min.

Validation

The validation of the analytical method developed with this study was carried out in accordance with the parameters and explanations specified in the ICH Q2 (R1) – Validation of Analytical Procedures Guidelines (ICH Q2 (R1), 2005).

In the specificity studies, the system received one injection each of mobile phase solution, placebo solution, standard solution, sample solution, and FAV + placebo solution. A DAD detector was used throughout this analysis.

In the system suitability studies, 6 consecutive injections were applied from each of the prepared standard and sample solutions.

For the limit of quantitative determination (LOQ), 6 consecutive injections of the 0.030 µg/mL LOQ solution were applied.

Table 1. Chromatographic conditions of the developed method

HPLC System	HPLC LC-20A (Shimadzu Corporation, Japan)
Dedector	SPD-M20A Diode Array Dedector (DAD)
Column	Kinetex® EVO C18
Column Dimensions	100Å, 250 x 4.6 mm, 5 µm
Mobile Phase/Dilution Solvent	Phosphate Buffer (10 mM KH_2PO_4 (pH 3.0)):Acetonitrile, (90:10, *v/v*)
Mode	Isocratic
Flow Rate	0.5 mL/min
Detection Wavelenght	222 nm
Column Temperature	30 ºC
Injection Volume	10 µL

These studies were performed such that the FAV peak height to noise to signal to noise ratio (S/N) was in the 10:1 range and the RSD% between FAV peak areas from 6 consecutive injections was less than 10.0. For the lower limit of detection (LOD), an injection of the 0.010 µg/mL LOD solution was performed. It was found that the signal to noise (S/N) ratio of the FAV peak height to noise, which was acquired from the LOD injection, varied between 2:1 and 3:1.

Three solutions were made at the accuracy parameter, one for each of the percent LOQ, 100 percent, and 150 percent recovery levels, and three injections were made from each solution. The precision parameter was analyzed in two steps. In the first step, for reproducibility, two standard solutions were prepared. 6 consecutive injections of the first standard solution and two consecutive injections of the second standard solution were performed. The RSD% between the FAV peak areas obtained from both standard solutions, the tailing factor, and the theoretical plate number were evaluated, and the recovery calculation was made. During the second phase, the intermediate precision study, all solutions were prepared and administered on a different day by a different analyst as described in the repeatability study.

For the robustness parameter, three injections of each of the standard and sample solutions were made for the normal analysis conditions of the method and modified conditions given in Table 2. During the robustness study, results from flow rate, column temperature, and wavelength were evaluated.

For the solution stability parameter, prepared standard and sample solutions were divided into two and stored under HPLC conditions and at refrigerator temperature (2-8°C). From the solutions in HPLC conditions, at the start, 6, 21, 27 and 45 hours 3 injections were given. Similarly, of the solutions kept at refrigerator temperature (2-8 °C), 3 injections were given at the beginning, and thereafter in the 4^{th}, 19^{th}, 27^{th}, and 45^{th} hours.

Degradation and Stress Studies

A FAV 200 mg film-coated tablet was exposed to the conditions given in Table 3. The data from the deterioration studies were compared with the percent area findings and FAV peak purity values of the normal condition sample that was first injected into the HPLC system in the degradation and stress studies.

Checking the suitability of the determined total impurity limit was evaluated by Arrhenius Equation (lnk = lnA - Ea / R x T). 6-month analysis results of the most degraded impurity of FAV (RRT 0.51) under 30 °C and 40 °C heat stress conditions and 7-day analysis results under 70 °C heat stress conditions were used in this equation.

RESULTS AND DISCUSSION

Method Development

Initially, the λ_{max} values of the FAV molecule were obtained from the UV-Visible spectra of the FAV solution (C_{FAV} : 0.01 mg/mL, methanol) and the solvent was 222 nm and 322 nm, respectively. By injecting the sample solution into the HPLC system, an extra impurity peak - RRT 0.51 was seen in the chromatogram of 222 nm compared to the chromatogram of 322 nm, thus 222 nm was chosen as the method wavelength in order to monitor this impurity.

Due to the polar and basic character of FAV (Pharmaceuticals and Medical Devices Agency, 2014) and the capacity of its hydroxyl group to make intramolecular hydrogen bonds, it was decided to test the C8 and C18 columns for chromatographic separation. In addition, due to the pKa value of the molecule being 5.1, attention was paid to ensure that the pH ranges of the preferred C8 and C18 columns were wide so that the pH range to which the column would be resistant corresponded to $pK_{aFAV} \pm 2$. As a result of the column trial studies, it was decided to choose the Kinetex® EVO C18 100Å 250 x 4.6 mm, 5 µm column as the stationary phase that would provide separation in this analytical method. Upon examination of the findings produced by this column, it was observed that the

Table 2. Robustness parameters and their initial & changed conditions

Parameter	Initial	Lower Limit	Upper Limit
Flow Rate	0.5 mL/min	0.45 mL/min	0.55 mL/min
Column Temperature	30 °C	28 °C	32 °C
Dedection Wavelength	222 nm	215 nm	230 nm
Different Column*	Kinetex® EVO C18 250 x 4.6 mm, 5 gm, 100Â		

**Only serial number/part number differs from the column that was used initially.*

Table 3. Stress conditions that FAV tablet was exposed*

Stress Condition	Stressor	Exposure Condition	Exposure Duration
Acidic	0.1 N HCI	60 ₀C	4 hours
Alkali	0.1 N NaOH	60 °C	4 hours
Oxidative	3% H_2O_2	60 °C	4 hours
Photolysis	UV light	In a petri dish under 500 W/m^2 UV light	7 days
Thermal	-	70°C ± 2°C, 100% RH ± 5% RH	7 days
Humidity	Distilled Water	-	8 hours

**In order to compare the decomposition and stress studies, the reference sample and placebo solution without any treatment were prepared. For all conditions, placebo solutions were prepared exposed to the same conditions. For alkaline, acidic, oxidative decomposition and humidity studies, empty solutions exposed to these conditions were prepared.*

injection repeatability was guaranteed and that the theoretical plate number values and tailing factor satisfied the acceptance standards.

During the determination of the mobile phase, the type, concentration and pH value of the buffer solution and the determination of the organic solvent were sequentially carried out. Phosphate buffer and acetonitrile were chosen as the first materials to be used because of their extremely low absorbance at wavelengths near 222 nm. Buffer concentration trials were started at 10 mM, since in most applications the buffer concentration in the mobile phase is sufficient at 5 - 10 mM (Dolan, 2011). 1/10 of the total volume was chosen for the acetonitrile ratio to be used as the other component of the mobile phase. While determining the pH value of 10 mM buffer, considering the pH value at which FAV is not ionized, pH 3.0 value was chosen from the three pH ranges (1.1-3.1, 6.2-8.2, 11.3-13.3) where the phosphate buffer is effective.

After determining the column and mobile phase, it was observed that the retention time of the last impurity (RRT 1.99) was approximately 17.1 minutes in injections made under these conditions. Considering this value, 25 minutes, which is close to 1.5 times the retention time of the last impurity, was determined as the analysis time.

Determination of Sample and Standard Solutions Concentrations and Impurity Specifications

The maximum recommended daily dose for a pharmaceutical form containing FAV molecule is 3200 mg/day (Pharmaceuticals and Medical Devices Agency, 2014). According to ICH Q3B (R2) (European Medicines Agency, 2006), for drugs with a maximum daily dose of more than 1.0 g, the reporting limit, the limit of unknown impurities, and the limit of known impurities were determined as 0.05%, 0.10%, and 0.15%, respectively.

Based on an unknown impurity limit (0.10%) and reporting limit (0.05%) determined according to the ICH Q3B (R2) guideline, the FAV concentration for the sample solution was determined as 0.5 mg/mL since, the LOQ% of FAV was below or equal to the reporting limit. The FAV concentration for the limit level solution was also determined as 0.5 µg/mL. FAV peak purity was achieved at both concentrations. The S/N value obtained from the chromatograms of the solution at the limit level concentration was determined as 108.17. Based on this value, the LOQ level was calculated as 0.030 µg/mL, the S/N value as 10.52, and the LOQ as 0.006 (below reporting limit - 0.05%). These obtained values and the peak purity of FAV proved that the determined sample solution concentration was appropriate according to the ICH Q3B (R2) guideline.

The total impurity limit for the FAAR1-V-01 tablet was determined as 0.5% which was the result of both the mathematical calculation of the stress/stability data of the tablet and the stress/stability studies using the reference product Avigan®

Tablet (Serial No: PC1021, Japan). Evaluations in these studies were made on the RRT 0.51 impurity with the highest % result showing a regular increase in the chromatograms. 'Guidance for Industry ANDAS: Impurities in New Drug Products' was used to determine the total impurity limit by comparing it with the original product to be evaluated in terms of quality (Food and Drug Administration, 2010). The accelerated period 40 °C and 70 °C analysis results of the FAV tablet and Avigan® tablet are shown in Table 4. While checking the compliance of the determined total impurity limit, regardless of the relevant compound specifications of the reference product, 6-month analysis results at 30 °C and 40 °C stress conditions and 7-day analysis results at 70 °C stress conditions over RRT 0.51 impurity in FAV Tablet were evaluated by Arrhenius Equation (lnk = lnA - Ea / R x T). In this way, the behavior of the RRT 0.51 impurity against temperature change was determined. According to the Arrhenius Graph in Figure 2 obtained with the stress stability results of the RRT 0.51 impurity with the highest increase in 3 different temperature conditions for the product FAAR1-V-01, the shelf life of this product was approximately 72 months. The determined shelf life of the reference product of Avigan® Tablet was 60 months (Pharmaceuticals and Medical Devices Agency, 2014). The mathematical result obtained from the graph with the total impurity limit determined, since it corresponds to the shelf life of the reference product, showed that the determined total impurity limit is suitable for this product during shelf life.

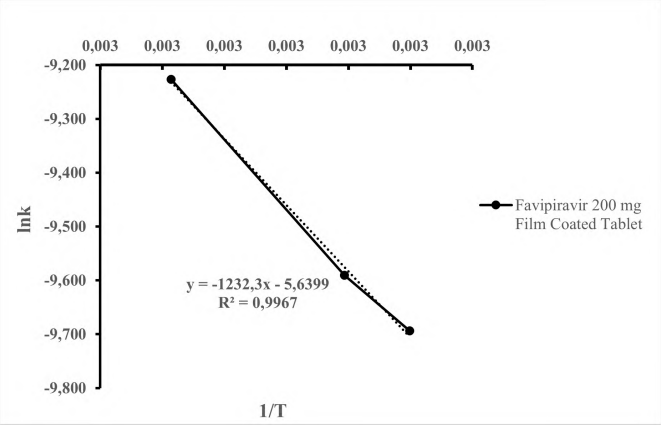

Figure 2. Arrhenius Graph for FAV 200 mg film-coated tablet.

Method Validation

It was observed that there was no interference between the FAV peak and the other peaks obtained in the chromatograms of the sample solution and placebo solution (Figure 3). FAV Peak purity index was also found between 0.99 and 1.00 as seen in Figure 3. The retention time, peak area, peak purity index, and single point threshold values of the FAV peak obtained from the injected solutions are reported in Table 5.

In the system suitability studies, the areas of FAV peak in all

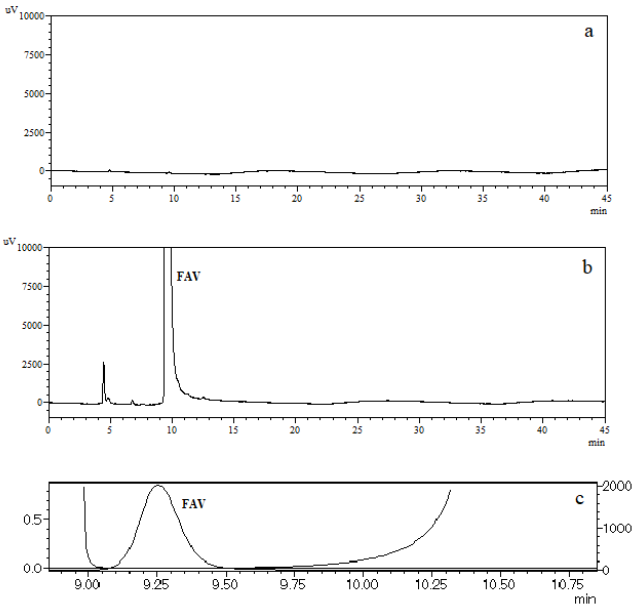

Figure 3. Representative chromatograms of placebo (a) and sample (b), and the figure of FAV peak purity (c).

chromatograms given separately from the standard and sample solutions, the standard deviation between the retention times and the peak areas, and the RSD% values were found to be less than 0.055.

In the LOD studies, the calculated S/N values of the LOD solution injection were found to be close to the ratio of 3:1 and these values provided the requested acceptance criterion. Similarly, the S/N ratios calculated from the LOQ solution injections were close to 10:1 and the RSD% value between the FAV peak areas in consecutive injections was below 10.0.

In the linearity graph obtained according to the least squares method from linearity studies, the peak areas corresponding to the concentrations were located directly above the line in the graph. The data of the obtained linearity equation are given in Table 6. From the reported values, the determination coefficient was 0.99980, which satisfies the acceptance criterion ($R^2 \geq 0.999$). At 2.54% the y-intercept criterion was obtained in accordance with the acceptance criterion (range ± 20.0% of the signal output by the standard solution).

Table 4. Temperature stress/stability results of FAV 200 mg film coated tablet

RRT 0.51 Impurity	FAV 200 mg Film Coated Tablet				
	Initial	3rd day	7th day	3rd month	6rd month
30°C ± 2°C, %65 RH[a] ± %5 RH[a]	0.019	-	-	0.025	0.056
40°C ± 2°C, %75 RH[a] ± %5 RH[a]	0.019	-	-	0.027	0.060
70°C ± 2°C, %100 RH[a] ± %5 RH[a]	0.019	0.039	0.078	-	-

[a] Relative Humidity

Table 5. Specificity results of FAV peak (222 nm) from different solutions

Solutions	Retention Time (minutes)	Peak Area	Peak Purity Index	Single Point Threshold
Mobile Phase/Dilution Solvent	-	-	-	-
Placebo Solution	-	-	-	-
Standard Solution	9.257	23187	0.999949	0.993503
Sample Solution	9.248	21328856	0.999999	0.999964
FAV + Placebo Spike Solution	9.261	23592	0.999962	0.988149

Table 6. Linearty parameters of the developed method

Parameter	**Result**
Linearity Range (p.g/mL)	0.030-0.750
Regression Equation	y=43971.286 x+582.978
Slope	43971.286
Intercept	582.978
Mean Correlation Coefficient, R	0.9999
Determination Coefficient, R^2	0.9998
y-Intercept Criterion (%)	2.54
LOD[a] (p.g/mL)	0.010
LOQb (p.g/mL)	0.030

[a]Limit of Detection; [b]Limit of Quantification

In the accuracy studies, the average recovery value at the LOQ%, 100% and 150% levels, were determined within the 90.0% - 110.0% limit. The results obtained are given in Table 7.

In the repeatability and intermediate precision studies, the results of 2 different standard solutions were all within the system suitability acceptance criteria. In both studies, the mean recovery values were found to be over 98% and the RSD% values were found to be below 0.28 (Table 8).

In the robustness studies, for both standard and sample solutions, the % change of FAV peak areas compared to the initial conditions was found to be less than 5.0 in both the column change and column temperature changes. The % change obtained in terms of flow rate and wavelength changes was found to be more than 5.0%. When the applied changes were evaluated in terms of sample solutions impurity results (%), it was seen that the results did not exceed the specification limits and similar results were obtained with the impurity results (%) obtained in the initial conditions.

The percent change between the standard and sample solutions held in refrigerated and HPLC settings at the beginning and injection times of the solution stability investigation was determined to be less than 5.0 for 45 hours in both scenarios. When the sample solution is evaluated in terms of impurities, no results exceeding specification limits for each unknown impurity and total impurity were observed for 19 hours under refrigeration conditions. However, the RRT 0.51 impurity showed a regular increase. The same impurity caused the sample solution

Table 7. Recovery results for FAV tablet samples

Concentration (p.g/mL)		Recovery (%)	RSD [b] (%)	Mean Recovery (%)
Added	Found (mean ± SD [a])			
0.030	0.032 ± 1.11	106.30	1.05	
0.500	0.480 ± 0.67	96.22	0.69	99.46
0.750	0.720 ± 0.80	95.85	0.84	

[a] Standard Deviation; [b] Relative Standard Deviation

Table 8. Intra-day & inter-day precision data for FAV tablet samples (n = 6)

Concentration (µg/mL)		Recovery (%)	RSD [b] (%)
Added	Found (mean ± SD [a])		
Intra-day			
0.501	0.492 ± 0.17	98.10	0.17
Inter-day			
0.504	0.496 ± 0.27	98.35	0.28

[a] Standart Deviation; [b] Relative Standart Deviation

results to exceed the limit from the 6th hour under HPLC conditions. Therefore, the stability time of the sample solution was determined by the 6-hour solution stability study performed in addition to both conditions. When all studies were evaluated, it was observed that the standard solution was stable for 45 hours under HPLC conditions and refrigerator conditions, but the sample solution was stable for impurities only for 2 hours under HPLC conditions and refrigerator conditions. According to this result, it was determined that the sample solutions should be injected into the system fresh after preparation.

Degradation and stress studies

The numerical data of all degradation studies obtained under alkaline, acidic, oxidative, thermal, humidity, and photolytic stress conditions are shown in Table 9.

In the degradation experiments carried out under alkaline conditions, only the RRT 0.54 impurity was detected in addition to the impurities in the normal condition sample. Results for this impurity were found to exceed each unknown impurity limit (0.10%). RRT 0.54 impurity and RRT 0.76 impurity, which were also detected in the normal condition sample, were observed as major impurities belonging to this condition. RRT 0.51, another impurity detected in the normal condition sample, increased with alkaline conditions, but the result was below the limit for each unknown impurity (Figure 4b).

No additional impurities were detected in the normal condition sample for degradation study under acidic conditions. RRT 0.51 impurity was observed as the major impurity for this condition. RRT 0.76 and RRT 1.18, the impurities in the normal condition sample, were the impurities that increased in acidic conditions; however, the results of both impurities under this condition were below each unknown impurity limit (Figure 4c).

In the oxidative conditions degradation study RRT 0.57, RRT 0.63, RRT 0.84, and RRT 1.31 impurities were detected in addition to the impurities in the normal condition sample. The results for impurities RRT 0.57, RRT 0.63, and RRT 0.84 remained below each unknown impurity limit (0.10%), while impurities RRT 0.51, RRT 0.76, and RRT 1.31 were observed as major impurities for this condition. RRT 1.99, one of the impurities in the normal condition sample, also increased with this condition, but each gave results below the unknown impurity limit (Figure 4d).

In the temperature effect study, RRT 0.54, RRT 1.31, and RRT 2.07 impurities were detected in addition to the impurities in the normal condition sample. Although RRT 0.51, RRT 0.76, and RRT 1.99 are the normal condition impurities, they were increased with the effect of temperature and all impurity results obtained as a result of this study were below each unknown impurity limit (0.10%). However, the RRT 0.51 impurity was increased under this condition, giving results above the reporting limit (0.05%) (Figure 5b).

In the humidity effect study, in addition to the impurities in the normal condition sample, RRT 0.54 and RRT 1.31 impurities were detected. The impurity RRT 0.51 in the normal condition sample increased with the effect of humidity and was close to each unknown impurity limit (0.10%) but still below each unknown impurity limit (Figure 5c).

In the photodegradation study, in addition to the impurities in the normal condition sample, RRT 0.54 and RRT 1.31 impurities were detected. The impurity RRT 0.51 increased with photodegradation and was detected close to each unknown im-

Table 9. Favipiravir 200 mg film coated tablet degradation results

	Reference	Alkali	Acidic	Oxidative	Thermal	Humidity	Photolysis
Favipiravir	99.867	95.699	88.261	94.120	99.830	99.833	99.864
RRT[a] 0.51	0.018	0.051	11.617	4.789	0.070	0.090	0.080
RRT[a] 0.54	-	0.128	-	-	0.005	0.029	0.027
RRT[a] 0.57	-	-	-	0.074	-	-	-
RRT[a] 0.63	-	-	-	0.007	-	-	-
RRT[a] 0.76	0.013	4.082	0.082	0.206	0.017	0.012	0.016
RRT[a] 0.84	-	-	-	0.007	-	-	-
RRT[a] 1.11	0.001	0.001	0.001	0.001	0.001	0.001	0.001
RRT[a] 1.18	0.005	0.005	0.006	0.004	0.005	0.005	0.003
RRT[a] 1.31	-	-	-	0.570	0.012	0.010	0.003
RRT[a] 1.99	0.003	0.003	0.003	0.019	0.006	0.003	0.007
RRT[a] 2.07	-	-	-	-	0.030	-	-
Total	99.907	99.969	99.970	99.797	99.976	99.983	100.001

[a] Relative Retention Time

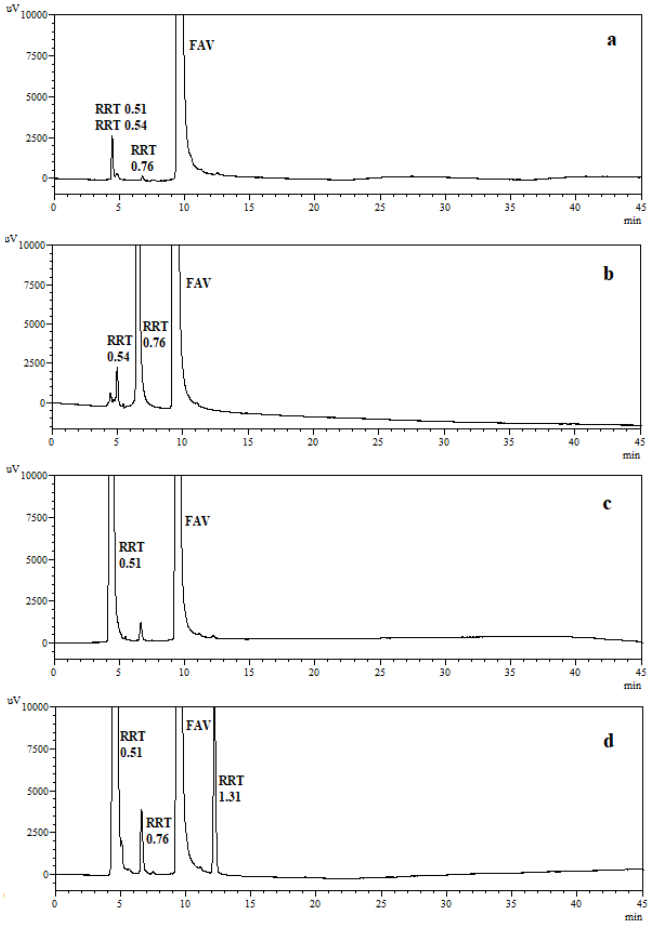

Figure 4. Chromatograms obtained under normal conditions (a) alkaline (b), acidic (c) and oxidative (d) stress conditions.

purity limit (0.10%). The other impurities, RRT 0.76 and RRT 1.99, which were found common in both conditions, were observed as impurities increasing with photodegradation. However, all impurity results obtained as a result of this study were below each unknown impurity limit (Figure 5d).

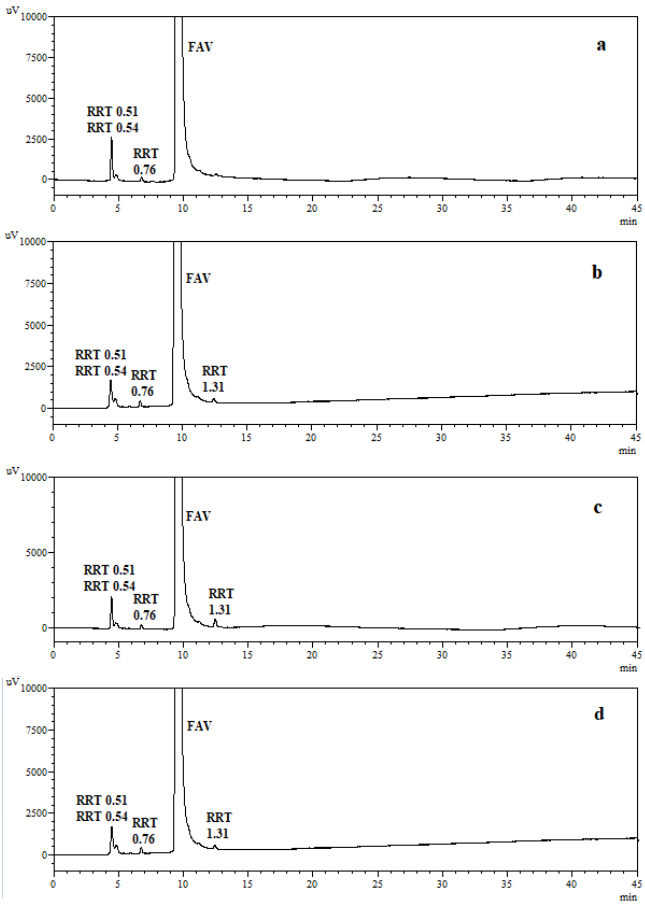

Figure 5. Chromatograms obtained under normal conditions (a), thermal (b), humidity (c) and photolytic (d) stress conditions.

CONCLUSION

Different medications were required by countries to treat the Covid-19 virus sickness, which can have a rapid and serious impact on public health. Drugs containing the FAV active ingredient were also used in this period. Currently, it is imperative for nations to manufacture these medications, and analytical techniques capable of guaranteeing the drug's quality are required. The method outlined in this study was developed to respond to this requirement. The developed method has some advantages including separating more than one impurity that does not interfere with the active ingredient of FAV, contributing to green chemistry with the use of a small number of organic solvents, and having a shorter analysis time compared to the analytical methods that determine impurities. Moreover, the developed method contributed to the analysis efficiency with low buffer solution concentration.

When the developed method is compared with the method given in Chinese patents, (Guangling et al., 2015 and Guangking et al., 2016) the method of the patent with an analysis time of 60 minutes is longer than the developed method. The LOD value of the patent method was reported as 0.1%. In the developed method, the LOD: 0.002%; R^2 was obtained as 0.9998. These values show that the linearity of the method and the detection limit are better than the Chinese patent methods. In the stability-indicating method published by Ali et al. (Ali et al., 2021), impurities were not identified one by one, and the degradation results were not published in detail. With the developed method, the impurities that occur in FAV and pharmaceutical preparations containing this active ingredient can be determined together and the conditions under which these impurities are formed can be explained supported by the results obtained from detailed degradation and stress studies.

In the developed method, the retention time of FAV was 9 minutes and the retention times of major impurities formed in alkaline, acidic, and oxidative conditions were approximately 4, 5, 7, and 12 minutes (RRT 0.51, 0.54, 0.76, 1.31). The total run time was completed in 25 minutes. The RSD% values of the method were obtained as 0.25 and the consistency between the results was supported by statistical tests. An average recovery of the active substance was 99.46% achieved with 5.03% RSD. The optimum time for which the sample solutions remained stable under HPLC conditions was found to be 2 hours, and for this reason, the sample solutions were given to the HPLC system immediately after preparation.

To determine the applicability of the validated method, pharmaceutical preparations containing FAV were kept under alkaline, acidic, oxidative conditions and exposed to high temperature, humidity, and photodegradation. Then, the impurity analyses of the pharmaceutical solid dosage form were successfully carried out with the developed method. Major impurities were detected in alkaline, acidic, and oxidative conditions. Although the impurities that increased when the same pharmaceutical preparations were kept under high temperature, humidity and light could be detected separately and the impurities formed remained below each unknown impurity limit (0.10%). This result showed that the preparations were resistant to these stress conditions. Since the analytical methods in which the impurity determination is given in detail with the degradation studies are not included in the literature, the developed method could not be compared from this perspective.

In conclusion, an HPLC method with high efficiency, reproducibility, and reliability was developed that can determine FAV and possible degradation impurities in solid dosage form. The developed method can be preferred in the pharmaceutical industry for its ease of use in the impurity analysis of pharmaceutical preparations containing FAV-active ingredients produced for antiviral treatment.

Peer-review: Externally peer-reviewed.

Author Contributions: Conception/Design of Study- S.E.T., B.G.; Data Acquisition- B.G.; Data Analysis/Interpretation- B.G.; Drafting Manuscript- S.E.T., B.G..; Critical Revision of Manuscript- S.E.T.; Final Approval and Accountability- S.E.T., B.G..

Conflict of Interest: The authors have no conflict of interest to declare.

Financial Disclosure: The authors declared no financial support.

Note: Section Editor was not involved in the evaluation and peer-review processes of the article. These processes were carried out by the Editor-in-Chief and the member editors of the editorial management board.

ORCID IDs of the authors

Büşra Gülşen 0000 0002 7029 8004
Sıdıka Ertürk Toker 0000 0002 6827 8362

REFERENCES

Ali, S.N.S., Mobina, L., Mehfuza, M., Seema, P., Ahmed, A., & Khan, G.J. (2021). Analytical method development and validation and forced degradation stability-indicating studies of favipiravir by RP-HPLC and UV in bulk and pharmaceutical dosage form. *Journal of Pharmaceutical Research International, 33*, 254-271. doi: 10.9734/JPRI/2021/v33i48B33283

Baranovich, T., Wong, S. S., Armstrong, J., Marjuki, H., Webby, R. J., Webster, R. G., & Govorkova, E. A. (2013). T-705 (favipiravir) induces lethal mutagenesis in influenza A H1N1 viruses in vitro. *Journal of Virology, 87*(7), 3741-3751. doi:http://dx.doi.org/10.1128/JVI.02346-12T

Bulduk, İ. (2020). HPLC-UV method for quantification of Favipiravir in pharmaceutical formulations. *Acta Chromatographica*, 33, 209-215. doi:10.1556/1326.2020.00828

Cuiyan, L., Yuanyuan, Z., Lichao, B., Yangjin, L., & Lei, L. (2015).

Content determination of favipiravir tablets by HPLC. *China Pharmacist*, 7, 1231-1233.

Delong, L., Abdelnabi, R., & Neyts, J. (2018). Favipiravir as a potential countermeasure against neglected and emerging RNA viruses. *Antiviral Research*, 153, 85-94. doi:10.1016/j.antiviral.2018.03.003

Dolan, J. (2011) (Accessed 2 March 2021) A Guide to HPLC and LC-MS Buffer Selection, https://www.hplc.eu/Downloads/ACE_Guide_BufferSelection.pdf.

Drugbank, Favipiravir (2021, March 1), https://go.drugbank.com/drugs/DB12466

Guangling, F., Wenjuan, D., Yuxiao, D., Ren-Yang, Z., Yan, G., Chong-Gang, D., & Jinrui, S. (2015). HPLC method for measuring related substances in Favipiravir (Chinese Patent No CN104914185A). Shandong Academy of Pharmaceutical Sciences, https://patents.google.com/patent/CN104914185A/en

Guangling, F., Wenjuan, D., Yuxiao, D., Ren-Yang, Z., Yan, G., Chong-Gang, D., & Jinrui, S. (2016). A kind of Favipiravir has the HPLC assay method of related substance (Chinese Patent No. CN104914185B) Shandong Academy of Pharmaceutical Sciences, https://patents.google.com/patent/CN104914185B/en

Guidance for Industry ANDAs: Impurities in Drug Products, Food and Drug Administration, (2010) (Accessed 23 March 2021) https://www.fda.gov/files/drugs/published/ANDAs–Impurities-in-Drug-Products.pdf

ICH Q2 (R1):Validation of Analytical Procedures: Text and Methodology, 2005, European Medicines Agency, (Accessed 12 March 2021) https://www.ema.europa.eu/en/documents/scientific-guideline/ich-q-2-r1-validation-analytical-procedures-text-methodology-step-5en.pdf

Kiso, M., Takahashi, K., Sakai-Tagawa, Y., Shinya, K., Sakabe, S., Le, M., Ozawa, M., Furuta, Y., Kawaoka, Y. (2010). T-705 (Favipiravir) Activity against Lethal H5N1 Influenza A Viruses. *Proceedings of the National Academy of Sciences of the United States of America*, 107, 882-887. doi: 10.1073/pnas.0909603107

Megahed, S. M., Habib, A. A., Hammad, S. F., & Kamal, A. H. (2020). Experimental design approach for development of spectrofluorimetric method for determination of favipiravir; a potential therapeutic agent against COVID-19 virus: Application to spiked human plasma. *Spectrochimica Acta Part A: Molecular and Biomolecular Spectroscopy*, 249, 1386-1425. doi:10.1016/j.saa.2020.119241

Japan Pharmaceuticals and Medical Devices Agency, 2014 Report on the deliberation results, Avigan 200 mg Tablet, (Accessed 31 December 2020) https://www.pmda.go.jp/files/000210319.pdf

Turkish Republic Ministry of Health, Covid-19 Information Platform, What is Covid-19? (December 2020) https://covid19.saglik.gov.tr/TR-66300/covid-19-nedir-.html

Yegorova, A. V., Scrypynets, Y. V., Leonenko, I. I., Umetskaya, I. V., & Voitiuk, O. D. (2020). Determination of favipiravir residues on the surfaces of pharmaceutical manufacturing equipment by HPLC, luminescence and spectrophotometry. *Odesa National University Herald Chemistry*, 25, 45-55. doi:10.18524/2304-0947.2020.4(76).216925

Watanabe, T., Kiso, M., Fukuyama, S., Nakajima, N., Imai, M., Yamada, S., . . . Kawaoka, Y. (2013). Characterization of H7N9 influenza A viruses isolated from humans. *Nature*, 501, 551-555. doi:10.1038/nature12392

How cite this article

Gülşen, B., & Ertürk Toker, S. (2024). Development and validation of stability indicating HPLC method for favipiravir used in the treatment of the Covid-19 disease. *İstanbul Journal of Pharmacy, 54*(2), 223–232. DOI: 10.26650/IstanbulJPharm.2024.1368223

İstanbul Journal of Pharmacy
Istanbul J Pharm2024, 54 (2): 233–239
DOI: 10.26650/IstanbulJPharm.2024.1349707

Original Article

Caffeine analysis in urine by gas chromatography mass spectrometry: A non-derivatization detection and confirmatory method

Eylem Funda Göktaş[1], Erol Kabil[1]

[1]İstanbul Pendik Veterinary Control Institute, Department of Pharmacology, Doping Control Laboratory , İstanbul, Türkiye

ABSTRACT

Background and Aims: Caffeine is a xanthine alkaloid found naturally in plants. Caffeine has cardiotonic and stimulant effects in humans and animals. For this reason, caffeine is on the monitoring list for human sports and is listed as a feed contaminant in horse racing. The aim of this study was to develop a rapid, practical, and specific method for the determination of caffeine in horse urine.

Methods: In the new method, the pH of the sample was adjusted by the addition of phosphate buffer, and after solid phase extraction, it was dissolved in methanol before being analysed by gas chromatography mass spectrometry without derivatization. The method was validated according to the European Commission's 2002/657/EC criteria.

Results: The effects of different cartridge brands, pH, and elution solution were determined. Intraday and interday CV% values are 2.8 and 5.2 for the International Residue Limit (IRL), respectively. Five levels (blank, 0.5xIRL, IRL, 1.5xIRL, and 2xIRL) were used in constructing the curve, and the R2 value was greater than 0.99. The analysis run was 11.8 min. The decision limit (CCα) was determined to be 56.7 ng/mL due to IRL. The detection limit of the method was calculated to be 3.3 ng/mL. The method was determined to be robust according to changes in extraction pH, phosphate buffer concentration, centrifugation time, hexane volume in the wash step, different grades of methanol, inlet temperature, and operator.

Conclusion: The applicability of the method was demonstrated by analysing positive and negative horse urine samples. Validation parameters showed the method to be selective, specific, and easy to apply.

Keywords: Caffeine, Gas chromatography-mass spectrometry, Urine

INTRODUCTION

Caffeine is a methylxanthine alkaloid that is naturally found in the environment (Greene, Woods, & Tobin, 1983). Due to its widespread use, caffeine can also be present in the metabolism as a result of environmental contamination. Pharmacologically, caffeine is an effective cardiotonic and diuretic for horses as it possesses pronounced effects on the central nervous system (Aramaki, Suzuki, Ishidaka, Momose, & Umemura, 1991). The International Federation of Horseracing Authorities (IFHA) has determined a 50 ng/mL residue limit for caffeine in horseracing due to the possibility that feed may contain caffeine contamination and environmental factors may affect its levels. In human sport, due to its positive effect on the cardiorespiratory system and brain functions, caffeine limit was determined above 12 µg/mL concentration from 1984 to 2004, but now it is on the World Anti-Doping Agency's monitoring list only (Büyüktuncel, 2010; Russo et al., 2018). Moreover, caffeine is listed chemicals with high production volumes of the United States Environmental Protection Agency and Food and Drug Administration regulations require beverage companies to list caffeine in the ingredients list on product labels ('CFR - Code of Federal Regulations Title 21', n.d.). Therefore, caffeine must be analysed in various matrices, and new and current methods are continually being developed.

Among the various sources of caffeine, tea leaves, coffee beans, cola nuts, and cocoa beans/leaves are widely consumed by humans (Shrivas & Wu, 2007). Caffeine is a polar characterised compound with the structure of xanthine (Figure 1). Because of its common use and presence in most plants, qualitative and/or quantitative analysis in biological samples (plasma, urine, etc), wastewater, feed, food products, and beverages is routinely performed. According to previous studies, by far the most common method of analysis has been the use of UV (ultraviolet) or MS (mass spectrometry) detectors coupled to liquid chromatography. However, the use of gas chromatography to analyse caffeine is quite limited notably in biological samples.

Corresponding Author: Eylem Funda Göktaş **E-mail:** eylemfundagoktas@gmail.com
Submitted: 25.08.2023 • **Revision Requested:** 23.10.2023 • **Last Revision Received:** 16.05.2024 • **Accepted:** 21.05.2024

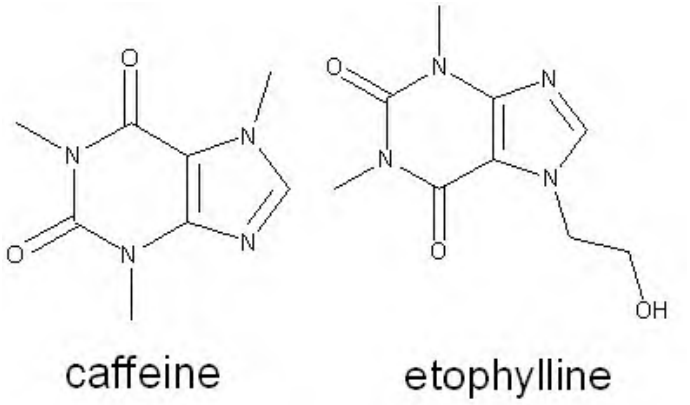

Figure 1. Structure of caffeine and etophylline

trometry allows trace-level, reproducible, and high-accuracy analyses.

Chromatographic determination requires the preparation of samples with liquid–liquid extraction (LLE) (Büyüktuncel, 2010; Del Coso et al., 2011; Ventura et al., 2003) or solid-phase extraction (SPE) (Thomas & Foster, 2004; Verenitch & Mazumder, 2008) as part of the sample preparation process, especially for biological samples. The presence of non-active substances such as salt, acids, bases, xenobiotics, proteins, nucleic acids, etc., which are factors that may make urine matrix complex, should be removed or minimised prior to chromatographic analysis. To achieve low detection levels, SPE is generally preferred due to its advantages in both extraction and enrichment.

By combining gas chromatography and mass spectrometry, high accuracy, reproducibility, and trace-level results can be obtained. Despite its powerful separation and identification properties, the use of gas chromatography mass spectrometry for the development of caffeine methods is limited. To demonstrate that gas chromatography is a useful alternative method for the analysis of caffeine without the need to derivatize the drug, a novel method has been developed. In this study, we propose a more practical, traceable, and validated caffeine analysis method in urine using gas chromatography mass spectrometry, compared with other available methods.

MATERIAL AND METHOD

Chemicals and Reagents

Reference standards for caffeine and etophylline (7-(β-hydroxyethyl)theophylline) (Internal Standard-IS) were purchased from Cayman Chemical (Michigan, USA). All standards of purity were ≥99%. The Elga-pure lab flex water purification system (Elga-Veolia Water Solutions&Technologies, UK) was used for water deionisation. n-hexane was purchased from VWR Chemicals (VWR International Fontenay Sous Bois, France). Chloroform and methanol were obtained from J.T. Baker (Gliwice, Poland). Potassium dihydrogen phosphate was purchased from Merck (Darmstadt, Germany). All chemicals were of analytical grade purity.

The automated solid-phase extraction (SPE) system was procured from Gilson (Gilson Aspec GX274 and operated by Trilution LH software). The SPE cartridge (UCT Xtract C18 Reverse Phase Hydrophobic Sorbent 500 mg/3 mL) was obtained from UCT (Philadelphia, USA). A vortex mixer (Allsheng MTV-100), laboratory centrifuge (Thermo Scientific Heraeus Cryofuge 5500i), and nitrogen evaporator (Biotage Turbo Vab LV) were used.

Urine samples (drug free samples), which were used for fortifying, were obtained from post-race samples that were free of the target analytes. The official samples were taken from post-race samples that were declared positive or negative after an accredited analysis. The Pendik Veterinary Control Institute Animal Experiments Local Ethics Committee approved this study (Approval no:08/2022-275).

Instrumental

GC-MS analyses were performed on an Agilent 7890A GC, 5975C mass spectrometer, and 7683 autosampler equipped with a bonded-phase fused-silica DB-5MS column (30 m length, 0.25 mm internal diameter, 0.25 µm film thickness, Agilent J&W, USA). Helium was used as the carrier gas at 1.0 mL/min, and the injection volume was 1 µL. The injection mode was splitless, the injector was heated at 300°C, and the transfer line temperature was 280°C. The temperature programme was 100°C (0.5 min), 100°C to 220°C (20°C/min), and 220°C to 300°C (15°C/min) and held for 5 min with a post temperature of 300°C (5 min). The run time was 11.8 min. The MS quadrupole and source temperatures were 150°C and 230°C, respectively. Screening analyses were performed in the Selective Ion Monitoring (SIM) acquisition mode with the monitoring

of characteristic ions for caffeine (m/z:194, 109, 82, 67) and etophylline (m/z:180, 224, 193, 95).

Preparation of the solutions

The primary stock standard solution was prepared in methanol at a caffeine concentration of 1 mg/mL of caffeine. A working solution of caffeine was prepared by diluting 100 µL of stock solution to 10 mL (10 µg/mL). Etophylline (IS) was prepared in methanol at a concentration of 50 µg/mL. All standard solutions were stored at 20°C in amber flasks.

Sample preparation

A total of 5 mL of urine sample was taken into a polypropylene tube. 25 µL of IS (50 µg/mL) and 4 mL phosphate buffer (1.0 M, pH 6) were added and mixed before centrifugation (4400 rpm, 15 min). The extraction procedure was modified according to a previously published method (Göktaş, Kabil, & Arıöz, 2020). The tubes were placed into an automated solid phase extraction device. Cartridges were preconditioned with 2 mL deionised water and 2 mL of methanol before loading the samples. The cartridge was then washed with 3 mL deionised water and 6 mL hexane and dried for 2 min. The analytes were eluted with 5 mL of chloroform and evaporated to dryness (N_2, 45°C). Before transfer to a vial, 50 µL of methanol was added to the sample, which was then mixed for 3 min. Subsequently, 1 µL of the sample was injected into the GC-MS system.

Parameters of validation

The method was validated according to the requirements of the guidelines of the European decision 2002/657/EC directive. The validation parameters for quantitation of confirmatory methods for authorised substances included precision, recovery, accuracy, linearity, decision limit (CCα), relative matrix effect, robustness and stability (Official Journal of the European Union, 2021).

For validation, linearity was calculated by preparing five levels (Blank, 0.5xIRL, IRL, 1.5xIRL and 2xIRL) of matrix-matched calibration curves. Drug-free samples were loaded with 25, 50, 75, and 100 ng/mL of caffeine and analysed on 3 separate days (n=6). These results were used to determine the precision, accuracy, and recovery.

For the calculation of LOD and LOQ, 10 samples were analysed after being fortified with 5 ng/mL (S/N>3) caffeine concentration and calculated according to the formula below.

$LOD=3x(sd/\sqrt{10})$

$LOQ=10x\ (sd/\sqrt{10})$

For the calculation of CCα, 20 blank samples were fortified at the IRL level (50 ng/mL) of caffeine and analysed. CCα was calculated by adding the obtained standard deviation multiplied by 1.64 to the mean value of the results. Six different blank and fortified urine samples analysed for selectivity. Robustness was determined by applying minor changes in the sections of analysis. In the stability study, a working solution was prepared and an appropriate volume of drug-free urine was fortified with 100 ng/mL caffeine. After the first analysis, fortified samples (containing 100 ng/mL caffeine) and working solutions (containing 5 µg/mL caffeine) were divided into three parts and stored at -20ºC (deep freezer), +4ºC (refrigerator) and +20ºC (room temperature). For calculation of the matrix effect, 20 blank samples were fortified after extraction with caffeine at the IRL concentration and compared with the same concentration of the pure solution of analyte. The matrix factor (standard normalised for IS) was calculated as follows.

MF (standard)=peak area of post-extraction/peak area of solution standard

MF (IS)= peak area of post-extraction IS/peak area of solution IS

MF (standard normalised for IS)=MF (standard)/MF (IS)

RESULTS AND DISCUSSION

Method Development

Selection of the internal standard was the first step in the study. Etophylline was chosen as the internal standard because of its structure similar to that of caffeine (Figure 1) and its ability to be detected without derivatization. After IS selection, a SIM method was developed using caffeine and etophylline standards by changing the gradient, flow rate, auxiliary temperature, gain factor, and other instrument parameters.

To select the appropriate cartridge for the extraction step, different brands of products were compared (UCT Xtract, CS-DAU503, and OASIS HLB). The same extraction method was applied to all cartridges. The results of the study showed that C18 cartridges (UCT Xtract) performed well in terms of abundance (Supplementary Material S1). Following this, the pH and eluted solution factors were examined (Supplementary Material S1). Based on the pKa of caffeine (10.4), the pH was adjusted to 6, 7, 8, and 9, followed by extraction after centrifugation. Additionally, acetone, dichloromethane, and chloroform elution solutions were tested and their abundances were compared (Supplementary Material S1). Previous studies have indicated that caffeine is more soluble in chloroform than in other solutions; therefore, chloroform was used for caffeine extraction (Shrivas Wu, 2007). The most effective results were obtained at pH 6 and elution with chloroform (Figure 2).

Validation

The validation parameters were calculated in accordance with the guidelines, and the data obtained are summarised in Table 1. Good linearity was achieved within the range with a correla-

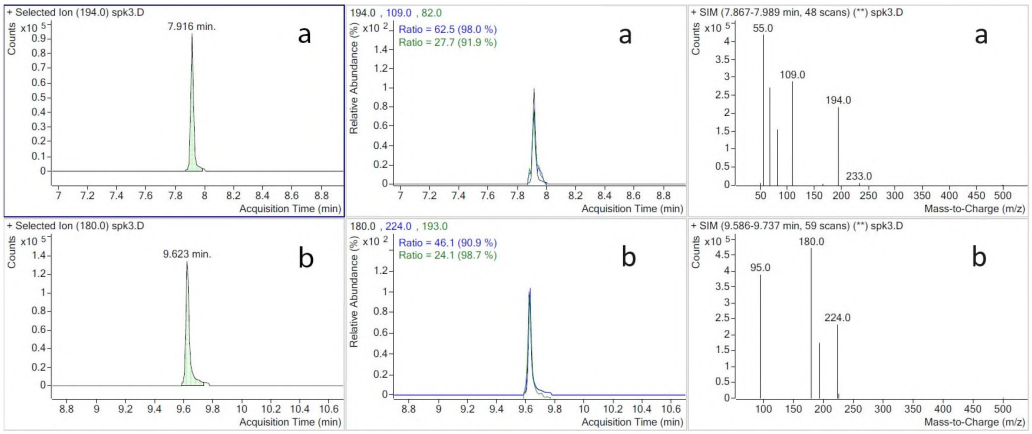

Figure 2. 50 ng/mL caffeine-fortified urine sample GC-MS chromatogram, characteristic ions, and spectra of caffeine (a) and etophylline (b).

tion coefficient (R2) of 0.9988 (Figure 3). The CV% values for precision were less than 16% and the recovery value deviated less than ±10%, which met the criteria of the guideline (Table 1). The low value of the calculated standard deviation for CC was an indication of the reproducibility and robustness of the method. In addition, the limit of detection (LOD) and limit of quantification (LOQ) were calculated to determine the performance of the method. LOD and LOQ were calculated as 3.3 and 10.9 ng/mL.

In a study using gas chromatography to quantify the caffeine concentration in urine doping control, it was concluded that 26.2% of urine samples were below 100 ng/mL, which is the LOD of the study (Del Coso et al., 2011). Therefore, it is important to detect caffeine at lower concentrations. When the current method was compared with other studies in urine (Del Coso et al., 2011; Xiong, Chen, He, & Hu, 2010), it was clear that the method was able to perform analyses with a lower detection limit.

Selectivity and specificity

Chromatograms of blank and fortified urine samples were compared, and no conflicts were detected. Theobromine (structurally similar), tripelennamine, pentoxifylline, tolmetin, pyrilamine, promazine, and zomepirac were fortified with caffeine to control specificity. No interference was detected on the chromatogram.

Robustness

Extraction pH (5 and 6), phosphate buffer concentration (1.0 M and 0.5 M), centrifugation time (15 min and 30 min), hexane volume (6 mL and 3 mL) in the washing step, different grades of methanol (HPLC and MS grade), inlet temperature (300°C and 200°C), and operator were determined and compared for robustness (Supplementary Material S2). According to the Youden test assessment, slight changes in parameter effects were insignificant for the method.

Relative matrix effect

For the evaluation of the matrix effect, the MF was calculated and found to be 1.01. The coefficient of variation of MF was less than 20%, and the relative matrix effect was not found to be significant for caffeine analysis.

Stability

To determine stability, samples were analysed at the end of week 2, week 4, month 3, and month 6 and compared with the results from fresh samples (Table 2). Data obtained were within the ±15% deviation criteria at +20°C after 1 month in the matrix. The results were in accordance with previous studies and revealed that the current method is compatible with other methods and that the results are mutually supportive (Göktaş et al., 2022; Ventura et al., 2003).

Real sample application

Official positive and negative samples were analysed using this method. According to the results, the concentration of real sample 1 was calculated to be 134.1 ng/mL (>56.7), and this sample was declared positive. On the other hand, the concentration of real sample 2 was calculated as 14.2 ng/mL (<56.7). Therefore, this sample was reported as negative. Another laboratory which is using a validated method confirmed these results.. Figure 4 shows a blank, a spiked sample at IRL (50 ng/mL), and the chromatograms of the positive and negative real samples, the product ion (m/z:194.0), two precursor ions (m/z:109.0 and 82.0), and the ion ratios. The results demonstrate the applicability of the method.

Table 1. Validation results for caffeine

Analytes	Fortified Con. (ng/mL)	Corr. coef.(R^2)	Interday (n=6) Measured concentration Mean±SD (ng/mL)	Interday (n=6) Precision CV (%)	Interday (n=6) Recovery (%)	Interday (n=6) Accuracy (%)	Intraday (n=6) Measured concentration Mean±SD (ng/mL)	Intraday (n=6) Precision CV(%)	Intraday (n=6) Recovery (%)	Intraday (n=6) Accuracy (%)	With-in Lab. Rep. (%) CV	CCα (ng/mL) (α=%5)
Caffeine	25.0	0.99	26.2 ± 1.9	7.4	104.7	4.7	26.3 ± 1.7	6.6	105.1	5.1	8.0	56.7
	50.0		48.2 ± 1.3	2.8	96.3	-3.7	48.7 ± 2.5	5.2	97.3	-2.7		
	75.0		76.5 ± 2.6	3.4	102.0	2.0	74.5 ± 3.3	4.4	99.3	-0.7		
	100.0		100.3 ± 2.1	2.1	100.3	0.3	101.1 ± 3.8	3.8	101.1	1.1		

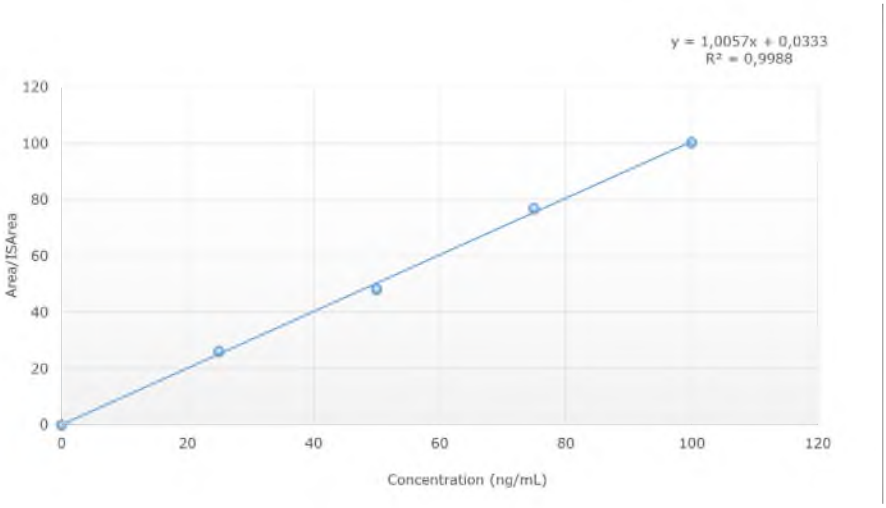

Figure 3. Matrix-matched calibration curve for caffeine

Table 2. Solution and matrix stability results of caffeine (Analyte Remaining (%) = $C_{\text{concentraion at time point}} \times 100/C_{\text{fresh}}$)

	Solution stability			Matrix stability		
Time	-20°C	+4°C	+20°C	-20°C	+4°C	+20°C
2 week	9.9	1.8	7.9	6.4	11.1	1.3
4 week	-3.3	0.1	-2.7	1.4	-5.7	-0.2
3 month	-2.3	-2.6	-4.0	5.4	1.2	-26.7
6 month	3.6	6.3	2.3	2.0	1.2	-35.3

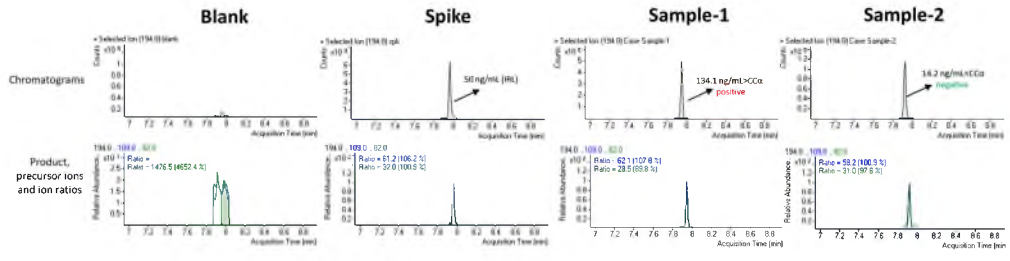

Figure 4. Blank, spiked sample at IRL (50 ng/mL), positive and negative real samples chromatogram, product ion (194.0), two precursor ion (109.0 and 82.0) and ions ratios

CONCLUSION

In summary, a sensitive, simple, and selective GC-MS method for the quantification of caffeine in horse urine has been developed and validated. A number of advantages distinguish this method from previously published methods, such as its low detection and quantification limits, short run time, simplicity, cost effectiveness, and selectivity. Additionally, since derivatization damages columns, the elimination of derivatization extends the column's lifetime and reduces analysis costs. The method has been validated for selectivity, linearity, precision, recovery, accuracy, relative matrix effect, robustness, and stability under various conditions in accordance with Decisions 2002/657/EC and 98/179/EC. Considering these advantages, this method shows promise for the detection of caffeine in various matrices such as wastewater, beverages, biological samples, and other environmental samples.

Ethics Committee Approval: The Pendik Veterinary Control Institute Animal Experiments Local Ethics Committee approved this study (Approval no:08/2022-275).

Peer-review: Externally peer-reviewed.

Author Contributions: Conception/Design of Study- E.F.G., E.K.; Data Acquisition- E.F.G.; Data Analysis/Interpretation- E.F.G.; Drafting Manuscript- E.F.G.; Critical Revision of Manuscript- H E.F.G., E.K.; Final Approval and Accountability- E.F.G., E.K.

Conflict of Interest: The authors have no conflict of interest to declare.

Financial Disclosure: The authors declared no financial support.

ORCID IDs of the authors

Eylem Funda Göktaş 0000-0002-1813-9188
Erol Kabil 0000-0002-0339-0353

REFERENCES

Al-Bratty, M., Alhazmi, H. A., Rehman, Z. U., Javed, S. A., Ahsan, W., Najmi, A., . . . Khalid, A. (2020). Determination of Caffeine Content in Commercial Energy Beverages Available in Saudi Arabian Market by Gas Chromatography-Mass Spectrometric Analysis. *Journal of Spectroscopy, 2020*, 1–9. doi: 10.1155/2020/3716343

Aramaki, S., Suzuki, E., Ishidaka, O., Momose, A., & Umemura, K. (1991). Pharmacokinetics of Caffeine and Its Metabolites in Horses after Intravenous, Intramuscular or Oral Administration. *Chemical & Pharmaceutical Bulletin, 39*(11), 2999–3002. doi: 10.1248/cpb.39.2999

Büyüktuncel, E. (2010). Simultaneous Determination of Theobromine, Paraxanthine, Theophylline, and Caffeine in Urine by Reversed-Phase High-Performance Liquid Chromatography with Diode Array UV Detection. *Analytical Letters, 43*(16), 2518–2524. doi: 10.1080/00032711003731357

Carregaro, A. B., Woods, W. E., Tobin, T., & Queiroz-Neto, A. (2001). Comparison of the quantification of caffeine in human plasma by gas chromatography and ELISA. *Brazilian Journal of Medical and Biological Research, 34*(6), 821–824. doi: 10.1590/S0100-879X2001000600019

CFR - Code of Federal Regulations Title 21. (n.d.). Retrieved 23 June 2023, from https://www.accessdata.fda.gov/scripts/cdrh/cfdocs/cfcfr/CFRSearch.cfm?fr=182.1180&SearchTerm=caffeine

Chi-Hang Chow, Kan, Y.-C., & Ho, K.-S. (2019). A Simple and Rapid Gas Chromatographic Method for Routine Caffeine Determination in Beverages using Nitrogen Phosphorus Detector. *Journal of Analytical Chemistry, 74*(8), 764–770. doi: 10.1134/S1061934819080045

Official Journal of the European Union L 180, (2021) 84-109. Retrieved from https://eur-lex.europa.eu/eli/reg_impl/2021/808/oj. Del Coso, J., Muñoz, G., & Muñoz-Guerra, J. (2011). Prevalence of caffeine use in elite athletes following its removal from the World Anti-Doping Agency list of banned substances. *Applied Physiology, Nutrition, and Metabolism, 36*(4), 555–561. doi: 10.1139/h11-052

Göktaş, E. F., Kabil, E., & Arıöz, F. (2020). Quantification and validation of nine nonsteroidal anti-inflammatory drugs in equine urine using gas chromatography–mass spectrometry for doping control. *Drug Testing and Analysis, 12*(8), 1065–1077. doi: 10.1002/dta.2864

Göktaş, E. F., Kabil, E., Yatanaslan, L., Güneş, E., & Dirikolu, L. (2022). Simultaneous quantification of caffeine and its main metabolites by gas chromatography mass spectrometry in horse urine. *Biomedical Chromatography, 36*(10). doi: 10.1002/bmc.5445

Greene, E. W., Woods, W. E., & Tobin, T. (1983). Pharmacology, pharmacokinetics, and behavioral effects of caffeine in horses. *American Journal of Veterinary Research, 44*(1), 57–63.

Holland, D. T., Godfredsen, K. A., Page, T., & Connor, J. D. (1998). Simple high-performance liquid chromatography method for the simultaneous determination of serum caffeine and paraxanthine following rapid sample preparation. *Journal of Chromatography B: Biomedical Sciences and Applications, 707*(1–2), 105–110. doi: 10.1016/S0378-4347(97)00590-2

Kertys, M., Žideková, N., Pršo, K., Maráková, K., Kmeťová, K., & Mokrý, J. (2021). Simultaneous determination of caffeine and its metabolites in rat plasma by UHPLC-MS/MS. *Journal of Separation Science, 44*(23), 4274–4283. doi: 10.1002/jssc.202100604

Lin, H.-J., Wang, M.-L., Chen, C.-W., Hwang, B.-S., Lee, M.-H., & Choong, Y.-M. (2020). A gas chromatographic method for determination of nicotinamide, paraben esters and caffeine in commercial health drinks, tonic drinks and cold formulas. *Journal of Food and Drug Analysis, 8*(3). doi: 10.38212/2224-6614.2830

Russo, M., Dugo, P., Fanali, C., Dugo, L., Zoccali, M., Mondello, L., & De Gara, L. (2018). Use of an Online Extraction Technique Coupled to Liquid Chromatography for Determination of Caffeine in Coffee, Tea, and Cocoa. *Food Analytical Methods, 11*(10), 2637–2644. doi: 10.1007/s12161-018-1247-5

Schneider, H., Ma, L., & Glatt, H. (2003). Extractionless method for the determination of urinary caffeine metabolites using high-performance liquid chromatography coupled with tandem mass spectrometry. *Journal of Chromatography B, 789*(2), 227–237. doi: 10.1016/S1570-0232(03)00065-5

Shrivas, K., & Wu, H.-F. (2007). Rapid determination of caffeine in one drop of beverages and foods using drop-to-drop

solvent microextraction with gas chromatography/mass spectrometry. *Journal of Chromatography A,* 1170(1–2), 9–14. doi: 10.1016/j.chroma.2007.09.020

Thomas, P. M., & Foster, G. D. (2004). Determination of Nonsteroidal Anti-inflammatory Drugs, Caffeine, and Triclosan in Wastewaterby Gas Chromatography–Mass Spectrometry. *Journal of Environmental Science and Health, Part A*, 39(8), 1969–1978. doi: 10.1081/ESE-120039368

Ventura, R., Jiménez, C., Closas, N., Segura, J., & De La Torre, R. (2003). Stability studies of selected doping agents in urine: Caffeine. *Journal of Chromatography B*, 795(2), 167–177. doi: 10.1016/S1570-0232(03)00557-9

Verenitch, S. S., Lowe, C. J., & Mazumder, A. (2006). Determination of acidic drugs and caffeine in municipal wastewaters and receiving waters by gas chromatography–ion trap tandem mass spectrometry. *Journal of Chromatography A, 1116*(1–2), 193–203. doi: 10.1016/j.chroma.2006.03.005

Verenitch, S. S., & Mazumder, A. (2008). Development of a methodology utilizing gas chromatography ion-trap tandem mass spectrometry for the determination of low levels of caffeine in surface marine and freshwater samples. *Analytical and Bioanalytical Chemistry, 391*(7), 2635–2646. doi: 10.1007/s00216-008-2174-x

Weimann, A., Sabroe, M., & Poulsen, H. E. (2005). Measurement of caffeine and five of the major metabolites in urine by high-performance liquid chromatography/tandem mass spectrometry. *Journal of Mass Spectrometry, 40*(3), 307–316. doi: 10.1002/jms.785

Xiong, J., Chen, J., He, M., & Hu, B. (2010). Simultaneous quantification of amphetamines, caffeine and ketamine in urine by hollow fiber liquid phase microextraction combined with gas chromatography-flame ionization detector. *Talanta, 82*(3), 969–975. doi: 10.1016/j.talanta.2010.06.001

Yang, F., Duan, X., Wang, Z., & Dong, Y. (2022). A Gas Chromatography Flame Ionization Detector Method for Rapid Simultaneous Separation and Determination of Six Active Ingredients of Anticold Drug. *Current Pharmaceutical Analysis, 18*(1), 71–81. doi: 10.2174/1573412917666210106115211

Zou, J., & Li, N. (2006). Simple and environmental friendly procedure for the gas chromatographic–mass spectrometric determination of caffeine in beverages. *Journal of Chromatography A*, 1136(1), 106–110. doi: 10.1016/j.chroma.2006.09.061

How cite this article

Göktaş, E.F., & Kabil, E. (2024). Caffeine analysis in urine by gas chromatography mass spectrometry: A non-derivatization detection and confirmatory method. *İstanbul Journal of Pharmacy, 54*(2), 233–239. DOI: 10.26650/IstanbulJPharm.2024.1349707

İstanbul Journal of Pharmacy
Istanbul J Pharm2024, 54 (2): 240–246
DOI: 10.26650/IstanbulJPharm.2024.1258232

Original Article

Stability indicating HPTLC method development and validation for the analysis of novel nitroimidazole antitubercular drug delamanid

Vaishali Pardeshi[1], Tushar Lokhande[2]

[1]Alard College of Pharmacy Marunji, Pune, India
[2]H.K. College of Pharmacy, Jogeshwari, Mumbai, India

ABSTRACT

Background and Aims: Delamanid is an active drug substance used in efficient treatment for multidrug-resistant tuberculosis (MDR TB). A straightforward, accurate, and precise HPTLC technique has been developed and validated for the study of the delamanid.

Methods: The samples were placed as bands on an aluminium TLC plate covered with silica gel. Delamanid was completely separated using ethyl acetate and n-hexane as the mobile phase; the RF value was 0.51 0.098. At 330 nm, densitometric detection was performed in the absorbance mode. This method led to the discovery of sharp, symmetrical, and well-defined peaks.

Results: A linear correlation was obtained for the concentration range of 200–1200 ng/spot, with a determination coefficient of 0.992. According to the requirements set out by the International Conference on Harmonisation, the method's accuracy, recovery, repeatability, and robustness were all validated. The limit of quantitation was determined to be 349.11 ng/spot, whereas the lowest detectable level was found to be 115.2 ng/spot. This approach permitted the analysis of delamanid in the presence of their degradation products created under various stress conditions, according to the findings of the validation research. delamanid degraded by 20.54% and 35.72% under alkaline and photodegradation conditions, respectively.

Conclusion: The established method might be used to evaluate the stability of delamanid in a commercial pharmaceutical dose form. Regarding HPTLC-induced degradation of delamanid, no prior technique has been documented. This technique was successfully used to quantify the amount of delamanid in its commercially available formulation.

Keywords: HPTLC, Method Development, Validation, Stability indicating method, Delamanid

INTRODUCTION

Delamanid is an effective substance used in the treatment of MDR TB. ®Deltyba is trade name of it. It is the foremost in a new class of TB drugs assigned as nitroimidazole. Chemically, Delamanid is (2R)-2-Methyl-6- nitro-2-[(4-{4-[4-(trifluoromethoxy)phenoxy]-1- piperidinyl} phenoxy) methyl]-2,3-dihydroimidazo[2,1- b][1,3]oxazole, as shown in Figure 1. Delamanid is used to treat people with pulmonary tuberculosis (TB) that is multidrug resistant. By preventing the production of mycobacterial cell wall constituents such as methoxymycolic acid and meromycolic acid, it functions as a prodrug (Field, 2013). For its analysis, no HPTLC technique is available. The objective of this study was to create a repeatable, exact, accurate, and specific HPTLC technique for investigating delamanid. The. According to the ICH guidelines, the developed technique was validated using the criteria of linearity, accuracy, precision, robustness, ruggedness, LOD, and LOQ (Field, 2013; Bahuguna & Rawat, 2020)

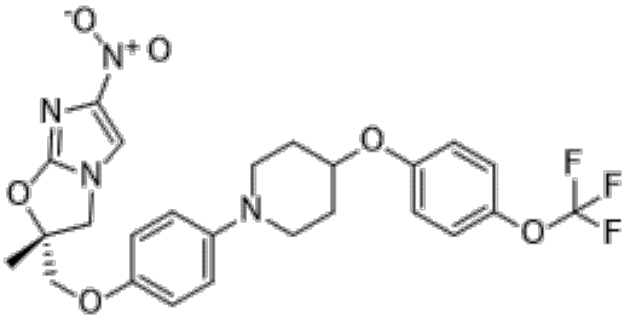

Figure 1. Structure of the Delamanid

Thin layer chromatography is a form of chromatography that

Corresponding Author: Vaishali Pardeshi **E-mail:** vaishali.pardeshi12@gmail.com
Submitted: 01.03.2023 • **Revision Requested:** 01.02.2024 • **Last Revision Received:** 03.02.2024 • **Accepted:** 17.05.2024

separates and analyzes mixtures using an inert backing and a thin stationary phase. Since the mid-1970s, with the introduction of contemporary methodological and instrumental advancements in TLC (known as high performance TLC), the use of this method in qualitative and quantitative analysis of pharmaceutical, environmental, toxicological, food, and agricultural samples has steadily increased. This tendency persists if certain quality control laboratories now frequently use quantitative HPTLC because of this pattern. The following are the main benefits of HPTLC: ease of use, minimal pre-treatment, effectiveness with small amounts of sample, parallel analysis of samples (up to 72 samples can be analysed concurrently and under identical conditions on a 20cm plate), numerous nondestructive detection methods (such as visualization and scan in visible or UV light at different wavelengths), a wide range of developing solvent options and low consumption of solvents. (In fact, the expenses associated with providing solvents and maintenance are much lower compared with HPLC). These benefits, with the method's dependability, sensitivity, and repeatability, make it a viable option for other chromatographic processes like HPLC. In the current work, a straightforward and practical analytical procedure using the HPTLC-densitometric method is described for the identification and quantitative measurement of delamanid in bulk drugs (Le Roux, Wium, Joubert, & Van Jaarsveld, 1992).

MATERIALS AND METHODS

Delamanid pure drug was obtained as a gift sample from Mylan, Hyderabad. HPLC grade Ethyl acetate, methanol, and n-hexane were purchased from Qualigen (India) Ltd., Mumbai, India. All other chemicals are of analytical grade from S.D. Fine Chemical Ltd., World, India. and the volumetric glassware of class A grade were used throughout the experimental work.

Instrumentation

For applying the samples to the HPTLC plate, a Camag Linomat automated sample applicator with a Linomat 100-L syringe 695.0014 was used. Chromatographic separations were performed on 20 20 cm aluminium packed plates that had silica layers pre-coated with 0.2 mm. The plates were developed ascendingly in a Camag twin-trough chamber with a stainless steel top for 20 20 cm plates. On a Camag TLC scanner III running WINCAT software with a D2lamp as the radiation source, densitometric scanning was performed (Ferenczi-Fodor, Renger, & Végh, 2010).

HPTLC analysis

Preconditioning: After selection of the chromatographic layer, plates were prewashed with methanol and then activated at 70°C for 60 min.

Sample application

The samples were spotted using an automated applicator at a constant application rate of 5 s/µL in bands that were 6 mm wide. There were 9 mm between each ring. The distances from the plate's bottom and left edge were maintained at 30 and 20 mm, respectively. Samples were placed under a continuous nitrogen gas drying stream at a constant 150 nL/s application rate.

Selection of suitable mobile phase

Different solvents like acetonitrile, petroleum a ether, formic acid, and methanol were tried in various combinations and compositions. Among them, ethyl acetate: n-hexane (70:30) solvent mixtures was selected for the method development.

Chromatographic development

The tank was saturated for 20 min before the spotted plate was inserted. Under tight light-protected conditions, 10 mL of the mobile phase was used to develop plates. Around 80 mm of development distance was present. Chromatography was conducted at a temperature of 25°C and a relative humidity of 33%.

Detection and scanning

After development, the plate was dried with a dryer for 1 min. Densitometric scanning was then performed in the absorbance mode using a D2 light source at 330 nm (λmax for the compounds). The monochromator bandwidth was maintained at 6 mm, and the dimension of the slit was set at 0.30 mm.

Preparation of stock and working solutions

A stock solution was prepared (1000 µg/mL) by dissolving and diluting 10 mg of delamanid in 10 mL methanol. The solution was sonicated for 10 min.

Calibration curve

The concentration 0.2 µL, 0.4 µL, 0.6 µL, 0.8 µL, 1 µL, 1.2 µL were applied in three replicates on the TLC plate. The spotted plates were developed and scanned as described above. The calibration curve was constructed by plotting average peak areas versus the corresponding amounts, and the regression equation was calculated for Delamanid.

RESULTS AND DISCUSSION

Method Development and Optimisation

Various chromatographic conditions were investigated to attain satisfactory results for the Delamanid qualitative and quantitative analyses. Developing the mobile phase individually on glass and aluminium TLC plate and comparing the results indicated that using aluminium backing plates produces well-defined spots with better resolution. Hence, in this work, aluminium sheet plates recoated with silica gel were selected as the stationary phase.

Method validation

HPTLC was performed as per the International Conference on Harmonization (ICH) guidelines Q2 (R1) linearity, accuracy, precision, robustness, specificity, limit of detection (LOD), and limit of quantitation (LOQ) (ICH, 2005).

Linearity

The linearity of the method was evaluated by constructing calibration curves at six concentration levels. The calibration curve (Figure 2) was plotted over a concentration range of 200–1200 ng/spot (Table 1). Aliquots of the standard working solution of delamanid were applied to the plate (0.2, 0.4, 0.6, 0.8, 1.0 and 1.2 µL/spot). The calibration curves were developed by plotting peak area versus concentrations (n = 6) with the help of the win CATS software. We obtained the linear equation y = 2.6001x + 165.72, where y is area and x is concentration. Figures 3 and 4 show the 2D Densitogram of the Delamanid and the 3D Densitogram of the Delamanid Standard (Rf 0.51 ± 0.098) respectively.

Table 1. Calibration parameters

Sr. No.	Conc.(ng/spot)	Area
1	200	602.4
2	400	1210.1
3	600	1771.5
4	800	2351.4
5	1000	2816.9
6	1200	3162.5

Precision

To assess the three sources of variance, accuracy was measured at three distinct concentration levels of 0.6, 0.8, and 1 µL/spot. When a densitometer measures the same location three times, the accuracy was initially evaluated. The same analyst on two separate days assessed repeatability under the same conditions.

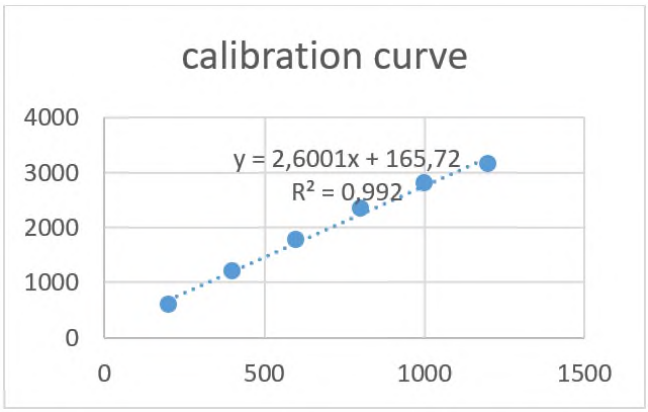

Figure 2. Calibration curve for Delamaid

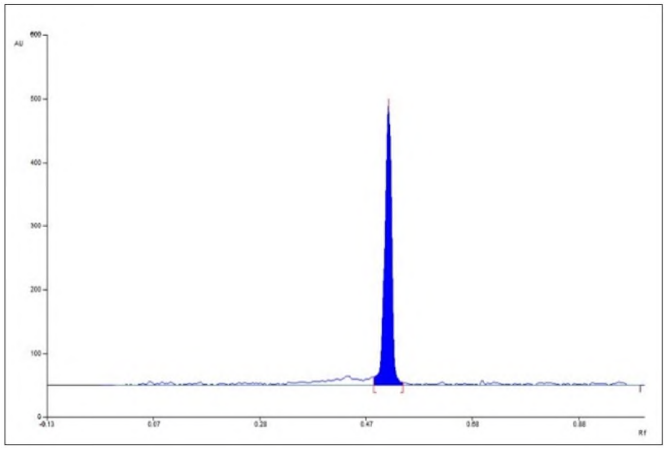

Figure 3. 2D Densitogram of Delamanid

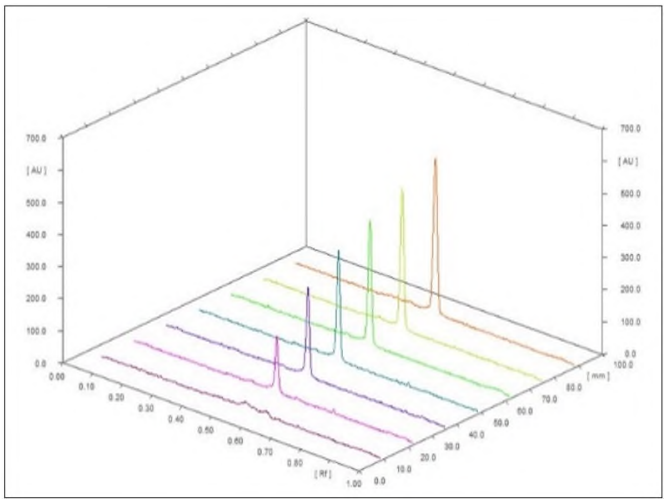

Figure 4. 3D Densitogram of Delamanid Standard (Rf 0.51 ± 0.098)

Second, the same answer is found thrice. The RSD values were under 3%, confirming both the appropriate intermediate accu-

racy and the strong repeatability of sample application and peak area measurement. RSD values between 1% and 5% in TLC densitometry are considered acceptable (Tables 2 and 3).

Accuracy (Recovery studies)

Recovery studies were carried out to assess the accuracy of the method. These studies were conducted at three levels. The percentage recovery was found to be within the limits shown in Table 4.

Robustness

Robustness was determined by altering chromatographic conditions like mobile phase composition as ethyl acetate: n-hexane (60:40). The low value of RSD indicates robustness of the method. The results are shown in Table 5.

LOD and LOQ

The sensitivity of the proposed method was estimated in terms of the limit of detection (LOD) and limit of quantitation. The ICH indicates that LOD (which they call DL, the detection limit) can be calculated as LOD = 3.3σ / S, and the limit of quantification (which they call QL, the quantitation limit) LOQ = 10σ / S. Here σ is the standard deviation of the response and S is the slope of the calibration curve. S is estimated from the slope of the calibration curve for the analyte.(Table 6)

Stress degradation studies of bulk drug

Stability studies were conducted to provide evidence on how the quality of drug varies under the influence of a variety of environmental conditions like hydrolysis, oxidation, and temperature. Dry heat and photolytic degradation were performed in the solid state.

Acid hydrolysis

To 1 ml standard stock solution of drug (1000 µg/ml), 1 ml of 0.1 N HCl was added and the volume was made to 10 ml with Acetonitrile to get 100 µg/ml solution. The solution was kept for 24 h in dark, neutralised with 0.1 N NaOH and 10 µl of this solution was applied to a TLC plate (1000 ng/band concentration). The acid degradation blank is prepared in the same way without using an analyte. Under acid hydrolysis, the percent recovery obtained for Delamanid was 98.74 % with no peak of degradants. A representative chromatogram is shown in Figure 5.

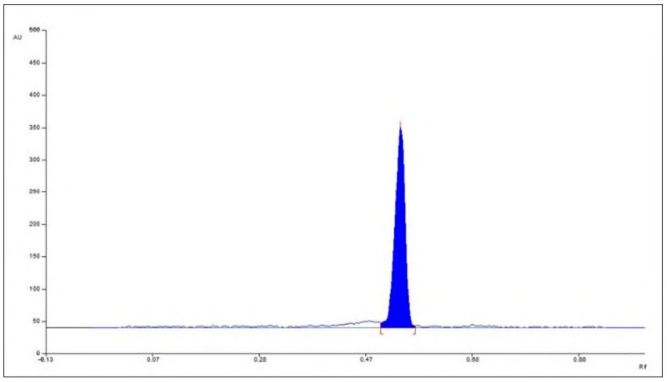

Figure 5. Densitogram of Delamanid after acid degradation

Alkaline hydrolysis

To 1 ml standard stock solution of drug (1000 µg/ml), 1 ml of 0.1 N NaOH was added, and the volume was made to 10 ml with Acetonitrile to get 100 µg/ml solution. The solution was kept for 24 h in dark, neutralised with 0.1 N HCl and 10 µl of this solution was applied to the TLC plate (1000 ng/band concentration). The alkali degradation blank is prepared in the same way without using an analyte. Under alkaline hydrolysis, the percent recovery obtained for delsmani was 79.46 % i.e.20.54 % degradation with one peak of degradants. A representative chromatogram is shown in Figure 6.

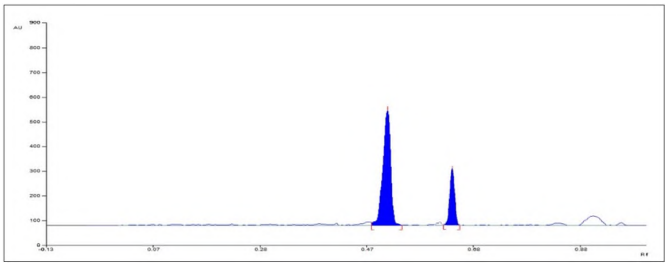

Figure 6. Densitogram of the Delamanid after alkaline degradation

Degradation under oxidative conditions

To 1 ml standard stock solution of drug (1000 µg/ml), 1 ml of 30 % H_2O_2 was added and the volume was made to 10 ml with Acetonitrile to get 100 µg/ml solution. The solution was kept for 24 h in dark and 10 µl of this solution was applied to the TLC plate (1000 ng/band concentration). The blank is prepared in the same way without using an analyte. Under oxidative degradation, the percent recovery obtained for Delamanid was 96.18% with no peak of degradants. A representative chromatogram is shown in Figure 7.

Table 2. Intraday precision results

Sr. no.	Conc. (ng/spot)	Area	Mean	S.D.	%RSD
1	600	1871.5	1872.53	17.6	0.9
2	600	1851.4			
3	600	1894.7			
4	800	2337.5	2348.16	7.73	0.32
5	800	2351.4			
6	800	2355.6			
7	1000	2775.6	2796.73	16.8	0.6
8	1000	2797.7			
9.	1000	2816.7			

Table 3. Interday precision results

Sr. no.	Conc.(ng/spot)	Area	Mean	S.D.	%RSD
1	600	1702.1	1724.1	21.0	1.2
2	600	1752.5			
3	600	1717.7			
4	800	2232.7	2258.6	29.0	1.3
5	800	2244.0			
6	800	2299.1			
7	1000	2655.8	2663.9	17.7	0.6
8	1000	2647.4			
9.	1000	2688.5			

Table 4. Results of recovery studies

%Recovery	Standard API	Admixture	Area	Mean	%Recovery.
50	0.4µl(400ng)	0.2 µl(200 ng)	1702.2	1728.36	100.1
50	0.4µl(400ng)	0.2 µl(200 ng)	1747.1		
50	0.4µl(400ng)	0.2 µl(200 ng)	1735.8		
100	0.4µl(400ng)	0.4 µl(200 ng)	2339.4	2318.83	103.5
100	0.4µl(400ng)	0.4 µl(200 ng)	2309.8		
100	0.4µl(400ng)	0.4 µl(200 ng)	2307.3		
150	0.4µl(400ng)	0.6 µl(200 ng)	2954.4	2922.03	106
150	0.4µl(400ng)	0.6 µl(200 ng)	2918.9		
150	0.4µl(400ng)	0.6 µl(200 ng)	2892.8		

Table 5. Robustness results

Conc.(µL)	Area	Mean	S.D.	R.S.D.
0.6 µL	1630.6	6329	18.3	1.1
0.6 µL	1592.6			
0.6 µL	1632.5			
0.8 µL	2424.6	8188.3	36.02	1.4
0.8 µL	2498.5			
0.8 µL	2419.8			
1.0 µL	2570.3	2560.96	18.7	0.7
1.0 µL	2534.8			
1.0 µL	2577.8			

Table 6. LOD and LOQ

Drug	LOD	LOQ
Delamanid	115.2 ng	349.11 ng

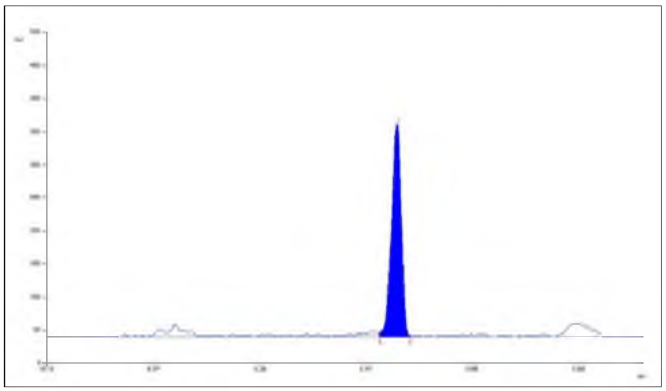

Figure 7. Densitogram of Delamanid after oxidation with 30 % v/v H_2O_2

Degradation under dry heat

In dry heat study drug sample is kept in an oven (1000 C) for a period of 2 h. A sample was withdrawn, 10 mg of it was dissolved in acetonitrile to obtain a solution of 1000 µg/ml and further diluted with Acetonitrile to get 100 µg/ml as final concentration and 10 µl of this solution was applied on a TLC plate (1000 ng/band concentration). Under dry heat degradation conditions, the percent recovery obtained for Delamanid was 98.93 % with no peak of degradants. A representative chromatogram is shown in Figure 8.

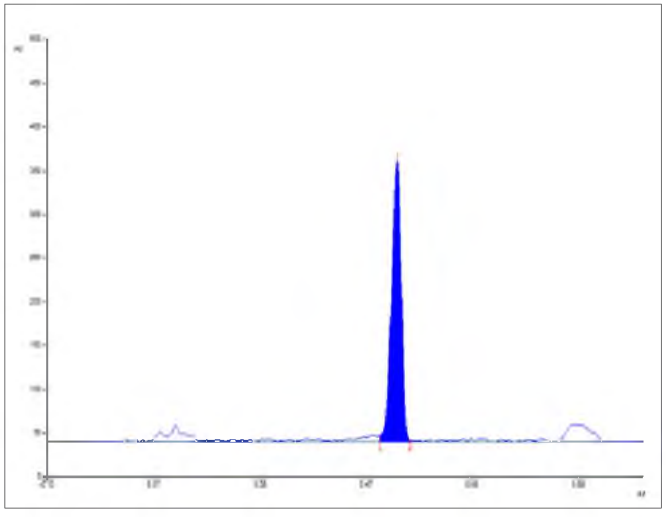

Figure 8. Densitogram of the Delamanid after dry heat degradation

Photo-degradation studies

The photodegradation stability of the drug was studied by exposing the drug to UV light providing illumination of NLT 200 watt hr/m^2 and exposure to cool white fluorescence light of NLT 1.2 million Lux-Hr. After exposure, 10 mg of drug was accurately weighed and transferred to 10 ml of volumetric flask; the volume was made up with Acetonitrile. Further dilution made with Acetonitrile to get 100 µg/ml as final concentration and 10 µl of this solution was applied to the TLC plate (1000 ng/band concentration). An average of 64.28 % of Delamanid was recovered i.e.35.72 % degraded with one peak of degradants after exposure to UV light, and an average of 99.08 % of Delamanid was recovered with no peak of degradants after exposure to fluorescence light. A representative chromatogram is shown in Figures 9 and 10, respectively (Guideline, 1996).

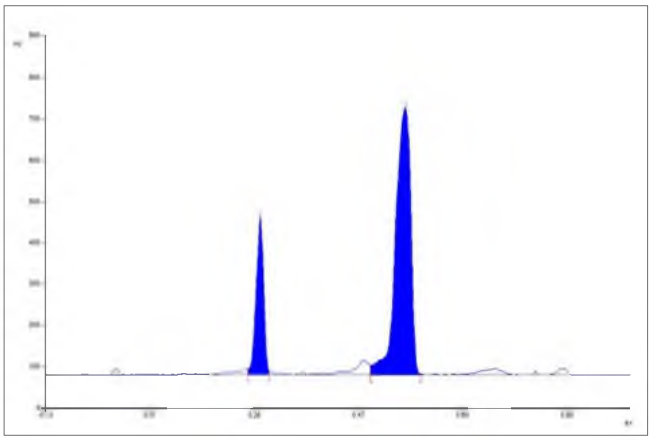

Figure 9. Densitogram of the Delamanid after UV illumination exposure

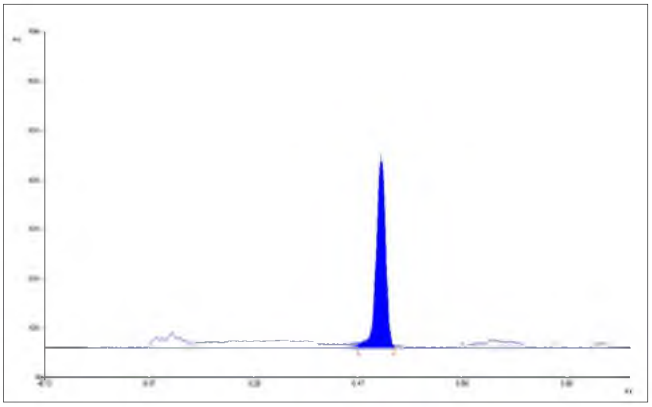

Figure 10. Densitogram of the Delamanid after fluorescent light exposure

Table 7. Summary of Degradation

Stress condition/Duration	% Recovery of the Analyte	RT of the degraded products
Acidic/2 N HClfor 24 h	98.74 %	-
Alkaline/1 N NaOH for 24 h	79.46 %	Degradant at Rf 0.65
Oxidative 30 % H_2O_2 at room temperature for 24 h	96.18 %	-
Dry heat / 100ºC/ 24 h	98.93 %	-
UV illumination NLT 200 W/m2	64.28 %	Degradant at Rf 0.29
Fluroscent light NLT 1.2 10^6 Lux h	99.08 %	-

CONCLUSION

For the examination of Delsmani, a new HPTLC densitometric technique was created, verified in accordance with the ICH criteria, and shown to be repeatable, precise, accurate, and robust. In comparison with other analytical techniques, the process is quick, easy, and moderately affordable. It is also practical enough to be recommended for the regular analysis of the delamanid. For the safety of patients, the quality of pharmaceutical goods is crucial. The presence of degradation chemicals or contaminants affects effectiveness and safety of medications. This study examined Delamanid's forced degradation under ICH-required conditions to examine its degradation profile and clarify the structures of the degradation products. A stability-indicating HPTLC technique that is green, sensitive, accurate, exact, economical, less time-consuming, cost-effective, and repeatable was created. The approaches were shown to be linear, exact, accurate, specific, and selective to the drug in the presence of degradation products in the validation trials. At room temperature, the medication is vulnerable to alkali hydrolytic and photolytic deterioration. The stability indication research was conducted in accordance with ICH Q1A (R2) recommendations.

Peer-review: Externally peer-reviewed.

Author Contributions: Conception/Design of Study- V.P.; Data Acquisition- V.P.; Data Analysis/Interpretation- T.L.; Drafting Manuscript- V.P., T.L.; Critical Revision of Manuscript- V.P., T.L.; Final Approval and Accountability- V.P., T.L.

Conflict of Interest: The authors have no conflict of interest to declare.

Financial Disclosure: The authors declared no financial support.

Acknowledgement: The authors are thankful to Mylan Lab, Hyderabad, India, for providing the gift sample. We are also thankful to the Principal Mahatma Gandhi Vidyamandir's Pharmacy College Panchavati Nashik for providing facilities for conducting this research work.

ORCID IDs of the authors

Vaishali Pardeshi 0000-0001-7636-9363
Tushar Lokhande 0000-0002-0735-3082

REFERENCES

Bahuguna, A., & Rawat, D. S. (2020). An overview of new antitubercular drugs, drug candidates, and their targets. *Medicinal research reviews, 40*(1), 263-292.

Ferenczi-Fodor, K., Renger, B., & Végh, Z. (2010). The frustrated reviewer—recurrent failures in manuscripts describing validation of quantitative TLC/HPTLC procedures for analysis of pharmaceuticals. *JPC-Journal of Planar Chromatography-Modern TLC, 23*(3), 173-179.

Field, S. K. (2013). Safety and efficacy of delamanid in the treatment of multidrug-resistant tuberculosis (MDR-TB). *Clinical Medicine Insights: Therapeutics, 5*, CMT-S11675.

Guideline, I. H. T. (1996). Stability testing: photostability testing of new drug substances and products. *Q1B, Current Step, 4*.

ICH, I. C. H. (2005). Topic Q2 (R1) validation of analytical Procedures: text and methodology. In *Int. Conf. Harmon* (Vol. 1994, p. 17).

Le Roux, A. M., Wium, C. A., Joubert, J. R., & Van Jaarsveld, P. P. (1992). Evaluation of a high-performance thin-layer chromatographic technique for the determination of salbutamol serum levels in clinical trials. *Journal of Chromatography B: Biomedical Sciences and Applications, 581*(2), 306-309

How cite this article

Pardeshi, V., Lokhande, T. (2024). Stability indicating HPTLC method development and validation for the analysis of novel nitroimidazole antitubercular drug delamanid. *İstanbul Journal of Pharmacy, 54*(2), 240–246. DOI: 10.26650/IstanbulJPharm.2024.1258232

İstanbul Journal of Pharmacy
Istanbul J Pharm2024, 54 (2): 247–254
DOI: 10.26650/IstanbulJPharm.2024.1450017

Original Article

Pharmacy students' awareness of LGBT people and related pharmaceutical knowledge levels

Nadir Yalçın[1], Zeynep Güneş[2]

[1]Hacettepe University, Faculty of Pharmacy, Department of Clinical Pharmacy, Ankara, Türkiye
[2]Hacettepe University, Faculty of Pharmacy, Ankara, Türkiye

ABSTRACT

Background and Aims: Historically marginalised by the health care staff, the disproportionate prevalence of health issues among LGBT people and cultural biases can often be overlooked by many practitioners.

Methods: This study aimed to enhance the awareness and knowledge of 4th and 5th year pharmacy students, who are rapidly progressing towards becoming future health care professionals, regarding health issues faced by LGBT people. We conducted a study in January-February 2024 in the form of an e-survey comprising demographics (Section 1), Hudson-Rickett Homophobia Scale (Section 2), and drug knowledge level (Section 3). Section 3 consisted of 19 multiple-choice questions divided into three categories: general illnesses (6 questions), hormone therapies (6 questions), and drug interactions (7 questions), with participants directed to select appropriate responses. Pre- and post-test correct answer rates were compared.

Results: A total of 140 students participated, with 53 from the 4th year and 87 from the 5th year. It was found that 28.6% of participants were identified as homophobic, with a higher percentage observed in males (45.5%) than in females (23.6%) (p=0.043). According to Poisson regression analysis, abeing acquaintedwith an LGBT individual was associated with 1.587 times decrease in the Hudson-Rickett Homophobia Scale score (p<0.001). Evaluation of correct responses to questions measuring drug knowledge revealed an increase in the mean (SD) number of correct answers from 10.31 (2.21) pre-test to 12.39 (2.64) post-test (p<0.001).

Conclusion: The study highlights inadequate education on LGBT health issues, the prevalence of homophobia among more than a quarter of students, and insufficient drug knowledge levels, yet a significant improvement was observed with the provision of brief information.

Keywords: Transgenders, attitude, pharmacotherapy, public health, side effects

INTRODUCTION

LGBT, which stands for Lesbian, Gay, Bisexual, Transgender, and Queer, is an umbrella term representing people in all segments of society, including intersex, asexual, and people who question their sexual orientation. (Hegazi & Pakianathan, 2022). The National Institute on Minority Health and Health Disparities has begun to recognise the LGBT community as a minority community facing inequalities in health care (Pérez-Stable, 2016).

Negative social life, limited knowledge of health providers about LGBT, fear of stigmatisation and marginalisation are barriers to the health of these people (Wang, Miao, & You, 2022). For example, in a survey conducted with LGBT people in Turkey, only 7 out of 278 participants stated that they did not experience any problems while receiving health care services. Approximately two-thirds of the participants stated that they were afraid to share their LGBT status with health providers, one-third stated that they could not get enough information, and one-fourth stated that they encountered negative behaviours when they did (Yasin, Çebi, & Şapçı, 2018).

Health problems that LGBT people are at risk for include depression, substance abuse, obesity, sexually transmitted diseases, cancer, and other chronic conditions that may occur in relation to these diseases. For example, the risk of depression and anxiety in LGBT people is 1.5 times higher than that in the general population (Mandap Madalene, Carrillo, & Youmans, 2014). According to Centres for Disease Control and Prevention (CDC) data, the risk of suicide in LGBT adolescents is five

Corresponding Author: Nadir Yalçın **E-mail:** nadir.yalcin@hacettepe.edu.tr
Submitted: 09.03.2024 • **Revision Requested:** 26.05.2024 • **Last Revision Received:** 27.05.2024 • **Accepted:** 31.05.2024

times higher than that in non-LGBT adolescents ("Disparities in Suicide," 2023).

When cancer is considered as an example of other diseases for which LGBT people are at risk, it is stated that LGBT people have less access to cancer screenings due to the negative behaviours they face in the health system (Banerjee, Staley, Alexander, Walters, & Parker, 2020). However, men who are gay, bisexual, or have sex with men are 80 times more likely to develop HIV or hepatitis-related anal cancer (Mandap Madalene et al., 2014). Studies have shown that lesbian and bisexual women have an increased risk of cancers caused by obesity and alcohol and tobacco addiction (Meads & Moore, 2013; Wakefield, 2021).

Pharmacists are the closest health advisors in the community and have responsibilities in LGBT health, such as providing information to patients about sexually transmitted diseases, improving patient medication adherence, recommending pre-exposure prophylaxis, monitoring hormone therapy in transgender people receiving hormone therapy, and communicating correctly without marginalising these people (Chaudhary, Ray, & Glass, 2021; Grundmann et al., 2020).

The aim of this study was to determine the awareness of LGBT people among the 4th-5th pharmacy students, who are about to graduate, to measure the homophobia scale, to evaluate the level of knowledge about the drugs administered to LGBT people, and to increase the awareness levels of the students with brief information in the survey.

MATERIALS AND METHODS

Study Design

An e-survey was designed for the study targeting fourth- and fifth-year students of Hacettepe University Faculty of Pharmacy. The duration of pharmacy education in Turkey is 5 years; they are preferred in the survey because they are competent compared to other grades. An Informed Consent Form was obtained from the participants in the survey applied in January-February 2024, and the study was approved by the Hacettepe University Health Sciences Research Ethics Committee (decision no: SBA 23/468, decision date: 03/01/2024).

Participation in the survey administered via Google Forms was voluntary. Volunteers were contacted through the students' class groups and class representatives, and an "Informed Consent Form" was presented to the volunteers on the home page of the survey. Volunteers were informed that the questionnaire consisted of three stages, that it would take 15 minutes to answer, and that they could stop answering the questionnaire at any stage. No personal data were collected at any stage of the survey. Announcements were made once in student groups to remind them of the survey. For the students to participate in the survey voluntarily without feeling any pressure, the responsible faculty member did not contact the students.

When the sample size was calculated taking into account the homophobia scale based on similar studies in the literature, it was planned to include a total of at least 122 students, 61 students each from the 4th and 5th grades, with an effect size of 0.60 and a sampling error of 0.05. Since the information presented in the questionnaire concerns occupational sciences, only students in the 4th and 5th grades were included. Thus, the awareness and knowledge levels of students who are close to graduation were evaluated using a questionnaire designed by reviewing the current and scientific literature and considering the core curriculum education.

The first part of this questionnaire, which consists of three parts, consists of questions to find out what grade the students are in, their average age, and whether they have received training on providing health services to LGBT people before. The Hudson and Rickett Homophobia scale was applied in the continuation of the questionnaire, and in the third part of the questionnaire, a 19-question test questioning the medication knowledge of LGBT people was applied, and the questions were divided into three sections. In the first of these sections, general information about LGBT people and disease incidences was included. The second section focussed on the possible side effects of hormone replacement therapy. In the third section, possible interactions that may be observed are mentioned. At the end of each section, information boxes related to the questions were added. The first information box and related questions fofocussedn the problems faced by LGBT people in Turkey while receiving health care services. In addition, diseases and conditions with a higher incidence in these individuals compared with the general population were summarised. The second information box and related questions focussed on the hormone therapies used during the gender reassignment process and the common problems encountered. Finally, the third information box and related questions focussed on the antiretroviral therapies and the common problems encountered with these therapies. After the information boxes, the questions were repeated and it was aimed to evaluate the pre-posttest (pre-posttest) awareness of the students. Such a questionnaire was designed to understand whether the students read the information given in the information boxes with understanding and to determine whether they instantly reflected their understanding of the related questions. At the same time, since there is not enough infrastructure and time to present the information to the students as education, we aimed to obtain instant feedback through the questionnaire. A detailed form of the questionnaire is included in the supplementary material.

Hudson and Rickett Homophobia Scale

In the second part of the questionnaire, the Hudson and Rickett Homophobia Scale, which has been translated from English into Turkish by Sakall and Uğurlu, was used (Arzu Kader Har-

manci Seren et al., 2023). There are 25 questions in the English version of the scale, and the statement "I am not uncomfortable walking around the parts of the city where homosexuals are concentrated" was removed from the Turkish version because it is not suitable for our country. The statements in the scale are scored between 1 and 6. 1 strongly disagree and 6 strongly agree, and the other options that the participants can choose are quite disagree/somewhat disagree/somewhat agree. The Cronbach's alpha value of the questionnaire was found to be 0.94, and its reliability was found to be high. In the scale, 50 points and above are considered increasing homophobia level, and the options scored between 1 and 6 were collected. In the 5th, 6th, 8th, 10th, 11th, 13th, 17th, 18th, 23rd, and 24th statements in the scale, the scores are reversed and summed (Arslantaş, 2017)

Survey Assessment

SPSS Version 23.0 statistical analysis programme was used to determine the demographic characteristics of the participants. As descriptive statistics, the mean and standard deviation or median and minimum-maximum values and interquartile range (IQR) were given for numerical variables and number and percentage values were given for categorical variables. We used the Kolmogorov-Smirnov test and graphical representations to analyse the normality assumption, which is one of the parametric test. In the comparison of numerical data, Student's t-test was used for normally distributed data, Mann–Whitney U test was used for non-normally distributed data, and Chi-Square test was used for the comparison of ratios. The relationship between numerical variables was analysed using the appropriate correlation test (Pearson or Spearman). Poisson regression analysis, a statistical analysis used to quantify the relationship between a criterion variable and one or more predictor variables, was used to determine the nature of the relationship between the variables. The pre- and post-information responses of pharmacy students were analysed by Wilcoxon test. The McNemar test was used to measure the significance of the change in the two-group dependent two-sample test. $p<0.05$ was considered statistically significant.

RESULTS

Demographic Characteristics

There were 146 students in the 4th grade and 162 students in the 5th grade, resulting in a total of 308 students in pharmacy school, and the survey participation rate was found to be 45.45%. A total of 140 students participated in the survey, 53 of whom were fourth graders and 87 of whom were fifth graders. When their biological sex was analysed, most of the students in both classes were female. When asked about their sexual orientation, the majority of respondents stated that they were heterosexual. When asked if they knew any LGBT people in their neighbourhood, 72.8% answered "yes". When asked whether they found the education provided in their faculty for these people adequate, only 11 students answered "yes". Finally, when asked if they were confident in providing health care services to these people, 30.2% of fourth graders and 37.9% of fifth graders answered "yes" (Table 1).

Hudson and Rickett Homophobia Scale

The answers given to 24 questions on the Hudson and Rickett Homophobia Scale vary in both classes. Although there is variability in the answers given to each question, there is no significant difference when the total score is compared in both classes. At the same time, when the participants were divided into two categories as homophobic and non-homophobic according to the predictive value, although there was no significant difference, 17 (32.1%) participants from the 4th grade and 23 (26.4%) participants from the 5th grade were homophobic individuals ($p>0.05$) (Table 2).

Assessment of the Drug Knowledge Level

According to the results obtained in the third and last part of the questionnaire to evaluate and increase the drug knowledge levels of the students in LGBT people, the general disease knowledge levels (1st information box), knowledge levels about hormone therapies (2nd information box), and drug interaction knowledge levels (3rd information box) increased significantly in both classes with the short information given ($p<0.05$). When the average of the total number of correct answers was analysed for both classes, it increased from 10.13 in the 4th grade to 12.72 after the information and from 10.43 to 12.18 in the 5th grade ($p<0.001$). When it is analysed whether the information is useful for the students based on the number of correct answers after reading the information boxes (pre-posttest) regardless of the class distinction, the average number of correct answers increased from 10.31 to 12.39 ($p<0.001$). However, when the number of correct answers of the classes before and after the information was compared separately, no significant difference was found ($p>0.05$) (Table 3).

Correlation and Regression Analyses

When the relationship between being homophobic and biological genders was analysed by chi-square test, 45.5% (15/33) of men were homophobic, while 23.6% (25/106) of women were homophobic ($p=0.043$). At the same time, only 2% (2/100) of non-homophobic and 22.5% (9/40) of homophobic students considered their level of knowledge sufficient ($p<0.001$). Nineteen (18.6%) of the students who acquainted with LGBT people and 21 (55.3%) of those who did not acquaint with LGBT people were in the homophobic category ($p<0.001$). When it was analysed whether being homophobic had an effect on the rate of correct answers given to the related knowledge level questions, it was found that it did not have a significant effect on all three knowledge levels and their total ($p>0.05$).

Table 1. Comparison of demographic characteristics of students

Variables	4th Grade (n=53)	5th Grade (n=87)	p
Age (years), mean (SD)	21.60 (0.66)	22.70 (0.83)	<0.001
Biological sex Female, n (%) Male, n (%) Not wishing to disclose, n (%)	 39 (73.6) 13 (24.5) 1 (1.9)	 67 (77) 20 (23)	 0.422
Sexual orientation Heterosexual, n (%) Bisexual, n (%) Not wishing to specify, n (%) Homosexual, n (%) Pansexual, n (%)	 48 (90.6) 3 (5.7) - - 2 (3.7)	 78 (89.7) 4 (4.6) 3 (3.4) 2 (2.3) -	 0.121
DAreyou acquainted with any LGBT people in your neighbourhood? Yes, n (%) No, n (%)	 40 (75.5) 13 (24.5)	 62 (71.3) 25 (28.7)	 0.729
Have you received any training on providing health care services to LGBT people? Yes, n (%) No, n (%)	 1 (1.9) 52 (98.1)	 - 87 (100)	 0.379
Do you think that the training given in your faculty on this subject is sufficient? Yes, n (%) No, n (%)	 5 (9.4) 48 (90.6)	 6 (6.9) 81 (93.1)	 0.592
Do you feel confident in providing health services to these people? (At the beginning of the survey) Yes, n (%) No, n (%)	 16 (30.2) 37 (69.8)	 33 (37.9) 54 (62.1)	 0.454
Do you feel confident in providing health services to these people? (At the end of the survey) Yes, n (%) No, n (%)	 27 (50.9) 26 (49.1)	 31 (35.6) 56 (64.4)	 0.422

* LGBT: Lesbian, Gay, Bisexual, and Transgender

Table 2. Hudson and Rickett Homophobia Scale

Items, n (%)	Strongly disagree	Disagree	Somewhat disagree	Neither agree nor disagree	Agree	Strongly agree	P
1-I feel uncomfortable being in a homosexual group. 4th Grade 5th Grade	46 (86.8) 20 (23)	6 (11.3) 16 (18.4)	- 15 (17.2)	1 (1.9) 19 (21.8)	- 6 (6.9)	- 11 (12.6)	<0.001
2-I get angry if someone of my own sex shows sexual interest in me. 4th Grade 5th Grade	38 (71.7) 12 (13.8)	11 (20.8) 17 (19.5)	3 (5.7) 14 (16.1)	1 (1.9) 18 (20.7)	- 11 (12.6)	- 15 (17.2)	<0.001
3-I would be disappointed if I found that my child was gay. 4th Grade 5th Grade	38 (71.7) 6 (6.9)	8 (15.1) 9 (10.3)	4 (7.5) 17 (19.5)	3 (5.7) 23 (26.4)	- 14 (16.1)	- 18 (20.7)	<0.001
4-I would be upset if I determined that my brother was gay. 4th Grade 5th Grade	35 (66) 9 (10.3)	13 (24.5) 9 (10.3)	4 (7.5) 13 (14.9)	1 (1.9) 24 (27.6)	- 13 (14.9)	- 19 (21.8)	<0.001
5-I like to participate in social activities with bisexual people. 4th Grade 5th Grade	19 (35.8) 1 (1.1)	12 (22.6) 5 (5.7)	6 (11.3) 12 (13.8)	10 (18.9) 32 (36.8)	4 (7.5) 14 (16.1)	2 (3.8) 23 (26.4)	<0.001

Table 2. Continued

6-I would not be disturbed to learn that my daughter's teacher is a lesbian. 4th Grade 5th Grade	37 (69.8) 9 (10.3)	9 (17) 19 (21.8)	2 (3.8) 12 (13.8)	17 (19.5)	3 (5.7) 11 (12.6)	2 (3.8) 19 (21.8)	<0.001
7-I get bored if someone of my own gender shows sexual interest in me. 4th Grade 5th Grade	40 (75.5) 7 (8)	8 (15.1) 13 (14.9)	3 (5.7) 10 (11.5)	- 17 (19.5)	2 (3.8) 18 (20.7)	- 22 (25.3)	<0.001
8-I would feel comfortable talking to a homosexual at a party. 4th Grade 5th Grade	42 (79.2) 12 (13.8)	7 (13.2) 24 (27.6)	- 21 (24.1)	1 (1.9) 11 (12.6)	- 7 (8)	3 (5.7) 12 (13.8)	<0.001
9-I would be disturbed to learn that my son's male teacher is homosexual. 4th Grade 5th Grade	39 (73.6) 10 (11.5)	8 (15.1) 18 (20.7)	2 (3.8) 11 (12.6)	2 (3.8) 15 (17.2)	2 (3.8) 11 (12.6)	- 22 (25.3)	<0.001
10-I does not mind working with a male homosexual. 4th Grade 5th Grade	48 (90.6) 22 (25.3)	3 (5.7) 20 (23)	1 (1.9) 14 (16.1)	- 11 (12.6)	- 9 (10.3)	1 (1.9) 11 (12.6)	<0.001
11-It does not bother me if a member of my own sex shows sexual interest in me. 4th Grade 5th Grade	33 (62.3) 3 (3.4)	12 (22.6) 8 (9.2)	2 (3.8) 11 (12.6)	3 (5.7) 22 (25.3)	2 (3.8) 15 (17.2)	1 (1.9) 28 (32.2)	<0.001
12-If I find that my child is gay. I will think that I am not a good parent. 4th Grade 5th Grade	48 (90.6) 19 (21.8)	4 (7.5) 29 (33.3)	1 (1.9) 13 (14.9)	- 11 (12.6)	- 7 (8)	- 8 (9.2)	<0.001
13-I do not feel uncomfortable finding someone of my own sex attractive. 4th Grade 5th Grade	32 (60.4) 1 (1.1)	9 (17) 4 (4.6)	4 (7.5) 14 (16.1)	6 (11.3) 18 (20.7)	1 (1.9) 16 (18.4)	1 (1.9) 34 (39.1)	<0.001
14-I am disgusted to see two men holding hands in public. 4th Grade 5th Grade	48 (90.6) 27 (31)	3 (5.7) 20 (23)	- 11 (12.6)	2 (3.8) 9 (10.3)	- 11 (12.6)	- 9 (10.3)	<0.001
15-It would bother me to find that my doctor is gay. 4th Grade 5th Grade	50 (94.3) 27 (31)	2 (3.8) 25 (28.7)	1 (1.9) 8 (9.2)	- 11 (12.6)	- 5 (5.7)	- 11 (12.6)	<0.001
16-It would disturb me to learn that my boss is homosexual. 4th Grade 5th Grade	51 (96.2) 27 (31)	2 (3.8) 25 (28.7)	- 8 (9.2)	- 9 (10.3)	- 7 (8)	- 11 (12.6)	<0.001
17-I would be proud if someone of my own gender showed sexual interest in me. 4th Grade 5th Grade	12 (22.6) 1 (1.1)	9 (17) 3 (3.4)	11 (20.8) 3 (3.4)	13 (24.5) 15 (17.2)	4 (7.5) 25 (28.7)	4 (7.5) 40 (46)	<0.001
18-Working with a female homosexual does not bother me. 4th Grade 5th Grade	45(84.9) 27 (31)	5 (9.4) 16 (18.4)	- 15 (17.2)	- 7 (8)	- 11 (12.6)	3 (5.7) 11 (12.6)	<0.001
19-I feel uncomfortable if my spouse or partner is interested in someoning of his/her own sex. 4th Grade 5th Grade	12 (22.6) 4 (4.6)	5 (9.4) -	3 (5.7) 1(1.1)	7 (13.2) 6 (6.9)	11 (20.8) 22 (25.3)	15 (28.3) 54 (62.1)	<0.001
20-It would disturb me to learn that my neighbour is homosexual. 4th Grade	52 (98.1)	1 (1.9) 20 (23)	- 9 (10.3)	-	- 8 (9.2)	-	<0.001

Table 2. Continued

5th Grade	29 (33.3)			11 (12.6)		10 (11.5)	
21- 21-Ild feel uncomfortable if I was weren in a pub frequented by bisexual people. 4th Grade 5th Grade	38 (71.7) 12 (13.8)	6 (11.3) 16 (18.4)	8 (15.1) 15 (17.2)	1 (1.9) 8 (9.2)	- 15 (17.2)	- 21 (24.1)	<0.001
22-It would disturb me to learn that the religious leader of the religion to which I belong is homosexual. 4th Grade 5th Grade	38 (71.7) 17 (19.5)	7 (13.2) 7 (8)	2 (3.8) 8 (9.2)	2 (3.8) 7 (8)	2 (3.8) 11 (12.6)	2 (3.8) 37 (42.5)	<0.001
23-It would not bother me to find that my best friend of my own sex is gay. 4th Grade 5th Grade	49 (92.5) 19 (21.8)	3 (5.7) 16 (18.4)	- 15 (17.2)	- 4 (4.6)	- 12 (13.8)	1 (1.9) 21 (24.1)	<0.001
24-It does not bother me if people of my own gender find me attractive. 4th Grade 5th Grade	41 (77.4) 5 (5.7)	7 (13.2) 16 (18.4)	2 (3.8) 25 (28.7)	1 (1.9) 6 (6.9)	- 17 (19.5)	2 (3.8) 18 (20.7)	<0.001
Homophobia score, median (min-max) 4th Grade 5th Grade	**33.33 (0-98.33)** **33.33 (1.67-98.33)** **33.33 (0-97.50)**						**0.572**
Weighted score, mean (SD) 4th Grade 5th Grade	**6.24 (4.43)** **6.64 (4.51)** **6.00 (4.39)**						**0.439**
Number of homophobic individuals according to the cut-off value (≥ 50 points), n (%) 4th Grade 5th Grade	**40 (28.6)** **17 (32.1)** **23 (26.4)**						**0.601**

Table 3. Distribution of mean correct answers before and after the three brief informations

	1. Info, mean (SD)			**2. Info, mean (SD)**			**3. Info, mean (SD)**			**Total**		
Grade	*Pretest*	*Posttest*	*P**	*Pretest*	*Posttest*	*P**	*Pretest*	*Posttest*	*P**	*Pretest*	*Posttest*	*P**
4th	4.47 (1.08)	4.85 (0.79)	0.008	2.91 (1.29)	3.92 (1.37)	<0.001	2.75 (1.01)	3.94 (1.56)	<0.001	10.13 (2.09)	12.72 (2.62)	<0.001
5th	4.45 (0.88)	4.66 (0.79)	0.046	3.11 (1.43)	3.94 (1.42)	<0.001	2.86 (1.14)	3.59 (1.36)	<0.001	10.43 (2.28)	12.18 (2.65)	<0.001
P**	0.735	0.130		0.383	0.801		0.866	0.153		0.429	0.167	
Total	4.46 (0.96)	4.73 (0.79)	0.002	3.04 (1.38)	3.94 (1.40)	<0.001	2.82 (1.09)	3.72 (1.45)	<0.001	10.31 (2.21)	12.39 (2.64)	<0.001

*Expresses the p values of the correct answers within classes before and after the information.
**Expresses the p-values of correct answers between classes.

When a Poisson regression analysis was conducted within the framework of demographic characteristics and knowledge levels to predict a student's homophobia score, it was found that having a male gender increased the homophobia score by 1.745 times (p<0.001) and having an LGBT acquaintance decreased it by 1.587 times (p<0.001). No statistically significant relationship was found with the other parameters.

DISCUSSION

To the best of our knowledge, this is the first study to measure the attitudes towards LGBT people, homophobia levels, and knowledge levels of pharmacy faculty students who receive intensive pharmaceutical education and focus on vocational courses in the last years of their education. In our study, while no relationship was found between homophobia and drug knowledge levels, the fact that homophobia was higher in males than in

females and that students who were acquainted with LGBT people had less homophobia were among the striking results.

Pharmaceutical care education for LGBT people is not provided in pharmacy faculties. In this regard, the fact that the majority of the students stated in the survey that they did not receive any training and that the training and themselves were inadequate reveals that such training programmes should be increased. It has been shown that with the LGBT health and practise elective course for pharmacy students in the USA, students have more knowledge about the health resources available for LGBT people and the barriers to treatment and are able to distinguish the health care needs of different members of the LGBT community (Jann, Penzak, White, & Tatachar, 2019). In another study conducted with pharmacy students, students stated that the problems of transgender people should be included in the curriculum (Knockel, Ray, & Miller, 2019). In general, it was observed that with the training provided, students became more confident in communicating with LGBT people and took medical histories of LGBT people more easily (Braun et al., 2017). For this reason, it is emphasised in the literature that training curricula, including LGBT health issues, should be developed and pedagogical practises in the training programmes of health professionals should be improved (Bleasdale, Wilson, Aidoo-Frimpong, Gabriel, & Przybyla, 2024).

Homophobia assessment studies conducted for students studying in health sciences are available in the literature. However, such studies on pharmacy students who will provide pharmaceutical counselling services are extremely limited. According to a study involving 2,531 students from medicine (33.1%), nursing (24.8%), pharmacy (11.9%), and other health sciences (midwifery, nutrition and dietetics, physiotherapy, health institution management) (30.2%) in Istanbul, medical students had the lowest homophobia score, and their mean scores were significantly lower than those of other students. Pharmacy students were the most likely to state that they would not provide health services to LGBT people. Pharmacy students also had the highest Hudson Rickets homophobia score (weighted score=4.09) (A. K. Harmanci Seren et al., 2023). The sociocultural living conditions of the students may have been effective because it was higher in our study (6.24). In addition, unlike this study, a significant difference was found between the genders in our study.

According to a study measuring the general perceptions and attitudes of pharmacy students towards the health of transgender people, 67% did not have confidence in their ability to treat transgender people before the course, while only 20% reported this deficiency after the course (Leach, Seung, & Layson-Wolf, 2019). In our study, while 40% of the students were confident about providing health care services to LGBT people before the information, this rate increased slightly (41.4%) after the information. This situation shows that students' 'elf-confidence in providing health care services to LGBT people is still insufficient. In another thesis study involving pharmacy faculty members, the mean Hudson and Rickets homophobia score was 88.12 for pharmacy and 88.94 for the general population. Although it is promising that the students included in our study as future health professionals have a lower score, it is estimated that it will decrease further with awareness and information training.

In addition to students, studies conducted with academic health professionals who have started their professional life are also included in the literature. According to a study in which the homophobia and knowledge levels of nurse educators in Turkey were evaluated, it was found that half of them had a high level of homophobia and lack of knowledge, and very little effort was made to acquire this knowledge (Aslan, Sahin, & Emiroglu, 2019). According to a thesis study evaluating the attitudes of medical faculty members towards LGBT people, 80.3% of them did not receive any training on this subject and 75% of them were homophobic (Arslantaş, 2017).

Our study has some limitations. Among the limitations of this study are that it was conducted as a single-centred study, other health sciences students were not included, and participation was low due to the sociocultural sensitivity of the subject. In addition, students who agreed to participate in the study were included. Therefore, the findings do not provide clear information about the students who did not participate. However, the knowledge level questions and information boxes in the last part of the questionnaire constitute a unique strength of our study.

CONCLUSION

Pharmacists are at the most convenient position to achieve meaningful changes in the way they treat, counsel, and interact with all patients, including those whose sexual orientation or gender identity is different from their own. It is therefore extremely important that sfuturepharmacists receive adequate education and training that recognises itheirrole in LGBT health and promotes culturally competent and equitable patient care. Therefore, the pharmacy curriculum needs to be revised accordingly. It is also essential that pharmacists address the problems of LGBT people with prescription and non-prescription drugs (non-adherence, adverse effects, drug interactions, drug abuse, etc.). In conclusion, the findings of our study suggest that education is inadequate, homophobia is seen in more than a quarter of the students, and knowledge levels are inadequate but significantly increased with the brief information provided. There is a need for large-scale, comparative studies that reflect the contributions of formal education to the provision of health care services for LGBT people.

Ethics Committee Approval: Ethical approval for the study was obtained from the non-interventional ethics committee of Hacettepe University on 03.01.2024 (Decision no: SBA 23/468).

Informed Consent: Inform consent was obtained from all participants included in the study.

Peer-review: Externally peer-reviewed.

Author Contributions: Conception/Design of Study- N.Y.; Data Acquisition- Z.G.; Data Analysis/Interpretation- N.Y.; Drafting Manuscript- N.Y, Z.G.; Critical Revision of Manuscript- N.Y.; Final Approval and Accountability- N.Y., Z.G.

Conflict of Interest: The authors have no conflict of interest to declare.

Financial Disclosure: The authors declared no financial support.

ORCID IDs of the authors

Nadir Yalçın 0000-0002-2280-8727
Zeynep Güneş 0000-0003-4454-4600

REFERENCES

Aslan, F., Sahin, N. E., & Emiroglu, O. N. (2019). Turkish nurse educators knowledge regarding LGBT health and their level of homophobia: A descriptive-cross sectional study. *Nurse Educ Today, 76*, 216-221. doi:10.1016/j.nedt.2019.02.014

Banerjee, S. C., Staley, J. M., Alexander, K., Walters, C. B., & Parker, P. A. (2020). Encouraging patients to disclose their lesbian, gay, bisexual, or transgender (LGBT) status: oncology health care providers' perspectives. *Translational behavioral medicine, 10*(4), 918-927.

Bleasdale, J., Wilson, K., Aidoo-Frimpong, G., Gabriel, S. J., & Przybyla, S. M. (2024). Lesbian, Gay, Bisexual, and Transgender (LGBT) Health Education in Healthcare Professional Graduate Programs: A Comparison of Medical, Nursing, and Pharmacy Students. *J Homosex, 71*(1), 193-206. doi:10.1080/00918369.2022.2111535

Braun, H. M., Ramirez, D., Zahner, G. J., Gillis-Buck, E. M., Sheriff, H., & Ferrone, M. (2017). The LGBTI health forum: an innovative interprofessional initiative to support curriculum reform. *Med Educ Online, 22*(1), 1306419. doi:10.1080/10872981.2017.1306419

Chaudhary, S., Ray, R., & Glass, B. (2021). Pharmacists' role in transgender healthcare: a scoping review. *Research in Social and Administrative Pharmacy, 17*(9), 1553-1561.

Disparities in Suicide. (2023). Retrieved from https://www.cdc.gov/suicide/facts/disparities-in-suicide.html#LGB

Grundmann, O., Segal, R., Pullo, J., Davis, L., Felix-Irizarry, Y., Da Silva, L., & Holets, T. (2020). The pharmacist as an LGBT ally. *American journal of pharmaceutical education, 84*(7), ajpe7835.

Harmanci Seren, A. K., Eskin Bacaksiz, F., Cakir, H., Yilmaz, S., Sukut, O., Turan, S., & Maghsoudi, N. (2023). A Cross-Sectional Survey Study on Homophobia Among Medical, Nursing, Pharmacy, and Other Health Sciences Students. *J Homosex, 70*(13), 3108-3124. doi:10.1080/00918369.2022.2087480

Harmanci Seren, A. K., Eşkin Bacaksiz, F., Çakir, H., Yilmaz, S., Sükut, Ö., Turan, S., & Maghsoudi, N. (2023). A Cross-Sectional Survey Study on Homophobia Among Medical, Nursing, Pharmacy, and Other Health Sciences Students. *Journal of Homosexuality, 70*(13), 3108-3124. doi:10.1080/00918369.2022.2087480

Hegazi, A., & Pakianathan, M. (2022). LGBT sexual health. *Medicine, 50*(4), 234-238.

Jann, M. W., Penzak, S., White, A., & Tatachar, A. (2019). An Elective Course in Lesbian, Gay, Bisexual, and Transgender Health and Practice Issues. *Am J Pharm Educ, 83*(8), 6967. doi:10.5688/ajpe6967

Knockel, L. E., Ray, M. E., & Miller, M. L. (2019). Incorporating LGBT health into the curriculum: Assessment of student pharmacists' knowledge and comfort level in caring for transgender patients. *Curr Pharm Teach Learn, 11*(9), 928-935. doi:10.1016/j.cptl.2019.07.001

Leach, C., Seung, H., & Layson-Wolf, C. (2019). Student pharmacists' perceptions of transgender health management. *Curr Pharm Teach Learn, 11*(12), 1254-1258. doi:10.1016/j.cptl.2019.09.015

Mandap Madalene, Carrillo, S., & Youmans, S. L. (2014). An evaluation of lesbian, gay, bisexual, and transgender (LGBT) health education in pharmacy school curricula. *Currents in Pharmacy Teaching and Learning, 6*(6), 752-758.

Meads, C., & Moore, D. (2013). Breast cancer in lesbians and bisexual women: systematic review of incidence, prevalence and risk studies. *BMC public health, 13*, 1-11.

Pérez-Stable, E. J. (2016, 04.01.2024). Director's Message. Retrieved from https://www.nimhd.nih.gov/about/directors-corner/messages/message_10-06-16.html

Wakefield, D. (2021). Cancer care disparities in the LGBT community. *Current Opinion in Supportive and Palliative Care, 15*(3), 174-179.

Wang, Y.-C., Miao, N.-F., & You, M.-H. (2022). Attitudes toward, knowledge of, and beliefs regarding providing care to LGBT patients among student nurses, nurses, and nursing educators: A cross-sectional survey. *Nurse Education Today, 116*, 105472.

Yasin, Y., Çebi, M. M., & Şapçı, İ. (2018). Web tabanlı bir araştırmanın düşündürdükleri üzerinden LGBTİ+ sağlığı. *Turkish Journal of Public Health, 16*(2), 106-116.

How cite this article

Yalçın, N., & Güneş, Z. (2024). Pharmacy students' awareness of LGBT people and related pharmaceutical knowledge levels. *İstanbul Journal of Pharmacy, 54*(2), 247–254. DOI: 10.26650/IstanbulJPharm.2024.1450017

İstanbul Journal of Pharmacy
Istanbul J Pharm2024, 54 (2): 255–267
DOI: 10.26650/IstanbulJPharm.2024.1359269

Review Article

Toxicity of serotonin-norepinephrine reuptake inhibitors (SNRIs) during pregnancy and lactation

Göksu Canıtez[1], Rahime Şimşek[2], Deniz Arca Çakır[3], Hülya Tezel Yalçın[4], Terken Baydar[4], Pınar Erkekoğlu[4]

[1]Hacettepe University Graduate School of Science and Engineering, Department of Bioengineering, Ankara, Türkiye
[2]Hacettepe University, Faculty of Pharmacy, Department of Pharmaceutical Chemistry, Ankara, Türkiye
[3]Hacettepe University, Vaccine Institute, Department of Vaccine Technology, Ankara, Türkiye
[4]Hacettepe University, Faculty of Pharmacy, Department of Pharmaceutical Toxicology, Ankara, Türkiye

ABSTRACT

Major depressive disorder (depression) is a severe mood disorder. Lifestyle changes during the COVID-19 pandemic contributed to the high incidence of depression in the population. The primary care treatment is provided by both psychotherapy and antidepressants. In the last 35 years, selective serotonin reuptake inhibitors (SSRIs) were used because of lower adverse effects when compared to tricyclic antidepressants and monoamine oxidase (MAO) inhibitors. However, selective serotonin–norepinephrine reuptake inhibitors (SNRIs), which are second-generation antidepressants, are preferred over first-generation antidepressants by some physicians as they have broad uses nowadays. Anxiety disorders, depression, social phobia, attention-deficit hyperactivity disorder (ADHD), obsessive-compulsive disorder (OCD), fibromyalgia syndrome, chronic neuropathic pain, and menopausal symptoms are among the conditions that can be treated with SNRIs. Although the effects of genetic factors and family history on these diseases, especially recurrence, are undeniable, these drugs provide a great deal of improvement. However, the use of SNRIs during pregnancy and lactation is still a debate. There is no definite judgment on whether a pregnant woman should use these drugs during pregnancy or not. As the rate of depression among pregnant women increases, this issue becomes more serious. A definitive answer has not been reached yet because studies on pregnant women cannot be carried out within the framework of ethical rules. In this review, the effects, toxicity, and safety of SNRIs during pregnancy and lactation are discussed.

Keywords: SNRI, antidepressant, serotonin, norepinephrine, pregnancy, lactation

INTRODUCTION

"Depression (major depressive disorder)" is associated with changes in a person's mood, interests, tastes, and cognitive behavior and with a loss of physical strength (Otte et al., 2016; American Psychiatric Association, 2023). Quality of life is negatively affected by depression (Yang et al., 2021; American Psychiatric Association, 2023). Premature birth, inadequate newborn weight, relapse, and postnatal problems are outcomes of untreated perinatal major depressive disorder and anxiety disorders during pregnancy (Robiyanto et al., 2023). Antidepressants can be prescribed during pregnancy for anxiety and major depressive disorders (Otte et al., 2016). The prevalence of antidepressant usage during pregnancy is estimated to be 3% worldwide for selective serotonin reuptake inhibitors (SSRIs), 0.73% for serotonin and norepinephrine reuptake inhibitors (SNRIs), and 0.38% for tricyclic antidepressants (TCAs) (Molenaar et al., 2020). Although the pathophysiology of depression and the toxic effects of antidepressants are subjects of intense research, there are different hypotheses for the neurobiology of depression, particularly in susceptible period, like pregnancy and lactation. This review will focus on SNRIs, which are second-generation antidepressants. The toxicity and safety of SNRIs are evaluated and their effects during pregnancy and lactation are discussed.

DEPRESSION AND PREGNANCY

"Antenatal depression" defines mild or major depression during pregnancy or a few months after pregnancy ends. This depression can be caused by changing hormonal activities or social and economic conditions. In addition, a family history of depression is an important factor (Ghimire, Papabathini, Kawuki, Obore & Musa, 2021).

Corresponding Author: Pınar Erkekoğlu **E-mail:** erkekp@yahoo.com
Submitted: 12.09.2023 • **Revision Requested:** 20.11.2023 • **Last Revision Received:** 17.01.2024 • **Accepted:** 27.02.2024

SECOND GENERATION ANTIDEPRESSANTS

Today, second-generation antidepressants with high efficacy and selectivity are chosen due to their lower adverse effects on both the mother and the child (Fasipe, 2018). New antidepressants are shown in Table 1.

SEROTONIN–NOREPINEPHRINE REUPTAKE INHIBITORS

SNRIs are compounds that inhibit presynaptic neuronal uptake of serotonin and norepinephrine (Figure 1). This mechanism ensures the activities of monoamines by staying in the central nervous system (CNS) for a longer period (Li et al., 2020).

SNRIs are now utilized as first-choice medications for treating major depressive disorder and anxiety, along with SSRIs. SNRIs provide a faster antidepressant effect compared to SSRIs due to the suppression of serotonin as well as norepinephrine reuptake, which is the primary distinction between SSRIs and SNRIs' mechanisms of action (MoA). Both classes have quite similar pharmacological activities on serotonin. The effect of SNRIs on serotonin is significantly greater than on norepinephrine (Snamina, Wietecha-Posłuszny & Zawadzki, 2019; American Psychiatric Association, 2023). MoA of SNRIs is dose dependent. They act as SSRIs at low doses, whereas norepinephrine reuptake inhibition occurs at higher doses (Fasipe, 2018). The fact that SNRIs suppress reuptake of serotonin as well as norepinephrine, unlike SSRIs, is due to their different affinities and selectivity levels of these two antidepressant class drugs to serotonin and norepinephrine transporters (SERT and NET, respectively) (Dale, Bang-Andersen & Sánchez, 2015).

Like SSRIs, SNRIs are well-tolerated, rapidly effective, and have fewer adverse effects (Fasipe, 2018). SNRIs inhibit the penetration of serotonin and norepinephrine into neurons and thus increase their levels in synaptic space (Banzi et al., 2015). These drugs also show activity in the hypothalamus, *amygdala*, and *locus coeruleus* as stress factors in these regions that are strongly affected by increased norepinephrine secretion. It was suggested that these drugs alter stress response and act in these specific regions of the brain such as the *amygdala* which is responsible for regulating responses to negative situations and activities of norepinephrine pathways located along peptide circuits (Gałecki, Mossakowska-Wójcik & Talarowska, 2018). In a study, it was reported that adverse effects such as nausea, fatigue, and diarrhea appeared in normal doses of SSRIs, while cardiac problems were experienced with increasing doses. This is attributed to the inhibition of norepinephrine reuptake (Park, Kim, Ko & Park,2021).

Globally, SNRIs are prescribed nearly >16 million times in a year (Park et al., 2021). The drugs classified as SNRIs by The Food and Drug Administration (FDA) are duloxetine, venlafaxine, desvenlafaxine, and levomilnacipran. In 2009, the FDA approved the SNRI milnacipran for the treatment of fibromyalgia. It is not used in the treatment of depression in the USA but acts as an antidepressant for treating depression (Lantz et al., 2003).

EFFECTS OF SNRIs DURING PREGNANCY AND LACTATION PERIOD

There is no definitive recommendation for the use of antidepressants during pregnancy. Although this is the case, the use of SNRIs and SSRIs in pregnancy has increased in recent years. However, women who use antidepressants before pregnancy usually discontinue this treatment at the beginning of the pregnancy due to concerns about the use of the medicine during this susceptible period (Zoega et al., 2015).

The hypothesis that SNRIs may pose potential risks in an unborn or newborn baby arises from their ability to pass the placenta and the blood–brain barrier (BBB). They are also secreted to human milk at certain levels. There are concerns that SNRIs can affect the functional development of the brain and can cause neurobehavioral, cognitive, emotional, and mental problems both in perinatal and early postnatal periods (Dubovicky, Belovicova, Csatlosova & Bogi, 2017). In a study, the relationship between antidepressant exposure during the third trimester of pregnancy and the risk of poor neonatal adaptation was investigated. The study's results showed that throughout the third trimester, there was a greater incidence of poor neonatal adaptation with SNRI therapy and antidepressant combination therapy than with bupropion monotherapy (Brumbaugh et al., 2023). Moreover, there are also risks for preterm birth, stillbirth, congenital malformations, low birth weight, seizures and respiratory difficulties, persistent pulmonary hypertension in newborns and infant deaths. In addition, conditions such as feeding and sleep disorders, excessive crying, unbalanced body temperature, vomiting, hypertonia, hypotonia, tremors, restlessness, and lower IQ scores in later life are considered characteristic features in newborns who are prenatally exposed to antidepressants. Infants with these symptoms have a longer hospital stay and need intragastric feeding and respiratory support (Dubovicky et al., 2017).

Although data on whether prenatal exposure to SSRIs/SNRIs causes some birth abnormalities, including heart defects, are conflicting, and persistent pulmonary hypertension (PPHN) in infants has been reported. This is explained by the mechanism suggesting "both SSRIs and SNRIs increase levels of serotonin in fetal circulation and cause vasoconstriction as well as an increase in the infant's pulmonary vascular resistance." (Masarwa et al., 2019).

Pregnant women exposed to SSRIs and SNRIs in the first trimester have a risk of giving birth to an infant with musculoskeletal problems as well as heart, craniofacial, digestive, and respiratory system disorders. Animal experiments suggested that altered serotonin levels could affect organogenesis and morphogenesis. Serotonin is vital for cellular development in early

Table 1. Pharmacological classes of second-generation antidepressants.

Pharmacological Class	Examples
SSRIs	Fluoxetine, Sertraline, Paroxetine, Citalopram, Escitalopram, Fluvoxamine
SNRIs	Venlafaxine, Desvenlafaxine, Duloxetine, Levomilnacipran
SARI	Trazodone, Nefazodone, Vortioxetine
SPARI	Vilazodone
SNRISA with potent antipsychotic D_2 receptor blockade/antagonism	Amoxapine
NRISA	Maprotiline
NASSA	Mirtazapine, Mianserin
NRIs	Reboxetine, Atomoxetine
NDRI	Bupropion
Atypical antipsychotics that exhibit weak D_2 receptor antagonism with potently strong 5-HT_{2A} receptor blockade	Olanzapine, Quetiapine, Risperidone, Lurasidone, Aripiprazole
NMDA-glutamatergic ionoceptor antagonist/inverse agonist/partial agonist that exhibit a direct action on excitatory glutamatergic neurotransmission system	Ketamine

SSRIs, Selective Serotonin Reuptake Inhibitors; SNRIs, Serotonin-Norepinephrine Reuptake Inhibitors; SARI, Serotonin receptor antagonists with serotonin reuptake inhibition; SPARI, Serotonin 5-HT_{1A} autoreceptor partial agonist with serotonin reuptake inhibition; SNRISA, Serotonin-norepinephrine reuptake inhibitor and serotonin receptos antagonism; NRISA, Norepinephrine reuptake inhibitor with serotonin receptors antagonism; NASSA, Noradrenergic α2-receptor antagonist with specific serotonergic receptors-2 and-3 antagonism; NRIs, Selective Norepinephrine Reuptake Inhibitors; NDRI, Norepinephrine-Dopamine Reuptake Inhibitor; NMDA,N-methyl-D-aspartate.

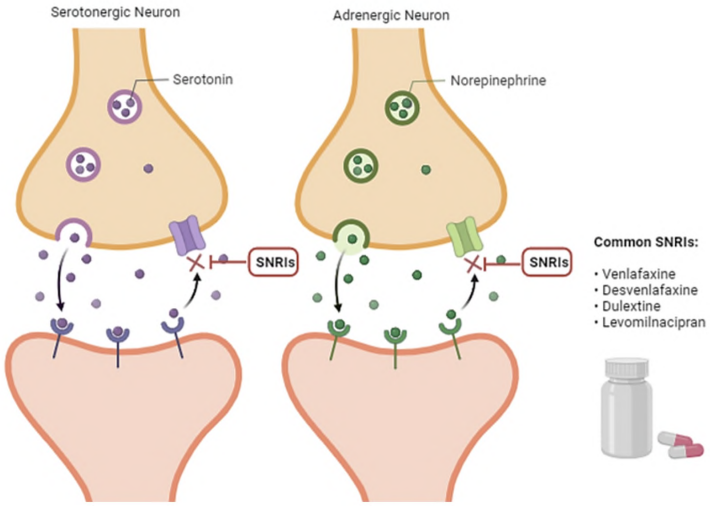

Figure 1. Action mechanism of serotonin-norepinephrine reuptake inhibitors (SNRIs)

organogenesis. Therefore, prenatal alterations in serotonin levels may cause various malformations in the newborn (Bérard, Zhao & Sheehy, 2017).

Although a significant relationship was not found in some studies, a study found an increased risk of ADHD in children of mothers who used antidepressants including SNRIs during their pregnancy (Uguz, 2018). A study on pregnant women prescribed at least two SNRI/SSRI drugs found that their children had a higher risk of developmental problems, such as language, and cognitive development aside from communication problems, lower social competence, and emotional maturity (Singal et al., 2020). Moreover, postpartum hemorrhage with an increase in gastrointestinal bleeding and preeclampsia may arise due to the use of SNRIs during pregnancy (Perrotta et al., 2019). Regarding their biological mechanism, SNRIs are especially anticipated to raise the risk of hypertensive disorders of pregnancy among antidepressants. It was suggested that SNRIs were associated with the risk of preeclampsia during the second trimester of pregnancy (Avalos, Chen & Li, 2015). Also in another study, an elevated risk for hypertensive disorders in pregnant women treated with SNRIs compared to those treated with SSRIs was found (Benevent et al., 2023).

The potential link between the use of antidepressants and metabolic problems has long been a contentious issue. The-

oretically, antidepressants can affect blood glucose levels directly through weight gain, by raising cellular insulin resistance, or by blocking pancreatic insulin production. Antidepressants have been shown to cause hyperglycemia in several animal experiments. Serotonin homeostasis is impacted by serotonin reuptake inhibitors blocking the serotonin reuptake transporter. However, when insulin resistance develops naturally during pregnancy, serotonin compensates this resistance. Their susceptibility to histamine and noradrenergic receptors may increase the incidence of gestational diabetes mellitus. Therefore, in a systematic review and meta-analysis, the gestational diabetes mellitus risk linked to antidepressant treatment during pregnancy was evaluated. The effects of TCAs, particularly amitriptyline, on glucose dysregulation appear to be more significant in the general population than those of SSRIs and SNRIs (Wang, Ying & Jiang, 2023).

FDA evaluates the use of antidepressants during pregnancy on a case–by–case basis, by making a risk–benefit analysis. According to these evaluations, most antidepressants are in category C, which means, "negative effects on fetus have been observed in animal studies, but there are no adequate and good human studies. The drug can only be used during pregnancy if it is essential" (Ray & Stowe, 2014). FDA pregnancy categories of SNRIs are given in Table 2 (Dandjinou, Sheehy & Bérard, 2019).

Amounts of SNRIs in breast milk may differ. Amounts of venlafaxine and desvenlafaxine passing into breast milk are usually moderate. There are insufficient studies on the safety of duloxetine in lactation and no reports for levomilnacipran (Drugs and Lactation Database, 2006). Lactation risk categories for some SNRIs given by the American College of Obstetricians and Gynecologists (ACOG) and the FDA are summarized in Table 3 (Armstrong, 2008).

UNDERSTANDING SNRIs

SNRI drugs show higher efficacy with improved response and remission rates vs. TCAs. In patients with high recurrence potential, SNRIs can be prescribed in high doses for long–term treatments. It is because they are well tolerated as they do not interact with muscarinic, histaminic, and α1-adrenergic receptors and they do not affect MoA. Only venlafaxine may exhibit some dopamine reuptake inhibition at high doses. Their specific MOA provides lower adverse effects. The likelihood of committing suicide in SNRI-using patients is less than TCAs although SNRI possess more risk than SSRIs. General adverse effects are nausea, vomiting, diarrhea, headache, dry mouth, cardiovascular symptoms, sexual problems, and syndrome of inappropriate antidiuretic hormone secretion (SIADH) (Lambert & Bourin, 2002; Lee & Chen, 2010).

Venlafaxine

Venlafaxine (1-(2-(dimethylamino)-1-(4- methoxyphenyl) ethyl)cyclohexan-1-ol) has phenylethylamine structure and is structurally different from other SNRI drugs because it contains two chemical rings (bicyclic) (Figure 2a). Venlafaxine is the first SNRI approved for major depression, anxiety, panic disorder, and social phobia by the FDA in 1993. A few years later, micro capsulated XR formulation was on the market. XR formula is used once a day while non–XR formulation should be taken twice daily. XR formula has clinical advantage of causing less nausea and dizziness at the start of treatment (Sansone & Sansone, 2014).

Pharmacokinetics

Venlafaxine is effectively absorbed after being administered orally. It has a 45% absolute bioavailability. A single oral dose of venlafaxine was at least 92% absorbed. Following twice-daily oral administration of an immediate-release formulation of 150 mg venlafaxine, the Cmax was 150 ng/mL and the Tmax was 5.5 hours. The active metabolite, desvenlafaxine (ODV), has a Cmax and Tmax of 260 ng/mL and 9 hours, respectively. The rate of absorption is slower with venlafaxine XR. However, it has a similar level of absorption as the formulation for immediate release. After once-daily administration of 75 mg venlafaxine XR, Cmax was 225 ng/mL and Tmax was two hours. The bioavailability of venlafaxine or ODV is not affected by food. The oral half–life is 5 hours while the half-life of the XR formulation is 11 hours. Venlafaxine's apparent volume of distribution (Vd) at steady state is 7.53.7 L/kg while ODV's is 5.71.8 L/kg. Venlafaxine is 27% bound to plasma proteins. Venlafaxine undergoes extensive presystemic hepatic metabolism by CYP2D6, 3A3, and 3A4. After CYP2D6-mediated demethylation, venlafaxine is metabolized to ODV (Yue et al., 2023). Even though it's not a frequent metabolic pathway, CYP2C9, CYP2C19, and CYP3A4 can N-demethylate venlafaxine to form N-desmethylvenlafaxine (NDV) (Fogelman et al., 1999). ODV and NDV are further metabolized by CYP isoenzymes 2C19, 2D6 and/or 3A4 to form N,O-didesmethylvenlafaxine (NODV). NODV is also metabolized to form N,N,O-tridesmethylvenlafaxine, possibly with glucuronidation. Within 48 hours, venlafaxine (87%) can be detected in urine [unconjugated ODV (29%), minor inactive metabolites (27%), conjugated ODV (26%), and unchanged venlafaxine (5%)] (Preskorn et al., 2009). Venlafaxine and ODV have an elimination half-life of 5±2 hours and 11±2 hours, respectively (Stahl, Entsuah & Rudolph, 2002; Sansone & Sansone, 2014).

Pharmacodynamics

Venlafaxine has 30-fold selectivity for serotonin reuptake compared to norepinephrine reuptake at the presynaptic terminal.

Table 2. Teratogenicity categories for SNRIs.

Drug Name	FDA Category	Possible Teratogenic Effects	Approved condition
Duloxetine	C	No teratogenic effect observed.	Major – depressive disorder, not clear for pediatric patients
Venlafaxine	C	No teratogenic effect observed.	Major – depressive disorder, not approved for pediatric patients
Desvenlafaxine	C	No teratogenic effect observed.	Major – depressive disorder, not approved for pediatric patients
Levomilnacipran	C	No teratogenic effect observed.	Major – depressive disorder, not approved for pediatric patients

Table 3. Lactation risk categories of SNRIs.

Drug Name	Lactation Risk Category
Venlafaxine	L3
Desvenlafaxine	No information
Duloxetine	Not applicable
Levomilnacipran	No information

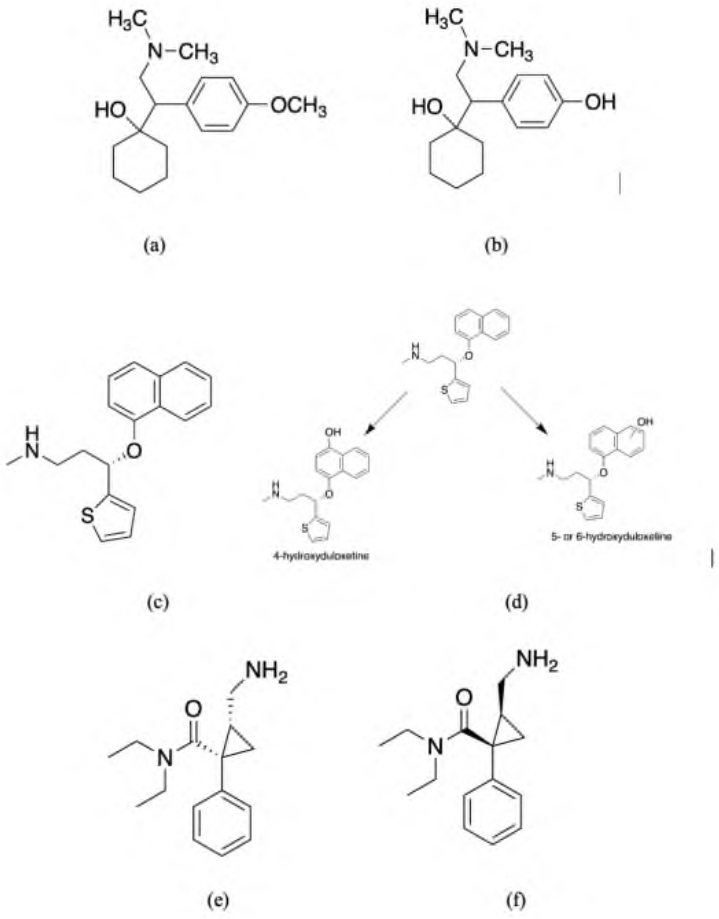

Figure 2. Chemical structure of SNRIsa. Venlafaxine; b. Desvenlafaxine; c. Duloxetine; d. Major metabolites of duloxetine. e. Levomilnacipran; f. Milnacipran.

At low doses, venlafaxine initially inhibits serotonin reuptake while at higher doses, it inhibits norepinephrine reuptake as well as serotonin. Therefore, adverse effects just as headache and nausea are related to serotonin uptake suppression while adverse effects such as dry mouth and sweating are due to norepinephrine reuptake suppression. At high doses, venlafaxine also inhibits dopamine reuptake (Sansone & Sansone, 2014).

In a study comparing venlafaxine and SSRIs, venlafaxine showed a much higher efficacy, possibly due to the "double effect". 75 mg daily intake fulfilled serotonin reuptake inhibition (Stahl et al., 2002; FDA, 2017).

Pregnancy

During the second and third trimesters, venlafaxine may increase the risk of pre-eclampsia and eclampsia. In one study investigating the relationship between gestational diabetes and antidepressants, pregnant women using venlafaxine had an increased risk compared to the control group (Dandjinou et al., 2019).

In another study investigating the relationship between venlafaxine therapy in the early period of pregnancy and preterm delivery, increased risks were observed. Children whose mothers used venlafaxine in the third trimester had withdrawal syndrome, preterm birth, neonatal seizures, and necrotizing enterocolitis (Bellantuono, Vargas, Mandarelli, Nardi & Martini, 2015). Partial clubfoot, hypospadias, and neural tube defects were also observed in children after their mother intake venlafaxine in first trimester. However, there is no clear evidence that prenatal venlafaxine exposure is the only reason for these malformations. In another study, researchers suggested that exposure of venlafaxine might lead to hypospadias (Lind et al., 2013).

Prenatal exposure caused slightly reduced IQ scores and a higher incidence of problematic behavior. Moreover, prenatally exposed newborns may experience poor neonatal adaptation syndrome. Scientists mention a "possibility" of all these conditions for SNRIs as there is lack of empirical studies where firm evidence can be reached (Dubovicky et al., 2017). Most of the research conducted on pregnant women exposed to venlafaxine have not found a conclusive link between miscarriage or serious birth abnormalities (Bellantuono et al., 2015).

Lactation

O-desmethylvenlafaxine can be found in most breastfed newborns' plasma, but rare adverse effects have been documented. Venlafaxine was not to be taken during nursing, and newborn or preterm infants who were breastfed should be watched for excessive sedation and proper weight gain. Evaluation of serum ODV levels is suggested. Venlafaxine was also suggested to cause withdrawal symptoms, but this has not been rigorously demonstrated (Koren, Moretti & Kapur, 2006; Boucher, Koren, & Beaulac-Baillargeon, 2009).

Desvenlafaxine

Desvenlafaxine [4-(2-(dimethylamino)-1-(1-hydroxycyclo hexyl) thylphenol] is an SNRI authorized by the FDA for the management of depression (Figure 2b). Desvenlafaxine was introduced into therapy in 2008 and is used as succinate salt. Because it is a metabolite of venlafaxine, they are structurally similar. After biotransformation, desvenlafaxine concentration in plasma is 2-3 times that of venlafaxine (Figure 3) (DeMaio, Kane, Nichols & Jordan, 2011; Sansone & Sansone, 2014; Magalhães, Alves, LLerena & Falcão, 2015).

Desvenlafaxine is superior to venlafaxine due to its proven high efficacy, safety profile, good tolerance, low effect on CYP450s, and once-daily use (Seo, Sohi, Patkar, Masand & Pae, 2010). According to the FDA, this single daily dose is 50 mg. Once a day treatment is sufficient.

Pharmacokinetics

Oral bioavailability is ~80% (Pae, 2011). Food does not affect the bioavailability of the drug, but the important thing is that orally taken drug is swallowed directly without chewing (FDA, 2011). Within 7.5 hours, peak plasma concentration is reached (Reddy et al., 2010). Cmax and Tmax of desvenlafaxin (ODV) were 290 ng/mL and three hours, respectively. Vd is 3.4 L/kg and binds 30% of plasma proteins. Drug concentration has no impact on the degree of protein binding (Liebowitz & Tourian, 2010; Reddy et al., 2010).

Just a small fraction of desvenlafaxine goes through oxidative N-demethylation via CYP43A4. Its metabolites are N,O-didesmethylvenlafaxine, benzylhydroxy desvenlafaxine, desvenlafaxine N-oxide and cyclohexane ring hydroxy desvenlafaxine, Desvenlafaxine also undergoes glucuronidation and desvenlafaxine O-glucuronide is the major metabolite. The main excretion route is by the kidneys. While 19% of the dose is excreted as the glucuronide metabolite and 5% as N,O-didesmethylvenlafaxine, the remaining 45% of the dose remains unchanged in the urine (Liebowitz & Tourian, 2010). Desvenlafaxine has an 11.1-hour half-life (Liebowitz & Tourian, 2010; Sansone & Sansone, 2014).

Pharmacodynamics

Desvenlafaxine has ten times greater affinity for inhibiting the reuptake of serotonin than norepinephrine transporters. Dopamine and norepinephrine transporters have lower affitinity. In *in vitro* experiments, desvenlafaxine did not inhibit MAO and desvenlafaxin nearly had no affinity for muscarinic, cholinergic, H1-histaminergic, and α1-adrenergic receptors, desvenlafaxin nearly had no affinity (Liebowitz & Tourian, 2010). In a study on male rats, desvenlafaxine reached to hypothalamus rapidly after oral administration (30 mg) and it significantly increased the amount of extracellular norepinephrine, suggest-

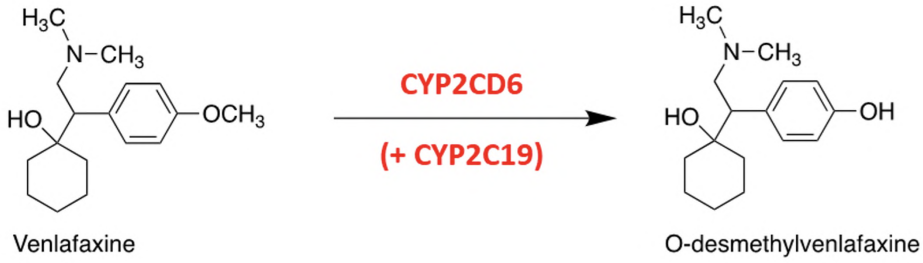

Figure 3. Biotransformation of venlafaxine to desvenlafaxine (ODV).

ing a good brain–plasma ratio and therefore it can be used in various CNS disorders (Deecher et al., 2006).

In a study conducted to improve the treatment of vasomotor symptoms that occur during menopause, desvenlafaxine was preferred despite being a new SNRI because its therapeutic efficacy is assumed to be due to its role in thermoregulation of norepinephrine and serotonin neurotransmitters in hypothalamus and dysfunction resulting from vasomotor symptoms. Women treated with desvenlafaxine showed a much higher rate of improvement compared to control group (Speroff et al., 2008).

Many studies have demonstrated safety, tolerability, and effectiveness of desvenlafaxine in both daily and fixed doses and flexible doses (100 mg, 200 mg, and 400 mg) (Liebowitz et al., 2008).

Pregnancy

There were no teratogenic effects when oral doses up to 300 mg/kg/day and 75 mg/kg/day were given to pregnant rats and rabbits during organogenesis. In reproductive developmental studies in rats and rabbits treated with desvenlafaxine succinate, there was no evidence of teratogenicity at a plasma exposure (AUC) that is up to 19-times (rats) and 0.5-times (rabbits) the exposure at an adult human dose of 100 mg per day. Yet, at highest dose, fetus weights showed decreases and delayed skeletal ossification was observed along with maternal toxicity (Pfizer Medical Information, 2021).

Lactation

Desvenlafaxine is eliminated in breast milk. Nursing mothers must discontinue using the medicine or stop breastfeeding based on the risks and benefits to the mother and child because controlled clinical trials are not available (Ilett, Watt, Hackett, Kohan & Teoh, 2010).

When given orally to pregnant rats during gestation and lactation at the maximum dose (300 mg/kg/day), there were increases in pup mortality during the first four days of lactation and decreases in pup weights, both of which had no apparent cause. The AUC exposure at the level that had no effect on rat pup mortality was 4.5 times higher than the exposure at a daily dose of 100 mg for adults. Desvenlafaxine medication for the mother had no impact on the pups' post-weaning development or ability for reproduction (Pfizer Medical Information, 2021).

Ten breastfeeding women (with a mean age of 4.3 months) receiving desvenlafaxine at a dose of 50 to 150 mg every day participated in a lactation study. Foremilk and hindmilk were collected over a 24-hour dosing period at steady state (up to 8 samples). The average relative baby dose was 6.8%, with a range of 5.8% to 8.1%. No adverse reactions were reported in newborns (Rampono, Teoh, Hackett, Kohan, & Ilett, 2011).

Duloxetine

Duloxetine, ((3S)-N-methyl-3-naphthalen-1-yloxy-3-thiophen-2-ylpropan-1-amine), is one of the first-line treatments for many diseases including fibromyalgia and major depressive disorder (Figure 2c). Duloxetine was introduced to treatment in USA in 2004 (Lantz et al., 2003; Lee & Chen, 2010; Fanelli, Weller & Liu, 2021; Knadler, Lobo, Chappell & Bergstrom, 2011). In addition to these disorders, SNRIs especially venlafaxine and duloxetine can also be used in the treatment of pain associated with cancer. Duloxetine may be preferred because of its higher affinity for noradrenergic transporters, but both medicines are recommended as equivalent first-line treatments (Zerfas, McGinn & Smith, 2023).

Pharmacokinetics

Mean bioavailability is 50%, with a wide variability between individuals (30-80%). As duloxetine can hydrolyze in acidic conditions, there is a necessity for enteric coating although enteric coating causes two hours of delay in absorption. Tmax is 6 hours including delay time. Food also leads to a delay in Tmax and 10% decrease in AUC. Along with those, taking duloxetine before sleep at night leads to a 4-hour lag time and 18% decrease in AUC with a 29% reduction in Cmax. The reason for the delay is delayed gastric emptying. However, they do not practically affect the clinical efficacy. Duloxetine is highly bound to proteins (90-99%, primarily albumin and α1-acid-glycoprotein) and is highly distributed. Duloxetine can cross

BBB. In both humans and animals, the amount of duloxetine in the cerebral cortex was found to be higher than in plasma. V_d is 1,620-1,800 L (Knadler et al., 2011).

Cytochrome P450 2D6 (CYP2D6) and cytochrome P450 1A2 (CYP1A2), two mitochondrial isoforms of cytochrome P450 isoenzymes, are primarily responsible for the metabolism of duloxetine (Yue et al., 2023). Five phenotypes (ultrarapid metabolizers, rapid metabolizers, normal metabolizers, intermediate metabolizers, and poor metabolizers) have been determined based on the enzymatic activity of different CYP2D6 polymorphisms. Because treatment response may vary due to CYP2D6 polymorphisms, personalized treatment approaches are very important to optimize major depression disorder management (Maciaszek et al., 2023). CYP2C9 is known to be a minor contributor in formation of 5-hydroxy metabolite. Hydroxylation occurs at 4-, 5-, or 6- positions on naphthalene ring (Figure 2d) and 4-hydroxy metabolite directly undergoes glucuronidation. 5- and 6-hydroxy metabolites undergo glucuronide or sulfate conjugation. Unknown metabolites lack clinical significance in overall profile of duloxetine. The half-life of duloxetine ranges between 78-17 hours, with a mean of 12 hours. Inter-individual variations are reported in the clearance of duloxetine (57-114 L/h). The concentration of the drug in the blood at a steady state increased by 2.3 and 2.6 times, respectively, with the dose doubling from 30 to 60 mg and from 60 to 120 mg. The 20% of duloxetine is eliminated in the feces as the parent drug, a 4-hydroxy metabolite, and an unidentified metabolite. Urine excretes 70% of duloxetine as conjugated metabolites. Biliary secretion may also be involved (Knadler et al., 2011).

Pharmacodynamics

Duloxetine inhibits the reuptake of serotonin and norepinephrine in neurons. It also has a weaker inhibitory effect on dopamine reuptake. The dopaminergic, adrenergic, cholinergic, histaminergic, opioid, glutamate, and -aminobutyric acid (GABA) receptors are not particularly stimulated by duloxetine. The dual action of duloxetine on serotonin and norepinephrine regulates emotions. Compared to venlafaxine, the affinity of duloxetine for suppression of serotonin and norepinephrine reuptake is partially more balanced (Frampton & Plosker, 2007).

CNS effects of duloxetine are mediated by its action on the external urinary sphincter. Due to increments in serotonin and norepinephrine levels in α1-adrenergic receptors, *Onuf's* nucleus, activation of 5-HT2 and 5-HT3 show increases. Both 5-HT2 and α1 are G_q (G_i/G_o) coupled receptors. When they are activated, the activity of the inositol trisphosphate/phospholipase C (IP3/PLC) pathway increases. This activation of the IP3/PLC pathway causes the release of intracellular calcium, which raises intracellular calcium levels and promotes neuronal excitability. On the other hand, 5-HT3 is a ligand-gated sodium channel allowing sodium to flow into neurons when it is activated. Increased sodium flow into neurons causes depolarization and the activation of voltage-gated channels is essential to produce action potentials. When each of these receptors is activated, they work together to enhance the pudendal motor nerve's response to glutamate. This response also provides duloxetine to act on the spinal cord and enables modulation of pain. Increased serotonin and norepinephrine levels in the dorsal horn of the spinal cord provide pain inhibition by activation of several receptors (i.e. α1-adrenergic and α2-adrenergic receptors, 5-HT1A, 5-HT1B, 5-HT1D, 5-HT2 and 5-HT3). GABAergic inhibitory interneuron connections that are activated block the transmission of painful impulses to the brain and the nociceptive projection neuron. Activation of G_q-coupled 5-HT1 and α2 receptors cause elevated potassium through inward rectifier channels and reduced adenylyl cyclase/protein kinase A signaling which participates in neuronal inhibition. These inhibitory receptors are present on the projection neuron itself as well as the dorsal root ganglion, which act to prevent the direct transmission of painful inputs (Wong et al., 1993; Millan, 2002; Gupta, Nihalani & Masand, 2007; Bellingham & Peng, 2010).

The safety, tolerability, and effectiveness of duloxetine are demonstrated in both daily and fixed doses and flexible doses (30 mg and 60 mg). The intended pharmacological effect of duloxetine and its hypertensive effect are connected. The vascular endothelium's adrenergic receptors are activated when norepinephrine availability increases. Vasoconstriction occurs as the Gq-coupled receptor mediating calcium releases from the sarcoplasmic reticulum to enhance smooth muscle contraction because the action of α1-adrenergic receptors predominates (Cowen, Ogilvie & Gama 2005).

Pregnancy

It has been demonstrated that duloxetine has adverse effects on postnatal and embryo/fetal development in animals. There is no sufficient and reliable research on pregnant women. Some neonates can need respiration support, tube feeding, and a longer hospital stay. Some of them wailed nonstop, experienced convulsions, had trouble breathing or eating, or had stiff or overly relaxed muscles. Therefore, if there is no immediate necessity, duloxetine should not be given to pregnant women or those planning to have children. (Cymbalta Product Monograph, 2021).

A recent study revealed information on pre/post-term births, ectopic pregnancies, and pregnancy outcomes of women exposed to duloxetine from the Lilly Safety System (LSS) and the FDA Adverse Events Reporting System. There were 400 pregnancies found in the LSS database. Most of the pregnancy outcomes that were categorized as "abnormal" were spontaneous abortions (n=41), perinatal complications (n=25), or premature births (n=19). In patients with abnormal pregnancy outcomes, relevant concomitant medication use, and relevant medical history were more frequently reported, compared to those with nor-

mal pregnancy outcomes. Considering all the available data, it was suggested that the "frequency of abnormal results reported in pregnancy cases with duloxetine exposure is generally consistent with historic control rates in the general population" (Hoog, Cheng, Elpers & Dowsett, 2013). In addition, there are similar results reported in 256 pregnant women taking duloxetine with a majority of intake during either of the trimesters (n=206) while others throughout pregnancy (Einarson et al., 2012). The rate of major congenital malformations (1.8% as hydronephrosis, kidney agenesis, and clubfoot) was within the general population's baseline rate (Einarson et al., 2012). Similar findings were obtained from two case reports performed by Briggs et al. (2009) and Bellantuono et al. (2013) who reported two cases of pregnant women exposed to duloxetine during pregnancy (60mg/day) (Briggs et al., 2009; Bellantuono, Marini & Lucarelli, 2013). Both suggested that healthy newborns were born from two mothers who took duloxetine during pregnancy.

In one case report, Eyal and Yaeger (2008) found that a newborn developed a neonatal "behavioral syndrome," characterized by poor muscle tone, respiratory distress, jitteriness, weak cry, low *Apgar* score, and seizures, born to a mother who took duloxetine throughout pregnancy (90 mg/day). Authors suggested that these symptoms could have developed as a result of discontinuation syndrome (Eyal & Yaeger, 2008).

Ankarfeldt et. al (2021) investigated the potential link between duloxetine exposure during pregnancy and birth defects or stillbirth in children. A population-based observational study was carried out using information from more than 2 million Danish and Swedish medical birth registrations from 2004 to 2016. It was found that there were no correlations between duloxetine exposure during pregnancy and the risk of abnormalities or stillbirth (Ankarfeldt et al., 2021).

Lactation

Duloxetine is eliminated in breast milk. The baby receives nearly 0.14% of the maternal dose on a mg/kg basis. Boyce et al., (2011) reported a newborn with no adverse effects whose mother was prescribed duloxetine in the second half of pregnancy (60 mg/day). The dose of duloxetine taken during pregnancy may be a crucial factor in adverse effects in prenatally exposed infants (Boyce, Hackett & Ilett, 2011). The safety of duloxetine in infants is not clearly established. Therefore, duloxetine is not recommended during nursing (Larsen et al., 2015).

Levomilnacipran (Fetzima)

Levomilnacipran ((1*S*,2*R*)-2-(aminomethyl)-*N,N*-diethyl-1-phenylcyclopropane-1 carboxamide, Figure 2e), is the enantiomer of milnacipran ((1*R*,2*S*)-2-(aminomethyl)-*N,N*-diethyl-1-phenylcyclopropane-1-carboxamide; Figure 2f) and is superior in the management of depression. Since it is used once a day, patient compliance is high and the drug is well tolerated (Bruno, Morabito, Spina & Muscatello, 2016). In addition, it has been shown to have -site amyloid precursor protein cleaving enzyme-1 (BACE-1) inhibitory activity. Thus, it has been experimentally shown that the compound may have a pleiotropic effect by inhibiting β-amyloid plaque formation (Fasipe, 2018).

Pharmacokinetics

After oral administration of an extended-release capsule of levomilnacipran, relative bioavailability was 92%. Intake of the drug with food does not affect its blood concentrations. After using extended-release capsules, the mean C_{max} was determined as 341 ng/mL, and the mean steady-state AUC was 5196 ng·h/mL. After oral intake, the drug has a T_{max} of 6-8 hours. In humans, there is no interconversion of stereoisomers. V_d is 387-473 L. Between 10 to 1,000 ng/mL of plasma concentrations, levomilnacipran is carried as 22% protein bound. Levomilnacipran is bio transformed by desethylation (mainly by CYP3A4 and by CYP2C8, CYP2C19, CYP 2D6 and CYP 2J2 to a lesser extent) to N-desethyl levomilnacipran and by hydroxylation to p-hydroxy-levomilnacipran. Both metabolites are glucuronidated later. The main excretion route for levomilnacipran and its metabolites is by kidneys. In the urine, about 58% of the dosage is eliminated unchanged, with the remaining 18% being accounted for by the primary metabolite N-desethyl levomilnacipran. Levomilnacipran glucuronide (4%), desethyl-levomilnacipran glucuronide (3%), p-hydroxy levomilnacipran glucuronide (1%), and p-hydroxylevomilnacipran (1%), are also urine detectable metabolites. It is found that these metabolites are inactive. 12 hours is the half-life, while 21 to 29 L/h is the average apparent total clearance (Bruno et al., 2016).

Pharmacodynamics

The exact antidepressant action mechanism is uncertain. However, it is hypothesized that it is connected to the accumulation of serotonin and norepinephrine in the central nervous system (CNS) due to an inhibition of their reuptake by transporters. Its inhibitory reuptake effect is more on norepinephrine rather than serotonin (Lee & Chen, 2010; Montgomery et al., 2013; Bruno et al., 2016;). In a rat study, levomilnacipran increased amounts of serotonin and norepinephrine in the frontal cortex but this increase was stronger for norepinephrine than serotonin (Auclair et al., 2013).

In a study of patients with major depression, patients treated with levomilnacipran showed significantly higher rates of improvement compared to the placebo group. In addition, it has played an important role in eliminating functional impairments that can occur during depression. Another factor observed was that a small number of patients discontinued to treatment of levomilnacipran compared to placebo. This suggests that the

drug is well-tolerated. However, patients treated with levomilnacipran had a higher mean heart rate, which was associated with increased noradrenergic activity (Montgomery et al., 2013).

Pregnancy

There are no sufficient controlled trials of levomilnacipran in pregnant women. The drug was not teratogenic in rats or rabbits when administered during the organogenesis phase up to 100 mg/kg/day (doses up to 8 or 16 times the MRHD of 120 mg on a mg/m2 basis, respectively). Rat fetus body weights were decreased, and skeletal ossification was postponed in both rats and rabbits. However, these effects were not seen in either species at doses up to 30 mg/kg/day (2.4 times MRHD in rats or 5 times MRHD in rabbits), which indicated that neither species experienced any adverse effects. Early postnatal pup mortality increased when pregnant rats were given 60 mg/kg/day (5 times MRHD) orally during organogenesis, pregnancy, and lactation. At 20 mg/kg/day (1.6 times MRHD), there was no pup death. Up to 8 weeks of age, pre- and post-weaning pup weight increase was decreased in the surviving pups. The progeny's physical and functional growth including their ability to reproduce remained unaffected. At 7 mg/kg/day (0.6 times the MRHD), no effects on body weight growth were seen. Levomilnacipran should be used in pregnant women by deciding based on the risks-benefits. (FDA, 2012).

Lactation

Levomilnacipran has been found in the milk of nursing rats. There have been no studies with nursing mothers who exposed to levomilnacipran in the literature. On the other hand, racemic form of milnacipran has modest amounts in breastmilk and was not anticipated to have any adverse effects on breastfed infants. Levomilnacipran should be used with caution while breastfeeding (Drugs and Lactation Database, 2006).

DISCUSSION AND CONCLUSION

Depression in pregnancy as well as in lactation may lead to severe consequences. Therefore, use of antidepressants during these periods may be needed. The usage of SNRIs during nursing and pregnancy has not been well studied. Even though the categorization of drugs in pregnancy (A, B, C, D and X) are discontinued by the FDA in 2015, FDA continues to be the initial phase of risk assessment. The current additional processes and the initial risk assessment are taken into consideration when making the final judgment about whether the drug can be used during pregnancy or not. On the other hand, drug use during lactation is being evaluated according to the Pregnancy and Lactation Labeling Rule (PLLR). The healthcare providers assess benefit versus risk and in subsequent counseling of pregnant women and nursing mothers who need to take medication according to the PLLR. When an information become s outdated, the PLLR also requires the label to be updated.

SNRIs used to be evaluated as category C by the FDA as negative effects on fetus have been observed in animal studies. These drugs can only be used during pregnancy if there is a clear necessity (Ray Stowe, 2014). Lactating mothers may also have post-partum depression. If a SNRI is the drug of choice, it should be used with caution, as there have been no well-designed or well-controlled studies on effects of SNRIs in postnatal period.

In conclusion, although SNRIs have fewer adverse effects and high efficacy, they should be used with caution during pregnancy and lactation. Well-controlled studies on large number of subjects are needed to show their safety during these two susceptible periods of life.

Peer-review: Externally peer-reviewed.

Author Contributions: Conception/Design of Study- R.G.C., R.Ş., T.B., P.E.; Data Acquisition- R.G.C., R.Ş., D.A.Ç.; Data Analysis/Interpretation- R.G.C., R.Ş., D.A.Ç., H.T., T.B., P.E.; Drafting Manuscript- R.G.C., R.Ş., D.A.Ç.; Critical Revision of Manuscript- H.T., R.Ş., T.B., P.E.; Final Approval and Accountability- R.G.C., R.Ş., D.A.Ç., H.T., T.B., P.E.

Conflict of Interest: The authors have no conflict of interest to declare.

Financial Disclosure: The authors declared no financial support

ORCID IDs of the authors

Göksu Canıtez	0009-0006-0672-2022
Rahime Şimşek	0000-0002-8467-6336
Deniz Arca Çakır	0000-0002-6110-1775
Hülya Tezel Yalçın	0000-0002-1843-3424
Terken Baydar	0000-0002-5497-9600
Pınar Erkekoğlu	0000-0003-4713-7672

REFERENCES

Ankarfeldt, M. Z., Petersen, J., Andersen, J. T., Li, H., Motsko, S. P., Fast, T. ... Jimenez-Solem, E. (2021). Exposure to duloxetine during pregnancy and risk of congenital malformations and stillbirth: A nationwide cohort study in Denmark and Sweden. *Plos Medicine*, 18(11), e1003851. https://doi.org/10.1371/journal.pmed.1003851

American Psychiatric Association (2023, September). Diagnostic and Statistical Manual of Mental Disorders (DSM-5-TR) [Web log post]. Retrieved from: https://www.psychiatry.org/psychiatrists/practice/dsm/updates-to-dsm/updates-to-dsm-5-tr-criteria-text

Armstrong, C. (2008). ACOG guidelines on psychiatric medication use during pregnancy and lactation. *American Family Physician,*

78(6), 772-778.

Auclair, A. L., Martel, J. C., Assié, M. B., Bardin, L., Heusler, P., Cussac, D. ... Depoortère, R. (2013). Levomilnacipran (F2695), a norepinephrine-preferring SNRI: profile in vitro and in models of depression and anxiety. *Neuropharmacology*, 70, 338–347. https://doi.org/10.1016/j.neuropharm.2013.02.024

Avalos, L. A., Chen, H., & Li, D. K. (2015). Antidepressant medication use, depression, and the risk of preeclampsia. *CNS Spectrums*, 20(1), 39–47. https://doi.org/10.1017/S1092852915000024

Banzi, R., Cusi, C., Randazzo, C., Sterzi, R., Tedesco, D., & Moja, L. (2015). Selective serotonin reuptake inhibitors (SSRIs) and serotonin-norepinephrine reuptake inhibitors (SNRIs) for the prevention of migraine in adults. *The Cochrane Database Of Systematic Reviews*, 4(4), CD002919. https://doi.org/10.1002/14651858.CD002919.pub3

Bellantuono, C., Marini, A., & Lucarelli, C. (2013). Infant health and neurodevelopmental outcomes following prenatal exposure to duloxetine. *Clinical Drug Investigation, 33*(9), 685 688. https://doi.org/10.1007/s40261-013-0112-y

Bellantuono, C., Vargas, M., Mandarelli, G., Nardi, B., & Martini, M. G. (2015). The safety of serotonin-noradrenaline reuptake inhibitors (SNRIs) in pregnancy and breastfeeding: a comprehensive review. *Human Psychopharmacology*, 30(3), 143–151. https://doi.org/10.1002/hup.2473

Bellingham, G. A., & Peng, P. W. (2010). Duloxetine: a review of its pharmacology and use in chronic pain management. *Regional Anesthesia And Pain Medicine, 35*(3), 294–303. https://doi.org/10.1097/AAP.0b013e3181df2645

Benevent, J., Araujo, M., Karki, S., Delarue-Hurault, C., Waser, J., Lacroix, I. ... Damase-Michel, C. (2023). Risk of Hypertensive Disorders of Pregnancy in Women Treated With Serotonin-Norepinephrine Reuptake Inhibitors: A Comparative Study Using the EFEMERIS Database. *The Journal Of Clinical Psychiatry*, 84(4), 22m14734. https://doi.org/10.4088/JCP.22m14734

Bérard, A., Zhao, J. P., & Sheehy, O. (2017). Antidepressant use during pregnancy and the risk of major congenital malformations in a cohort of depressed pregnant women: an updated analysis of the Quebec Pregnancy Cohort. *BMJ Open*, 7(1), e013372. *https://doi.org/10.1136/bmjopen-2016-013372*

Boucher, N., Koren, G., & Beaulac-Baillargeon, L. (2009). Maternal use of venlafaxine near term: correlation between neonatal effects and plasma concentrations. *Therapeutic Drug Monitoring*, 31(3), 404–409. https://doi.org/10.1097/FTD.0b013e3181a58fb4

Boyce, P. M., Hackett, L. P., & Ilett, K. F. (2011). Duloxetine transfer across the placenta during pregnancy and into milk during lactation. *Archives Of Women's Mental Health, 14*(2), 169–172. https://doi.org/10.1007/s00737-011-0215-5

Briggs, G. G., Ambrose, P. J., Ilett, K. F., Hackett, L. P., Nageotte, M. P., & Padilla, G. (2009). Use of duloxetine in pregnancy and lactation. *The Annals Of Pharmacotherapy*, 43(11), 1898–1902. https://doi.org/10.1345/aph.1M317

Brumbaugh, J. E., Ball, C. T., Crook, J. E., Stoppel, C. J., Carey, W. A., & Bobo, W. V. (2023). Poor Neonatal Adaptation After Antidepressant Exposure During the Third Trimester in a Geographically Defined Cohort. *Mayo Clinic Proceedings. Innovations, Quality & Outcomes*, 7(2), 127–139. https://doi.org/10.1016/j.mayocpiqo.2023.02.002

Bruno, A., Morabito, P., Spina, E., & Muscatello, M. R. (2016). The Role of Levomilnacipran in the Management of Major Depressive Disorder: A Comprehensive Review. *Current Neuropharmacology*, 14(2), 191–199. https://doi.org/10.2174/1570159x14666151117122458

Cowen, P. J., Ogilvie, A. D., & Gama, J. (2005). Efficacy, safety, and tolerability of duloxetine 60 mg once daily in major depression. *Current Medical Research And Opinion*, 21(3), 345–356. https://doi.org/10.1185/030079905X30680

Dale, E., Bang-Andersen, B., & Sánchez, C. (2015). Emerging mechanisms and treatments for depression beyond SSRIs and SNRIs. *Biochemical Pharmacology*, 95(2), 81–97. https://doi.org/10.1016/j.bcp.2015.03.011

Dandjinou, M., Sheehy, O., & Bérard, A. (2019). Antidepressant use during pregnancy and the risk of gestational diabetes mellitus: a nested case-control study. *BMJ Open*, 9(9), e025908. https://doi.org/10.1136/bmjopen-2018-025908

Deecher, D. C., Beyer, C. E., Johnston, G., Bray, J., Shah, S., Abou-Gharbia, M., & Andree, T. H. (2006). Desvenlafaxine succinate: A new serotonin and norepinephrine reuptake inhibitor. *The Journal Of Pharmacology And Experimental Therapeutics*, 318(2), 657–665. https://doi.org/10.1124/jpet.106.103382

DeMaio, W., Kane, C., Nichols, A., & Jordan, R. (2011). Metabolism studies of desvenlafaxine. *Journal Of Bioequivalence & Bioavailability, 3*(7), 151-160. https://doi.org/10.4172/jbb.1000076

Dubovicky, M., Belovicova, K., Csatlosova, K., & Bogi, E. (2017). Risks of using SSRI / SNRI antidepressants during pregnancy and lactation. *Interdisciplinary Toxicology*, 10(1), 30–34. https://doi.org/10.1515/intox-2017-0004

Einarson, A., Smart, K., Vial, T., Diav-Citrin, O., Yates, L., Stephens, S. ... Einarson, T. R. (2012). Rates of major malformations in infants following exposure to duloxetine during pregnancy: a preliminary report. *The Journal of Clinical Psychiatry*, 73(11), 1471. https://doi.org/10.4088/JCP.12l08013

Eyal, R., & Yaeger, D. (2008). Poor neonatal adaptation after in utero exposure to duloxetine. The American Journal Of Psychiatry, 165(5), 651. https://doi.org/10.1176/appi.ajp.2008.07071194

Fanelli, D., Weller, G., & Liu, H. (2021). New Serotonin-Norepinephrine Reuptake Inhibitors and Their Anesthetic and Analgesic Considerations. *Neurology International*, 13(4), 497–509. https://doi.org/10.3390/neurolint13040049

Fasipe, O. J. (2018). Neuropharmacological classification of antidepressant agents based on their mechanisms of action. *Archives Of Medicine And Health Sciences, 6*(1), 81-94. https://doi.org/10.4103/amhs.amhs_7_18

FDA Approved Drug Products. (2011). PRISTIQ® (desvenlafaxine) Extended-Release Tablets. Retrieved from: https://www.accessdata.fda.gov/drugsatfda_docs/label/2012/021992s030lbl.pdf

FDA Center for Drug Evaluation and Research. (2012). F2695 (Levomilnacipran HCl). Retrieved from: https://www.accessdata.fda.gov/drugsatfda_docs/nda/2013/204168Orig1s000PharmR.pdf

FDA Approved Drug Products. (2017). EFFEXOR XR® (venlafaxine Extended-Release) Capsules. Retrieved from : https://www.accessdata.fda.gov/drugsatfda_docs/label/2017/020699s107lbl.pdf

Fogelman, S. M., Schmider, J., Venkatakrishnan, K., von Moltke, L. L., Harmatz, J. S., Shader, R. I., & Greenblatt, D. J. (1999). O- and N-demethylation of venlafaxine in vitro by human liver microsomes and by microsomes from cDNA-transfected cells: effect of metabolic inhibitors and SSRI antidepressants. *Neuropsychopharmacology: Official Publication Of The American College Of Neuropsychopharmacology*, 20(5), 480–490. https://doi.org/10.1016/S0893-133X(98)00113-4

Frampton, J. E., Plosker, G. L. (2007). Duloxetine: a review of its use in the treatment of major depressive disorder. *CNS Drugs*, 21(7),

581–609. https://doi.org/10.2165/00023210-200721070-00004

Gałecki, P., Mossakowska-Wójcik, J., & Talarowska, M. (2018). The anti-inflammatory mechanism of antidepressants - SSRIs, SNRIs. *Progress In Neuro-Psychopharmacology & Biological Psychiatry*, 80(Pt C), 291–294. https://doi.org/10.1016/j.pnpbp.2017.03.016

Ghimire, U., Papabathini, S. S., Kawuki, J., Obore, N., & Musa, T. H. (2021). Depression during pregnancy and the risk of low birth weight, preterm birth and intrauterine growth restriction- an updated meta-analysis. *Early Human Development*, 152, 105243. https://doi.org/10.1016/j.earlhumdev.2020.105243

Gupta, S., Nihalani, N., & Masand, P. (2007). Duloxetine: review of its pharmacology, and therapeutic use in depression and other psychiatric disorders. *Annals Of Clinical Psychiatry : Official Journal Of The American Academy Of Clinical Psychiatrists*, 19(2), 125–132. https://doi.org/10.1080/10401230701333319

Hoog, S. L., Cheng, Y., Elpers, J., & Dowsett, S. A. (2013). Duloxetine and pregnancy outcomes: safety surveillance findings. *International Journal Of Medical Sciences, 10*(4), 413–419. https://doi.org/10.7150/ijms.5213

Ilett, K. F., Watt, F., Hackett, L. P., Kohan, R., & Teoh, S. (2010). Assessment of infant dose through milk in a lactating woman taking amisulpride and desvenlafaxine for treatment-resistant depression. *Therapeutic Drug Monitoring,* 32(6), 704–707. https://doi.org/10.1097/FTD.0b013e3181f88f70

Knadler, M. P., Lobo, E., Chappell, J., & Bergstrom, R. (2011). Duloxetine: clinical pharmacokinetics and drug interactions. *Clinical Pharmacokinetics*, 50(5), 281–294. https://doi.org/10.2165/11539240-000000000-00000

Koren, G., Moretti, M., & Kapur, B. (2006). Can venlafaxine in breast milk attenuate the norepinephrine and serotonin reuptake neonatal withdrawal syndrome. *Journal Of Obstetrics And Gynaecology Canada : JOGC = Journal D'obstetrique Et Gynecologie Du Canada : JOGC,* 28(4), 299–301. https://doi.org/10.1016/S1701-2163(16)32135-1

Lambert, O., & Bourin, M. (2002). SNRIs: mechanism of action and clinical features. *Expert Review Of Neurotherapeutics*, 2(6), 849–858. https://doi.org/10.1586/14737175.2.6.849

Lantz, R. J., Gillespie, T. A., Rash, T. J., Kuo, F., Skinner, M., Kuan, H. Y., & Knadler, M. P. (2003). Metabolism, excretion, and pharmacokinetics of duloxetine in healthy human subjects. Drug Metabolism And Disposition: The Biological Fate Of Chemicals, 31(9), 1142–1150. https://doi.org/10.1124/dmd.31.9.1142

Larsen, E. R., Damkier, P., Pedersen, L. H., Fenger-Gron, J., Mikkelsen, R. L., Nielsen, R. E., ... Danish Society of Clinical Pharmacology (2015). Use of psychotropic drugs during pregnancy and breast-feeding. *Acta Psychiatrica Scandinavica. Supplementum*, (445), 1–28. https://doi.org/10.1111/acps.12479

Lee, Y. C., & Chen, P. P. (2010). A review of SSRIs and SNRIs in neuropathic pain. *Expert Opinion On Pharmacotherapy*, 11(17), 2813–2825. https://doi.org/10.1517/14656566.2010.507192

Li, J., Lu, C., Gao, Z., Feng, Y., Luo, H., Lu, T. ... Luo, Y. (2020). SNRIs achieve faster antidepressant effects than SSRIs by elevating the concentrations of dopamine in the forebrain. *Neuropharmacology*, 177, 108237. https://doi.org/10.1016/j.neuropharm.2020.108237

Liebowitz, M. R., Manley, A. L., Padmanabhan, S. K., Ganguly, R., Tummala, R., Tourian, K. A. (2008). Efficacy, safety, and tolerability of desvenlafaxine 50 mg/day and 100 mg/day in outpatients with major depressive disorder. *Current Medical Research And Opinion*, 24(7), 1877–1890. https://doi.org/10.1185/03007990802161923

Liebowitz, M. R., & Tourian, K. A. (2010). Efficacy, safety, and tolerability of Desvenlafaxine 50 mg/d for the treatment of major depressive disorder:a systematic review of clinical trials. *Primary Care Companion To The Journal Of Clinical Psychiatry*, 12(3), PCC.09r00845. https://doi.org/10.4088/PCC.09r00845blu

Lind, J. N., Tinker, S. C., Broussard, C. S., Reefhuis, J., Carmichael, S. L., Honein, M. A., ... National Birth Defects Prevention Study (2013). Maternal medication and herbal use and risk for hypospadias: data from the National Birth Defects Prevention Study, 1997-2007. *Pharmacoepidemiology And Drug Safety*, 22(7), 783–793. https://doi.org/10.1002/pds.3448

Maciaszek, J., Pawłowski, T., Hadryś, T., Machowska, M., Wiela-Hojeńska, A., & Misiak, B. (2023). The Impact of the CYP2D6 and CYP1A2 Gene Polymorphisms on Response to Duloxetine in Patients with Major Depression. *International Journal Of Molecular Sciences*, 24(17), 13459. https://doi.org/10.3390/ijms241713459

Magalhães, P., Alves, G., LLerena, A., & Falcão, A. (2015). Clinical drug-drug interactions: focus on venlafaxine. *Drug Metabolism And Personalized Therapy*, 30(1), 3–17. https://doi.org/10.1515/dmdi-2014-0011

Masarwa, R., Bar-Oz, B., Gorelik, E., Reif, S., Perlman, A., & Matok, I. (2019). Prenatal exposure to selective serotonin reuptake inhibitors and serotonin norepinephrine reuptake inhibitors and risk for persistent pulmonary hypertension of the newborn: a systematic review, meta-analysis, and network meta-analysis. *American Journal Of Obstetrics And Gynecology, 220*(1), 57.e1–57.e13. https://doi.org/10.1016/j.ajog.2018.08.030

Millan M. J. (2002). Descending control of pain. *Progress In Neurobiology*, 66(6), 355–474. https://doi.org/10.1016/s0301-0082(02)00009-6

Molenaar, N. M., Bais, B., Lambregtse-van den Berg, M. P., Mulder, C. L., Howell, E. A., Fox, N. S. ... Kamperman, A. M. (2020). The international prevalence of antidepressant uses before, during, and after pregnancy: A systematic review and meta-analysis of timing, type of prescriptions and geographical variability. *Journal Of Affective Disorders, 264*, 82–89. https://doi.org/10.1016/j.jad.2019.12.014

Montgomery, S. A., Mansuy, L., Ruth, A., Bose, A., Li, H., & Li, D. (2013). Efficacy and safety of levomilnacipran sustained release in moderate to severe major depressive disorder: a randomized, double-blind, placebo-controlled, proof-of-concept study. *The Journal Of Clinical Psychiatry, 74*(4), 363–369. https://doi.org/10.4088/JCP.12m08141

Otte, C., Gold, S. M., Penninx, B. W., Pariante, C. M., Etkin, A., Fava, M. ... Schatzberg, A. F. (2016). Major depressive disorder. *Nature Reviews. Disease Primers, 2*, 16065. https://doi.org/10.1038/nrdp.2016.65

Pae C. U. (2011). Desvenlafaxine in the treatment of major depressive disorder. *Expert Opinion On Pharmacotherapy*, 12(18), 2923–2928. https://doi.org/10.1517/14656566.2011.636033

Park, K., Kim, S., Ko, Y. J., & Park, B. J. (2021). Comparison of risk of cardiovascular disease related adverse events between selective serotonin reuptake inhibitor users and serotonin norepinephrine reuptake inhibitor users in Korean adult patients with depression: retrospective cohort study. *Psychiatry Research, 298*, 113744. https://doi.org/10.1016/j.psychres.2021.113744

Perrotta, C., Giordano, F., Colombo, A., Carnovale, C., Castiglioni, M., Di Bernardo, I. ... Viganò, C. (2019). Postpartum Bleeding in Pregnant Women Receiving SSRIs/SNRIs: New Insights From a Descriptive Observational Study and an Analysis of Data from the FAERS Database. *Clinical Therapeutics, 41*(9), 1755–1766. https://doi.org/10.1016/j.clinthera.2019.06.008

Preskorn, S., Patroneva, A., Silman, H., Jiang, Q., Isler, J. A., Burczynski, M. E. ... Nichols, A. I. (2009). Comparison of the

pharmacokinetics of venlafaxine extended release and desvenlafaxine in extensive and poor cytochrome P450 2D6 metabolizers. *Journal Of Clinical Psychopharmacology, 29*(1), 39–43. https://doi.org/10.1097/JCP.0b013e318192e4c1

Rampono, J., Teoh, S., Hackett, L. P., Kohan, R., & Ilett, K. F. (2011). Estimation of desvenlafaxine transfer into milk and infant exposure during its use in lactating women with postnatal depression. *Archives Of Women's Mental Health, 14*(1), 49–53. https://doi.org/10.1007/s00737-010-0188-9

Ray, S., & Stowe, Z. N. (2014). The use of antidepressant medication in pregnancy. *Best Practice & Research. Clinical Obstetrics & Gynecology, 28*(1), 71–83. https://doi.org/10.1016/j.bpobgyn.2013.09.005

Reddy, S., Kane, C., Pitrosky, B., Musgnung, J., Ninan, P. T., & Guico-Pabia, C. J. (2010). Clinical utility of desvenlafaxine 50 mg/d for treating MDD: a review of two randomized placebo-controlled trials for the practicing physician. *Current Medical Research And Opinion, 26*(1), 139–150. https://doi.org/10.1185/03007990903408678

Robiyanto, R., Roos, M., Bos, J. H. J., Hak, E., van Puijenbroek, E. P., & Schuiling-Veninga, C. C. M. (2023). Switching pattern and dose adjustment of antidepressants before and during pregnancy. *Archives Of Women's Mental Health, 26*(5), 685–696. https://doi.org/10.1007/s00737-023-01355-8

Sansone, R. A., & Sansone, L. A. (2014). Serotonin norepinephrine reuptake inhibitors: a pharmacological comparison. *Innovations In Clinical Neuroscience, 11*(3-4), 37–42. https://www.ncbi.nlm.nih.gov/pubmed/24800132

Seo, H. J., Sohi, M. S., Patkar, A. A., Masand, P. S., & Pae, C. U. (2010). Desvenlafaxine succinate: a newer antidepressant for the treatment of depression and somatic symptoms. *Postgraduate Medicine, 122*(1), 125–138. https://doi.org/10.3810/pgm.2010.01.2106

Singal, D., Chateau, D., Struck, S., Lee, J. B., Dahl, M., Derksen, S. ... Brownell, M. (2020). In Utero Antidepressants and Neurodevelopmental Outcomes in Kindergarteners. *Pediatrics, 145*(5), e20191157. https://doi.org/10.1542/peds.2019-1157

Snamina, M., Wietecha-Posłuszny, R., & Zawadzki, M. (2019). Postmortem analysis of human bone marrow aspirate - Quantitative determination of SSRI and SNRI drugs. Talanta, 204, 607–612. https://doi.org/10.1016/j.talanta.2019.06.054

Speroff, L., Gass, M., Constantine, G., Olivier, S., & Study 315 Investigators (2008). Efficacy and tolerability of desvenlafaxine succinate treatment for menopausal vasomotor symptoms: a randomized controlled trial. *Obstetrics And Gynecology*, 111(1), 77–87. https://doi.org/10.1097/01.AOG.0000297371.89129.b3

Stahl, S. M., Entsuah, R., & Rudolph, R. L. (2002). Comparative efficacy between venlafaxine and SSRIs: a pooled analysis of patients with depression. *Biological Psychiatry, 52*(12), 1166–1174. https://doi.org/10.1016/s0006-3223(02)01425-7

Uguz F. (2018). Maternal Antidepressant Use During Pregnancy and the Risk of Attention-Deficit/Hyperactivity Disorder in Children: A Systematic Review of the Current Literature. *Journal Of Clinical Psychopharmacology, 38*(3), 254–259. https://doi.org/10.1097/JCP.0000000000000868

Wang, X. Y., Ying, X. H., & Jiang, H. Y. (2023). Antidepressant use during pregnancy and the risk for gestational diabetes: a systematic review and meta-analysis. *The Journal of Maternal-Fetal & Neonatal Medicine: The Official Journal Of The European Association Of Perinatal Medicine, The Federation Of Asia And Oceania Perinatal Societies, The International Society Of Perinatal Obstetricians, 36*(1), 2162817. https://doi.org/10.1080/14767058.2022.2162817

Wong, D. T., Bymaster, F. P., Mayle, D. A., Reid, L. R., Krushinski, J. H., & Robertson, D. W. (1993). LY248686, a new inhibitor of serotonin and norepinephrine uptake. *Neuropsychopharmacology: Official Publication Of The American College Of Neuropsychopharmacology, 8*(1), 23–33. https://doi.org/10.1038/npp.1993.4

Yang, L., Wu, Z., Cao, L., Wang, Y., Su, Y., Huang, J. ... Fang, Y. (2021). Predictors and moderators of quality of life in patients with major depressive disorder: An AGTs-MDD study report. *Journal Of Psychiatric Research, 138*, 96–102. https://doi.org/10.1016/j.jpsychires.2021.03.063

Yue, M., Kus, L., Katta, S., Su, I., Li, L., Haas, D. M., & Quinney, S. K. (2023). Pharmacokinetics of Antidepressants in Pregnancy. *Journal Of Clinical Pharmacology, 63 Suppl 1*(Suppl 1), S137–S158. https://doi.org/10.1002/jcph.2282

Zerfas, I., McGinn, R., Smith, M. A. (2023). Pharmacologic Management of Cancer-Related Pain in Pregnant Patients. *Drugs, 83*(12), 1067–1076. https://doi.org/10.1007/s40265-023-01906-4

Zoega, H., Kieler, H., Nørgaard, M., Furu, K., Valdimarsdottir, U., Brandt, L., & Haglund, B. (2015). Use of SSRI and SNRI Antidepressants during Pregnancy: A Population-Based Study from Denmark, Iceland, Norway and Sweden. *Plos One, 10*(12), e0144474. https://doi.org/10.1371/journal.pone.0144474

How cite this article

Canıtez, G., Şimşek, R., Arca Çakır, D., Tezel Yalçın, H., Baydar, T., & Erkekoğlu, P. (2024). Toxicity of serotonin-norepinephrine reuptake inhibitors (SNRIs) during pregnancy and lactation. *İstanbul Journal of Pharmacy, 54*(2), 255–267. DOI: 10.26650/IstanbulJPharm.2024.1359269